P-001

PIPELINE STATUS AND PETROLEUM PRODUCTS RECOVERY
(SYSTEM 2E, 0-54 KILOMETERS SEGMENT CASE STUDY)

[1]Ogbonna F Joel, [2]Franklin. C. Chukwuma, [3]Emenike. N. Wami, [4]Grace C. Akujobi-Emetuche

[1, 4]World Bank African Centre of Excellence, UniPort, Choba.

[2]Dept. of Chemical Engineering, UniPort, Choba.

[3]Dept of Chem/Petro-Chem, Engrg. RSUST, Nkpolu, Port Harcourt.

Corresponding Author's e-mail: graceakujobi_emetuche@yahoo.com

Other Authors: ogbonna.joel@ipsng.org; fochukwuma@yahoo.com; profwami@yahoo.com

Abstract:

The objective of this work is to determine the effect of pipeline age on interface monitoring along the 54 kilometer/4100m³ multiproduct single pipeline. Having considered the topography and environmental issues, the result showed that current line fill calculated at kilometers 52, 53, 54, 55, 56 and 57 were 3,795m³, 3,868m³, 3,941m³, 4,014m³, 4,087m³, and 4,160m³ respectively. The designed line fill of 4100m³ covers apparent distance of 0 to 56.2km. The result aids in estimating the product arrival, interface cutting or tank diversion time. The effect of reduced flow rate and line pressure was also considered. In order not to exert more stress on the aged and attacked pipeline, average flow rate achieved over a period of 4 years is 86% (PMS-89%, DPK-85%, AGO-83%) of minimum design rate, and this distorts the pipe length/line fill determined at designed pressure and flow rate.

Keywords: pipeline, line fill, interface monitoring and flowrate

1.0 Introduction

Pipeline is a system of connected lengths of pipe, usually buried or laid on the seabed that is used for transporting production fluid (oil or gas) (Bai 2014). Challenges of pipeline transportation include vandalism, maintenance, security concerns, pipeline age on the line, issues related to thwarted pipeline interface monitoring, flow rate and pressure need to be monitored regularly for through a multi-products single pipeline. Pipeline repairs introduce serious alteration in the original design parameters, on the designed line fill, flow regimes and line content recovery.

Interface monitoring and cutting have also become problematic resulting to product contamination and sometimes diversion into the extended pipeline route. This is experienced when water is trailing the petroleum product.

Pipeline installed 25 years ago with 6.35mm (0.25inch) wall thickness may have reduced in wall thickness to 5.08mm (0.20inch) or less due to corrosion, (Menon 2004). Therefore the allowable internal pressure will have to be reduced in the ratio of the wall thickness, compared with the original design pressure. System 2E (Port Harcourt - Aba) pipeline is designed and stalled over 30 years ago to transport refined petroleum products in batches (one at a time). In line with the pipeline engineering position, there is need for periodic review and evaluation of the problems associated with design and operation of the pipeline (Vincent-Genod, 1984). The objective is to find out the:

(a) Efficiency of the 54 kilometer/4100m³ pipeline installed over 30 years ago.

(b) Cause of interface monitoring challenge on 54 kilometer/4100m³ multiproduct single pipeline segment.

(c) Effect of pipeline age on the initial design parameters, line fill and product delivery.

1.1 Considerations and Assumptions

Using field data, the distribution of the velocities inside the pipe were reviewed under laminar (Re less than 2000), smooth turbulence (Re 1000 to 4000), and rough turbulent (Re more than 4000), flow conditions. According to McAllister (2009), the smooth turbulence has turbulent in the middle of the pipe and laminar around the rough wall surface of the pipe. Practically most pipelines operate in the transition zone between the smooth turbulence and the rough flows.

In this preliminary work, the efficiency of more than 30 years old battered pipeline with known design parameters is appraised to know whether the initial line fill still holds in the known length of pipeline and diameter. Since crude oil and finished product are non-compressible Newtonian liquids (Vincent-Genod 1984), using the principles of fluid flow, pipe sizing, and non-compressible Newtonian liquid laws, the actual line fill per kilometer within the referenced segment was considered.

Secondly, the collated field data was analyzed and used for determination of actual flow regimes using the known parameters of the petroleum products. This was checked using the fundamental laws, dimensionless coefficient

derived by Osborne Reynolds number (Incropera & Dewitt 2005); (Sinnott & Towler 2011); (Bratland 2013) and Chukwuma 2004).

The confirmation of the flow regime was carried out using the principles of flow in circular pipes.

1.2 Line Fill considerations

There is need to know the volume of liquid contained in a pipeline. For circular pipes the volume can be calculated by multiplying the internal cross-sectional area by a given length. The pipeline information for the study is tabulated on Table 1:

Table 1. Designed parameters for the referenced pipeline segment

S/N	Designed Parameters	Dimension
1	Length of pipe (L)	54km
2	Line fill (V)	4100m³
3	Minimum designed flow rate	270m³/hr
4	Maximum designed flow rate	290m³/hr
5	Pipe internal diameter (D)	12inches (0.3048m)
6	Main line pressure: Minimum	25kg/cm²
7	Main line pressure: Maximum	35kg/cm²
8	Operating Pressure: Minimum suction	3.5kg/cm²

Source: Referenced pipeline segment operations manual, July, 1980

2.0 Methodology

The most critical consideration is the reconfirmation of pipe line fill in volumes of batches. There is need to confirm the volume of petroleum products contained in the 54 kilometer pipeline segment between the pump station and the receiving Depot. The figures used are four years real time data collated from the industry. The data was analyzed and using statistical methods and engineering correlations. Data for this study was generated from field records and were analyzed using tables, charts and related engineering equations. The calculated figures from field data were compared with the original design information from the operating manual. The study is limited to pumping activities on petroleum product pipeline covering 54 kilometers from Rivers State to Abia State axis and from 2011 to 2014.

2.1 Line fill calculations

Using circular pipes formula, the volume can be calculated by multiplying the internal cross- sectional area by a given length. If the pipe internal diameter is D inches and length is

L (ft,), the volume (ft³) of this length of pipe according to Menon, (2004) is

$$V = 0.8754\left(\frac{D^2}{144L}\right) \qquad (1)$$

where V = Volume (ft³), Simplifying.

$$V = 5.4542 \times 10^{-3} D^2 L \qquad (2)$$

Therefore the volume of liquid contained in a mile of a pipe, also called line fill volume is calculated as follows:

$$V_L = 5.129(D)^2 \qquad (3)$$

Where V_L = line fill volume of pipe, bbl/mile, D = pipe internal diameter, inches

$$V_L = 5.129 \times 12in \times 12in = 738.576 barrel/mile$$

Carrying out detailed and careful conversion,

$$V_L = \frac{(738.576 barrel \times 0.159 m^3)}{mile \times 1 barrel} \qquad (4)$$

$$= 117.434 m^3/mile$$

$$V_L = \frac{(117.434 m^3 \times 1 mile)}{mile \times 1.609 km} \qquad (5)$$

$$= 72.9857 m^3/km$$

Calculating line fills (V_L) along kilometers 52, 53, 54, 55, 56 and 57. Calculated volumes are presented in table 1.

Using conventional cylindrical pipes formula, the volume can be calculated by multiplying the internal cross-sectional area by a given length too. This time the formula is $V = \pi r^2 L$ (6)

Where V is line fill volume of pipe, (m³/km); and L (km) is the length of the pipe while r is radius of pipe internal diameter, (mm).

2.2 Appraisal of petroleum products flow rates

The pumping flow rates for the respective products were collated for four years. Annual average flow rates for the products were plotted and compared with the designed. These were done to ascertain the effect of pipe age and other upsets on initial designed minimum and maximum flow rates.

3.0 Results and Discussion

3.1 Line fill confirmation

This was done using circular and cylindrical pipeline equations. The pipeline under review is a 12inch, 54 kilometer pipeline with designed line fill of $4100m^3$. From records this line has suffered numerous breaks (willful drilling, valve insertion, slicing and ruptures) which resulted to pegging, clamping and welding.

Table -1: Line Fill Calculation

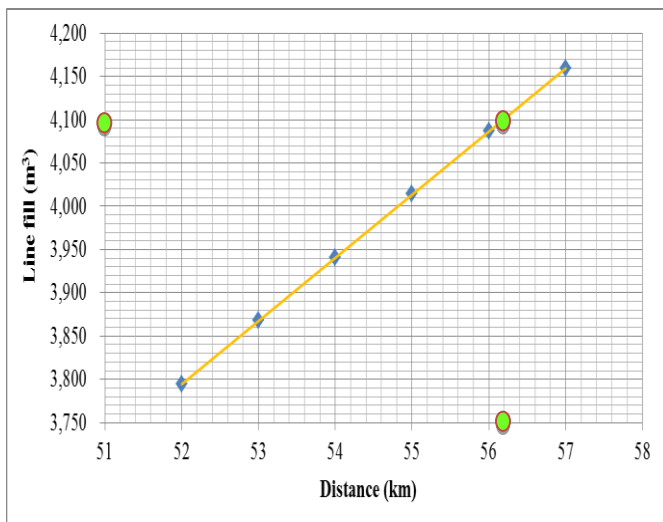| S/N	Length of pipe (km)	Volume in the line (m^3)	
		Circular Pipeline	Cylindrical pipes
1	52	3,795	3,796
2	53	3,868	3,867
3	54	3,941	3,940
4	55	4,014	4,013
5	56	4,087	4,088
6	57	4,160	4,159

Figure 1: Line-fill versus distance

From the reconfirmation calculation, the $4100m^3$ capacity 12inch (0.3048m) pipeline segment being studied stretches beyond 54 kilometers and the receiving Depot could by this calculation be situated at kilometer 56.2. Also the aged pipe wall thickness could have reduced by 0.2inch (5.08mm) or more due to wear and tear thereby taking less volume than designed line fill. This explains why there is interface monitoring challenges and product contamination in batch pumping where different products trail one another. For a pumping operation comprising of three or more products with different densities and viscosities, the interface has always been monitored using the designed length of 54km. This has always affected the expected time of arrival of product adversely. This also explains why there are traces of product on by-pass line, especially where water is leading the products, and the water is meant to be diverted for hydro-testing on the extended pipeline segment.

3. 2 Design and actual flow rates compared

The current actual flow rates of the respective products pumped were collated, analyzed, plotted and compared with the designed minimum and maximum vales. The average flow rates collated from 2011 to 2014 revealed that they are below the minimum designed flow rate of $270m^3/hr$. The analyzed data is presented on Table 2 while the plot is in Figure 2.

Table 2: Comparative analysis of design and actual flow rates

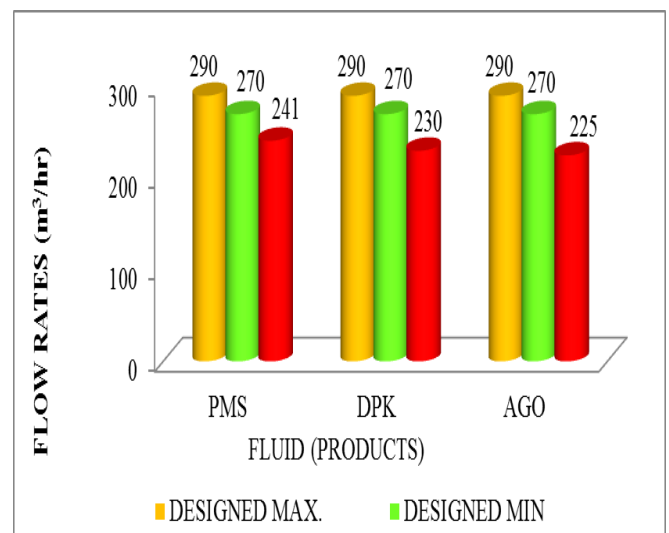| Product	Flow Rates (m^3/hr)			
	Designed (Max)	Designed (Min)	Average: 2011-2014	% = $\frac{Average \times 100}{Designed\,(Min)}$
AGO	290	270	225	83
DPK	290	270	230	85
PMS	290	270	241	86

Figure 2: Comparative analysis of design (maximum, minimum) and actual flow rates

4.0 Conclusion

From the investigation and the results obtained, the following conclusions were drawn.

The Shashi's referenced equation for volume of circulalr pipes gives almost the same result as the conventional volume of cylindrical pipe equation. Product pipeline installed more that 25years old will not have the same delivery efficiency due to corrosion attack on its internal diameter.

Current line fill at kilometers 52, 53, **54,** 55, **56** and 57 are 3,795m^3, 3,868m^3, 3,941m^3, 4,014m^3, 4,087m^3, and 4,160m^3 respectively. The designed line fill of 4100m^3 covers apparent distance of 0 to 56.2km and not 0 to 54 as contained in operating manual. Average flow rate achieved over a period of 4 years is 86% (PMS-89%, DPK-85%, AGO-83%) of minimum design rate of 270m^3/hr. This undoubtedly is part of the reason for contamination, diversion of part of batched products into wrong tanks or by-pass line.

References

Bai, Q and Bai, Y (2014). *Subsea Engineering Handbook,* 301353375.

Brantla, O. (2009). *Pipe Flow 1: Single-phase Flow Assurance* .ISBN 978-616-335-925-4.

Brantla , O. (2013). *Pipe Flow 2: Multi-phase Flow Assurance.* ISBN 978-616-335-926-1.

Chukwuma, F. O. (2004). *Introduction to Process Dynamics and Control.* Port Harcourt: M & J Grand Orbit Communications Limited.

De Nevers, Noels (2005): *Fluid Mechanics for Chemical Engineer*s. 3rd ed. New York: McGraw-Hill.

Gakkai, O. Y. (2009: Flow within circular pipes. Japan Society of Applied Physics through the Institute of Pure and Applied Physics: JAP, Volume 48, issues 1-2.

Green, D. W. and Perry, R. (2007). *Perry's Chemical Engineers' Handbook*, 8th ed., New York: Mcgraw Hill Professional.

Incropera, F. P and DeWitt, D. P. (2005). *Fundamentals of Heat and Mass Transfer*. 5th ed., New York: John Wiley & Sons.

Islam, R (2014). Flow Assurance, Technology & Engineering/Chemical & Biochemical, Wiley, ISBN 0470626089, 9780470626085.

Joel, O.F and Udofia O.O. (2012). Pipeline Vandalism in Nigeria. Recommended Best Practice of checking the menace, 36th Annual SPE International Technical Conference and Exhibition, in Lagos-Nigeria, August 6-8, 2012.

McAllister, E. W. (2009). *Pipeline Rules of Thumb Handbook. A Manual of quick, accurate to everyday pipeline Engineering problems.* 7th ed., Oxford OX2 8DP, UK: Gulf Professional Publishing, Jordan Hill.

Menon, E. S. (2004). *Liquid Pipeline Hydraulic*. New York: CRC Press.

Sinnott, R. and Towler, G. (2011). *Chemical Engineering Design. Coulson and Richardson Chemical Engineering Series,* Volume 6, 5th ed., New York: Elsevier

Vincent-Genod, J (1984). *Fundamentals Pipelines Engineering*. France: Technip Publishing Company.

P 002

PROCESS EVALUATION OF NIGERIA'S ARTISANAL ("ILLEGAL") PETROLEUM REFINERIES FOR EFFECTIVE AIR POLLUTION CONTROL

Akeredolu, F.A. and Sonibare, J.A*.
Environmental Engineering Research Laboratory
Department of Chemical Engineering
Obafemi Awolowo University
Ile-Ife
* asonibar@yahoo.com; fakered@oauife.edu.ng

Abstract:
The present inability of Nigeria's refining capacity to meet about 70% of its domestic demand have compelled the re-introduction of an age-long indigenous petroleum refining technology in some parts of Niger Delta area of the country for survival. In this article, the locations of the petroleum refineries in Nigeria were identified using secondary data. Life cycle analysis was then carried out to evaluate their air quality impacts. The study confirms that operations of the refineries severely impair air quality. It also shows that the present adopted approach by regulators to control operations of the over 20,000 petroleum refineries processing about 150,000 bpd of crude oil in Nigeria damages air quality more than what the refining process does thus demanding a new and better approach. The study suggests a quick and immediate intervention of every stakeholder including the Nigerian Society of Chemical Engineers (NSChE) to access the refineries for technical evaluation of their operations and possible modifications of the adopted processes. With this, the air pollution associated with their present operations and regulations can be controlled.

Keywords: *Petroleum, Refineries, Process, Air Pollution, Artisanal*

1.0   Introduction

The unconventional method of petroleum refining presently practiced in some parts of Niger Delta region of Nigeria poses air pollution challenges that may damage the airshed beyond repair if prompt actions are not taken to address the problem. Due to many reasons including inability of Nigeria's refining capacity to meet its domestic demand and the current high unemployment rate of youths in the country, there has been a re-introduction of an age-long indigenous petroleum refining technology in some parts of Niger Delta area of the country for survival. These petroleum refineries, are called artisanal refineries by the operators but classified as illegal refineries by the regulators.

Energy shortage is a perennial problem in Nigeria. Though the country has four petroleum refineries with total 445,000 bpd installed capacity insufficient to meet the national demand of over 750,000 bpd (Nkaginieme, 2012) when operated at full capacity, they presently perform below installed capacity. The local refining capacity between 2010 and 2014 was 9.17 – 43.36% (NNPC, 2014) as presented in Table 1. While the country daily received 17.38 – 64.39 million litres of refined petroleum products under the same period (Table 2), the daily locally refined products were 5.54 – 10.61 million litres (Table 3). Though Rice (2012) reported that Nigeria's domestic refineries satisfy only 25 percent (maximum) of domestic consumption, local refining in 2014 was 8.6% of the total refined petroleum products supply to the market (Table 3).

Unlike in the other parts of the world where local refining capacity increases with increased demand, it is the reverse in Nigeria. An instance is Korea that had its first petroleum refinery of about 35,000 bpd in 1964 almost the same time with Nigeria's first Port Harcourt refinery with

Table 1: Nigeria's 5-Year Domestic Refining Capacity Utilization (%)

Refineries/Year	2010	2011	2012	2013	2014
Kaduna	20.46	22.17	29.12	29.33	12.90
Port Harcourt	9.17	12.24	11.95	9.18	12.24
Warri	43.36	27.99	27.88	35.99	19.28

Source: Table 18.02 of NNPC (2014)

Table 2: Nigeria's 5-Year Average Daily Petroleum Products Distribution (litres)

Refineries/Year	2010	2011	2012	2013	2014
PMS	17,407,000	15,584,790	13,746,670	43,546,500	47,669,800
HHK	1,832,000	2,467,690	1,782,650	7,297,590	7,901,700
AGO	2,409,230	2,679,160	1,854,050	7,755,500	8,819,630

Source: Table 21.05 of NNPC (2014)

Table 3: Nigeria's 5-Year Average Daily Domestic Major Petroleum Products Yield (litres)

Refineries/Year	2010	2011	2012	2013	2014
PMS	2,660,651.13	4,543,216.51	4,036,769.26	4,402,444.40	1,929,902.15
HHK	2,200,297.65	2,539,847.79	2,049,308.30	2,526,487.40	1,553,072.89
AGO	3,046	3,528	3,104	3,284	2,058

	,881.55	,802.58	,199.84	,908.94	,352.94

Source: Calculated from Table 19.02 of NNPC (2014)

60,000 bpd capacity commissioned in 1965. While Korea refining capacity became 2,438,000 bpd in 1997 (Moon, 1997), Nigeria is yet to improve on its 450,000 bpd local refined capacity attained in 1988 though her population increased from 90.77 million in 1988 to 178.5 million in 2014 (WorldBank, 2015).

Apart from the general petroleum products shortage in the country, the peculiarities of Niger Delta terrain create supply gap in the area even when available in the other parts of the country. The Nigerian National Petroleum Corporation (NNPC) supplies refined petroleum products to the riverine communities in the Niger Delta through floating stations which have been reported to be grossly inadequate to effectively service the population, thereby nullifying the impact these station could have made in bridging the gap (Naanen and Tolani, 2014). Since the growth in population, among other factors, attracts increased petroleum products demand (Abila, 2015), Nigerian market uses alternative refined petroleum products supply route to fill the gap. While government relies on importation (Siddig et al., 2014) some individuals in the Niger Delta area of the country where there is abundant crude oil, rely on indigenous petroleum refining technology known as artisanal or illegal refinery (Plate 1). It is also referred to as "Kpoo Fire" or "bush refinery" in some parts of the operational areas.

Plate 1: A Typical Nigeria's Artisanal Refinery

Though many studies reported different origins of these refineries in the country, it is commonly accepted that it was re-introduced between 2005 and 2009 ((SocialAction, 2014); Naanen, and Tolani, 2014; and (HEDA, 2015)). According to Social Action (2014), the Biafran side of the Civil War between 1967 and 1970, innovated the technology for small scale refining to meet its refined petroleum products' needs. Why some also claim that the technology was introduced by unknown oil engineers to unemployed young men in the Niger Delta, others believe that the practice was started by makers of local alcoholic beverage (local gin) who were distilling palm wine. The technology resurrected in the militants camps, was taken back to the villages by the militants after the amnesty in 2009 and is presently a core part of the local economy of many Niger Delta communities (HEDA, 2015). The refined products (Plate 2) find their way as far as Lagos.

Plate 2: Typical Artisan Refineries Products

Operations of these refineries are structured with adequate strategies for survival (Attah, 2012). Each refinery has camp within which it operates with an average-sized camp employing about 12 - 20 people. In the camps are different categories of people including young men and women (16 – 30 years old) working on refining process with older men and women (30 – 60 years old) managing the site, purchasing crude and distributing refined products. The people are trained engineers (UNEP, 2011) and boat yards operators among others (Obenade and Amangabara, 2014).

Similar to Illegal hunting, logging, and mining across the country (FMEnv, 2014), the refineries rely on illegal bunkering for crude petroleum. About 25% of stolen crude oil find their way into their camps after payment of monetary compensation (HEDA, 2015) and unemployed youths find oil pipelines running through the areas as easy targets ((Anejionu, Ahiarammunnah, and Nri-ezedi, 2015); (Isumonah, 2015)) thus contributing to the crude oil. Nigeria high annual youth unemployment (Table 4) could partly be responsible for their ready availability.

Table 4: Nigeria's 4-Year Unemployment Rates by Age Group (%)*

Year/Age Group	15 – 24	25 – 34	35 – 44	45 – 54	55 – 64
2008	30.2	15.7	10.5	9	12.2
2009	41.6	17	-	11.5	16.7
2010	25.2	20.7	-	19.9	21.3
2011	37.7	22.4	-	18	21.4

Source: ABS (2014)

The refining process yields diesel, petrol, kerosene, bitumen and waste products with yields of each product depending on refining

methods and geological properties of crude oil. The product yield of a typical refinery are 2% PMS, 2% HHK, 41% AGO and 55% waste (HEDA, 2015). These are distributed and sold to large domestic and regional markets including the legal markets.

This study identified the locations of the artisanal petroleum refineries in Nigeria using secondary data. Life cycle analysis was carried out to evaluate their processes for air pollutants sources. The impetus is the desire to find how these refineries can be regulated for acceptance by regulators as a developed indigenous technology tackling refined petroleum products shortage in the country. With this, it is strongly believed that their air pollution impacts can be controlled for improved air quality availability in their area of operations.

2. Materials and Methods

Though the original intention of this study was to do physical counting of artisanal refineries scattered over the Niger Delta region of Nigeria for their physical processes evaluation, this preliminary study relied on extensive literature survey due to inaccessibility of the areas of operations.

From the literature, the locations of these refineries were identified and processes technically evaluated. Material balance analysis was carried out on their production to characterize air emissions for pollutants and processes by which they are generated. ISO 14040 (ISO, 2006), a basic requirements of ISO 14000 (ISO, 2000) on the principles and framework of environmental audit was used in the study with emphasis on its step two, the life cycle inventory analysis. It involves identifying and quantifying emissions to air, releases to water and land (only air in this study), use of raw materials and energy, waste and by-products, and physical size. The basic steps recommended in ISO 14049 (ISO, 2000a) in goal and scope definition and inventory analysis of audit were

strictly followed in strategy development for the study. In the inventory analysis, the major inputs and outputs of each of the unit operations in the artisanal refineries were identified as recommended in ISO 14049. Using HEDA (2015) estimates and assuming 41% AGO product fraction yield, the average daily AGO of 30 – 150 barrels production between 18:00 Hrs and 6:00 Hrs in a typical artisanal refinery translate to about 70 – 360 barrels (14000 – 72000 litres) of daily crude oil processing. These were used in air emissions calculation from the artisanal refineries using the daily crude oil processing.

3. Results and Discussions

In this section are reported the locations of the artisanal petroleum refineries in Nigeria as obtained from the surveyed secondary data. The evaluated processes and the sources of air pollutants from the refineries are also presented with their potential air pollutants quantified. Finally the possible controls are recommended. Recommendations were made on how these refineries can be regulated for acceptance by regulators as a developed indigenous technology tackling refined petroleum products shortage in the country.

3.1 Location of Nigeria's Artisanal Refineries

Due to some peculiarities of these artisanal refineries including the illegality of their operations in the country, they are all located in the creeks, forest and villages in the oil producing areas of Niger Delta (Figure1) where crude oil tapping operation points and water are easily accessed. However shadiness of their activities makes it difficult to establish their present number in the country from any of the previous studies reviewed.
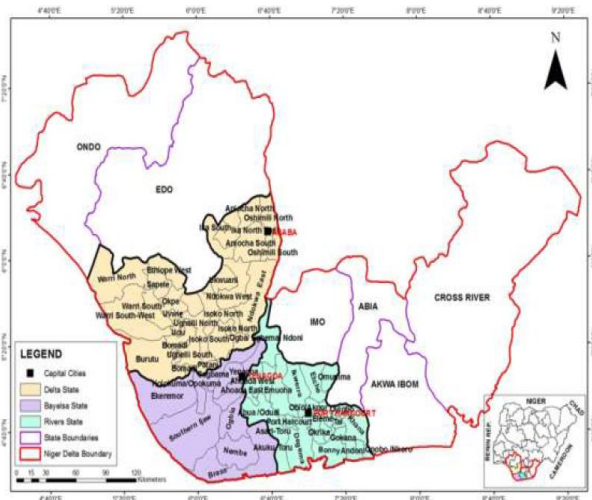
Fig. 1: Niger Delta Area Hosting Nigeria's Artisanal Refineries (Naanen and Tolani, 2014)

Through the activities of Joint Task Force (JTF) purposely established to destroy this indigenous refining technology in the country, there is an idea of how many they are. While about 600 of the refineries were destroyed in Ogoni by JTF in December 2009, about 800 operators of these refineries surrendered in the same area in March 2010 (Plate 3). In this same period, JTF estimate of such refineries was 1,500 (Naanen and Tolani, 2014). In 2012 JTF destroyed 7378 of the refineries (Table 5). There are over 20,000 of these refineries in the country (Unachukwu, 2012).

Plate 3: Surrendered Artisanal Refining Equipment

Table 5: Destroyed Illegal Refineries between July – December, 2012

Month	Average Destroyed
July	1157
August	1209
September	1034
October	998
November	1546
December	1434
Total	7378

Source: (MoD, 2013)

3.2   Technical Evaluation of Process Activities of Nigeria's Artisanal Refineries

The main activities of the artisanal refineries include taking in of crude oil, refining, and products delivery to customers. Some unit operations are required to get these activities accomplished in the plants. Unlike in the conventional petroleum refinery where a variety of processes including separation, petroleum conversion, petroleum treating, feedstock and product handling are employed in conjunction with auxiliary facilities, Nigeria's artisanal refineries mainly include some elements of separation processes, feedstock and product handling. The process typically involves crude oil boiling in metal pipes and drums welded together and the resultant fumes collection, cooling and condensation in tanks (UNEP, 2011). The distilleries are heated on open fires fed by crude oil tipped into pits in the ground.

The first stage in artisanal refining operation in Nigeria is the creation of tapping point where crude oil supply is achieved by engaging specialists who drill holes and install valves (tap installation) on them for siphoning crude from the pipelines that crisscross the operations area (Plate 4). Whenever crude is required for refining, artisan refineries operators purchase crude oil from the operators of the tapping point

(Plate 5) into "Cotonou Boat" (tapping point operation). On arrival through the "Cotonou Boat" (Plate 6) from the tapping point (crude oil supply), camp workers transfer the cold crude oil to a storage tank using a rubber hose and pump (Plate 7). The "Cotonou Boat" is big wooden boat powered by gasoline or diesel engine filled with crude oil and conveyed same to the artisanal refinery. The storage tanks include large locally made "GEEPEE" tanks (Plate 8) and open-air pits (Plate 9) which are large holes dug in the ground, clad with plastic or other synthetic material for prevention of crude oil leakage.

In the refinery, crude oils are left for 2 – 3 days to allow gas contents reduction by evaporation. They are then sent to the oven, a metal tank of various sizes and dimensions constructed from the conventional metal barrel (Plate 10), through pump or manually (Plate 11) for refining (local refining stage). These ovens are of different sizes including 10 in 1, 30 in 1, 60 in 1 or 100 in 1 capacity. A typical 10 in 1 oven is a barrel of 2000 litres capacity or the conventional 200 litre barrel multiplied by 10.

Plate 4: Typical Crude Pipelines in Niger Delta

Plate 5: Typical Crude Oil Tapping Point

Plate 6: Loaded "Cotonou Boat" with Crude

Plate 7: Typical Crude Oil Hose

Plate 8: Typical Crude Oil Storage Tanks

Plate 9: Typical Crude Oil Storage Pit

Plate 10: Typcical Artisanal Refinery's Oven

Plate 11: Manual Crude Transfer to Oven

They are characterized by two openings at the top where gas is further vented. The oven is placed or elevated from the ground with a pit dug underneath where crude oil and its residue are dispensed to help in igniting fire (Plate 12). Dry woods are added and thereafter ignited to produce the fire needed to heat up the crude oil inside the oven. The pit underneath the oven is intermittently replenished with oil and dry wood to sustain the fire. Detergent is poured into the oven already filled with crude oil for air emissions suppressions.

An elevated wooden or metal box with several metal pipes (Plate 13) connected to the oven serves as a cooler in the refining process. This cooler is sporadically replenished with water pumped directly from nearby river or stream. The pumped water, appropriately called coolant by the refiners, provides a cooling effect to the oil migrating from the oven to the cooler through the metal pipes linking the cooler to the oven. Connected to the cooler with metal pipes, is the receiver, a metal container receiving the refined products (Plate 14). The cooler is always carefully located between the oven and the receiver.

After about 2 - 3 hours when the heat underneath the oven would have reached a temperature of about 200 °C, PMS starts trickling to the receiver (Plate 14). A typical oven of 20 in 1 capacity (that is 4000 litres capacity) for example, would approximately produce 1 barrel or drum (200 litres) of PMS which trickles out from the cooler into the receiver. At between 200 and 250 °C, about 1 barrel or drum (200 litres) of kerosene will also start flowing from the cooler into the receiver. However kerosene flow is accompanied by gas vented through a line of vertical pipes in addition to the openings on top of the oven. Some artisanal refineries use electric fan powered by electric generator and placed close to the oven opening to re-direct the gas away from the oven and avoid potential fire-outbreak that could arise were the emitted gas ever to interact with the fire from oven.

At around 300 °C, a mixture of AGO and HHK gushes out of the cooler into the receiver. The air emissions from the oven will subside after approximately 3 drums (600 litres) of the mixture of AGO and HHK have surged out of the receiver. Once the air emission recedes, the fire underneath the oven is diminished.

Lastly, at about 350 °C or higher, there will be steady flow of AGO from the cooler into the receiver. As soon as this point is attained, the fire underneath the oven is increased for improved yield. The terminal end of this refining process occurs when smoke starts emitting from the oven indicating no more refined products are left in it (Plate 15). The fire underneath the oven is then extinguished using water from hoses connected to the nearby stream or river.

Plate 12: Fire Preparation for Refining

Plate 13: Cooler Connected to the Oven

Plate 14: Receiver of Refined Products

Plate 16: Manual Products Evacuation

Plate 15: Smoke Emitting Ovens

Plate 17: Artisanal Refinery Products in Storage Pit

The refined products are manually collected or drained out (Plate 16) with machines from the receiver into empty drums or the "Cotonou" boats and sold to buyers who visit the refineries on schedules (products distribution and sales). They may also be stored in underground storage tanks (Plate 17).

On completion of the refining process, the space at the side of the oven with a connecting pipe and channelled to a waste-pit is opened for the residue to flow into the waste-pit (Plate 18). The residue could be re-used to ignite and fuel the heating fire underneath the oven in future refining cycles. According to Social Action (2014), a 20 in 1 capacity oven (4000 litres) usually yields between 18-19 barrels or drums of refined products (3600 – 3800 litres) which implying that only about one or two drums (200 – 400 litres) of oil are lost in the refining process.

Plate 18: Typical Waste Pit

Plate 19 JTF in an Artisana Refinery Site
(Pictures from Social Action (2014); Naanen and Tolani (2014); UNEP (2011); HEDAS (2015) and MoD (2013))

These wastes are also reported not to be entirely lost but part of residue used in future refining process as fuel for igniting and sustaining the refining fire. However, HEDA (2015) reported 2% PMS, 2% kerosene, 41% diesel and 55% waste generation in the artisanal refineries. The refining process (Figure 2) in the refineries is a simple fractional distillation (locally called "cooking"), where crude oil is heated and condensed into separate petroleum products.

3.2 Identification of Unit Operations in Nigeria's Artisanal Refineries

Like the conventional petroleum refineries, operations in these artisanal refineries can be divided into two broad sections including the ancillary and specific operations. In the ancillary operations, fuel, water, and air are used to support specific operations which include crude oil siphoning, crude oil transport and storage, crude oil refining and refined petroleum products discharging. The entire route is summarized in Figure 2. Their identified unit operations with sources of air emissions are summarized in Figure 3.
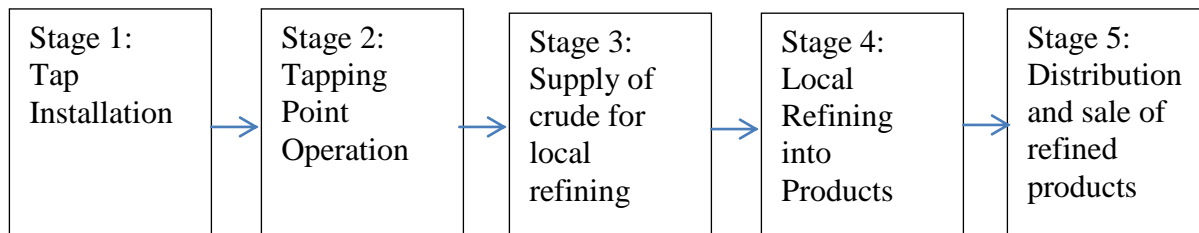
| Stage 1: Tap Installation | → | Stage 2: Tapping Point Operation | → | Stage 3: Supply of crude for local refining | → | Stage 4: Local Refining into Products | → | Stage 5: Distribution and sale of refined products |

Fig. 2: Typical Artisanal Refineries Flow Diagram

Emissions of VOCs ↑   Emissions of VOCs and combustion products ↑   Emissions of VOCs and combustion products ↑   Emissions of VOCs ↑   Emissions of VOCs ↑

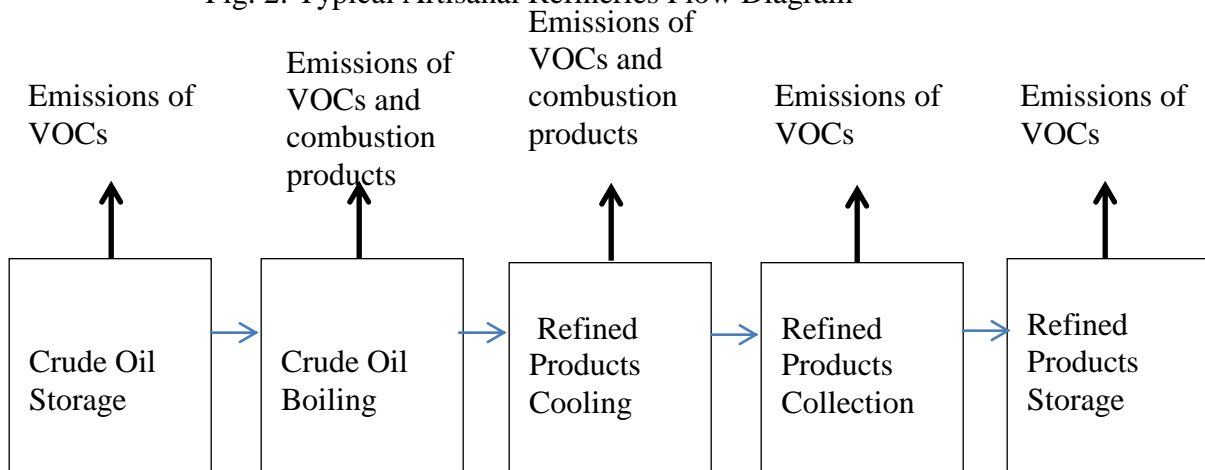| Crude Oil Storage | → | Crude Oil Boiling | → | Refined Products Cooling | → | Refined Products Collection | → | Refined Products Storage |

Fig. 3: Typical Artisanal Refineries Process Flow Diagram and Sources of Air Emissions

Due to crude oil composition, VOCs are common emissions associated with their refining process. These are carbon-based components of crude oil that evaporate at room temperature. However the key combustion products include carbon monoxide (CO), oxides of nitrogen (NO_X), Sulphur dioxide (SO_2) and particulate matter (PM). While CO is as a result of During tap installation to create tapping point for crude oil supply to the refinery, boats and electric power generators required in pipeline drilling are sources of combustion products while VOCs are released from the first crude oil obtained before tap installation. Similarly during the tapping point operation these VOCs are emitted from crude oil siphoning to the boats while combustion products are emitted from the engines powering the boats and the pumps. These sources also emit both VOCs and Combustion products expected from these fuels will be emitted into the atmosphere as air pollutants. In stage 4 which is the refining process, emissions of VOCs are expected from crude oil boiling (distillation process) in the ovens as part of the vent gas while oxidation of

incomplete combustion of carbon in the fuel, SO_2 may be from oxidation of sulphur and its allied compounds present in the fuel. The NO_X may be prompt or thermal depending on the source of the oxidized nitrogen which may be those present in the fuel or the combustion air. Particulate matter is also usually attributed to incomplete combustion process.

combustion products during the transfer of the siphoned crude oil to the artisanal refineries. During storage before refining, VOCs are emitted from the storage tanks or storage pits and while transferring them to the oven for refining, VOCs are emitted. If the transfer to the oven is pump-assisted, emission of combustion products are experienced in the areas of operations. Heating of the ovens for refining requires heat provision which is accomplished by wood and crude oil burning.

some components of the crude oil in the oven may also result in the emissions of combustion products. As summarized in Figure 4, VOCs may also be emitted from refined products cooling, collection and storage.
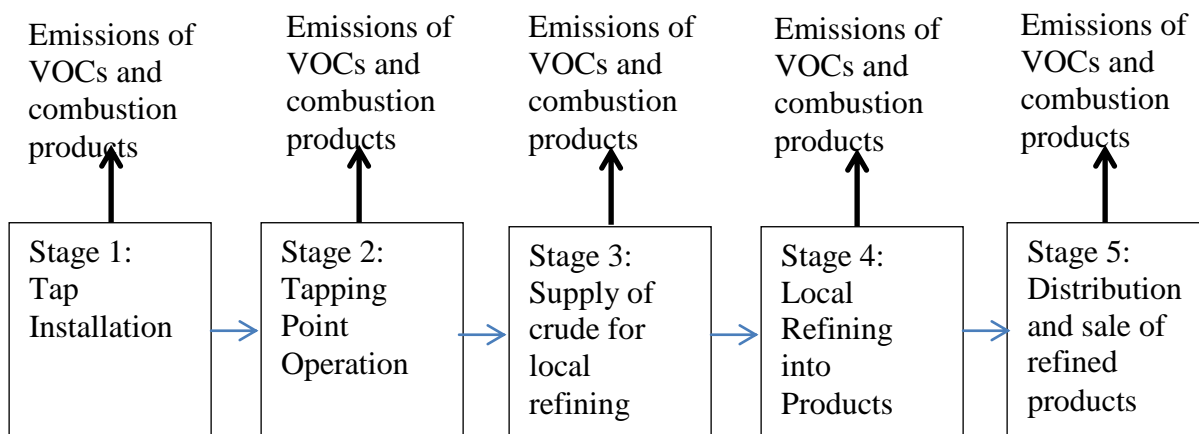

Fig. 4: Typical Artisanal Refining and Air Emissions Sources

Refined products loading into the boats for distribution is a known source of VOCs while combustion products are released from operations of pump if product loading is pump-assisted. Also, emissions of combustion products

are common experienced in the engines powering the boats used for products distribution. From the waste pits, the possibility of VOCs emissions is very high due to the nature of the wastes composition.

A major source of air emissions from these artisanal refineries identified in the course of this study is the usual sudden decommissioning of the refineries by the regulators. Whenever any of the artisanal refineries locations is sighted, the regulators move in to destroy it through burning (Plate19f). Usually these burnings are accompanied by large emissions of air pollutants including VOCs arising from evaporation of spilled crude oils and combustion products associated with crude oil burning.

3.3   Air Emissions from Nigeria's Artisanal Refineries Operations

Though there are many products and wastes outputs from operations of these artisanal refineries as earlier identified in this study, the focus is on air emissions for the purpose of recommending appropriate control measures for their control. As summarized in Table 6, there are several unit operations that result in air emissions in the artisanal refineries.

Table 6: Identified Sources of Air Emissions in Nigeria's Artisanal Refineries

VOCs Sources	Combustion Products Sources
Tapping installation	Tapping installation
Tapping point operation	Tapping point operation
Crude transfer to the Refinery	-
Crude Storage	-
Crude Transfer to the Oven	Crude Transfer to the Oven
Oven heating	Oven heating
Crude boiling	Crude boiling
Products cooling	-
Products collection	-
Products storage	-
Products evacuation from the refinery	Products evacuation from the refinery

From the daily 70 bbls crude oil processing, the estimated total VOCs emissions in the artisanal refineries are 0.0098 – 8.120 kg/day with total of 24.7898 kg/day but from the 360 bbls/day processing, these VOCs emissions are 0.0504 – 41.7600 kg/day with 127.4904 kg/day as total (Table 7). In the two daily crude oil processing handling rates, the minimum and maximum VOCs emissions are from products cooling and crude transfer respectively. Though tapping installation, oven heating and crude boiling as well as product storage are also major sources of VOCs emissions in the artisanal refineries, lack of emission factors for these activities made impossible for the emissions levels determination in this study.

Table 7: VOCs Emissions from Typical Nigeria's Artisanal Refineries

Sources	Emissions (kg/day)	
	From 70 bbls/day	From 360 bbls/day
Tapping installation	-	-
Tapping point operation	8.12	41.76
Crude transfer to the Refinery	8.12	41.76
Crude Storage	0.308	1.584
Crude Transfer to the Oven	8.12	41.76
Oven heating		-
Crude boiling		-
Products cooling	0.0098	0.0504
Products collection	0.056	0.288
Products storage		-
Products evacuation from the refinery	0.056	0.288
Total	24.7898	127.4904

Splash loading VOCs emission factor = 580 mg/L transferred (Table 5.2-5 AP-42); AGO 4 mg/L transferred; Cooling tower 0.7 kg/10⁶ L cooling water (Table 5.1-2); VOC from crude oil storage tanks 0.022 kg/day/m³ of stored crude (NPI, 2013)

Since these estimated VOCs emissions are fugitive in nature, they will be difficult to control in the artisanal refineries due to the nature of their operations which make it difficult for them to be properly organised. Implementing any control technology in their present form will be

difficult to achieve if not impossible though this is needed to reduce the present levels of VOCs emissions (Figure 5).
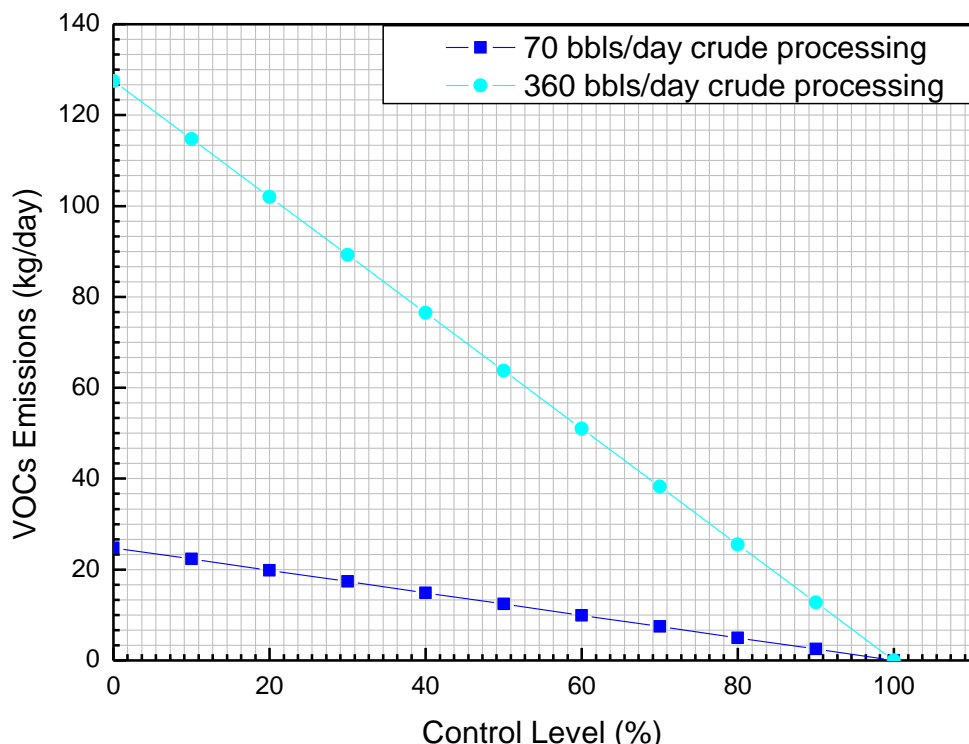

Fig. 5: VOCs Control Implementation in the Nigeria's Artisanal Refineries

For example, tapping points are operated under fear of being caught by regulator thus being carried out without any adequate precaution to prevent VOCs emissions. Crude transfer to the refinery is also done in not too different an atmosphere from tapping point operations. Crude storage in these refineries are being carried out in storage tanks not properly designed for this purpose. Though an activity of this nature in the refinery will require the use of fixed or floating roof storage tanks, the unconventional tanks employed in these refineries as earlier identified during technical review of the processes suggests that VOCs emissions from storage activities in the artisanal refineries will be difficult to accomplish. The present form of products collection and evacuation supports product agitation and unguarded exposure thus subjecting them to conditions that will encourage VOCs emissions from such activities.

Except manual execution of these two activities are discontinued, their control will not be achieved. However the nature of operations in these refineries indicates that except the operators of the refineries are educated on the danger associated with their present approach, the manual products collection and evacuation will be sustained.

As presented in Table 8, the current destruction method of Nigeria's artisanal refineries by the regulators indicates the presence of emissions of combustion products including CO, NO_X, and VOCs whenever any of these refineries are destroyed through burning. From a typical refinery handling 70 bbls of crude oil per day, the estimated levels of combustion products are 36.5 – 219.2 kg/day with a total of 300 kg/day but 187.9 – 1127.5 kg/day with a total of 1547.2 kg/day from those handling 360 bbls/day (Table

8). While the minimum emission is from NO_X the maximum is from CO.

Table 8: Air Emissions from Nigeria's Artisanal Refineries Destruction by JTF (kg)

Pollutants	Emission Factor*	Emissions (kg/day)	
		From 70 bbls/day Processing	From 360 bbls/day Processing
CO	18 kg/ton	219.2	1127.5
NO_X	3.7 kg/ton	45.1	231.8
VOCs	3 kg/ton	36.5	187.9
Total		300.8	1547.2

*Source: NPI (2013)

From the artisanal refineries destroyed between July and December 2012, emissions of CO into the ambient environment were 218761.6 - 1617257.6 kg/month while NO_X and VOCs were 45009.8 - 332747.8 kg/month and 36427.0 - 269297.0 kg/month respectively (Table 9). If these refineries daily handle 360 bbls, the emitted CO, NO_X and VOCs during the destruction by the regulators were 1125265.0 - 8318842.6 kg/month, 231304.5 - 1709984.3 kg/month and 187544.2 - 1386473.8 kg/month respectively (Table 9).

Table 9: Air Emissions from Destroyed Illegal Refineries between July – December, 2012 (kg)

Month	Average Destroyed	From 70 bbls/day Processing			From 360 bbls/day Processing		
		CO	NO_X	VOCs	CO	NO_X	VOCs
July	1157	253614.4	52180.7	42230.5	1304540.6	268155.6	217423.4
August	1209	265012.8	54525.9	44128.5	1363171.7	280207.5	227195.3
September	1034	226652.8	46633.4	37741.0	1165855.7	239648.1	194309.3
October	998	218761.6	45009.8	36427.0	1125265.0	231304.5	187544.2
November	1546	338883.2	69724.6	56429.0	1743145.9	358313.3	290524.3
December	1434	314332.8	64673.4	52341.0	1616863.7	332355.3	269477.3
Total	7378	1617257.6	332747.8	269297.0	8318842.6	1709984.3	1386473.8

Conclusion and Recommendations

The locations of Nigeria's artisanal petroleum refineries have been identified in this study with technical review of their processes undertaken. Life cycle analysis was then carried out to evaluate their air quality impacts. The study confirms they are located in the creeks, forest and villages in the oil producing areas of Niger Delta where crude oil tapping operation points and water are easily accessed. Operations of the refineries severely impair air quality. Emissions of VOCs from daily 70 bbls crude oil processing in these refineries are 0.0098 – 8.120 kg/day with total of 24.7898 kg/day but from the 360 bbls/day processing, they are 0.0504 – 41.7600 kg/day with 127.4904 kg/day as total. It also shows that the presently adopted approach by the regulators to control operations of the artisanal petroleum refineries damages air quality of their environment more than what the refining process does. From 70 bbls/day crude oil processing, the estimated levels of combustion products including CO, NO_X and VOCs are 36.5 – 219.2 kg/day with a total of 300 kg/day but 187.9 – 1127.5 kg/day with a total of 1547.2 kg/day from those handling 360 bbls/day. From the artisanal refineries destroyed between July and December 2012 with daily 70 bbls crude oil processing, emissions of CO into the ambient environment were 218761.6 - 1617257.6 kg/month while NO_X and VOCs were 45009.8 - 332747.8 kg/month and 36427.0

- 269297.0 kg/month respectively. If these refineries daily handled 360 bbls, the emitted CO, NO_X and VOCs during the destruction by the regulators were 1125265.0 - 8318842.6 kg/month, 231304.5 - 1709984.3 kg/month and 187544.2 - 1386473.8 kg/month respectively.

For air quality degradation effects of these artisanal refineries to be immediately arrested, it is recommended that efforts are made by every stakeholder including the Nigerian Society of Chemical Engineers (NSChE) to open a line of communication with the regulators on how these refinery sites can be accessed for air quality assessment. Also, there is the immediate need for technical evaluation of these artisanal refineries

adopted processes to identify the areas necessary for improvement so that the intended fractional distillation of crude oil by the refineries operators can be accomplished with ease and reasonable level of certainty. To achieve this, the stakeholder may want to consider the option of legalising the artisanal refineries if only for the environmental benefit. Organising the operators into cooperative societies would have been an option to give them ease of access to crude oil. The release of initial seed money for crude oil acquisition by the Federal, State or Local Governments may be a way to open up the sector for the necessary reformation. The Ministry of Niger Delta Affairs, the Niger Delta Development Commission (NDDC), the Niger Delta Amnesty Programme (NDAP) and relevant non-governmental organizations (NGOs) may be very useful on this. This is because most of the artisanal refineries buy the crude oils processed in the refineries and if credible alternative sources can be provided with the necessary support, it may not be too difficult to open up the sector for the necessary reforms that will be beneficial to the environment.

References

Abila, N. (2015). Econometric Estimation of the Petroleum Products Consumption in Nigeria: Assessing the Premise for Biofuels Adoption. *Renewable Energy, 74*, 884 - 892.

ABS (2014). Annual Bureau of Statistics. *Federal Office of Statistics, Abuja. Nigeria*, 169 pp.

Anejionu, O. C. D., Ahiarammunnah, P. O. N., and Nri-ezedi, C. J. (2015). Hydrocarbon pollution in the Niger Delta: Geographies of impacts and appraisal of lapses in extant legal framework. *Resources Policy, 45*, 65 - 77.

Attah, T. (2012). Oil theft and artisanal (illegal) refining in Nigeria – scale, impacts and the need for a multi-dimensional response. *Chatham House – Gulf of Guinea Security Conference*, 7

FMEnv. (2014). Nigeria: Fifth National Biodiversity Report. Federal Ministry of Environment, Abuja. 58.

HEDA. (2015). Communities, Not Criminals. *HEDA Resource Centre, Human and Environmental Agenda,* [www.hedang.org/ouroilourcurse](Accessed July 25, 2015).

ISO. (2000). Environmental management — Life Cycle Assessment — Life Cycle Impact Assessment. *International Organization for Standards, ISO 14042:2000 (E)*, 15.

ISO. (2000a). Environmental management — Life cycle assessment — Examples of application of ISO 14041 to goal and scope definition and inventory analysis. *International Organization for Standards, ISO 14049:200 (E)*.

ISO. (2006). Environmental management — Life cycle Assessment — Principles and Framework. *International Organization for Standards*, ISO 19011:12006 (E).

Isumonah, V. A. (2015). Minority political mobilization in the struggle for resource control in Nigeria. *The Extractive Industries and Society, Accepted*, 9.

MoD. (2013). Brief for Ministerial Platform on the Activities and Programmes of the Ministry of Defence from June 2012 to Date. *Nigeria's Federal Ministry of Defence, Abuja*, 167.

Moon, Y. S. (1997). The Outlook of the Korean Petroleum Industry and its Deregulation Process. *Energy Policy, 25*(12), 983 – 988.

Naanen, B., and Tolani, P. (2014). Private Gain, Public Disaster: Social Context of Illegal Oil Bunkering and Artisanal Refining in the Niger Delta. *Niger Delta Environment and Relief Foundation (NIDEREF), Port Harcourt, Nigeria*, 123.

Nkaginieme, U. (2012). Challenges of Building a New Private Refinery in Nigeria: Licensees Experience So Far. *Proceedings of the Nigerian Refining Capacity Summit Organized by the House of Representatives Committee on Petroleum Resources (Downstream), March 28th – 29th, 2012*.

NNPC. (2014). NNPC Annual Statistical Bulletin. *Nigerian National Petroleum Corporation, Abuja*, 52.

NPI. (2013). National Pollutant Inventory: Emission Estimation Technique Manual for Oil and Gas Extraction and Production Version 2.0. *Australian Government Department of Sustainability, Environment, Water, Population and Communities. Commonwealth of Australia, Canberra, Australia*, 36 pp.

Obenade, M., and Amangabara, G. T. (2014). The Socio-Economic Implications of Oil Theft and Artisanal Refining in the Niger Delta Region of Nigeria. *International Journal of Science and Research, 3*(7), 2390 - 2394.

Siddig, K., Anguiar, A., Grethe, H., Minor, P., and Wahmsley, T. (2014). Impacts of Removing Fuel Subsidies in Nigeria on Poverty. *Energy Policy, 69*, 165 - 178.

SocialAction. (2014). Crude Business: Oil Theft, Communities and Poverty in Nigeria. Social Development Integrated Centre. *Port Harcourt*, 69 pp.

Unachukwu, E. (2012). Reducing Dependence on Imported Fuel through Promotion and Investment in Small and Medium Scale Refineries. *Proceedings of the Nigerian Refining Capacity Summit Organized by the House of Representatives Committee on Petroleum Resources (Downstream), March 28th – 29th, 2012*, 23pp.

UNEP. (2011). Environmental Assessment of Ogoniland. *United Nations Environment Programme, Nairobi, Kenya*, 257 pp.

WorldBank. (2015). Nigeria: Country at a Glance. *The World Bank Washington DC, USA*, 32.

P 003

DEMULSIFICATION OF CRUDE OIL EMULSION USING BLEND OF TRIETHANOLAMINE AND PROPAN-2-OL

*[1]Akinyemi O.P., [2]Udonne J.D., [3]Oyedeko K.F.K.

[1,2,3]Chemical and Polymer Engineering Department, Lagos State University, Epe Campus, Lagos
*poakinyemi@yahoo.com; [2]udonne.joseph@gmail.com; [3]kfkoyedeko@yahoo.com

Abstract

For economic and operational reasons, it is necessary to separate the water completely from the produced crude oil i.e. the water/crude oil emulsions have to be broken (demulsified). The effect of blends of triethanolamine (TEA) and propan-2-ol on crude oil emulsions were assessed experimentally via centrifugation at different revolution per minute (RPM). It was observed that appropriate blending of TEA with propan-2-ol will enhance its performance as a demulsifier. About 33.3% blending of TEA with propan-2-ol could double the performance of TEA as demulsifier of crude oil emulsions.
Keywords: *Triethanolamine (TEA), propan-2-ol, emulsions, demulsifiers, water separation*

1.0 Introduction

Water-in-oil emulsions may be encountered at all stages in the petroleum production and in the processing industry. The presence of water in crude oil is typically undesirable and can result in high pumping costs and pipeline corrosions as well as increase in the cost of transportation. Water must be removed (to a level of <1%), in a process that is usually called demulsification or dehydration (Wang, *et al,* 2012). This consists of process forces coalescence of water droplets and producing their separation by settling. The droplets in emulsion are stabilized by the asphaltene and resin fractions of the crude oil (Rondon, *et al,* 2006). There are other numerous parameters that contribute to the stability of the interfacial film and as a result to emulsion stability, such as water pH and the additive content (Poteau *et al*., 2005; Fortuny *et al*., 2007; Al-Sabagh, et al, 2012; Daaou and Bendedouch, 2012), but these effects show different behavior for various oil origins (Pathak and Kumar, 1995). For example, Daaou and Bendedouch (2012) studied the effect of pH on Algerian crude oil emulsions and suggested that a neutral medium is more efficient than an acidic or basic environment for stabilizing the emulsions. Fortuny *et al*. (2007) studied the effects of salinity, temperature, water content and pH on the stability of crude oil emulsions based on microwave treatment and showed that, in emulsions containing high water contents, the rate of demulsification is high, except when high pH and salt content were simultaneously involved. Additionally, Moradi *et al*. (2011) studied the impact of salinity on crude oil/water emulsions by measuring the droplet-size distribution visualized by an optical microscopy method, and found that emulsions are more stable at lower ionic strength of the aqueous phase.

On the other hand, demulsifiers are organic molecules which when dissolve in emulsion at low concentration have the ability to adsorb and locate at the interfaces of droplets in emulsion (Udonne, 2012). To choose the most effective demulsifiers, a screening process involving the price of demulsifiers should be considered. Hajivand and Vaziri (2015) investigated the influence of a wide range of chemical demulsifiers on destabilization of the emulsion and observed that triethanolamine was one of the effective demulsiifer for the emulsions tested, more effective than urea, but could not perform as others. This study is therefore designed to investigate the possibility of improving the performance of triethanolamine as demulsifier using alcohol and formulate a cheaper demulsifier for water-in-oil emulsion in crude oil production.

2.0 Materials and Methods

Crude oil emulsions used for these sets of experiments were obtained from two fields in Niger Delta region of Nigeria and the chemicals used were analytical reagent grade of triethanolamine (TEA) and propan-2-ol obtained from BDH Chemical Ltd, Poole England. The experiments were carried out using bottle test method as described by Udonne (2012). In the first experiment, 20ml of the emulsion samples were measured into the four centrifuge cups and inserted into the centrifuge. The centrifuge was set at 2000rpm and was allowed to run for 5mins and 10mins. The water separation was recorded for pure sample without demulsifier. The experiment was repeated for the two samples without demulsifier at 3000rpm within the same range of time and water separated recorded. The second set of experiments were carried out at 2000rpm and

3000rpm for 5mins using pure triethanolamine (TEA) and pure propan-2-ol as demulsifiers with doping ratio of 0.5%v/v, 1.0%v/v, 1.5%v/v, 2.0%v/v, 2.5%v/v for demulsifier in the emulsion. The mixture of triethanolamine and propan-2-ol were prepared in ratio 1:1 and 2:1 (TEA to propan-2-ol) by volume. The resulting mixtures were used to dope the crude oil emulsions as demulsifiers at ratio of 0.5%v/v, 1.0%v/v, 1.5%v/v, 2.0%v/v, 2.5%v/v. The third sets of experiment were carried out using the blends of TEA and propan-2-ol following the previous procedure and water separation recorded.

The water separation percentage (V%) was determined using

$$V\% = \frac{Vol.\ of\ water\ separated\ (v_2)}{vol.of\ crude\ oil\ emulsion\ (v_1)}\ x\ 100 \qquad (1)$$

3.0 Results and Discussion

The results obtained showed that water-in-oil in the undoped crude oil samples could not be separated by ordinary centrifugal agitation (Table 1). Pure triethanolamine displayed better performance as emulsion breaker over propan-2-ol as shown in Tables 2 and 3. For higher RPM operation of the centrifuge each of the demulsifier performed better on the samples tested. Also, the results showed that appreciable quantities of pure demulsifier are required to separate

Table 1. Performance of Emulsion samples without addition of demulsifier

RPM	Time (mins)	Emulsion (ml)	Water separation (%v/v) Sample A	Sample B
2000	5	20	0.0	0.0
	10	20	0.0	0.0
3000	5	20	0.0	0.0
	10	20	0.0	0.0

Table 2. Effects of Pure Chemical additives on the crude oil emulsion for sample A

Quant-ity of demulsi fier (%v/v)	Emul sions (ml)	Water separation % for 2000RPM		Water separation % for 3000RPM	
		TEA	Propan -2-ol	TEA	Propa n-2-ol
0.5	20	1	-	1.50	-
1.0	20	2	-	3.00	-
1.5	20	3	0.6	6.00	1.00
2.0	20	4	0.6	6.25	1.00
2.5	20	5	0.75	6.25	1.25

reasonable quantity of water from the emulsions of the samples studied. For instance only 5% of water could be separated by 2.5%v/v of TEA at 2000RPM in sample A while similar percentage of propan-2-ol could only separate 0.75%v/v (Table 2). For sample B, 3.5% water was separated from the emulsion by 2.5% TEA at 2000RPM spin of the centrifuge while propan-2-ol could not break-out any water from the sample at the same revolution (Table 2). Thus, TEA acted as an effective demulsifier for both samples to certain extent which is in agreement with the observation of previous researches (Hajivand and Vaziri, 2015).

Table 3. Effects of Pure Chemical additives on the crude oil emulsion for sample B

Quant-ity of demulsi fier (%v/v)	Emul sions (ml)	Water separation % for 2000RPM		Water separation % for 3000RPM	
		TEA	Propan -2-ol	TEA	Propa n-2-ol
0.5	20	-	-	0.10	-
1.0	20	-	-	0.25	-
1.5	20	-	-	3.00	0.05
2.0	20	3.0	-	3.50	0.25
2.5	20	3.5	-	3.75	2.25

Blend of TEA with propan-2-ol improve its performance as the demulsifier as indicated by Figures 1 to 4. The results indicate that there is better level of separation when about 33.3% of the TEA-propan-2-ol mixture is made up of propan-2-ol (2:1). The improvement is about 100% for sample A (see Figures 1 and 2). The propan-2ol may have increased the Hydrophile-Lipophile Balance (HLB) of the triethanolamine and eventually increased its potency as a demulsifiers. The

increased in HLB enabled the demulsifier blend to migrate faster toward the interface and formed a continuous hydrophilic pathway existing between the dispersed water droplets. This leads to a rupture of the interfacial oil film surrounding the water droplets. This corroborate the findings of Al-Sabagh *et al*. (2012) which noted that the higher the HLB, the higher the demulsification efficiency of a demulsifier. It also gives credence to the fact that alcohol as a modifier helps demulsification process (Hajivand and Vaziri, 2015). In addition, the demulsifier blend may have altered significantly the physical properties of the interfaces. The adsorption and location behaviors can be attributed to the emulsion nature and the chemical structure of demulsifier combined both a polar and a non-polar group into a single molecule. To accommodate for dual nature, molecules of the blended demulsifier adsorb and locate at interfaces so that the polar groups remain in the water while the non-polar groups in crude oil (Al-Sabagh *et al*., 2012).
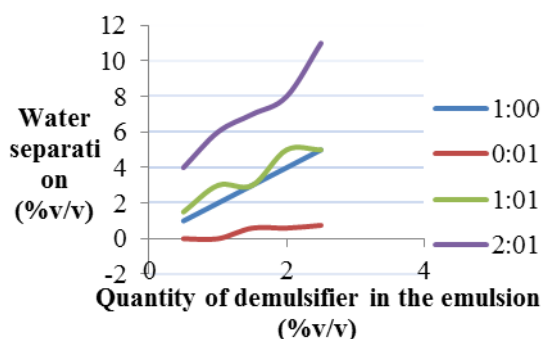
Figure 1. Effects of demulsifiers and their blends on Sample A at 2000RPM and 5mins
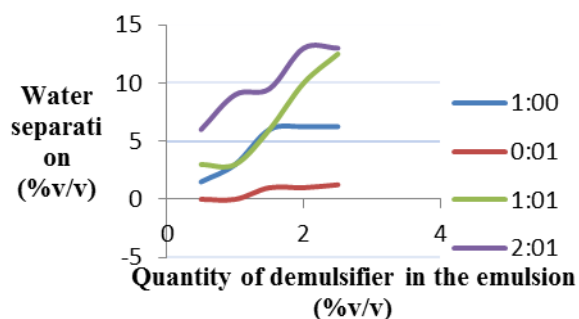
Figure 2. Effects of demulsifiers and their blends on Sample A at 3000RPM and 5mins

A look at the performance of the blend on sample B (see Figures 3 and 4) showed similar trend as that of sample A. Greater performance of the blends were obtained with 3000RPM spin of the samples. Thus, the
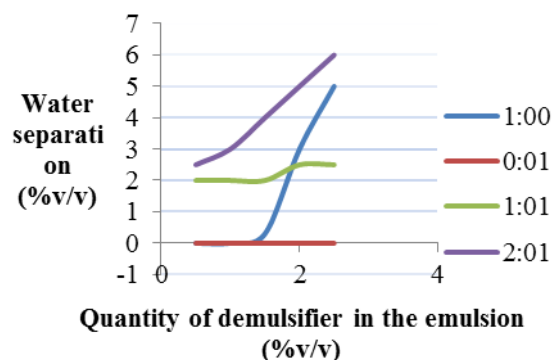
Figure 3. Effects of demulsifiers and their blends on Sample B at 2000RPM and 5mins

higher spinning of the centrifuge enhance better performance of the blend of the additives. This gives credence to the findings of Udonne (2012) that higher spin can increase the emulsion breaking.

The comparison of the performance of the pure demulsifiers and their blends on sample A of the crude oil emulsions as shown by Figures 1 and 2, shows that the performance of the TEA in breaking the water-in-oil emulsion was greatly improved by blending it with small quantity of the propan-2-ol especially at 2000RPM spin of the centrifuge. It was also observed
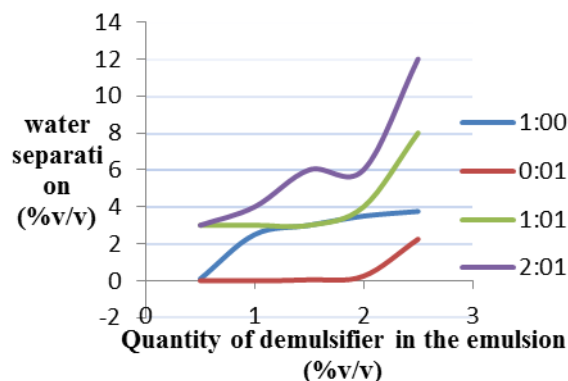

Figure 4. Effects of demulsifiers and their blends on Sample B at 3000RPM and 5mins

that demulsifier formed by 50% blending of TEA with propan-2-ol (1:01) exhibit virtually similar performance on sample A as pure TEA (see Figure 1). It is very likely that a little quantity of propan-2-ol added to the TEA was able to increase its ionic strength to the level required to separate the polar component of the emulsions and as well provide more aliphatic ends to interact with the non-polar component of the crude oil thereby enhancing more separation of the water.

4.0 Conclusion

Two crude oil emulsions sample were investigated for performance of triethanolamine blend with with propan-2ol

as demulsifiers. Triethanolamine can act as an effective demulsifier to a certain extent. In the study conducted on samples A and B, propan-2-ol though displayed low performance as demulsifier on the samples but when combined with triethanolamine in appropriate proportion improved the performance of TEA as demulsifier. Blend of TEA with 33.3% by volume of propan-2-ol will significantly increase the performance of TEA.

5.0 REFERENCES

Al-Sabagh A. M., Nasser N. M. and Khamis E. A (2012). Demulsification of Crude Oil Emulsions Using Ethoxylated Aliphatic Amine Polyesters as Novel Demulsifiers. *International Journal of Science and Research*: 2319-7064 Impact Factor: 3.358

Daaou, M. and Bendedouch, D. (2012) Water pH and surfactant addition effects on the stability of an Algerian crude oil emulsion. *Journal of Saudi Chemical Society*, 16, 333-337

Fortuny, M., Oliveira, C. B. Z., Melo, R. L. F. V., Nele, M., Coutinho, R. C. C. and Santos, A. F. (2007). Effect of salinity, temperature, water content, and pH on the microwave demulsification of crude oil emulsions. *Energy Fuels*, 21, 1358-1364.

Hajivand P. and Vaziri A. (2015). Optimization of Demulsifier Formulation for Separation of Water from Crude Oil Emulsions. *Brazilian Journal of Chemical Engineering* Vol. 32, No. 01, pp. 107 - 118,

Moradi, M., Alvarado, V., and Huzurbazar, S., (2011). Effect of salinity on water-in-crude oil emulsion: Evaluation through drop-size distribution proxy. *Energy & Fuels*, 25, 260-268.

Pathak, A. K. and Kumar, T., (1995). Study of indigenous crude oil emulsions and their stability. In: Proceedings of PETROTECH-95, the First International Petroleum Conference and Exhibition, New Delhi, January 9-12

Poteau, S., Argillier, J. F., Langevin, D., Pincet, F. and Perez, E. (2005). Influence of pH on stability and dynamic properties of asphaltenes and other amphiphilic molecules at the oil-water interface. *Energy & Fuels*, 19, 1337-1341.

Rondon, M.; Bouriat, P. and Lachaise, J., (2006). Breaking of Water-in-Crude Oil Emulsions. 1. Physicochemical Phenomenology of Demulsifier Action, *Energy & Fuels,* 20 (2006) 1600-1604.

Udonne J. D. (2012). Chemical treatment of emulsion problem in crude oil production. *Journal of Petroleum and Gas Engineering*, Vol. 3(7), pp. 135-141, December 2012

Wang, J. J.; Wang, X. K. and Sha, Z. L. (2012). Demulsification of Crude Oil Emulsion using Propylene Oxide-Ethylene Oxide Block Copolymer. *Advanced Materials Research*, 361-363 598-602.

P 004

CHARACTERIZATION OF THREE NATURAL FIBRES FOR FABRICATING FIBRE REINFORCED POLYMER COMPOSITES

*E.N. Ikezue, O. D. Onukwuli and V. C. Ezechulwu
Chemical Engineering Department
Anambra State University
Uli, Nigeria

*Email address: eddikezue@yahoo.com
Cell Phone: +2348037440725

Abstract:

Three natural fibres okro bast fibre (Hibiscus Esculentus) Banana Pseudo-stem fibre (Musa Acuminata) and Abari Bast fibre (Uremia Lobata) were characterized using the different chemical methods to obtain the various component ie Cellulose, hemicellulose, lignin, water soluble pectin, ash, wax or lipid. These fibres were obtained from plants through retting method and drying after the respective extraction and then chemically treated for five treatment solutions in order to macerate the fibres for their compatibility and bond adhesion with the polymer matrix resin- polyester resin. The result show that Abari fibre has 69.06% cellulose, 12.58% in hemicelluloses 9.96% lignin 2.04% waxes then Okro has 53.54% cellulose 28.94% hemicelluloses 18.22% lignin, banana fibre has 64.10% cellulose 19.19% hemicelluloses 11.22% lignin. This show that Abari fibre has the highest cellulose content followed by banana fibre and then Okro and this will imply that Abari fibre will have the highest mechanical strength.

Keywords: *Natural fibre, mechanical properties, composites, bond adhesion, mercerization, Ligno-cellulosic fibre, biodegradability, moisture sorption.*

Introduction

The structure and chemical make-up of natural fibres varies greatly and depends on the source and many processing variables. However some generalizations are possible. Natural fibres are complex, three dimensional, polymer composites made primarily of cellulose, hemicelluloses, pectins and lignins. These hydroxyl-containing polymers are distributed through the fibre wall. The major chemical components of selected natural fibres are listed in the table 1 below;

Table 1.0: Chemical Composition (5) of Selected Natural Fibres

Species	Cellulose	Ligning	Pectin
Flax	65-85	1-4	5.12
Kenaf	45-57	8-13	3.5
Sisal	50-64	-	-
Jute	45-63	12-25	4-10
Bamboo	40-50	20-30	0-1
Coir	40-45	34-36	0-1

of the three major components, cellulose shows the least framework components of the fibre, it is a highly crystalline, linear polymer of anhydroglucose molecules with a degree of polymerization (n) of around 10,000; it is the main component providing the strength, stiffness and structural stability. Hemicelluloses are branched polymers containing five and six carbon sugars of varied chemical structure, the molecular weights of which are well below those of cellulose but which still contribute as a structural component of wood. Portions of the hemicelluloses are polymers of five-carbon sugars and are called pentosans (Adil et al 2001)

Lignin is an amorphous, cross-linked polymers network consisting of an irregular array of variously bonded hydroxyl-and methoxy substituted phenlpropane units. The chemical structure varies depending on its source. Lignin is less polar than cellulose and acts as a chemical adhesive within and between fibres (Ayman 2003).

Pectin's are complex polysaccharides, the main chains of which consist of a modified polymer of glycournoic acid and residues of rhamnose. Their side chains are rich in rehamose, galactose and arabinose sugars. The chains are often cross-linked by calcium ions, improving structural integrity in pectin-rich areas. Pectins are important in non-wood fibres, especially bast fibres. The lignin, hemicelluloses, and pectins collectively function as matrix adhesive, helping to hold together the cellulosic frame work structure of the natural composite fibre (Ankit et al 2005).

Natural fibres also contain lesser amounts of additional extraneous components, inducing low molecular

weight organic components (extractives) and inorganic matter (ash). Though often small in quantity, extractives can have large influences on properties such as color, material, such as rice hulls, causes some concern about their abrasive nature.

Mechanical Performance of Natural Fiber

Due to different species, a natural variability within species, and differences in climates and growing seasons, natural fibre dimensions (table 2) as well as physical and mechanical performance can be highly variable. Methods of producing fibres with more reproducible properties are the goal of major research efforts. Most natural fibres have a maximum density of about $1.5gcm^{-3}$. Though some natural fibres such as wood are hollow and have low densities in their native states, they are often densified during processing. Nevertheless, even the maximum density of these fibres is considerably less than that of inorganic fibres such as glass fibres. As such, their low density makes them attractive as reinforcement in applications where weight is a consideration (Tang 1997).

Table 2.0: Dimensions of Selected Natural Fibers

Fibre type	Length (mm)		Width (mm)	
	Average range	Range	Average range	Range
Flax	33	9-70	19	5-38
Hemp	25	5-55	25	10-51
Jute	5	2-6	21	14-33
Sisal	3	1-8	20	8-41
Kenaf	2	2-5	20	10-25
Coir	1	-	-	15-45
Flax	-	3-8	-	15-45

Though variable, high aspect rations are found, especially for flex and hemp. The mechanical performance (table 3) of the fibres is good, but not as good as that of synthetic fibres such as glass. However their densities are considerably lower. The balance of significant reinforcing potential at low cost and low density is part of the reason why they are attractive to industries such as the automotive industry (Bledzki 2007).

Table 3.0: Mechanical Properties of Selected Organic and Inorganic Fibers

Fibre/fibre bundles	Density (gcm^{-3})	Stiffness (Gpa)	Strength (MPa)	Strain
Glass	249	70	2700	-
Kevlar	1.44	124	2800	2.5
Nylon -6	1.15	1.8-23	503-690	17-45
Polypopylene	0.91	1.62.4	170-325	80-100
Flax	1.4	50-70	500-900	1.5-4.9
Hemp	1.48	30-60	300-500	2-4
Softwood	1.4	10-50	100-170	-
Hardwood	1.4	10-70	90-180	-

Moisture and Durability

The major chemical constituents of natural contain hydroxyl and other oxygen-containing groups that attract moisture through hydrogen bonding. The moisture content of these fibres can vary greatly depending on fibre type. The processing of the fibre can also have a large effect on moisture sorption. The table above shows the wide range of moisture contents for different natural fibres at several relative humidity. This hygroscopicity can create challenges both in composite fabrication and in the performance of the end product. If natural fibres are used, a process that is insensitive to moisture must be used or the fibres must be dried before or during processing. Natural fibres absorb less moisture in the final composites since they are at least partially encapsulated by the polymer matrix. However, even small quantities of absorbed moisture can affect performance. Moisture can plasticize the fibre, altering the composites performance. Additionally, volume changes in the fibre associated with moisture sorption can reduce fibre-matrix adhesion and damage the matrix. Method of reducing moisture sorption include (i) adequately dispersing and encapsulating the fibres in the matrix during compounding (ii) limiting fibre content, (iii) improving fibre-matrix bonding, (iv) chemically modifying the fibre, or (v) simple protecting the composite from moisture exposure (Bradshwa 2003).

MATERIALS AND METHOD

The fibres for the bio-chemical analysis were all cut into small strips with razor blade. The strips were small enough to be placed in a Wiley Mill. All of this material was ground in the Wiley Mill. The material was then placed in a shaker with sieves to pass through a No. 40 mesh sieve (425-µm) yet retained on a No. 60 mesh sieve (250-µm). The resulting material was placed in glass jars labeled with appropriate

code for chemical analysis. The grinding process was the same as above described.

All tests were conducted at the polymer laboratory, department of Biochemistry, University of Nigeria, Nsukka under the standards of American Society for Testing and Materials (ASTM) except for alcohol-toluene solubility of fibres and results of the analysis are shown in Table 5. There was a minor modification for extractive content test. Instead of benzene solutions, the exact standard that was followed for each chemical property performed is presented in Table 4.0.

Table 4.0: Standards Followed for Chemical Analysis

S/N	Property	Standard
1.	Alcohol-toluene solubility	ASTMD 1107-56 (Reap proved 1972)
2.	Hot-water solubility	ASTM 1110-56 (Reap proved 1977)
3.	Klason Lignin	ASTMD 1106-56 (Reap Proved 1977)
4.	Holocellulose	ASTMD 1104-56 (Reap Proved 1978)
5.	Alpha-cellulose	ASTMD 1103-60 (Reap proved 1978)
6.	Ash Content	ASTMD 1102-84 (Reap proved 1990)

Each test was conducted using 3 replications. It was necessary to conduct additional experimentation when analyzing for alcohol-toluene extractive content and holocellulose content. The alcohol-toluene test is the starting material for many of the other experiments. Both the lignin and holocellulose content test are performed with extractive-free fibres that is derived from the alcohol-toluene extractive test. Additionally, holocellulose is a necessary preparatory stage in order to determine alpha-cellulose content (Do Masden 2004).

Alcohol-Toluene Solubility of Fibres

The extraction apparatus consisted of a soxhlet extrication tube connected on the top end of a reflux condenser and joined at the bottom to a boiling flask. A two-gram oven-dried sample was placed into a cellulose extraction thimble. The thimble was plugged with a small amount of cotton and placed in a soxhlet extraction tube. The boiling flasks contained a 2:1 solution of 95 percent ethyl alcohol and distilled toluene respectively and were placed on a heating mantle. The extraction was conducted for eight hours at the rate of approximately six siphoning per hour.

When the extraction was completed, all of the remaining solution was transferred to the oiling flask which was heated on a heating mantle until the solution was evaporated. The flasks were oven-dried at $103+2^0$C, cooled in a desiccator, and weighed until a constant weight was obtained.

The following formula was used to obtain the alcohol-toluene solubility content of fibres:
Alcohol – toluene solubles (percent
$[W_2/W_1]$ x10   [1]
Where,
W_1 = weight of oven-dry test specimen (grams).
W_2 = weight of oven-dry extraction residue (grams).

A minor change was made since it was necessary to conduct additional experiments in order to provide sufficient extractive-free fibres for other chemical property experiments. Therefore, the sample size was increased to 20 grams and the extraction time to forty-eight hours.

Hot-Water Solubility of Fibres

A two-gram sample was oven-dried and placed into a 250ml Erlenmeyer flask with 100ml of distilled water. A reflux condenser was attached to the flask and the apparatus was placed in a gently boiling water both for three hours. Special attention was given to insure that the level of the solution in the flask remained below that of the boiling water. Samples were then removed from the water bath and filtered by vacuum suction into a fritted glass crucible of known weight. The residue was washed with hot tap water before the crucibles were oven dried at $103+2^0$C. Crucibles were then cooled in a desiccators and weighed until a constant weight was obtained.

The following formula was used to obtain the hot-water solubility of fibres:
Hot-water soluble (percent)
$[W_2/W_1]$ x 100   [2]
Where,
W_1 = Weight of oven-dry test specimen (grams).
W_2 = weight of oven-dry specimen after extraction with hot water (grams).

Klason Lignin in Fibres

A one-gram, oven-dried sample of extractive-free fibres was placed in a 150ml beaker. Fifteen ml of cold sulfuric acid (72 percent) was added slowly while stirring and mixed well. The reaction proceeded for two hours with frequent stirring in a water bath maintained at 25^0C. When the two hours had expired, the specimen was transferred by washing it with 560 ml of distilled water into a 1,000 ml flask, diluting the concentration of the sulfuric acid to three percent.

An allihn condenser was attached to the flask. The apparatus was placed in a boiling water bath and the insoluble material was allowed to settle. The contents of the flasks were filtered by vacuum suction into a fritted-glass crucible of known weight. The residue was washed free of acid with 500ml of hot tap water and then oven-dried at 103 ± 2^0C. Crucibles were then cooled in a desiccators and weighed until a constant weight was obtained.

The following formula was used to obtain the lignin content of fibres:

Klason lignin content in fibres (percent) = $[(W_4-W_3)/(100-W_2] \times (100-W_1)$ [3]

Where,

W_1 = alcohol-toluene extractive content (grams).

W_2 = weight of oven-dry extractive-free sample (grams).

W_3 = Weight of oven-dried crucible (grams).

W_4 = Weight of oven-dried residue and crucible (grams)

Holocellulose in Fibres

A two-gram sample of oven-dried extractive-free fibres was weighed and placed into a 250ml flask with a small watch glass cover. The specimen was then treated with 150ml of distilled water, 0.2ml of cold glacial acetic acid, and one gram of $NaClO_2$ and placed into a water bath maintained between 70^0C-80^0C. Every hour for five hours 0.22ml of could glacial acetic acid and one gram of $NaClO_2$ was added and the contents of the flask were stirred constantly. At the end of five hours, the flasks were placed in an ice water bath until the temperature of the flasks was reduced to 10^0C.

The contents of the flask were filtered into a coarse porosity fritted-glass crucible of known weight. The residue was washed free of ClO^2 with 500ml of cold distilled water and the residue change color from yellow to white. The crucibles were then over-dried at 103 ± 2^0C, then cooled in a desiccators, and weighed until a constant weight was reached.

The following formula was used to determine the holocellulose content in fibres:

Holocellulose content in fibres (percent) = $[(W_4-W_3)/(100-W_2) \times (100-W_1)$ [4]

Where,

W_1 = alcohol-toluene extractive content (grams).

W_2 = weight of oven-dry extractive-free sample (grams).

W_3 = Weight of oven-dried crucible (grams).

W_4 = Weight of oven-dried residue and crucible (grams).

Alpha-Cellulose in Fibres

A three gram oven-dried sample of holocellulose was placed in a 250ml Erlenmeyer flask with a small watch glass cover. The flasks were placed into water bath that was maintained at 25^0C. The sample was then treated with 50ml of 17.5 percent NaOH and thoroughly mixed for one minute. After the specimen was allowed to react with the solution for 29 minutes, 50ml of distilled water was added and mixed well for another minute. The reaction contained for five more minutes.

The contents of the flask were filtered by aid of vacuum suction into a fritted glass crucible of known

weight. The residue was washed first with 50ml of 8.3 percent NaOH, then with 40ml of 10 percent acetic acid. The residue was washed free of acid with 1,000 ml of hot tap water. The crucible was oven-dried in an oven at 103 ± 2^0C, then cooled in a desiccator, and weighed until a constant weight was reached.

The following formula was used to obtain the alpha-cellulose content in fibres:

Alpha-cellulose (percent) = $[(W_4-W_3)/(100-W_2] \times W_1$

[5]

Where,

W_1 = Holocellulose content (percent).

W_2 = weight of oven-dry holocellulose sample (grams).

W_3 = Weight of oven-dried crucible (grams).

W_4 = Weight of oven-dried residue and crucible (grams)

Ash Content in Fibres

Ignite an empty crucible and cover in the muffle at 600^0C, cool in a dessicator, and weight to the nearest 0.1mg. Put about 2 gram sample of air-dried fibres in the crucible, determine the weight of crucible plus specimen, and place in the drying oven at 103 ± 2^0C with the crucible cover removed. Cool in a desiccators and weight until the weight is constant. Place the crucible and contents in the muffle furnace and ignite until all the carbon is eliminated. Heat slowly at the start to avoid flaming and protect the crucible from strong drafts at all times to avoid mechanical loss of test specimen. The temperature of final ignition is 580^0C to 600^0C. Remove the crucible with its contents to a dessicator, replace the cover loosely, cool and weight accurately. Repeat the heating for 30 min periods until the weight after cooling s constant to within 0.2mg.

The following formula was used to obtain the ash content in fibres:

Ash content (percent) = $[W_2/W_1] \times 100$ [6]

Where,

W_1 = Weight of ash (grams).

W_2 = weight of oven-dry sample (grams).

The effects of age, height, layer on fibres chemistry were evaluated by analysis of variance at the 0.05 level of significance.

Table 5.0: Chemical Composition of Fibres

S/N	Fibres	Cellulose (%w/	Hemicellulose	Lignin (Klason	Cellulose (%	Wxes	Ash

		w)	(%w/w)	(%w/w)	/Lignin ratio	w/w)
1.	Banana	64.10 ±0.33	19.10 ±0.66	11.22 1±0.20	>2.0	-	-
2.	Okro	53.54 ±0.03	28.94 ±0.04	18.22 ±0.71	>2.0	-	-
3.	Abari	69.06 ±0.03	12.58 ±0.04	9.96.2 2±0.7	>2.0	2.04	-

Results and Discussion

From the results shown in table 5, we could observe that the lignin content of okro bast fibre is the highest showing that it will be more susceptible to bio degradiability and it's moisture absorbing capacity will be higher than the other two fibres. Also the Abari fibre has the highest cellulose content making it more acceptable as a reinforcing agent for fabricating polymer composites.

Natural fibres absorb less moisture in the final composites since they are at least partially encapsulated by the polymer matrix. However, even small quantities of absorbed moisture can affect performance. Moisture can plasticize the fibre, altering the composites performance. Additionally, volume changes in the fibre associated with moisture sorption include (i) adequately dispersing and encapsulating the fibres in the matrix during compounding (ii) limiting fibre content, (iii) improving fibre-matrix bonding, (iv) chemically modifying the fibre, or (v) sample protecting the composite from moisture exposure (Ching et al 2005).

REFERENCES

Adil A.L. – Mayah, Khaled A. Soudki Alan Plumtree (2001). Experimental and Analytical Investigation of a stainless steel anchorage for CFRP prestressing tendons. *PCI Journal* Pp 88-100 vol. 8 No 1 (2001).

Anders Carolin (2003). carbon fibre Reinforced Polymers for strengthening of structural elements. PhD *Thesis in Structural Eng. University of Technology Lulea-Sweden.* http//www.ce.;uth.se/Pp. 1-43.

Anders Carolin (2001) *Strengthening of structures with CFRP* Licentiate thesis in structural Engineering Lulea University of Technology Lulea-Sweden 2001:01 Pp 13-24.

Ayman S. Mosallam, Khalid M. Mosallum (2003). *Strengthening of two way concrete slabs with FRP composite laminates.* Construction and Building materials journal vol. 17 No 1 Pp 43-54.

Antonio Nanni (2004) *Fibre Reinforced Polymer composites for infrastructure strengthening – from research to practice.* Published online pp 3-16.

Ankit Srivastava, Amit Agarwal D. Chakraborty and A. Dutta (2005) Control of Smart Laminated FRP Structures using Artificial Neural Networks *Journal of Reinforced Plastics and composites* vol. 1353 Pp 1353-1364.

Anders Thygesen (2006). *Properties of hemp fibre polymer composites. An optimization of fibre properties using novel defibration methods and fibre characterization* PhD thesis at Royal Agricultural and Veterinary University of Denmark Pp. 23-30.

Arura H., Hopper P., and Dear J.P. (2010). *Impact and Blast Loading of Glass fibre Reinforced Polymer Campsites.* Proceedings of the IMPLAST 2010 conference, October, 12-14 Providence Rhode Island USA Pp 1-10.

Benjamin Tang (1997). *Fibre Reinforced Polymer Composites Applications* in USA-Federal Highway administration workshop proceedings Jan 28-29.

Bo Madsen and Hans Lilholt (2003) *Physical and Mechanical* Properties of unidirectional plant fibre composites an evaluation of the influence of porosity. *Composite science and technology journal* vol. 63 (2003) pp 1265-1272.

Bledzki A.K., Mamum O. Faruk A.A. (2007). Abaca Fibre Reinforced Pp composites and Comparison with jute and flax Pp composites *Express polymer letters* vol. 1. No II pp. 755-762.

Brian S. Hayes and Luther M. Gammon (2010). *Optical microscopy of fibre Reinforced composites* ASM International, the materials information society, materials park Ohid 44073-0002 USA Pp. 3-10.

Bradshwa R.D, F.T, fisher, L.C. Brinson (2003). Fibre waviness in nanotube Reinforced polymer composites – II: modeling via numerical approximation of the dilute

strain concentration tensor. *Composites science and technology Journal* Vol. 63 (2003) Pp. 1705-1722.

Ching Au and Ural Buyukozturk (2005). Effect of fibre orientation and ply mix on fiber Reinforced Polymer confined concrete *Journal of composites for construction* vol. 9, No. 5 Pg 397406.

Do Masden (2004). *Properties of plant fibre Yarn polymer composites, an experimental study*

by G-DTU, Report R-082 Technical University of Denmark Pp. 20-27.

Emmanuelle David, Chafika Djelal, Francois Buyle-Bosin (1998) *Repair and strengthening of reinforced concrete Barns using composite materials* 2ⁿᵈ International PhD symposium in Civil Engineering Budapest Hungary Pp 1-8

P 005

ALTERNATIVE APPROACH TO PINCH ANALYSIS IN THE REVAMP OF REFINERY'S CRUDE DISTILLATION UNIT (CDU)

[1*]Oghenejoboh, K. M and [2]E. O. Ohimor
[1]Department of Chemical Engineering, Delta State University, Oleh Campus, P.M.B 22, Oleh
[2]Department of Chemical Engineering, College of Engineering, Federal University of Petroleum Resources, Ugbomro, Effurun
Corresponding author: kmoghene@yahoo.com; [2]ohimortog@yahoo.com

Abstract:
The primary objective of a crude distillation unit (CDU) revamp is to maximize the use of existing equipment thereby minimizing costs. Minimizing cost requires identifying the flow scheme that will circumvent major unit bottlenecks without compromising reliability and operability. To many, pinch analysis holds the key to better heat management during a major CDU revamp. However, pinch analysis lacks appreciation for the interrelationship between crude unit revamp heat recovery, distillation and crude hydraulic limitations. Practical options to pinch analysis advanced in this study include increasing crude charge rate at constant product yield, increasing heat recovery through product rundown, optimal utilization of existing surface area as well as the modification of the vacuum column from two to three product draws to increase the temperature of the heat available
Key words: *Pinch analysis, refinery, CDU revamps, energy optimization, investment cos*

1.0 Introduction

Refinery's crude distillation unit (CDU) is among the highest consumer of energy as a result of large scale heating and cooling of process stream and equipment. Part of the energy requirement of the CDU is provided for, by integrating the crude with various cuts from the distillation unit in a heat exchanger network known as the pre-heat train. In this era of increasing cost and limited resources, the design of associated heat exchanger networks that will meet the required duties in the CDU had been a major challenge facing process engineers (Sauer, 2000). The objective of an energy efficient heat exchanger network is to satisfy the flow sheet heating and cooling at a minimum total cost (Patwardhan and Ratnam, 1999). This is achieved by an orderly and appropriate arrangement of units in the network by means of pinch analysis (Bassey, 1996). Pinch analysis which was developed based on targeting techniques enables designers to know the minimum energy requirement of a system's heat exchanger network so that the units can be arranged in a controlled and cost effective manner (Linnhoff and Tjoe, 1986). The efficiency of energy recovery in the preheat train of the CDU had improved greatly through pinch analysis (Fraser and Gillespite, 1992; Manjusha et al., 2013). Ogboja and Usman had even reported energy saving of the order of 20-30% through pinch analysis. Pinch analysis becomes inadequate when undertaking a major revamp of the crude distillation unit (CDU) since it relies more on theoretical design without sufficiently considering fouling and operability realities (Barletta and Steve, 2012). CDU revamp becomes necessary when there is need to increase crude charge rate and or to increase product yield and quality. To achieve these revamp objectives, there is need for increased heat input to the crude oil preheat (heat

recovery) and more heater duty. However, this requires an appreciation of the relationship between crude units revamp heat recovery, distillation and crude hydraulic limitations which cannot be adequately address by the use of pinch analysis. In the present study these limitations are analysed.

2.0 CDU Revamp Objectives

It is customary that most refineries' crude distillation units operate far below the designed capacity, especially in Nigeria. This is as a result of improperly executed design work, since most designers focus solely on office-based computer modeling, calculations and equipment specification sheet which do not always provide actual equipment performance. Turn around maintenance for our refineries are generally between seven to eight years or even more, and this long maintenance interval had resulted in lost profits due to poor reliability or unstable operations. Poor reliability and operability have increased unscheduled shutdown to correct revamp design errors.

Crude unit revamp objectives and specific units' constraints will normally differ, however, all crude unit revamps have the same common global limits that must be eliminated. Crude hydraulics, heat input, distillation and heat removal limits are common to all crude unit revamps. The challenge therefore is to determine the appropriate process scheme that will satisfy processing objectives and capital investment criteria, while taking advantage of low cost opportunities resulting from under-utilised equipment (Flower and Linnhoff, 1979). Therefore, revamps include more crude capacity, improved product yields or better product quality. These objectives affect the crude hydraulics, heat input, column performance and heat removal. Increasing crude charge rate as well as product

yield and quality requires more heat input to the crude oil which can only be done by increasing the crude oil preheat resulting in more fired heater duty. Pinch analysis, though effective in improving heat integration in CDU and other chemical processes lacks appreciation for the interrelationship between crude unit revamp heat recovery and crude hydraulics limitations (Linnhoff and Tjoe, 1986; Fraser and Gillespite, 1992; Bassey, 1996; Ogboja and Usman, 1999)

3.0 Practical CDU Revamp Options

Practical solutions require detailed understanding of current bottlenecks and the potential options to be considered given the specific limits. The various practical options available to a CDU revamp engineer, some of which had been implemented with great success by many refineries are discussed below

3.1 Heat Management

One of the major objectives of a CDU revamp is to operate as close as possible to the unit's designed capacity and this requires increasing crude charge rate as well as product yield and quality. Increasing crude charge rate will increase heat inputs at constant product yield, which will invariably lead to increase in product yield by vapourising more crude oil in the vacuum column. Higher heat input can improve product quality through better fractionation (Shirazi et al., 2014). Increasing crude oil heat input by a significant amount without large increase in exchanger surface area minimizes cost and avoids constructability issues.

Heat recovery can be increased if product rundown, condenser and pump-around heat is discarded to air or cooling water if the temperature level is high enough, since product rundown heat below $120^o – 135^oC$ is difficult to recover to crude because the atmospheric column condenser temperatures are typically $120 - 135^oC$ when full range naphtha is the overhead product. Potential pump-around heat sources include light vacuum gas oil (LVGO), air/water loses, heavy vacuum gas oil (HVGO) and other pump-around air/water loses. Heat input and recovery can be increased by judiciously utilizing existing surface area, increasing surface area or shifting product cut-point between atmospheric and vacuum column. Process flow scheme changes that better utilize existing surface area with small piping changes are always the best option for cost consideration. Increasing surface area in the same service does not require process flow scheme change. Diesel and AGO product yield shift between the vacuum and atmospheric columns increases the temperature of the oil from about $135-163^oC$ to $274-360^oC$, thereby increasing the HVGO pump-around temperature while decreasing the LVGO pump-around heat loses to air and water.

Another way of minimizing the exchanger surface area and pump-around circulation rate is to increase the HVGO draw temperature, because the HVGO pump-around is usually the largest heat input to crude oil. The LVGO and HVGO draw temperatures are normally in the range of between $138-160^oC$ and $232-282^oC$ respectively and these sometimes act as feed to the fluid catalytic cracking (FCC) unit. The LVGO pump-around heat is usually discarded to air, cooling water or used for steam generation since it is too low to exchange with crude oil

Modifying the vacuum column from two to three product draws to increase the temperature of the heat available is another viable option that can be exploited. This option reduces the total surface area required for a given heat duty. Moving product draw locations above the pump-around or adding another pump-around lower in the atmospheric column increases heat source temperature and increased pump-around circulation rate will increase exchanger outlet temperature which will invariably raise the exchanger log mean temperature difference (LMTD). In many instances adding a third vacuum product draw and pump-around is significantly cheaper than maintaining two product draws because large temperature shifts can be achieved in the process (Barletta and Martins, 2001; Majumder, 2013). The added pump-around also acts as a heat exchanger in the pre-heat train by providing extra energy integration as well as increasing the cold reflux to the column thereby enhancing better separation (Kamel et al., 2013). Barletta and Martins (2001) illustrated this as shown in Figure 1, where the three product draw temperatures were $104-138^oC$, $232-240^oC$ and $304-321^oC$ respectively. It was noticed that changing both the product draw temperature and the quality of heat available from the middle vacuum gas oil (MVGO) and HVGO pump-around dramatically reduced exchanger surface area, pump-around circulation rate and potential HVGO pump-around piping modifications which led to minimum revamp cost. Unless the revamp engineer is experienced adding a third pump-around will not be identified by a pinch analysis
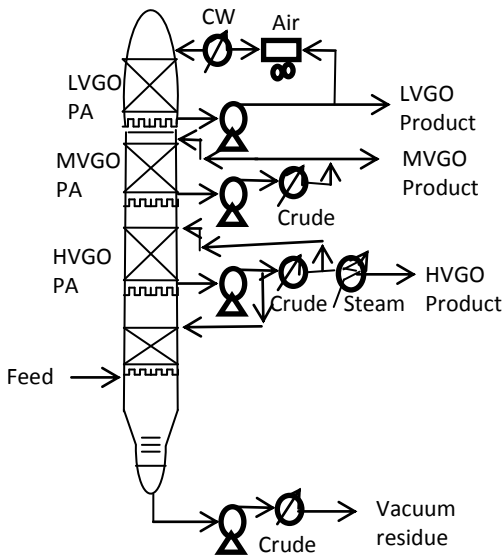
wisdom to have actual performance information on the specific unit being revamped so that prudent investment decision can be made. If there will be need for alternative process flow scheme, this will have to be evaluated based on field data and base-case equipment performance (Karnel et al., 2012). Revamp case process flow scheme and equipment performance modeling are normally done concurrently to establish the direction of a revamp. It is very important to be conscious of the cost of alternative process flow scheme being considered and this require a thorough detailed engineering design otherwise scope growth will occur and it can be significant

A process flow scheme modification that can be used to increase crude charge rate capacity is shown in Figure 2. The flow scheme which was implemented as a revamp option (Barletta and Martins, 2001) required large increase in both pump-around flow rates to meet future operating heat removal needs. Changes include

- Column internals
- Column nozzles
- New piping
- New pumps

The process flow scheme was not changed for this modification and a major scope growth occurred as the engineering works progressed. It is therefore very important not to compromise unit reliability and operability during scope rationalization exercises. Fixed equipment reliability including fixed heaters, heat exchanger networks and distillation equipment will normally determine run length and profitability during operations. It is one thing to target a seven to eight or more years run and it is another to actually achieve it without large economic penalties over long period of time.

Figure 1 Modified three-product column
(Adapted from Barletta and Martins, 2001)

3.2 Minimum Capital Flow Sheet Modifications

Scope growth is a major problem usually encountered during a revamp operation because many companies approach the feasibility stage of design work by focusing solely on office-based computer modeling and calculation sheets which do not always identify the high cost changes that may arise in the course of operation due to actual equipment performance. A major challenge during a CDU revamp is the selection of a minimum capital cost process flow scheme that will provide a balance between the crude charge hydraulics and heat integration. Crude charge system pressure drop depends on accurate prediction of future operations with different exchanger network design. Crude preheat train pressure drop which is a function of exchange fouling and type of fouling cannot be accurately calculated with any exchanger model unless field data is available.

Field pressure measurements should normally be used to adjust the exchanger program calculated pressure drop otherwise revamped unit pressure drop might be under-predicted resulting in a crude charge rate limit. Many a times, office-based rules for exchanger pressure drop are too conservative, leading to high investment cost to eliminate perceived limits that do not exist. It is a course of

Figure 2 Modified three-product column (Adapted from Barletta and Martins, 2001)

3.3 Economics Considerations

The revamp engineer should always be conscious of cost. For cost-effective revamp operations, there will be need to balance the cyclic interaction between crude charge hydraulics, heat input and removal (Sauer, 2000). The dilemma that most revamp engineers usually face is to find a process scheme that meets the flash drum pressure and temperature requirements. The flash drum operating pressure and temperature are variables that depend on the flash drum design. The amount of vapour that leaves the drum as well as the amount of crude that is flashed is a function of these parameters. Hence, the operation of the flash drum is a major factor influencing the system hydraulics. For example, if the revamp objective is to increase the crude charge rate by a fixed percentage, one possibility of achieving that is to move one exchanger from flashed crude to desalted crude service. This will allow the flash drum operating pressure and temperature to be increased to maintain a constant vapour flow rate, thereby maintaining flash crude composition. While this system helps the flashed crude, it can significantly increase the pressure drop through the desalted crude to flash drum system. Desalted crude pumps may be limited, however, they cost less to replace or revamp than flashed crude pumps

4.0 Conclusion

From the discussion above, it is clear that the primary goal of CDU revamp is to maximize the use of existing equipment thereby minimizing investment costs. Therefore effective revamp exercise needs to meet the unit processing objectives and control capital investment and operable design. A perfect design that is never built due to high capital cost will not increase the refiner's profitability, while a low cost design that is not reliable or is difficult to operate can cause an unscheduled shutdowns resulting in serious loses. Pinch analysis, though effective in process heat integration, becomes ineffective in CDU revamps where heat source temperature changes play a vital role in minimizing costs. Heat source temperature changes can be economically handled by increasing the vacuum product draw and pump-around from two to three. In a typical case study, Diesel and AGO product yield shift between the vacuum and atmospheric columns was shown to have increased the temperature of the oil from about 135-163°C to 274-360°C, thereby increasing the HVGO pump-around temperature while decreasing the LVGO pump-around heat loses to air and water while the incorporation of an additional pump-around in the vacuum unit increased the

product temperatures to; 104-138°C, 232-240°C and 304-321°C respectively. It was noticed that changing both the product draw temperature and the quality of heat available from the middle vacuum gas oil (MVGO) and HVGO pump-around dramatically reduced exchanger surface area, pump-around circulation rate and potential HVGO pump-around piping modifications which led to minimum revamp cost. However, adding a third pump-around will not be identified by a pinch analysis unless the revamp engineer is experienced.

References

Barletta T and Martins G (2001) Revamping Conceptual Process Design, Petroleum *Technology Quarterly, Winter* 2001/2002, pp. 41- 46

Barletta T and White S (2012) Designing a Crude Unit Heat Exchanger Network, Sour & Heavy, www.eptq.com Assessed 23/05/2015

Bassey EN (1996) Pinch Method of Synthesis in Improving performance of Process Heat Recovery Network, *JNSChE,* Vol 5 (1), pp. 117-124

Flower JR and Linnhoff B (1979) Using Pinch Technology for Process Retrofit, *JAIChE* 24, pp. 633

Fraser DM and Gillespie NE (1992) The Application of Pinch to Retrofit Energy Integration of an Entire Refinery, *IChE* 70 (A)

Kamel D, Gadalla M and Ashour F (2013) New Retrofit Approach for Optimisation and Modification for a Crude Distillation System, *Chemical Engineering Transactions* 35, pp. 1363-1365

Linnhoff B and Tjoe TN (1986) Using Pinch Technology for Process Retrofit, *Chem. Eng.* 93 (8), pp. 47-50

Majumder K (2013) High-Capacity Tray for Debottlenecking a Crude Distillation Unit, *PTQ (Q 1,* pp.73-75

Manjusha P, Pradyumna S, Dawande SD and Kanse N (2013) Heat Integration of Crude Organic Distillation Unit, *Res. J. Engineering Sci.* 2 (2), pp. 47-50

Ogboja O and Usman MA (1999) Upgrading the performance of the Port-Harcourt Refinery using Pinch Technology, In: Proceedings of the 29th Annual Conf. of NSChE, pp.132-134

Patwardhan VS and Ratnam R (1991) Sensitivity Analysis for Exchanger Networks, *Chem. Eng. Sci.* 46 (2), pp. 456

Sauer R (2000) Low Technology Enhances Reactions Lowering Cost, Improving Yields, *Chemical Processing*, *October,* pp. 53-54

Shirazi L, Babakhani EG and Zamani Y (2014) Feasibility of Revamping of Atmospheric Tower of Refinery, *Petroleum and Coal* 56 (3), pp. 320-321

P 006

USE OF RECYCLE COMPENSATOR CONFERS ROBUSTNESS ON SYSTEMS WITH RECYCLE

*Taiwo, O., Adeyemo, S. O. and Bamimore, A.

Process Systems Engineering Laboratory, Obafemi Awolowo University, Ile-Ife, Nigeria
*femtaiwo@yahoo.com; adeyesam@yahoo.com; ayobamimoreonline@yahoo.com

Abstract:

*The paper brings to bare inherent robustness of recycle compensated plants which are lacking in uncompensated plants. Such plants which have Right Half Plane (RHP) poles in the forward path were considered. Proportional-Integral-Derivative (PID) controllers with set-point filters and two-Degree-of-Freedom (2DoF) Proportional-Integral/Derivative (PI/D) controllers were designed using a method in the literature and SIMULINK auto-tuning facility respectively. The controller parameters were optimized using MATLAB **fmincon** command to minimize rise-time and calculated IAE values during response to unit step input. This was done for both the compensated and uncompensated plants. In both cases, simulations were done for situations when there are variations in some parameters in the plant models. It was observed that compensated plants were less sensitive to parameter variations than the uncompensated plants which in some cases lost stability even with optimized controller parameters.*

Keywords: *Recycle plant, recycle compensator, 2DoF controller, parameter variation, robustness.*

1.0 Introduction

Recycle operation is widespread in process industries as it enhances reuse of matter and energy in unit processes. Despite the economic attractiveness of this, recycle has been known to have detrimental effects on process dynamics (Denn and Lavie, 1982; Taiwo, 1986; Morud and Skogestad, 1994; and Lakshminnarayanan and Takada, 200). Taiwo and Krebs (1996) concluded from these that response time of the process with recycle can be substantially longer than the response time of the process in the forward path alone. Also, the gain of plants with recycle can be substantially greater than that of the forward path alone. In order to keep the steady state advantage while preventing the dynamic penalty, Taiwo (1985, 1986 and 1996) proposed the recycle compensator. Taiwo *et al* (2014) already established that the controllers designed for recycle compensated systems often perform well on the uncompensated system even above those designed directly from the uncompensated systems.

While Marquez *et al* (2012) addressed the control of delayed recycling systems with unstable first order forward loop, in a more recent work, Bamimore and Taiwo (2015) designed a recycle compensator for processes that lose stability as a result of recycle. This paper is an extension of the work to show how compensated plants (that are open-loop unstable and also with delays) outperform uncompensated plants even with optimal control systems when some process parameters are not exactly known.

In section 2, we discuss briefly the methods employed in the design and optimization of the control systems while in section 3 the methods are demonstrated on both recycle compensated and uncompensated plants in which we have variation in process parameters. The results of the simulations are discussed in section 4 and conclusions are made.

2.0 Methodology

Going by the findings of Taiwo and co-workers (2014), one can proceed on the design of a controller for a recycle plant by considering only the forward path transfer function having designed a recycle compensator for the system because such controllers have been found to often perform well on the uncompensated system even above those designed directly from the uncompensated systems. We employ two strategies in this work to design controllers for the systems.

First, we consider a method proposed by Lee and co-workers (2000) for systems that are open-loop unstable and also with time delay. By this method, we obtained PID controllers of the structure shown in Figure 1. The PID controller, C and the corresponding set-point filter, f_R take the form

$$C = P + \frac{I}{s} + Ds, \quad f_R = \frac{1}{\alpha s + 1} \qquad (1)$$

The resulting controller parameters were optimized for minimized rise-time and IAE during response to unit step changes.
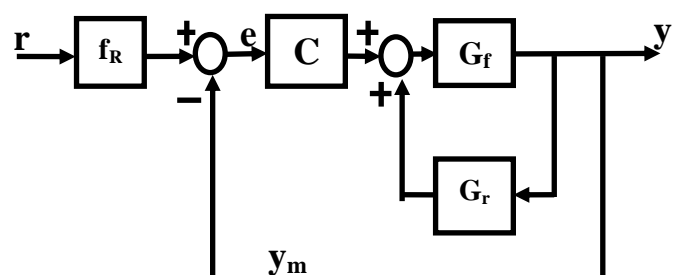
Figure 1: Application of Lee *et al* (2000) Control Structure to System with Recycle

Secondly, we obtained another set of controller parameters by employing SIMULINK auto-tuning facility for 2DoF control of the system. The 2DoF controller has been employed severally to eliminate *derivative* and *proportional kick* that may arise from sudden changes in set-point and hence the error, *e* (Seborg *et al*, 2004). Large overshoots that often result from such sudden changes are avoided by basing the proportional and derivative actions on the measurement y_m, rather than on the error signal, *e*. One way of representing the 2DoF controller is as shown in Figure 2.
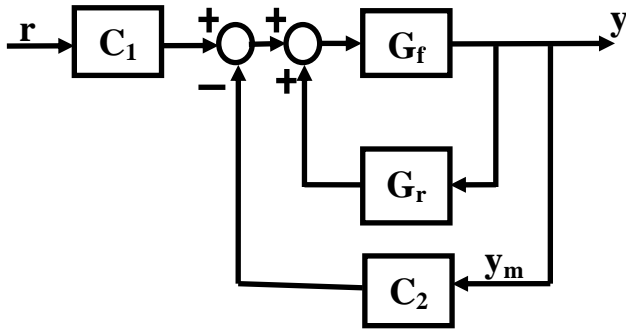
Figure 2: 2DoF Control Structure for System with Recycle

The relations describing the above controller is given as

Feedback controller: $C_2 = P + \frac{I}{s} + \frac{Ds}{\frac{1}{N}s+1}$

Pre-compensator: $C_1 = bP + \frac{I}{s} + \frac{cDs}{\frac{1}{N}s+1}$ (2)

For good reference tracking and disturbance rejection, we make the set-point weighting parameters *b* and *c* zero thus leaving us with $C_1 = \frac{I}{s}$. The controller parameters were also optimized as the former both for the recycle compensated and uncompensated plants. The parameters of the forward path process such as the gain, time delay and time constant were then subjected to variations to examine the robustness of each control system with both the recycle compensated and uncompensated plants.

3.0 Illustrative examples

3.1 Example 1: Consider the high-order unstable recycling system for which we have

Plant (Forward path):
$$G_f(s) = \frac{10}{(s-0.3)(s+2)(s^2+8s+20)(s^2+6s+13)} e^{-0.4s}$$

Recycle path: $G_r(s) = \frac{5}{(s+5)(s^2+2s+10)} e^{-0.5s}$ (3)

To apply the method proposed by Lee *et al* on the forward plant $G_f(s)$, there is need to approximate the stable part to a first order lag for which we now obtain

$$G_f(s) = \frac{0.0192}{(s-0.3)(0.6076s+1)} e^{-1.1534s}$$ (4)

The optimized controller parameters for this example (both recycle compensated and uncompensated plants) are summarized in Table 1.

Table 1: Controller Parameters for Example 1

Plant	P	I	D	α	IAE
Compensated	31.9981	2.6964	14.0860	10.7642	5.87
Uncompensated	32.2036	4.6412	20.0681	9.8013	6.73

Figures 3 and 4 present the simulation plots for the recycle compensated and uncompensated plants with process parameter variations. The greater adverse effects of these
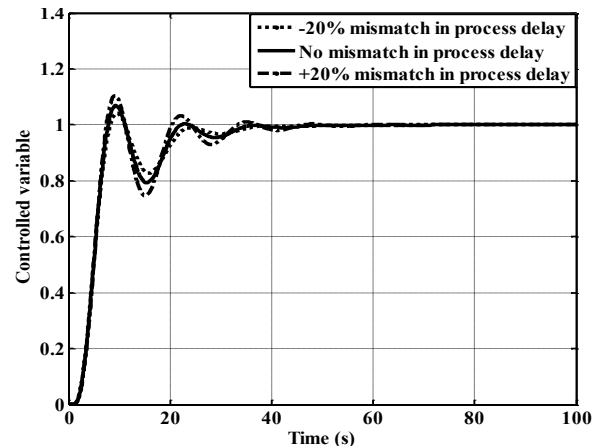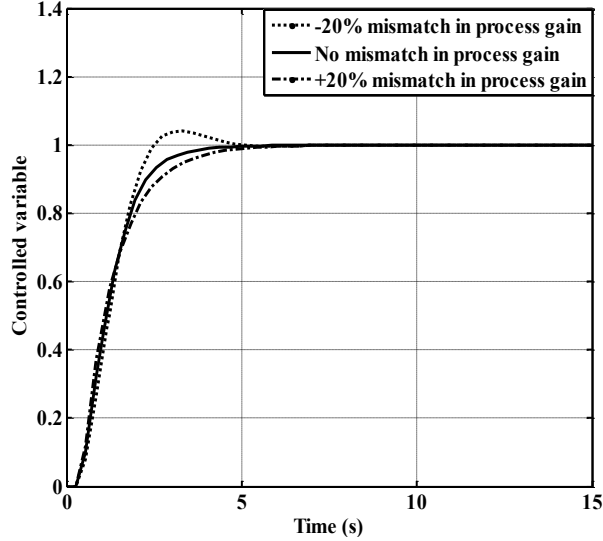

3(a)

126
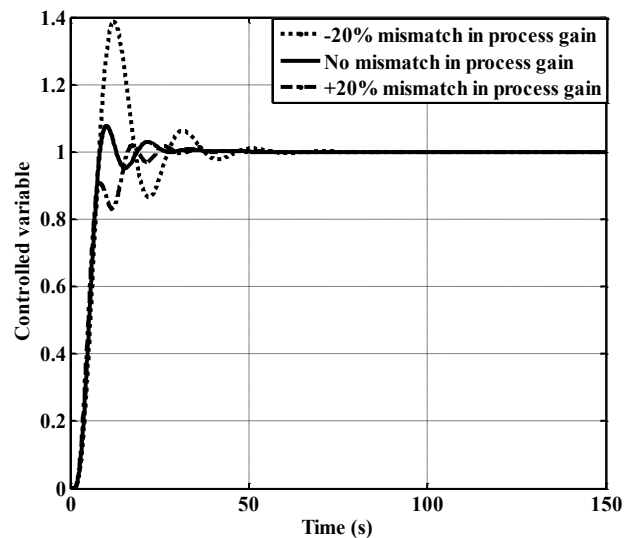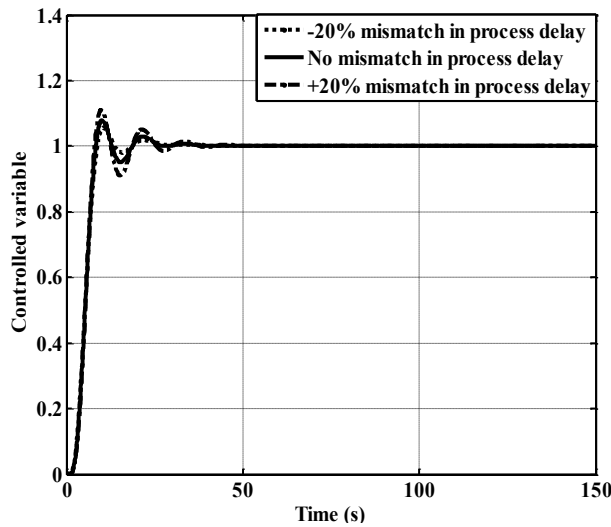
3(b)

Figure 3: Response of Compensated Plant with Process Parameter variations to Unit Step Input
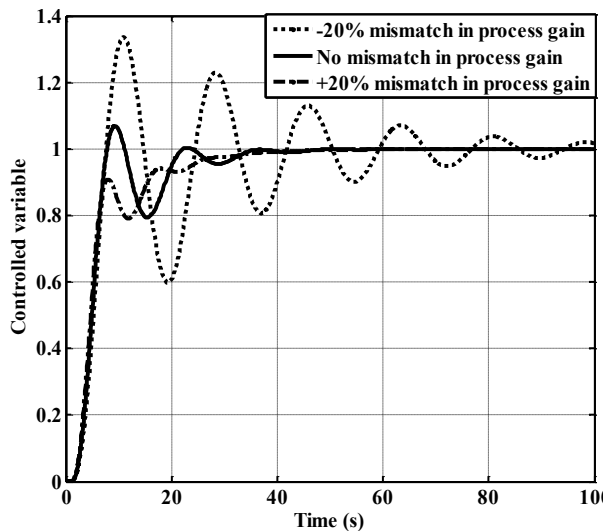
4(a)

4(b)

Figure 4: Response of Unompensated Plant with Process Parameter variations to Unit Step Input

variations on the performance of the uncompensated plant are very evident in the large undershoot and oscillations experienced when there was -20% mismatch in the forward path process gain K.

3.2 Example 2: Here we consider a reactor-separator-recycle process (Bequette, 2003) which has time delays at both the forward and recycling paths. It is a first order delayed unstable process given by

Plant (Forward path): $G_f(s) = \frac{0.8713}{(s-0.6439)} e^{-0.28s}$

Recycle path: $G_r(s) = \frac{-5.6579}{(s+3.402)} e^{-0.32s}$ (5)

The optimized controller parameters for this example (both recycle compensated and uncompensated plants) are presented in Table 2.

Table 2: Controller Parameters for Example 2

	P	I	D	N	∝	IAE
Recycle Compensated Plant						
Lee *et al*	3.1869	1.7698	0.2734	-	1.7373	0.6401
2DoF PI	2.0590	0.7616	-	-	-	1.7540
2DoF PID	2.4265	1.3203	0.5698	0.0805	-	1.3220
Uncompensated Plant						
Lee et al	3.3314	3.0229	0.4477	-	2.6962	3.0000
2DoF PI	3.1981	0.7834	-	-	-	5.2170
2DoF PID	5.3383	1.3203	0.5698	0.0805	-	4.8220

Figures 5 through 10 show the simulation responses of both the compensated and uncompensated plants with process parameter variations and with the above controllers. It would

127

be noted that the 2-DoF PID controller went unstable when there was -20% mismatch in process time constant τ and +20% mismatch in process time delay θ. Other controllers were also observed to oscillate repeatedly and were at best at the verge of instability. This is contrary to the smooth and stable responses of the recycle compensated plants with the different controllers.
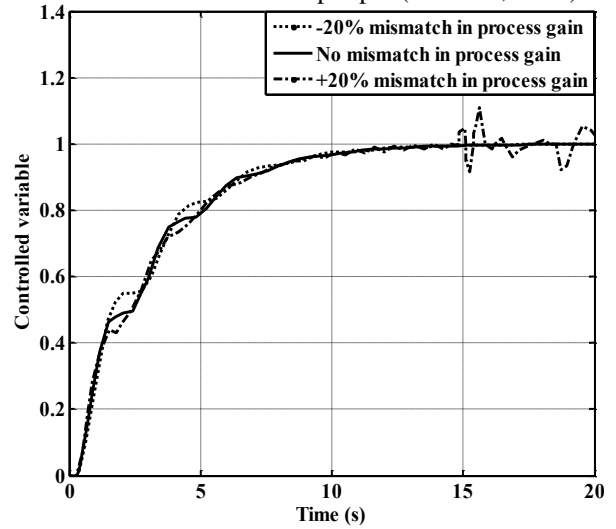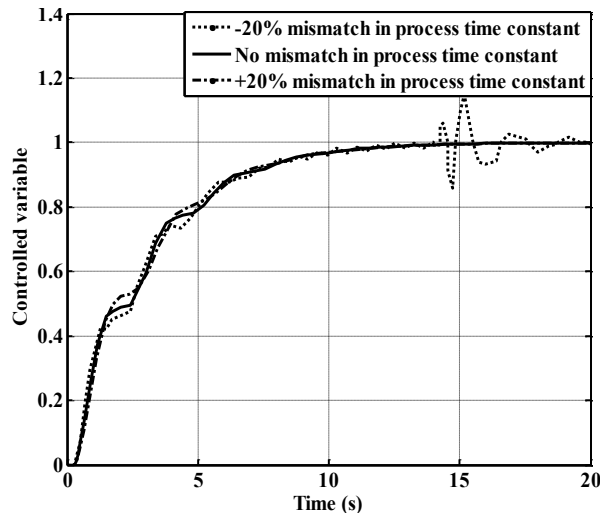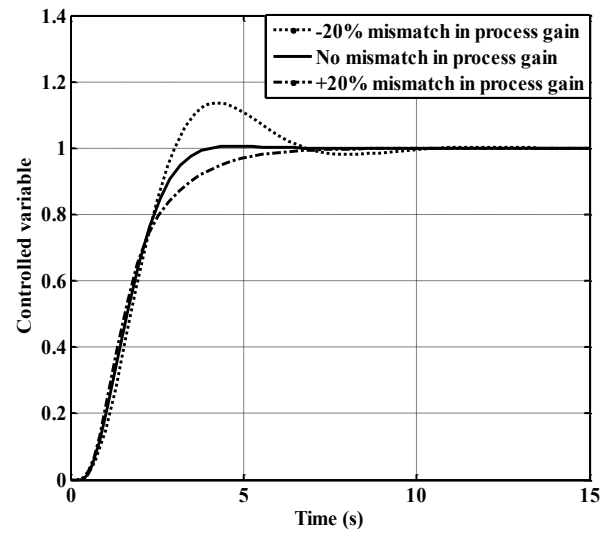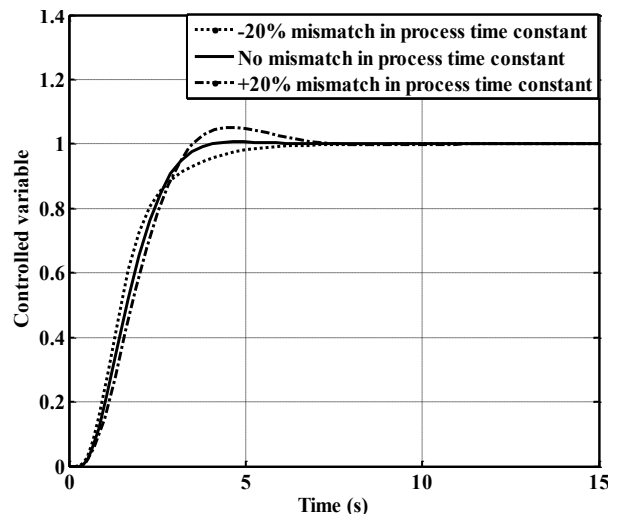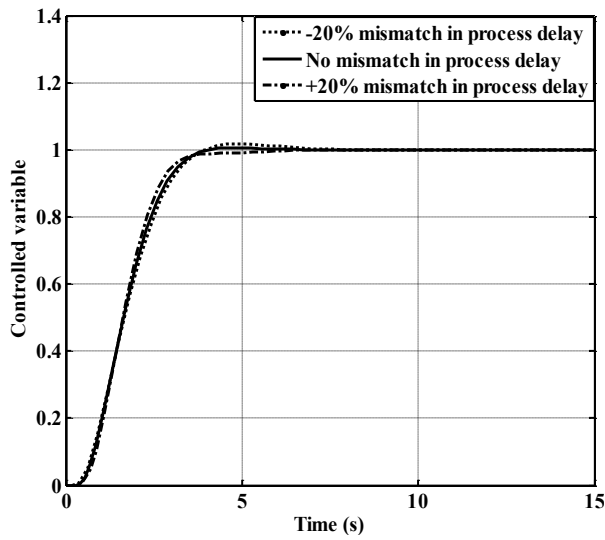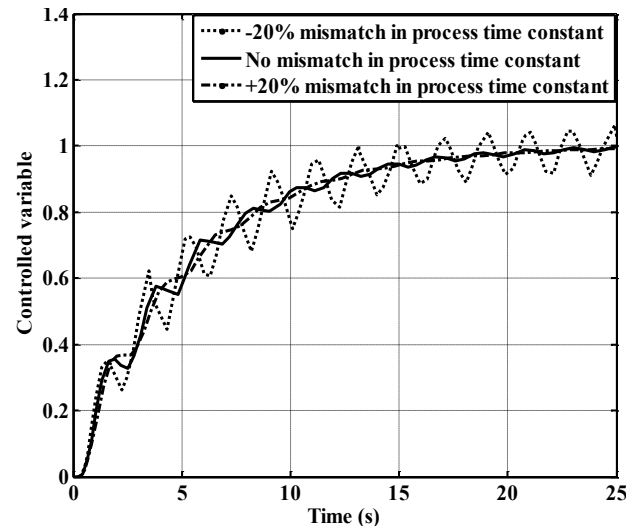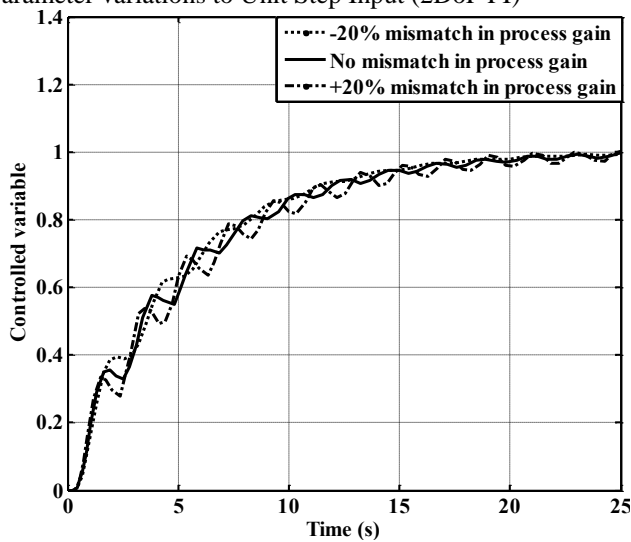

5(a)
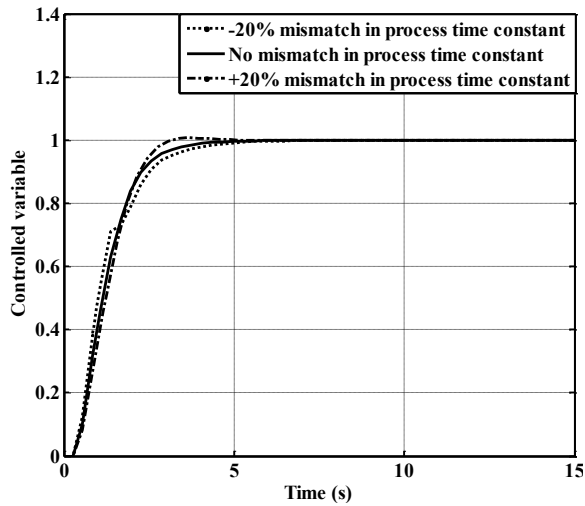
5(b)
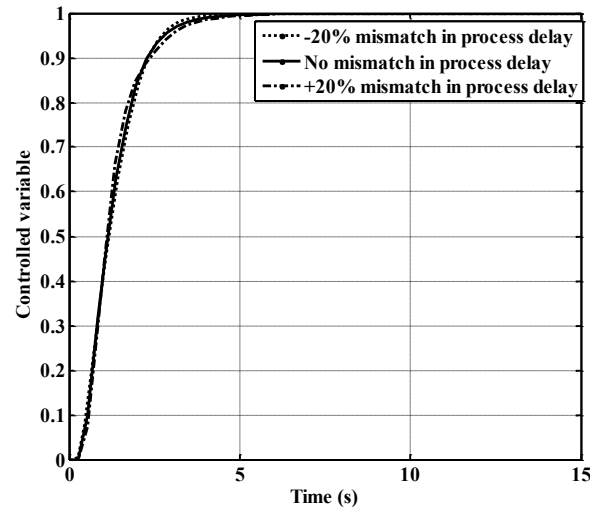
5(c)

Figure 5: Response of Compensated Plant with Process Parameter variations to Unit Step Input (Lee *et al,* 2000*)*

6(a)

6(b)

7(a)
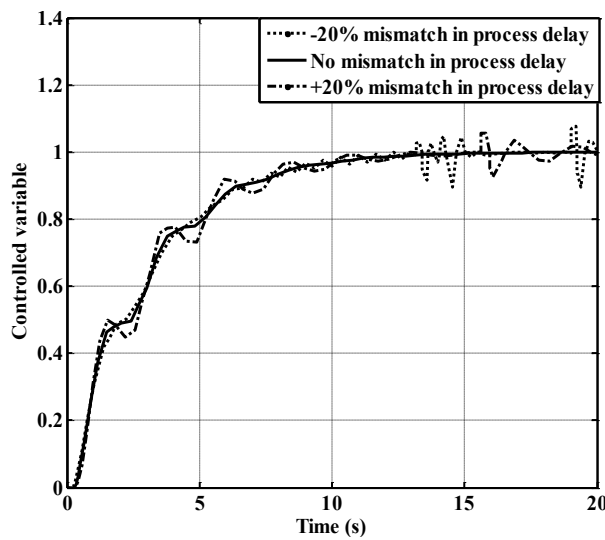
6(c)

7(b)

Figure 6: Response of Uncompensated Plant with Process Parameter variations to Unit Step Input (Lee *et al*, 2000*)*
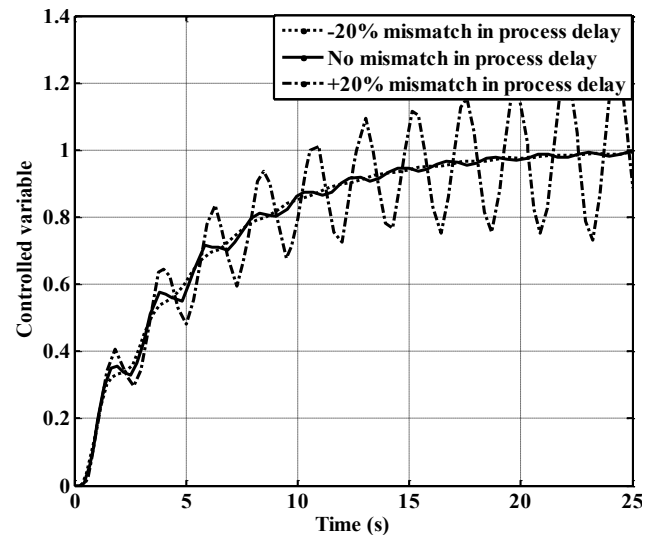
7(c)

Figure 7: Response of Compensated Plant with Process Parameter variations to Unit Step Input (2DoF PI)
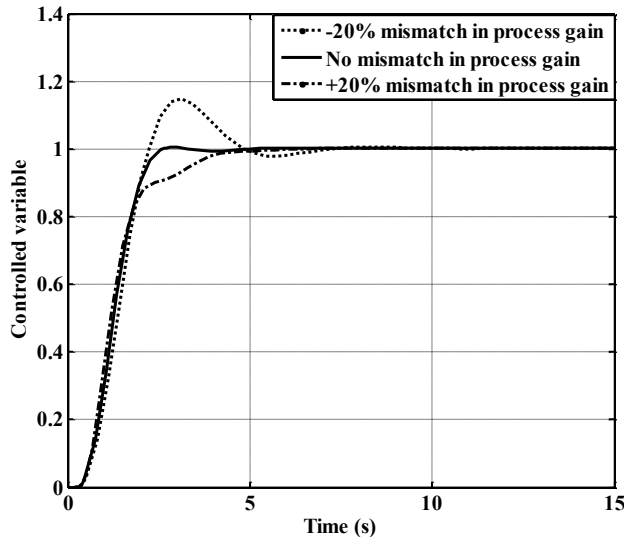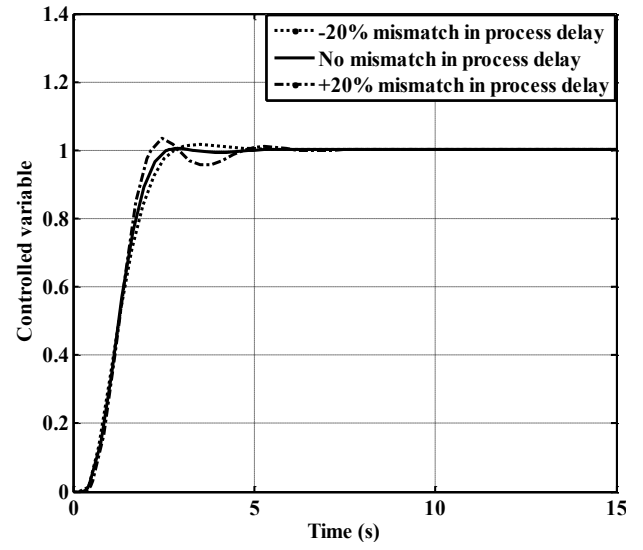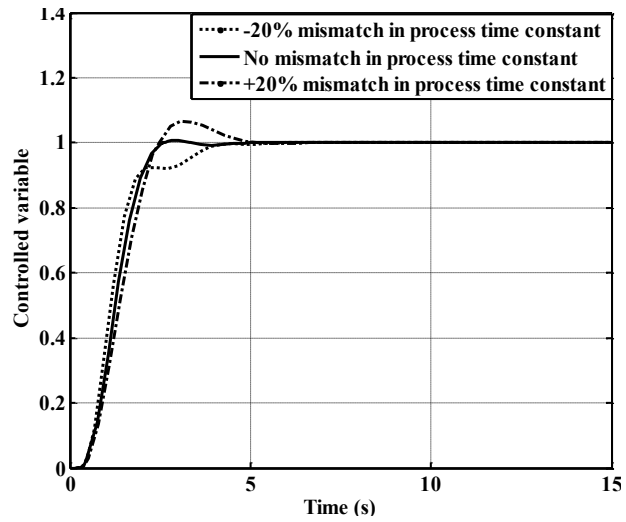

8(a)

8(b)

8(c)

Figure 8: Response of Uncompensated Plant with Process Parameter variations to Unit Step Input (2DoF PI)
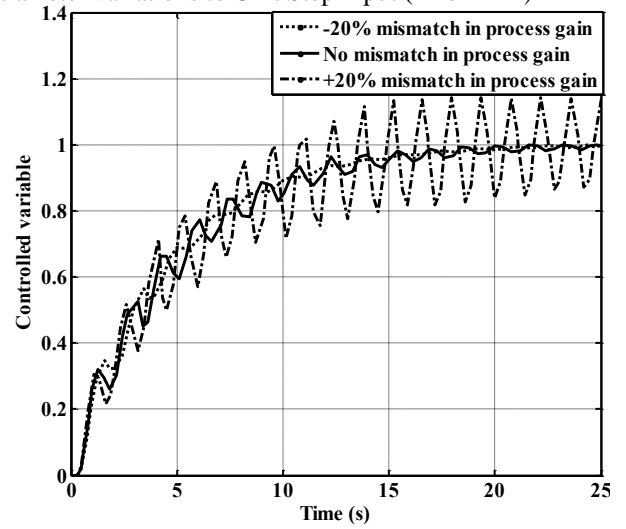
9(a)

9(b)
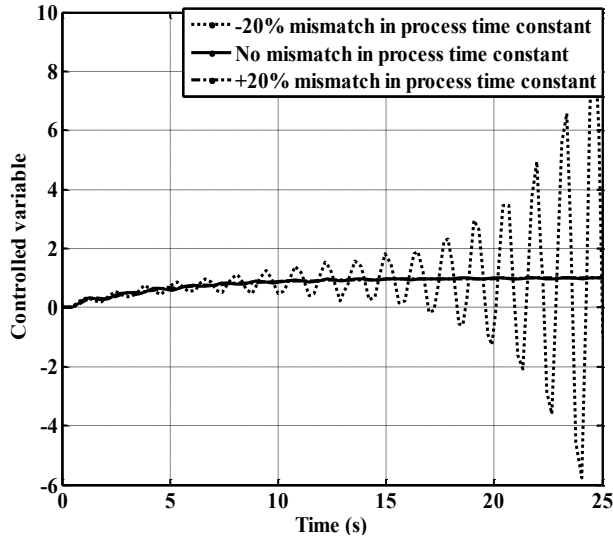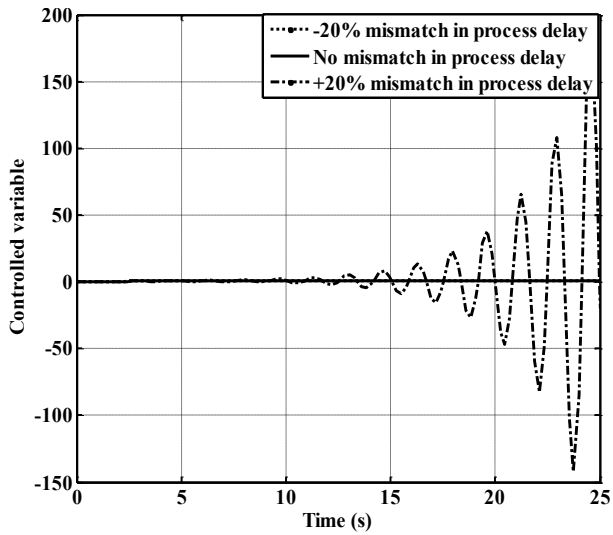

9(c)

Figure 9: Response of Compensated Plant with Process Parameter variations to Unit Step Input (2DoF PID)

10(a)

10(b)

3.3 Example 3: This is similar to Example 2 but differs in the fact that we now have a positive recycle unlike the negative recycle transfer function in Example 2.

$$Plant\ (Forward\ path):\ G_f(s) = \frac{0.8713}{(s-0.6439)}e^{-0.28s}$$

$$Recycle\ path: \qquad G_r(s) = \frac{5.6579}{(s+3.402)}e^{-0.32s} \qquad (6)$$

Note that the recycle compensated plant remains the same as we have in Example 2. Hence, only the controller parameters and simulation plots for the uncompensated plant are now presented in Table 3 and Figures 11 through 13 respectively.

Table 3: Controller Parameters for Example 3

	P	I	D	N	∝	IAE
		Uncompensated Plant				
Lee et al	4.0182	1.5461	0.0086	-	2.1183	2.0410
2DoF PI	4.118	0.7616	-	-	-	2.5710
2DoF PID	4.4690	1.3051	0.4946	0.1240	-	1.9590

10(c)

11(a)

Figure 10: Response of Uncompensated Plant with Process Parameter variations to Unit Step Input (2DoF PID*)*

11(b)

13(a)

11(c)
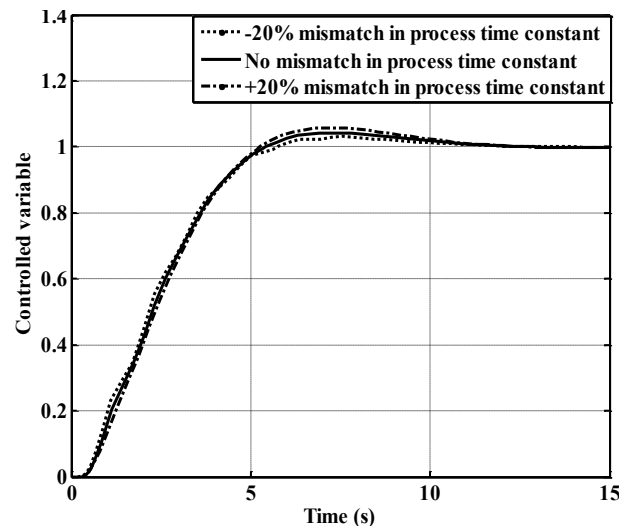
13(b)

Figure 11: Response of Uncompensated Plant with Process Parameter variations to Unit Step Input (Lee *et al*, 2000*)*
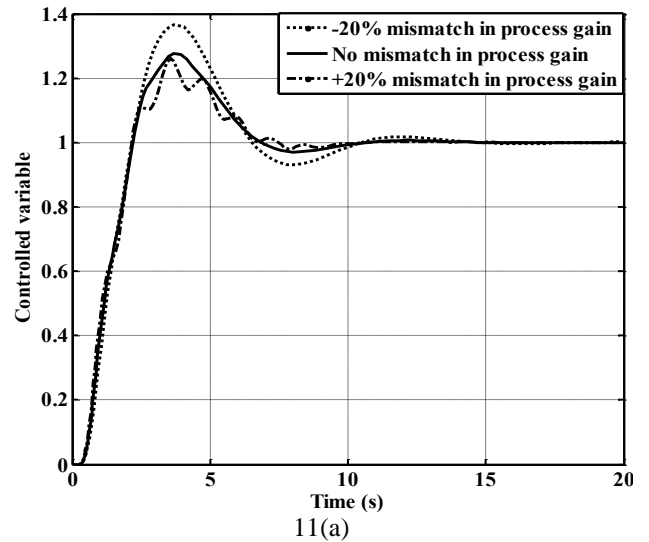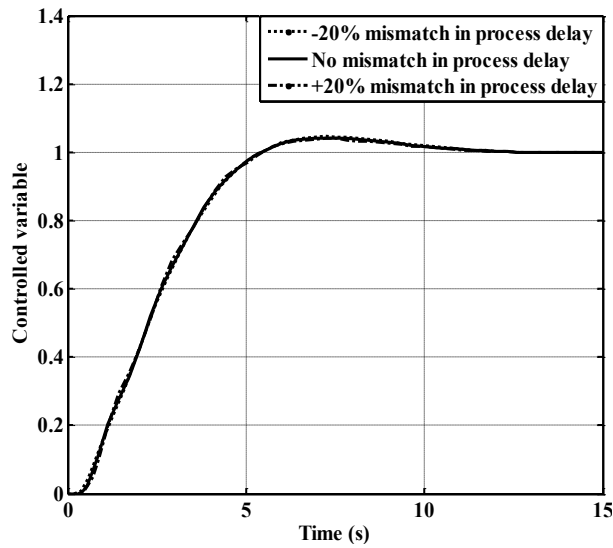
12(c)

Figure 12: Response of Uncompensated Plant with Process Parameter variations to Unit Step Input (2DoF PI)
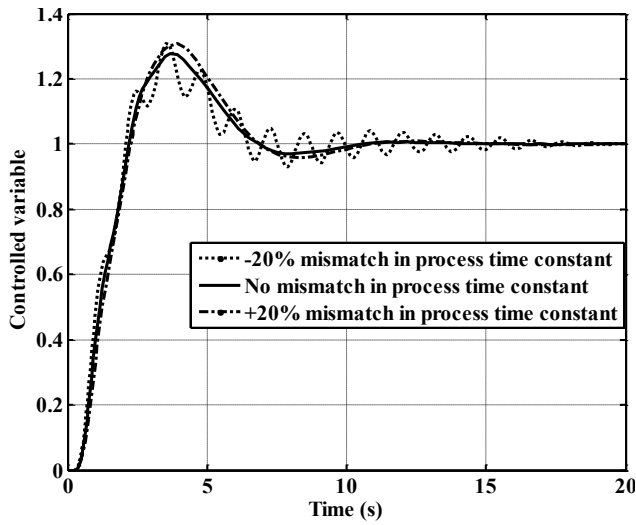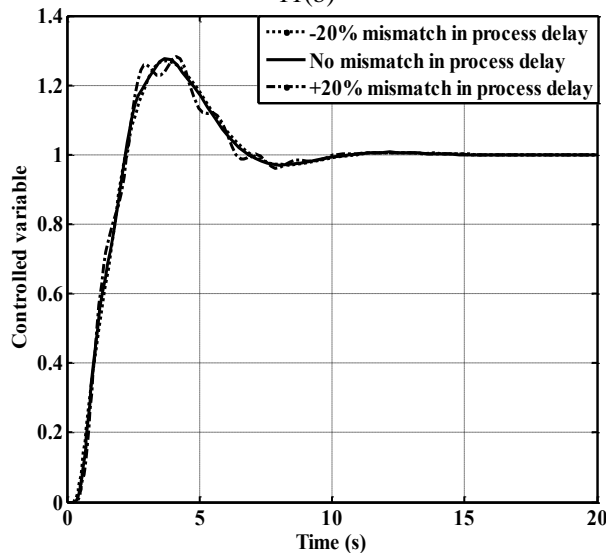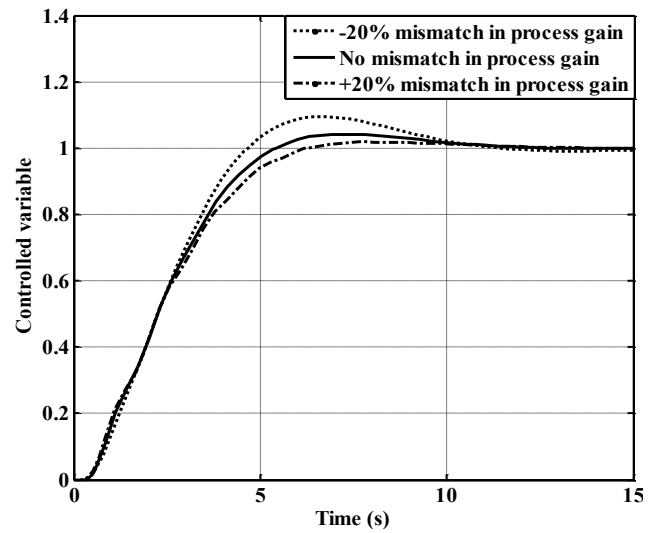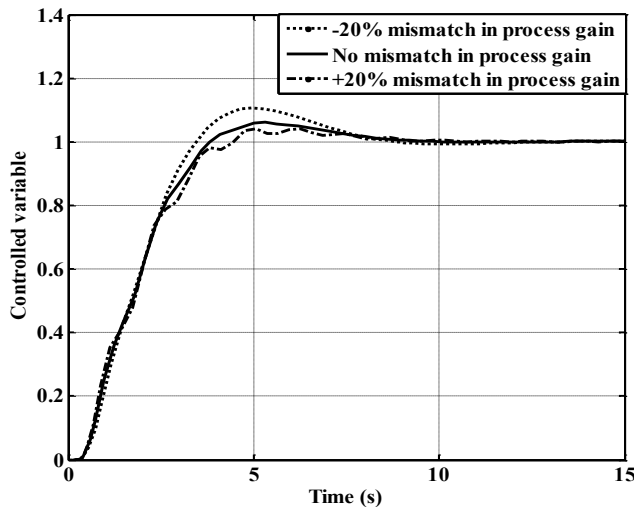

13(a)
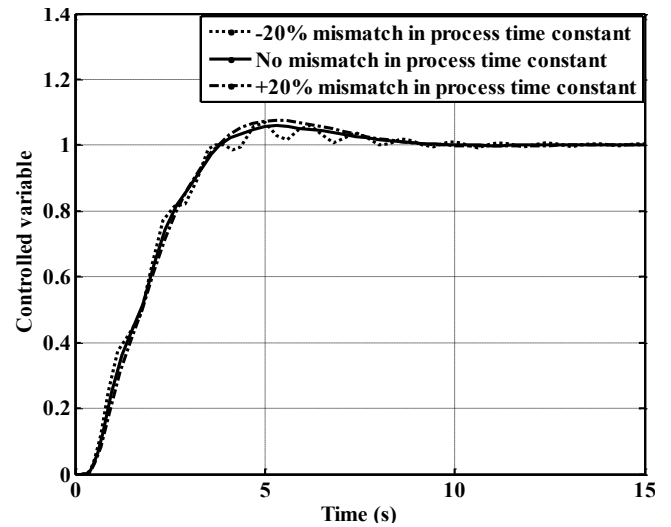
13(b)
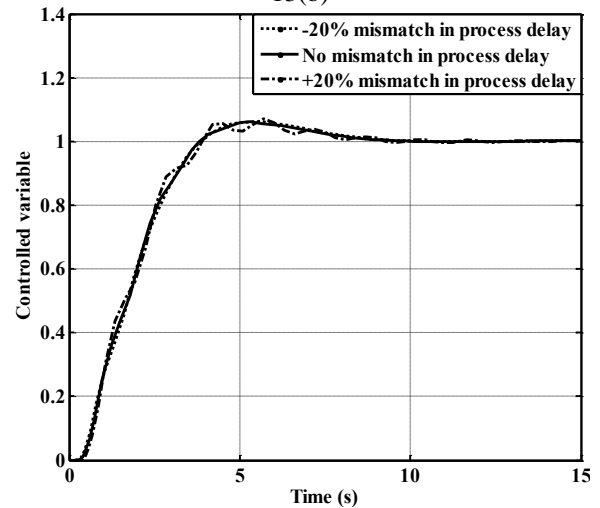
13(c)

Figure 13: Response of Uncompensated Plant with Process Parameter variations to Unit Step Input (2DoF PID)

The above simulation plots again show that besides the slower responses of recycle plants without recycle compensators, variation in process parameters often result in oscillatory responses that can be avoided by implementing a recycle compensator on the system. Notwithstanding, it should be noted that the oscillations in this case where we have positive recycle is less than for the case of Example 2 where we have negative recycle.

4.0 Conclusions

Stable and optimal controllers were designed for recycle systems which have unstable poles in the forward path using two different methods. The control systems were simulated

both for when recycle compensators are considered and when not. The recycle systems without recycle compensators were observed to be more sensitive to variations in process parameters (gain, time delay and time constant) and in a number of cases, the system went unstable unlike recycle compensated plants which robustly responded to set-point changes at the face of parameter variations.

5.0 References

Bamimore, A. and Taiwo, O. (2015). Recycle Compensator Facilitates Rapid Parameterization of Proportional Integral/Derivative (PI/D) Controllers for Open-Loop Unstable Recycle Processes. *Industrial Engineering Chemistry Research*, 54, 5115-5127.

Bequette, B. W. (2003). *Process Control: Modeling, Design and Simulation.* Prentice Hall.

Denn, M.M. and Lavie, R. (1982). Dynamics of plants with recycle*, Chem. Eng. J.* 24:55-59.

Lakshminarayanan, S. and Takada, H. (2001). Empirical modelling and control of processes with recycle: some insights via case studies, *Chemical Engineering Science*, 56:3327–3340.

Lee, T., Lee, J. and Park, S. (2000). PID Controller Tuning for Integrating and Unstable Processes with Time Delay. *Chemical Engineering Science*, 55, 3481-3493

Marquez, J. F., del Muro, B., Velasco, M., Cortes, D. and Sename, O. (2012). Control of delayed recycling systems with unstable first order forward loop. *J. Process Control, 22*, 729-737.

Morud, J. Skogestad, S. (1994): Effects of recycle on dynamics and control of chemical processing plants. *Comp. Chem. Eng*. 18: S529-S534.

Seborg, D. E., Edgar, T. F. and Mellichamp, D. A. (2004). *Process Dynamics and Control.* John Wiley & Sons, Inc.

Taiwo, O. (1986). The design of robust control systems for plants with recycle*, Int. J. Contr.*, vol 43, pp 671 - 678.

Taiwo, O. and Krebs, V. (1996). Robust control system design for plants with recycle. *Chem. Eng. J.,* vol 61, pp 1- 6.

Taiwo, O. (1985). The dynamics and control of plants with recycle*, J. Nig. Soc. Chem. Eng.,* vol 4, pp 96 - 107.

Taiwo, O., Bamimore, A., Adeyemo, S. and King, R. (2014). On Robust Control System Design for Plants with Recycle. In: Proceedings of the 19th World Congress, The International Federation of Automatic Control, Cape Town, South Africa.

P 007

THERMODYNAMIC ANALYSIS AND OPTIMIZATION OF DISTILLATION COLUMN: A GUIDE TO IMPROVED ENERGY UTILIZATION

[1]Umo A. M. and [2]*Bassey E. N.

[1]Department of Chemical and Petroleum Engineering, University of Uyo, Uyo, Nigeria.
[2]Department of Chemical/Petrochemical Engineering, Akwa Ibom State University, Ikot Akpaden, Nigeria.
*umoaniediong@gmail.com ;*enbassey@yahoo.co.uk Tel:+2348023443589*

Abstract:

Energy consumption no doubt contributes a lot to the cost of production. To maximize profit, energy loss due to lost work must be minimized during production. Thus in this research, thermodynamic analysis was used to determine the energy efficiency of a propane–propylene splitter. In addition, the thermodynamic analysis was used to identify scope for possible modification and to set target for the column modification. The result indicated that the thermodynamic efficiency of the system was increased by 2.2% and the lost work in the column was reduced by 21.7Kw/hr. This was achieved by sacrificing only 2Kw/hr increase in the column minimum work.

1. INTRODUCTION

The excessive cost of separation systems results partly because of energy dissipation or lost work, hence the present trends explore the use of thermodynamics analysis in reducing the cost of separation systems, particularly in distillation operations. Thermodynamic analysis emphasizes the use of first and second law of thermodynamics and may be applied through pinch analysis and the exergy analysis to identify and quantify the energy dissipation and define targets for energy consumption (Demirel, 2004).

The minimum thermodynamic condition for a distillation column is zero thermodynamic loss or reversible operation within the column, the stage-enthalpy or temperature-enthalpy profile of these conditions is called the Column Grand Composite Curve (CGCC). The CGCC can be used to identify scope for modification and set target for column modification or to integrate it most efficiently within the process train. It is a technique to enable designers apply the principle of pinch to distillation column design and modification to give a clearer picture of the thermodynamic consequences of the design alteration. Despite the benefit of CGCC, Dhole and Linnhoff (1993) observed that one of the reasons CGCCs have not been used more often is the difficulty of constructing them due to the fact that at minimum thermodynamic condition, the column needs infinite stages and infinite numbers of side condensers and reboilers. In addition, to identify and quantify unused parts of available energy and determine the thermodynamic efficiency of distillation systems, exergy analysis is used (Demire, 2004). Exergy is a measure of the quality and efficient use of energy (Ghorbani, Maleki, Salehi, Salehi and Amidpour, 2013) and is therefore a useful tool for optimization of energy system consumption.

The aim of this paper is to illustrate the application of thermodynamic analysis in optimization of distillation column energy utilization. In this study, thermodynamic analysis of propane-propylene splitter case study was carried out to optimize its energy consumption and reduce operational cost. The propylene – propane splitter unit in this case study shown in Figure 1, is a part of a polypropylene plant which comprises propylene purification, polymerization, additive and extrusion units. The plant was designed to produce 35,000 metric tonnes of polypropylene resin per year (Odigo, 2003). The purification area upgrades 73 mole percent propylene from a fluid catalytic cracking (FCC) unit to a minimum of 94 moles percent in the propylene - propane splitter.
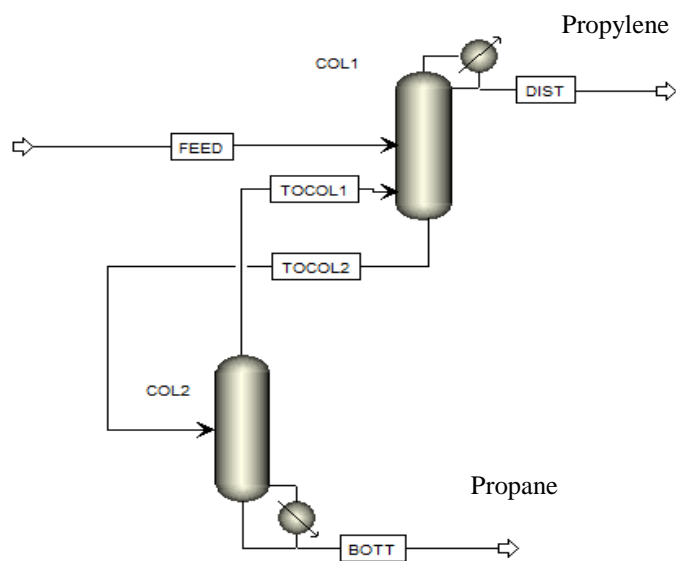

Figure 1. Schematic of Propylene-Propane Splitter

2. THEORY

2.1. Column Grand Composite Curve (CGCC)

The construction of the CGCC starts from a converged simulation (Dhole and Linnhoff, 1993), where the mole fraction of liquid (X^*), vapor (Y^*) for both light and heavy key components, vapor enthalpy (H_G^*), liquid enthalpy (H_L^*), molar flows of equilibrium vapor (G^*) and liquid stream (L^*) are obtained for each stage. The minimum vapor (G_{min}) and liquid (L_{min}) flows are obtained at each stage temperature by simultaneously solving equation (1) and (2)

$$G_{min} \qquad G_{min} Y_L^* - L_{min} X_L^* = D_L \qquad (1)$$
$$G_{min} Y_H^* - L_{min} X_H^* = D_H \qquad (2)$$

To get the temperature-enthalpy picture for the minimum thermodynamic condition, the minimum vapor and liquid flows are expressed in terms of enthalpies. The enthalpies of the minimum vapor and liquid flows are obtained using direct molar proportionality, equations (3) and (4).

$$H_{Gmin} = H_G^* \left({}^{G_{min}} / {}_{G^*} \right) \qquad (3)$$

$$H_{Lmin} = H_L^* \left({}^{L_{min}} / {}_{L^*} \right) \qquad (4)$$

Enthalpy balance is carried out in each stage to calculate the enthalpy deficit (H_{def}) at each stage temperature, using equation (5) for stages before the feed stage and equation (6) for stage at and after the feed stage (Dhole and Linnhoff, 1993). However, Bandyopadhyay (1998) and Demirel (2006) opined that at the feed stage, mass and energy balances differ from a stage without feed and finite changes of composition and temperature disturb the reversible operation. Thus we have the modified feed enthalpy deficit as equation (7). The CGCC is obtained by plotting temperature or stage number versus enthalpy deficit.

$$H_{def} = H_{Lmin} - H_{Gmin} + H_D \qquad (5)$$

$$H_{def} = H_{Lmin} - H_{Gmin} + \left(H_D - H_{feed} \right) \qquad (6)$$

$$H_{def,F} = Q_c + D[H_D + \frac{H_L (X_D - Y_L^*)}{Y_F^* - X_L^*} - \frac{H_V (X_D - X_F^*)}{(Y_F^* - X_F^*)}] \qquad (7)$$

2.2. EXERGY LOSS PROFILES

The expressions for exergy, entropy and energy balances were derived by Demirel (2004) and Demirel (2006). The energy balance in a distillation column is expressed as in equation (8)

$$\frac{d(mU)_{sys}}{dt} + \Delta(\dot{m}H)_i - \dot{Q}_0 - \sum_j \dot{Q}_j + \sum_k \dot{W}_k \qquad (8)$$

where the first term is the change in internal energy, the second is the net change of enthalpy of an input or output

stream i within the control volume, $\dot{Q}_0$ is the heat input rate from the surroundings, $\dot{Q}_j$ is the heat input rate from a reservoir *and* $\dot{W}_k$ shows the work done by the system. Also, the entropy balance is expressed in equation (9)

$$\frac{d(mS)_{sys}}{dt} + \Delta(\dot{m}S)_i - \frac{Q_0}{T_0} - \sum_j \frac{Q_j}{T_j} = \sigma \qquad (9)$$

The term σ shows the rate of entropy production due to irreversibility, which is zero when processes and heat flows between the system and its surrounding are reversible. To eliminate $\dot{Q}_0$ from equations (8) and (9), equation (9) is multiplied by the temperature of the environment T_0 and the result is subtracted from Equation (8). The resulting equation (10) is the exergy balance for a distillation column (Olakunle and Oluyemi, 2008).

$$\frac{d[m(H-T_0S-PV)]_{sys}}{dt} + \Delta[\dot{m}(H - T_0S)]_i - \sum_j \left(1 - \frac{T_0}{T_j}\right) Q_j +$$
$$\sum_k W_k + T_0\sigma = 0 \qquad (10)$$

The term $H - T_0S$ in equation (10) is called the availability (A) and the term $T_0\sigma$ is called the lost work (LW) or exergy lost if $T_0\sigma \geq 0$. The lost work is that portion of the total work that is necessary to overcome thermodynamic inefficiency due to driving forces within the system; it identifies and quantifies the power lost due to various irreversibilities and relates the evolution of a system to the environmental conditions. Applying equation (10) on a system at steady state in the absence of the work, the lost work in the system obtained as shown in equation (11)

$$LW = \Sigma(\dot{m}A)_{in} - \Sigma(\dot{m}A)_{out} + \Sigma\left[\left(1 - \frac{T_0}{T}\right)q\right]_{in} +$$
$$\Sigma\left[\left(1 - \frac{T_0}{T}\right)q\right]_{out} \qquad (11)$$

Similarly, applying equation (10) in an adiabatic system at a steady state in which the lost work is negligible, the minimum work in the system is obtained as shown in equation (12)

$$W_{min} = \Sigma(\dot{m}A)_{out} - \Sigma(\dot{m}A)_{in} \qquad (12)$$

The thermodynamic efficiency of the system, equation (13) is computed using the lost work and the minimum work, when $W_{min} > 0$.

$$\eta = \frac{W_{min}}{LW + W_{min}} \qquad (13)$$

Heat Flow [kcal/h]	8455410.08	7530102.71

3. METHODOLOGY

Thermal analysis of the propylene – propane splitter was carried out using the Aspen Plus simulator Version 11.1 through its column targeting tool for rigorous column calculations. The column grand composite curve obtained from Aspen Plus RadFrac was used in this study. For each of the simulations, the Peng-Robinson (PR) property package was used. The Initial Plant Operating Data are as shown in Table 1.

The thermal analysis was used in identifying design targets for improvements in energy consumption and efficiency based on the concept of minimum thermodynamic condition (MTC) for a distillation column. Sensitivity analysis was carried out to study the interactive effect of those process variables involved in the operation of the propane-propylene splitter case study. The analysis provided a tool that was used in the optimization of the operating condition of the propane-propylene splitter. The efficient operating criterion considered was the mole fraction of propylene in the distillate, which should be a minimum of 0.94. Thermal analysis of the optimized splitter was also carried out to determine the extent of improvement achieved.

Table 1. Initial Plant Operating Data (Umo and Bassey, 2013)

Item	Feed	Product	Bottom
Material stream			
Vapour Fraction	1.00	0.00	0.00
Temperature [C]	53.00	41.75	54.24
Pressure [bar]	18.23	17.22	19.25
Molar Flow [kgmole/h]	290.70	246.96	43.74
Mass Flow [kg/h]	12344.37	10419.80	1924.57
Liquid Volume Flow [m3/h]	23.82	20.03	3.79
Heat Flow [kcal/h]	-227856.96	-43.83	-1156869.77
Component Mole Fraction			
Propylene	0.81	0.946	0.043
Propane	0.19	0.054	0.957
Reflux ration = 10.2			
Energy Stream	Qc		Qr

4. RESULT AND DISCUSION

4.1. EXERGY ANALYSIS FOR OPERATING CONDITION MODIFICATION

The propane-propylene splitter in our case study is operated with its feed stage located at tray 38. However, it was designed to operate at a feed stage of 90. Exergy analysis of the column was used to show the thermodynamic implication of the decision to change the feed stage location by the plant operators.

Table 2. Exergy analysis for feed stage location in the propane-propylene splitter.

	Column minimum work (watt)	Column lost work (watt)	Thermodynamic efficiency (%)	% propylene in distillate
feed stage at stage 90	9786	137536	6.6	95.2
feed stage at stage 38	3743	134631	2.7	94.6

The change of feed stage location from stage 90 to stage 38 shows the reduction of the thermodynamic efficiency of the column by 3.9%. However, while the effect of this change on the purity of the distillate at the same distillate rate is almost insignificant (i.e. 0.6% reduction in purity of the distillate), exergy analysis reveals that the decision to change the feed tray location by the plant operators has saved the company 6.04Kw/hr of energy due to the reduction in the minimum work required in the column.

4.2. IDENTIFYING TARGET FOR POSSIBLE MODIFICATION

The column grand composite curve (CGCC) presents the results of the thermodynamic analysis of the column for possible modification towards achieving the best energy performance. The common considerations for column modification that may be identified in the CGCC are scope for the reflux, feed preheating/cooling and side condenser/reboiler modification. These were based on the condition that the feed condition has been chosen appropriately *beforehand (D*ohle and Linnoff, 1992).
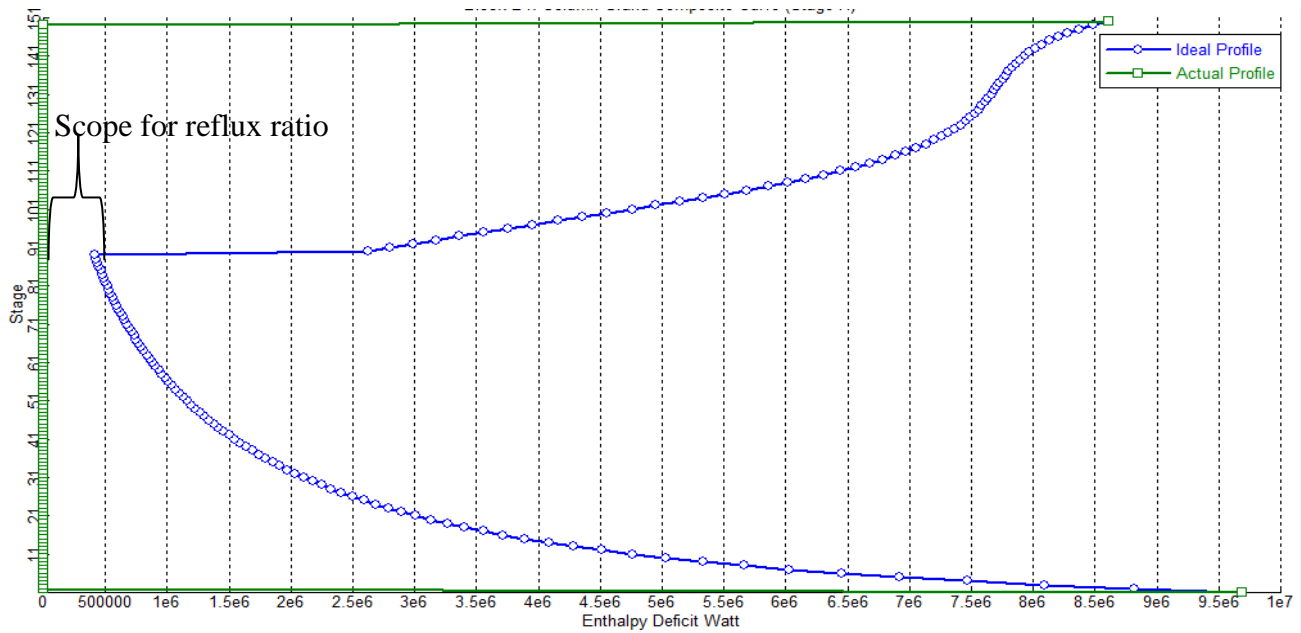
Figure 2: CGCC for feed stage at tray 90

The horizontal distance between the CGCC pinch point and the vertical axis represents the scope for reflux ratio as shown in the propane-propylene splitter case study CGCC with feed stage at tray 90, Figure 2.
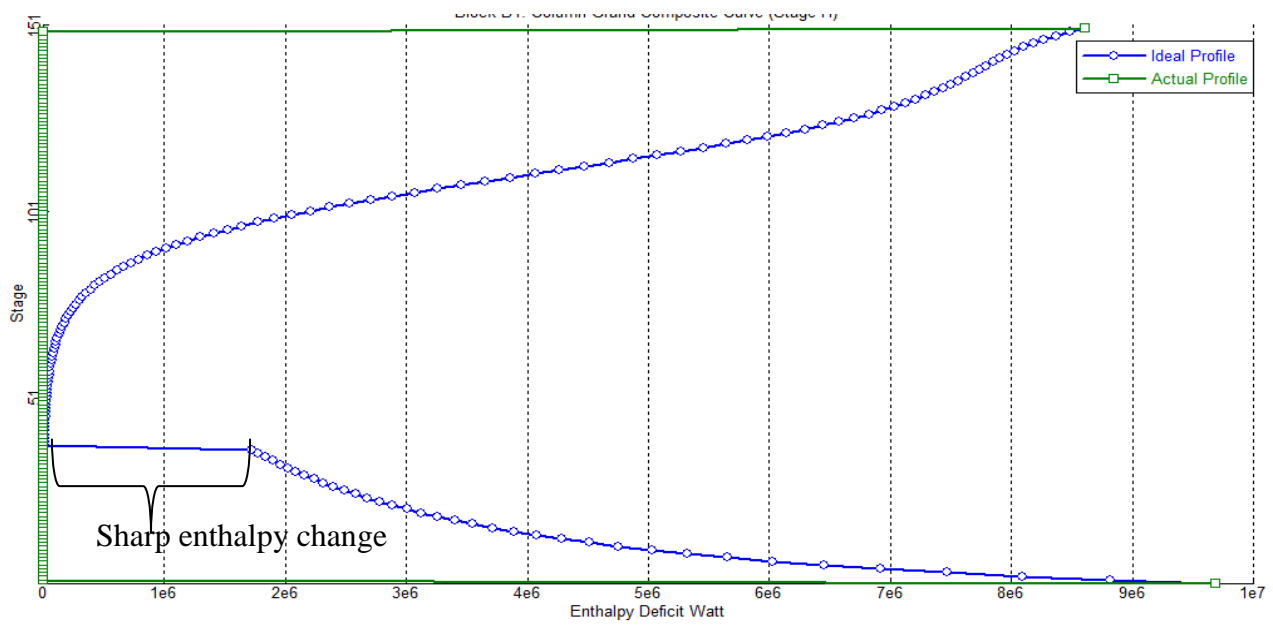
Figure 3: CGCC for feed stage at tray 38

The minimum work in the splitter was reduced by changing the feed stage to tray 38, at this condition, the CGCC Figure 3 indicates that there is no scope for reflux ratio reduction in the splitter. Thus to optimize the energy consumption of the splitter, it was necessary to identify other conditions for possible modification.

The next consideration is to identify a sharp change in enthalpy. A sharp enthalpy change in a CGCC indicates excessive subcooling/heating of the stream. This sharp enthalpy change increases the condenser and reboiler load. To reduce this load,Dohle and Linnoff (1992) suggested the use of either feed preheating/cooling or the use of side condenser/reboiler. They prefered feed preheating/cooling to side condensing/reboiler. Their reason being that Feed conditioning offers a more moderate temperature level and is external to the column unlike side condensing/reboiling. However, in this study, the adjustment of feed stage and pressure of the column is used to reduce the condenser and reboiler load. This approach is chosen because it enables the effective utilization of energy in the distillation column without additional capital cost as only adjustments of operating condition are involved.

4.3. OPTIMIZATION OF COLUMN ENERGY UTILIZATION

The operating condition; reflux ratio, column pressure and feed stage are variables which were chosen to optimize the energy efficiency of the distillation column using response surface optimization as shown in Figure 4 (Umo and Bassey, 2013).

In this work it was necessary to carry out exergy analysis to determine the implication of applying the result of the optimization process on the thermodynamic efficiency of the column.The work as shown in Table 2 indicats that the lost work in the column was reduced by 21.7Kw/hr. This was achieved by sacrificing only 2Kw/hr increase in the column minimum work. While the overal thermodynamic efficiency of the system has increased by 2.2%.

Further the exergy loss profile in Figures 5 and 6 indicates that the maximum exergy loss occurred in the stripping section of the column between stage 140 and 130. A comparison of Figure 5 and 6 shows that the maximum exergy loss has been reduced from 4.74kw/hr to 3.74Kw/hr by implementing the optimization result. In addition, comparing the CGCC of the splitter before optimization, Figure 2 with the CGCC after optimization in Figure 7, it is observed that the enthalpy deficit due to sharp enthalpy change has been reduced from 1700Kw to 800Kw
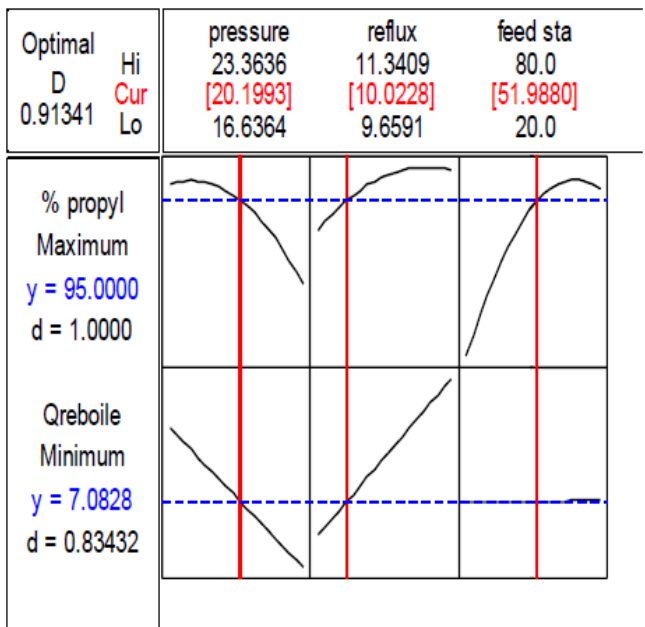

Figure 4: optimisation of the splitter

.

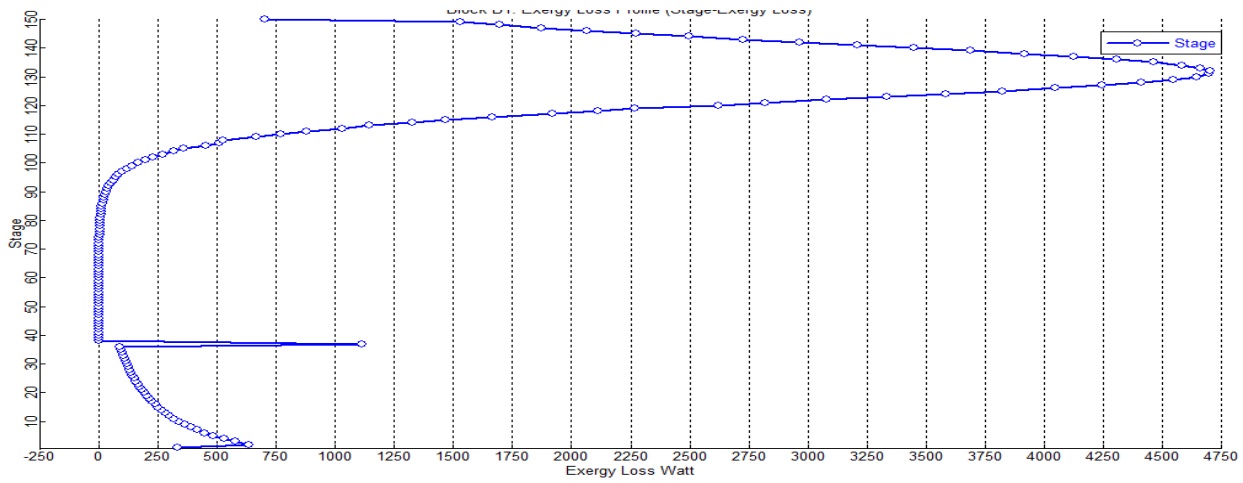Figure 5: exergy loss profilefor feed stage at tray 38
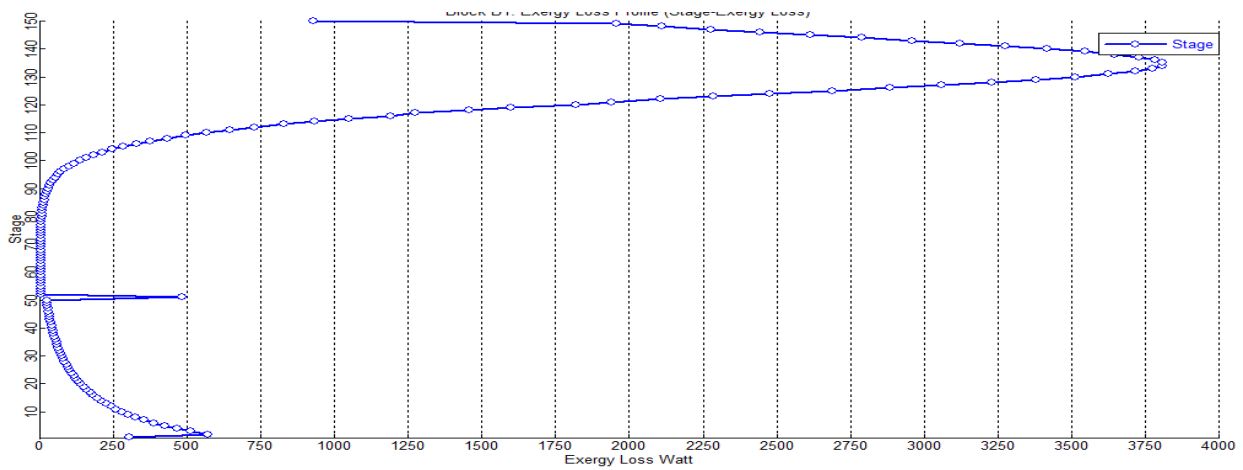

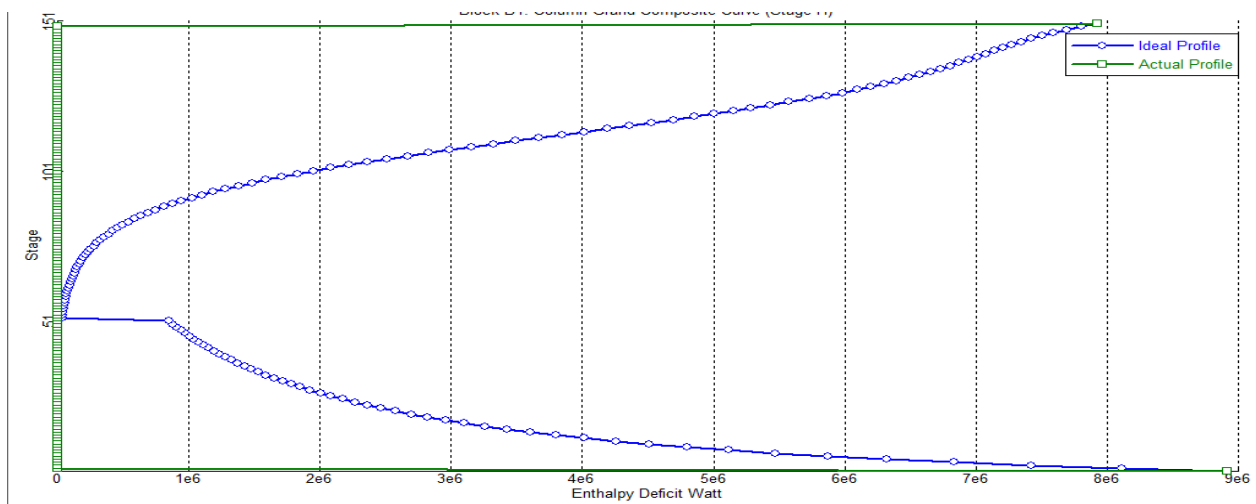Figure 6: exergy loss profile for the optimized operating conditions

Figure 7: CGCC for the optimized operating conditions

142

Table 3. Exergy analysis for column before and after optimization

Operating condition	Column minimum work (watt)	Column lost work (watt)	Thermodynamic efficiency (%)	% propylene in distillate
Before optimization	3743	134631	2.7	94.6
After optimization	5838	112926	4.9	95.0

5. CONCLUSION

In this reseach, thermodynamic analysis was carried out on the propane-propylene splitter unit to identify possible modification towards achieving the best energy performance. Amongst other considerations for column modification, adjustment of operating conditions (reflux ratio, column pressure and feed stage) was profered followed by process optimization on the splitter. Additionally, thermodynamic analysis was used to ascertain the implication on the energy efficiency, of applying the optimization result in the system. The result indicated that the thermodynamic efficiency of the system was increased by 2.2% and the lost work in the column was reduced by 21.7Kw/hr. This was achieved by sacrificing only 2Kw/hr increase in the column minimum work.

REFERENCE

Bandyopadhyay, S., Malik, R. and Shenoy, U. (1998).Temperature-enthalpy curve for energy targeting of distillation columns. *Comput. & Chem. Eng.*, 22(12), pp. 1733-1744.

Demirel, Y. (2004). Thermodynamic Analysis of Separation Systems. *Separation Science and Technology*, 39 (16), pp. 3897-3942.

Demirel, Y. (2006). Retrofit of Distillation Columns Using Thermodynamic Analysis. *Separation Science and Technology*, 41 (5), pp. 791-817.

Dhole, V. and Linnhoff, B. (1993).Distillation column targets. *Comput. Chem. Eng.,* 17(5), pp. 549-560.

Ghorbani, B.,Maleki, M., Salehi, A., Salehi, R. and Amidpour, M.(2013).Optimization of Distillation Column Operation by Simulated Annealing. *Gas Processing Journal*,1 (2), pp. 49-63.

Odigo, B. (2003). *Evaluation of Propane – Propylene Splitter in WRPC*. Unpublished Report. NSE Technical Report.

Olakunle, M. and Oluyemi, Z. (2008).Distillation Operation Modification with Exergy Analysis. In: Proceedings of the 38th NSChE conference, Oct 30 – Nov 1, Effurun, Nigeria.

Umo, A. and Bassey E. (2013).Simulation and Performance Analysis of Propylene-Propane Splitter in Petroleum Refinery Case Study. In: Proceedings of the 43rd NSChE conference, Nov 4-6, Uyo, Nigeria.

HEAT EXCHANGER NETWORK OPTIMIZATION OF NAPHTA HYDROTREATING UNIT OF A NIGERIAN REFINERY USING PINCH ANALYSIS

*[1]AZEEZ O. S, [2]SUNDAY U. B and [3]SULEIMAN, B

DEPARTMENT OF CHEMICAL ENGINEERING, FEDERAL UNIVERSITY OF TECHNOLOGY, MINNA, NIGERIA

*Corressponding author: tosin.azeez@futminna.edu.ng;bilyaminusuleiman@futminna.edu.ng

ABSTRACT

Energy integration of the Naphtha hydro treating unit (NHU) of a Nigeria Refinery Company was carried out using Pinch Technology. It was revealed that the traditional requirements of utilities for heating and cooling of streams are 21,080,000Kcal/h and 19,340,000Kcal/h respectively. When pinch technology was adopted for the same process, the heating and cooling utilities requirements are 13,950,000Kcal/h and 12,210,000Kcal/h respectively. Optimum minimum temperature difference of 13ºC was obtained for the determination of utility requirements. The temperature at the pinch point was found to be 205ºC. For the minimum approach temperature, the utilities targets were found to be 11,940,000Kcal/hr and 10,200,000Kcal/hr for hot and cold utilities respectively. For maximum energy recovery, the total numbers of heat exchangers is 23. Pinch analysis is seen to be an efficient technique for energy integration that saves more energy and utilities cost than the traditional energy technique.

Key Words:*cold stream, hot stream, cold utilities, hot utilities, minimum approach temperature, maximum energy recovery, optimum temperature.*

1.0 INTRODUCTION

The cost of energy usage has contributed to the global cost of production in process industries. This has the tendency to affect the profit made by industries negatively. Recently, the cost of energy increased tremendously, and what happened then is still possible because of the volatility in oil market.. When the price of oil continued to climb in the recent past, the sustainability of industrial development became an issue of concern at the period. Though, the price of oil has fallen drastically at the moment, energy conservation still remains the focus of many process industries since oil price and cost of energy are very relevant to their existence. In any industrial process design, it is economical to maximize the process-to-process heat recovery and to minimize the utility usage. In order to achieve maximum energy recovery or minimum energy requirement (MER,) heat exchanger network (HEN) has been synthesized using either the pinch technology or mathematical programming (Linnhoff and Ahmad, 1989; Salomeh *et al.,* 2008; Azeez, *et al.*, 2013). Pinch technology has been widely studied for HEN synthesis (Hallale and Fraser, 1998; Linnhoff and Ahmad, 1990; Linnhoff, et al.,1982). Mathematical programming techniques have also been used as energy optimization tools (Azeez *et al.,* 2013; Isafiade and Fraser, 2008).

Therefore, efforts towards reducing energy and costs of production have been continuously explored.

Based on the thermodynamic principles, pinch technology offers the opportunity to integrate the energy in a process for optimum cost. It also helps to evolve design with reduced capital cost and energy requirements. It can as well be used for the modification of existing processes by way of retrofitting. The main advantage of pinch technology is its ability to set an energy target before starting the design. The energy target provides the minimum theoretical energy required for the process (Akande, 2007). Linnhoff et al. (1979) in their work explain the relation between the minimum temperature difference ΔTmin and energy recovery, using the composite curves in a similar manner to Huang and Elshout (1976). Linnhoff and Hindmarsh (1983) presented and use the pinch point as the most constrained region of a design. In their method, the task was divided into two at the pinch point as separate systems (above and below the pinch point). In the design of a network, it must starts at the most constrained region of the system, which is immediately above or below the pinch point (Hallale, 1998). Feasibility criteria that are normally used to decide which streams are to be matched are contained in Smith (2005).

Evaluation of maximum energy recovery and minimum number of units at ΔTmin values made it possible for a design engineer to distinguish between a good and a bad network structure before the design. Various researchers have discussed targeting for minimum heat exchanger area in relation to heat content and the composite curves. The approached is based on equal heat transfer coefficients between all matches in the network and on vertical counter-current heat transfer between the composite curves. General overviews of pinch based synthesis and design are contained in Nishida et al. (1981); Smith (2005); Westerberg (1980) along with those earlier mentioned. However, Townsend and Linnhoff (1984) in their work

extended the approach to account for individual heat transfer coefficients for each streams using the Bath formula, with consideration for the spaghetti network. Their formulation is though an approximation but works well in many situations (Azeez, *et al*., 2013).

Ahmed and Linnhoff (1984) studied cost targeting for the cost effective ΔTmin before design. The cost of energy, cost of minimum number of units, and cost of heat exchanger area at different values of ΔTmin were evaluated and drawn in a cost -ΔTmin plot, from which the cost-effective ΔTmin was selected. Ahmed and Smith (1989) further worked on cost targeting where they developed a technique that enabled capital cost targets to take into account different materials of construction, pressure ratings, and heat exchanger type. Concept of supertargeting was presented by Hallale and Fraser (2000) where they used pinch-based techniques for mass exchanger networks.

In this research, pinch technology has been used to evaluate the hot and cold utility requirement of a naphtha hydrotreating unit (NHU) of a Nigerian refinery. In the research, it was assumed that traditional method can as well be used to effect energy need in the process. A comparison between the traditional method and the pinch analysis for energy usage was then made to know the amount of energy savings that is possible for the process.

The need for the reduction in total annual cost (TAC) in refineries production process through the reduction in energy usage in terms of utility is the motivation for this research.

2.0 METHODOLOGY

Materials

The material used for this research work is sourced from the Process Flow Diagram (PFD) of NHU of the refinery.

Methodology

Below is the necessary steps taken in the analysis, designing and optimization of any heat integration problem:

2.1 Data Extraction:

Data extraction is time consuming in the task of pinch analysis. It involves the identification of the hot and cold process streams as well as utilities in the process line. That is, those streams that need to be cooled and those that need to be heated alongside their thermal properties, flowrates, phase changes and the temperature through which they must be cooled or heated. The information above can be available in the PFD, in the field (from the plant personnel) or using of modeling tools such as simulation and data reconciliation for set of consistent and reliable data. As shown in Table 1, the extracted data of the NHU is from the PFD.

Table 1: Data of NHU extracted fro PFD

Stream no	Stream Type	Supply Temperature (°C)	Target Temperature (°C)	Heat Duty (Kcal/hr)
1	Cold	39	293	2.416×10^6
2	Hot	370	125	2.416×10^6
3	Cold	293	370	6.38×10^6
4	Hot	125	48	5.93×10^6
5	Hot	48	40	5.20×10^5
6	Hot	46	40	3.50×10^5
7	Cold	40	133	6.41×10^6
8	Hot	237	133	6.41×10^6
9	Hot	77	48	4.39×10^6
10	Hot	48	40	5.60×10^5
11	Cold	200	237	1.47×10^7
12	Hot	221	190	4.20×10^6
13	Cold	137	137.2	4.20×10^6
14	Hot	72	55	5.09×10^6
15	Hot	55	35	2.30×10^5
16	Hot	137	48	2.10×10^6

17	Hot	48	40	1.70×10^5

3.0 RESULT AND DISCUSSION

The data extracted from the Process Flow Diagram (PFD) were inputted into the "Aspen Energy Analyzer" software and the results obtained are d-iscussed as follows:

3.1 The Composite Curve of NHU

The composite curve of NHU is plotted as the temperature against enthalpy for hot and cold streams as shown in Figure 1. It determines the minimum targets for energy requirement.
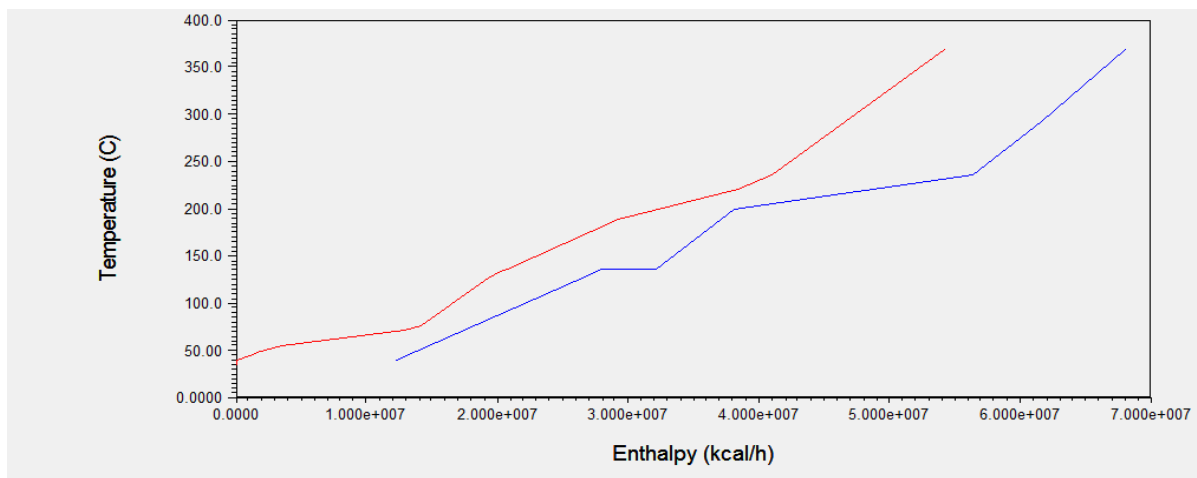
Figure 1: The composite curve of NHU

The composite curve plot of NHU as generated by the package is shown in Figure 1 having the hot composite curve represented in red while the cold composite curve is represented in blue. The maximum heat recovery possible for the process is represented by the overlap between the hot and the cold composite curves. The composite curves are closest to each other at the hot stream temperature of 220ºC and cold stream temperature of 200ºC (that is, they are 20ºC apart which is the initial ΔTmin taken). It equally reveals the minimum hot utility (Q_{HMIN}) and minimum cold utility (Q_{CMIN}) requirements as an overshoot of the cold composite curve and the hot composite curve to be 13,950,000Kcal/h and 12,210,000Kcal/h respectively
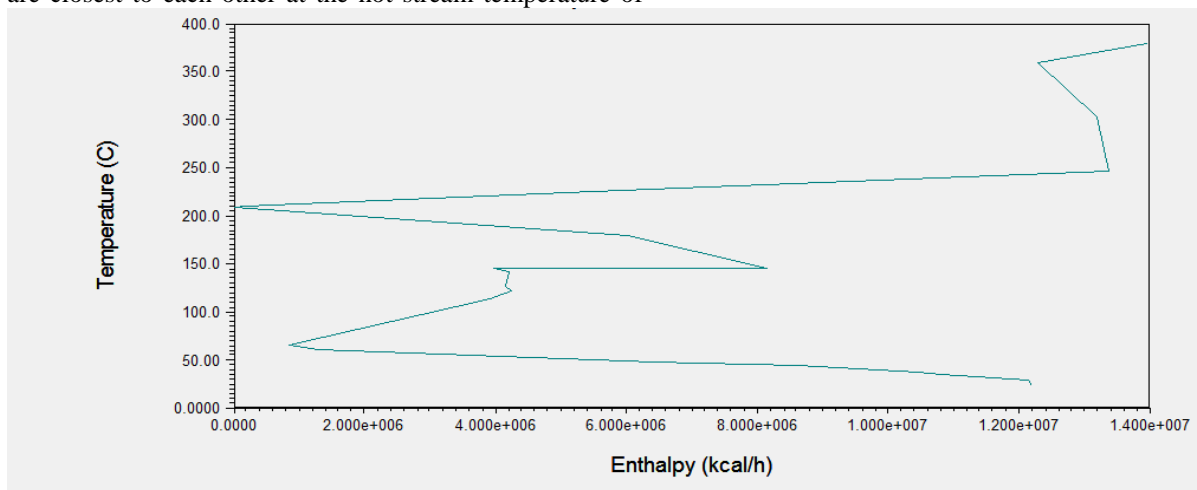
Figure 2: The Grand Composite Curve of NHU

3.2 The Grand Composite Curve of NHU

In the Grand Composite curve shown in Figure 2, the pinch occur at a point where the curve touches the temperature 220ºC and it divides the curve into two regions, that is, above pinch and below pinch. The minimum utility requirement for both hot and cold are represented by the distance between the end of the above and the below curves regions and the temperature

3.3 Energy Requirement Results of NHU

The results obtained are shown in Tables 2 to 5. The traditional energy requirements are calculated result from the process flow diagram while the energy target values are from the analysis using the program

Table 4: Comparison of Energy Requirement between traditional approach and pinch analysis

Table 2: Traditional Energy Requirement values

Minimum hot Utility Requirements (Kcal/h)	Minimum cold Utility Requirements (Kcal/h)
21,080,000	19,340,000

Table 3: Energy Target Values of NHU based on pinch Analysis

Initial ΔT_{min} (ºC)	Pinch Tempe-rature (ºC)	Energy Target (Q_{Hmin}) (Kcal/h)	Energy Target (Q_{Cmin}) (Kcal/h)
20	220	13,950,000	12,210,000

Table 5 shows the energy requirements at optimum ΔTmin values where a further reduction in energy usage was observed. At optimum ΔTmin , minimum number of heat exchange units targeted is 23 which is higher than that obtained for initial ΔTmin which is 17 units. Azeez, *et al.* (2013) however, observed that lower number of units does not eventually translate to lower TAC. The network design for this NHU is shown in Figure 3 while Figure 4 indicates the pinch position in the network.

	Energy Requirement (Kcal/h)		Savings (%)
	Traditional	Pinch Analysis	
Energy Target (Q_{Hmin})	21,080,000	13,950,000	33.82
Energy Target (Q_{Cmin})	19,340,000	12,210,000	36.87
Total Energy	40,420,000	26,160,000	35.28

Table 5: Energy Target Result Based on optimum ΔTmin

Optimum ΔTmin (ºC)	Pinch Temperature (ºC)	Energy Target (QH min) (Kcal/h)	Energy Target (QCmin) Kcal/h
13	205	1.194×10^7	1.020×10^7

The minimum heating and cooling requirements for the traditional approach is shown in Table 2 while Table 3 shows the pinch analysis energy requirement. A table of comparison for the values is shown in Table 4 and from observation; a significant savings of energy requirement is noticed. Saving of 33.82% and 36.87% for hot and cold respectively and the overall savings is found to be 35.28% which is a good saving for refineries.

3.4 Design of Heat Exchanger Network for NHU
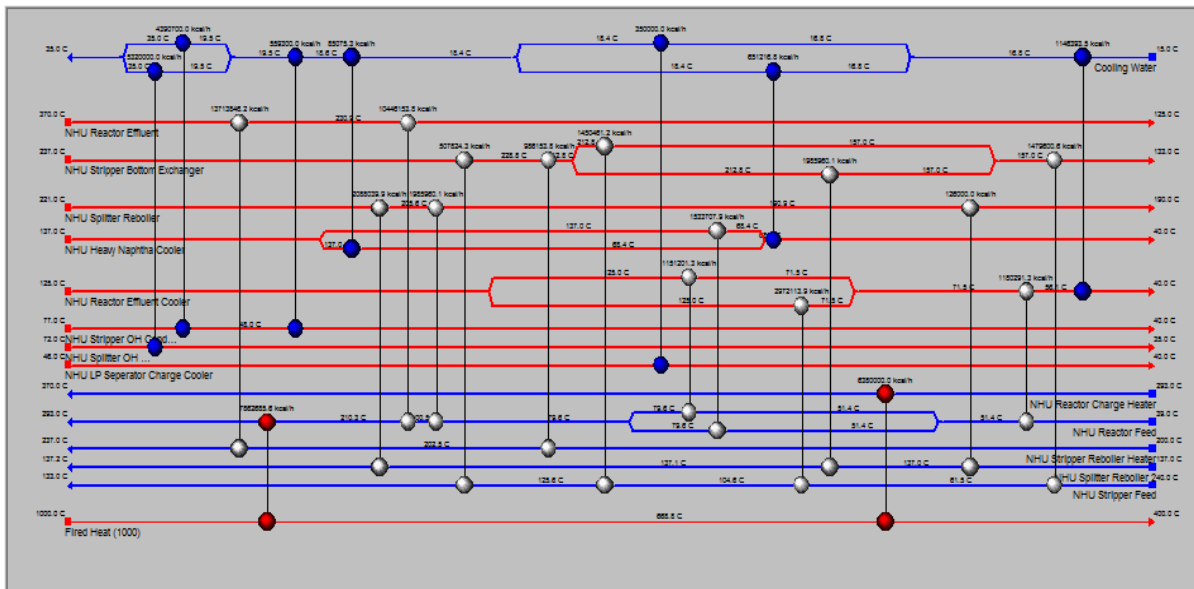
Figure 3: Complete HEN Design of NHU
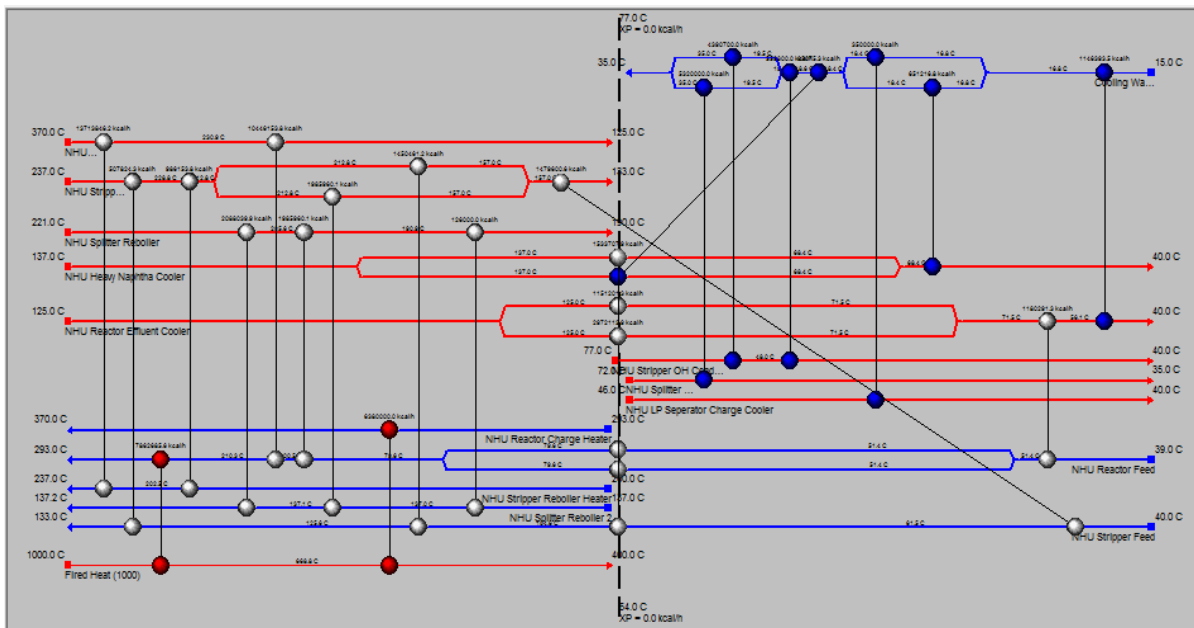
Figure 4: HEN Design showing the Pinch Line

4.0 Conclusions

The following conclusions were drawn from the result of the analysis:

1. The pinch point for the analysis was found to be 220ºC and the minimum temperature approach of 20ºC was used to determine the energy target.

2. For minimum approach temperature of 20ºC, the utilities targets were found to be 13,950,000Kcal/h and 12,210,000Kcal/h for hot and cold utilities respectively.

3. The optimum ΔTmin was found to be 13ºC, and the utilities targets were found to be

11,940,000Kcal/h and 10,200,000Kcal/h for hot and cold utilities.

4. Energy savings were found to be more using pinch analysis as an energy integration technique than the traditional energy technique.

5.0 References

Ahmad, S. and Linnhoff, B. (1984). "Overall cost targets for heat exchanger networks. "
In *IChemE Annual Research Meetingg*. Bath, UK.

Ahmad, S. and R. Smith,(1989). "Targets and Designfor Minimum Number of Shells in Heat
Exchanger Networks." *Chemical Engineering Research & Design,* **67**, (September): pp. 481-494

Akande H. F. (2007). Energy Integration of Thermal Hydro-dealkylation Plant, *M. Eng Thesis*, FUT Minna, Minna, Nigeria.

Azeez O. S, Isafiade A.J, Fraser D.M, (2013). ''Supply-based superstructure synthesis of heat
and mass exchange networks'' *Computer and Chemical Engineering,*. **56**. pp. 184 - 201

Hallale, N. (1998). Capital cost targets for the optimum synthesis of mass exchange networks, *PhD thesis*, Department of Chemical Engineering, University of Cape Town.

Hallale, N. And Fraser, D. M. (1998). Capital cost targets for mass exchange networks, a special case: Water minimization, *Chem. Eng. Science*. **53**,(2), pp. 293 -313
Hallale, N and Fraser, D. M. (2000). Supertargeting for Mass exchange Networks. Part 1, Targeting and Design technique. *Trans IChemE,* **78**, Part A. pp. 202 – 207.

Huang, F. And Elshout, R. V. (1976). " Optimizing the heat recovery of crude units" *Chem. Engng Prog*. **72**, pp. 9-23.

Isafiade, A.J. and Fraser, D. M. (2008). Interval based MINLP superstructure synthesis of heat exchange networks, *Chem. Eng. Research. Des.* **86**(3), pp. 245 – 257.

Linnhoff, B., D.R. Mason, and I. Wardle, (1979)."Understanding heat exchanger networks. "
Computers& Chemical Engineering, 3(1-4): p. 295-302

Linnhoff, B., Townsend, D. W., Boland, D., Hewitt, G. F., Thomas, B.E.A., Guy, A.R. and Marsland, R.H. (1982). A user guide on process integration for the efficient use of energy. The institute of chemical engineering, U.K.

Linnhoff, B. and Ahmad, S. (1989). Supertargeting: Optimum synthesis of energy management systems. *ASME J. Energy Resource Tech.*, September **111** (3)pp. 121-130.

Linnhoff, B. and Ahmad, S. (1990). Cost Optimum heat exchanger networks (Part 1). *Comp. & Chem. Eng*., **14**(7),pp. 729 – 750.

Linnhoff B. and Hindmarsh, E. (1983). Pinch Design Method of Heat Exchanger Network,
*Chemical Engineering Science,***38** (5), pp. 745-763

Nishida, N., G. Stephanopoulos, and A.W. Westerberg ,(1981). A review of process
synthesis. *American Institute of Chemical Engineers Journal*, **27**(3): pp.321-349.

Salomeh C, Dargahi R, Mahdavi A. (2008). Modification of Preheating Heat Exchanger Network in Crude Distillation Unit of Arak Refinery Based on Pinch Sama, Technology, WCECS (ISBN: 978-988-98671-0-2)

Smith R. (2005). Chemical Process Design and Integration. John Wiley & Sons, Ltd. England

Townsend, D.W. and B. Linnhoff. 1984. "Surface Area Targets for Heat Exchanger
Networks." in*IChemE Annual Meeting*. Bath, England.

P 009

OIL AND GAS CHALLENGES AND ENVIRONMENTAL SOLUTIONS

[1]Otu, F. I., [2, *]Otoikhian, S. K. and [3]Diamond, B

[1]Department of Mechanical Engineering, Federal University of Technology, Akure

[2,*]Department of Chemical Engineering Technology, Auchi Polytechnic, Auchi

[3]Department of Mechanical Engineering Technology, Auchi Polytechnic, Auchi

Corresponding e-mail: kev4za@yahoo.com ; otoigunvin@gmail.com

Abstract

The oil and gas industry is an essential pillar of the nation's economy. The challenges in the industry can be solved through public private partnership. Pipeline vandalism, frequent changes in national oil and gas company management and its incoherent policy, oil bunkering, insurgency, fluctuating crude oil prices, business joint venture and decay of infrastructures, gas flaring and gas pricing were identified as the key problems. The solutions are: The Federal Government should develop national plan for critical infrastructure. The pipelines Act, Cap 338 of 1990, the Oil Pipeline Regulations and the Miscellaneous Offence Act (1984) should be harmonized. Security forces, people of host communities and their rulers should be used to monitor pipelines and other facilities. Reorganization and restructuring of the national oil and Gas Company, adequate punishment for oil thieves, the setting up of modular refineries, social security schemes, provision of social amenities and payment of compensation were seen as solutions. Other solutions include diversification of the fuel and non-fuel mix, rehabilitation of damaged infrastructures, reduction of federal government stake in joint ventures to 40-49% share, reduction in gas flaring, gas pricing reforms and the upgrading of information and communication technology facilities.

Keywords: *Pipeline vandalism, gas flaring, oil thieves, modular refinery, gas pricing.*

1.0 Introduction

Oil and gas is an essential pillar of the rapid socioeconomic development of any nation. It is used to power agricultural, commercial, domestic, transport machineries and industrial which are used for productive and transportation activities that facilitate economic growth and development (Bhardwaj, 2013). All nations of the world, both oil and gas producing and non oil and gas producing alike, depend on energy and a slight change in the cost of energy normally affects all sectors of the economy. In order words, high energy cost leads to high cost of production of goods and services as well as high cost of commodities in the market. This is why it becomes imperative for some countries of the world to regulate the prices of oil and gas in order to ensure that the cost of production is maintained at a minimal level while the prices of commodities are not beyond the reach of the common man. The rapid devaluation of the naira can be attributed in part to lower oil prices which have wiped out billions of naira in market capitalization for Nigeria's fledging indigenous oil and gas companies and with it a good percentage of the value of our recently rebased economy (Ajumogobia, 2015). The exploration, production and marketing of oil and gas products are not without their challenges. The challenges of oil and gas industry vary from one place to another. Nevertheless, there are some problems which are common to the industry all over the world. In the light of this, this study will classify oil and gas key challenges into two broad categories: local problems and general problems. The local problems are peculiar to the Nigerian situation while general problems are found in all regions of the world where oil and gas industries

are located. The dwindling fortunes of the oil and gas industry are affected by the following unrelated factors. According to Ajumogobia 2015, pipeline vandalism, oil theft, militancy, frequent changes of the management of NNPC, ageing assets and volatility of oil prices, gas flaring and gas pricing are the key challenges.

2.0 Challenges and Solutions
2.1 Pipeline Vandalism

The effects of pipeline vandalism and its negative socio-economic impact on our country cannot be overemphasized. This economic sabotage is often caused by oil thefts. This menace has become a cankerworm in the socio-economic and political fabric of the nation Nigeria. Its attendant adverse effects on the investment inflow into the country cannot be over emphasized. It is estimated that a total of 16083 pipeline breaks were recorded within the last 10 years and 10 millions barrels of crude oil valued at 894 million dollars were lost to pipeline vandalism within the same period (NEITI, 2014). Pipeline vandalism in 2011, 2012 and 2013 were 4468, 3708 and 3571 respectively (PPMC, 2014). The following are some of the negative effects of pipeline vandalism which is frequently the results of oil bunkering. It caused a drop in oil production as a result of shut down by oil and gas firms. Some of the gas-powered stations are not producing due to absence of gas supply while most of the stations are generating electricity below the maximum levels. The Port Harcourt Refinery Company Limited which is composed of two refineries restricted its refinery operation to about three months in 2014 due to pipeline breakage and rupturing (PPMC, 2015). It requires some joint effort of all and sundry to tackle the problem of pipeline vandalism because of the negative implications it had on the nation's economic growth. This issue should be tackled culturally, psychologically and economically. The Federal Government needs to develop national plan for critical infrastructure and key resources protection similar to the United States' National Infrastructure Protection Plan (NIPP) (Momoh, 2014). Also, there is need to harmonize the Oil Pipelines Act, Cap 338 of 1990, the Oil Pipelines Regulations which are made pursuant to the Act and the Miscellaneous Offences Act (1984). The lingering disruption of pipelines in the country has resulted in the use of Marine vessels for crude oil deliveries to the refineries. The option of transporting by marine vessels has increased the operational cost of refining in the country (Momoh, 2014). The Directorate of State Security Service (DSS) in collaboration with the Nigerian Security and Civil Defense Corp (NSCDC), the armed forces and the police as well as the local vigilante group, the people of the host communities of the pipeline right of way and their traditional rulers would be able to provide a formidable force to counter pipeline breakage and oil and gas production disruption. Furthermore, there should be amnesty programme and a social security scheme for the restive youths in the host communities as well as provision of social amenities that make life comfortable and have a sense of belonging to the host communities of the pipeline right of way in order to pacify them.

2.2 Oil and Gas Company Management:

Incoherent oil and gas policy is also a major challenge of the oil and gas sector in Nigeria. This is due partly to the frequent change of important officials of NNPC and the Department of Petroleum Resources (DPR). For instance, since the NNPC was created 38 years ago, it has had 16 Group Managing Directors. In 30 years from 1977 to 2007 there were nine - an average of one every three years. Thereafter, appointments to that office became even more frequent. Similarly, the Department of Petroleum Resources (DPR) has had a similar high personnel turnover - six DPR directors in seven years (Ajumogobia, 2015). Pragmatic reforms to boost accountability and transparency should be implemented in Nigerian's oil and gas industry.

There should be full scale reorganization and restructuring of the Nigerian National Petroleum Corporation and its subsidiaries as this would help make the corporation a globally competitive company. Furthermore, the Petroleum Industry Bill (PIB) should be given the attention it deserves by the National Assembly and the controversial oil subsidy should be removed.

2.3 Oil Bunkering: Oil bunkering is one of the major challenges confronting the oil and gas sector. In 2013 a new and frightened phenomenon emerged. It was revealed by the Finance Minister then that Nigeria was losing up to 400,000 barrels per day to crude oil theft. This damaging phenomenon is completely inexplicable, especially in the light of vehement denials of collusion and assurances of our security agencies of their resolve to stop oil theft. Though apparently reduced from that incredible level the current estimates of approximately 150,000 barrels per day are an indication of a serious malaise. Nigeria lost a total of 10.9 billion dollars to oil theft between 2009 and 2011 (Ajumogobia, 2015). This economic sabotage and the inherent loss of human lives due to pipeline explosion can be curbed by enacting a law prohibiting oil bunkering and long term of imprisonment clearly spelt out in the law and there should be constant surveillance of our pipelines by the security forces, the host communities and their rulers.

2.4 Militancy or Insurgency: Militancy or Insurgency has been identified as one of the accompany problems of many years of neglect of the host communities by oil and gas prospecting companies. It has a political dimension and youth restiveness is linked to political pressures. Vandalism of infrastructural facilities is consistently carried out during insurgency, despite the inadequacy in infrastructural provision (Ola and Adewale, 2014). The personnel of the oil and gas companies and their facilities are also attacked. The non-challant attitude of the oil and gas companies towards clearing up polluted environments by the oil spillage has pitted them severally against their host communities. The spiraling effect has led to widespread canalization of oil pipelines with the attackers claiming that their source of livelihood, farming and or fishing, had been decimated by the companies with little or no compensation (Huffington, 2015). This problem can be curtailed by provision of social security schemes for the youths and the provision of social amenities like electricity and healthcare facilities. Furthermore, story boards can be geared towards solving the problem of environmental pollution in the Niger Delta region. It deals with the simulation of industrial accidents (gas leakages) and condensate. This can be employed towards building a framework involving "knowledge base" with the use of Narrative Knowledge Representation Language (NKRL) which involves the collection of formal statement with negligible loss of information (Bhardwaj, 2013).

2.5 Fluctuating Crude Oil Prices: Crude oil price fell from a high value of 150 dollars per barrel in the middle of 2008 to less than 40 dollars per barrel at the beginning of 2009. Crude oil and gas prices is determined to some extent by political unrest and instability in different parts of the globe, supply of commodity in the world oil and gas market as well as technological innovations. For example the political crisis in the Middle East and exploration of shale oil by the United States of America has resulted to the recent fluctuation in crude oil price. The fluctuation in crude oil prices can lead to variation in energy per unit price, the acute shortage of skilled manpower due to early retirements as well as slow approval of new projects in the oil and gas industry (Bhardwaj, 2013). The shock resulting from fluctuation in crude oil prices can be absorbed through systematic diversification of the oil and gas sector, variation in the transport fuel mix such as premium motor spirit (petrol or gasoline), diesel, Dual Purpose Kerosene (DPK), Aviation Turbine Kerosene (ATK), household kerosene, Pour Fuel Oil (LPFO), shale oil or bitumen derived crude

oil, bio-fuels, biodiesel and bio-ethanol. Again, atomization of drilling mechanism and robotic technology can play an essential part towards ameliorating this problem.

2.6 Business Joint Venture: Lack of investment based on the joint venture structure in particular and the inability of NNPC constrained by budget limitations to always meet its financial obligations to the joint venture, for replacement of ageing and dilapidated assets, especially pipelines and depots many of which have long passed their 'shelf life' is another risk factor that will continue to affect the efficiency and well being of industry by substantially increasing operating costs and environmental pollution (Ajumogobia, 2015). This problem can be solved by compelling the Ministries of Petroleum Resources and Finance to incorporate the existing joint venture companies in the upstream petroleum industry with the Federal Government opting to make a minority stake of 40-49% apart from being listed on the Nigerian Stock Exchange market. All dilapidated assets, pipelines and depots, should be replaced and/or repaired.

2.7 Gas Flaring: Gas flaring is one of the key challenges facing the oil and gas industry. Many countries of the World have taken advantage of the economic benefits which flared gas may present, through re-injection into the fields of associated gas or conversion into liquid natural gas (LNG), domestic cooking gas and plastic production. The quantity of flared gas could also be used for the development of gas reserves to fuel the power section through the construction of gas-fired power points and gas pipelines for delivery of gas to power plants as well as gas-utilizing fertilizer and petrochemical industries. The problem of gas flaring has remained unresolved in Nigeria for many decades (Adejugbe *et al.* 2014). According to statistical data obtained from NNPC, Nigeria lost about one billion dollars from oil companies flaring gas between January to September 2014. Nigeria has the largest natural gas reserves on the African continent with about 187 trillion cubic feet of proven gas reserves and 600 trillion cubic feet of unproven gas reserves. The adverse consequences of gas flaring are numerous. Some of them are huge economic waste in form of lost revenue from gas as already mentioned. Flared gas is known to contain toxic substances which cause respiratory disease and air pollution, leading to the depletion of the ozone layer, ultimately having an adverse effect on weather and climate (Adejugbe *et al.* 2014). Gas flaring has not been eliminated as a result of lack of political will on the part of the government, the unavailability of the infrastructure required to control gas flaring and perhaps there is no available market for domestic gas products as well as the low price of gas.

To solve these gas teething problems the government should establish a strategic gas development framework in form of incentives and desirable large-scale capital investment. Also, the government should encourage gas utilization and flaring reduction which requires sustainable investment in infrastructure. There should be strict measures to ensure the effectiveness of anti-gas flaring protocols and a mandatory requirement for a gas flaring plan to be submitted by all oil and gas operating companies in the country to the appropriate government regulatory authority in the oil and gas sector.

2.8 Gas Pricing: There has been a controversy between investors on gas projects and the NNPC and the government for over a decade now on gas pricing. This has a disastrous consequence on the economic development of the gas sector. To this end, there should be price reforms, improvement in regulatory arrangements, redefinition of the role of public companies in the gas sector and a workable alternative to the current NNPC joint venture financing system and implementation of the Gas Master Plan (Asu, 2015).

3.0 Conclusion

Information and communication technology facilitates in the oil and gas industry should be upgraded to meet up with the current advanced technological trends whereby information and automatic devices including robotics are highly needed to solve these challenges in the present day oil and gas industry.

4.0 Reference

Adejugbe, A and Onamade, B. (2014): In an article entitled 'Nigeria: Gas Flaring in Nigeria, Challenges and Investment Opportunities' in Strachan Partners of 31 July 2014.

Ajumogobia, O. (2015): In an article titled 'Ajumogobia Identifies Challenges in Nigeria's Oil and Gas Sector' in This Day Live of 12 February 2015.

Asu, F. (2015): In an article titled 'Nigeria Loses 170 billion naira to Gas Flaring', in Punch of 2 January 2015.

Asu, F. (2014): In an article titled 'Pipeline Vandalism and its far-reaching effects on Nigeria, in Business Day of 27 August 2014.

Bhardway, A. (2013): Challenges and Solutions in an Upstream and Downstream Oil and Gas Operation. Published in Houston, Texas in USA

Huffington, A. (2015): In an article titled 'The problem with Private Refining in Nigeria' in Nairaland Forum of 11 May, 2015.

Joda, A. (2015): In an article titled Oil and Gas Committee Set Targets for Government' in Ahmed Joda Led Transition Committee's recommendation on oil and gas industry, published in Premium Times of 27 July 2015.

Momoh, H. (2014): In an article titled 'Pipeline Vandalism and its far-reaching effects on Nigeria' in Business Day of 27 August 2014.

NEITI, Nigeria Extractive Industry Transparency Initiative (2014): In an article titled 'Pipeline Vandalism and its far-reaching effects on Nigeria' in Business Day of 27 August 2014

NNPC, Nigerian National Petroleum Corporation (2015): NNPC website publications June 2015.

PPMC, Pipelines and Products Marketing Company (2014): PPMC A Subsidiary of Nigerian National Petroleum Corporation in NNPC website publications in June 2014.

PPMC, Pipeline and Products Marketing Company (2015): PPMC A Subsidiary of Nigerian National Petroleum Corporation in NNPC website publications in June 2014.

Ola, A. B. and Adewale, Y.Y. (2014): Infrastructural Vandalism in Nigerian Cities: The case of Osogbo, Ogun State. Research on Humanities and Social Sciences Vol.4 No.3

Primeast Corporation (2015): Top 5 Challenges Facing Oil and Gas Companies.http://primeast.com/news/top5challengesfacingoilandgascompanies.

Yusuf, Y. (2014): 'Pipeline Vandalism and its Socio-economic Effects on the Nation' a paper delivered at the Annual Conference of the National Association of Energy Correspondents (NAEC) in Lagos held on 21 August 2014

P 010

DEVELOPMENT OF PRIVATE REFINERIES IN NIGERIA

[1]Otu, F. I., [2,]Otoikhian, S. K. and [2]Anakhu, A. E*
[1]Department of Mechanical Engineering, Federal University of Technology, Akure
[2]Department of Chemical Engineering Technology, Auchi Polytechnic, Auchi
*Corresponding e-mail: kev4za@yahoo.com ; otoigunvin@gmail.com

Abstract

Nigeria is a member of the Organization of Petroleum Exporting Countries (OPEC). That not withstanding it is an importer of refined petroleum products. This paper explores the development of small-scale modular private refineries and large-scale conventional private refineries. Some of the major problems encountered in the process of developing private refineries in Nigeria were discussed. These are government regulation of refined petroleum product prices, low profit margin in a regulated economy, hostile environment, lack of funds and lack of crude oil in the refinery site. Solutions were offered to these problems in order for the smooth development of private refineries. These solutions are the establishment of modular and conventional private refineries, conducive operating environment, deregulation of the downstream oil sector, mobilization of funds by Nigerian businessmen, setting up of refinery technical crew and the diversification of the products from the private refineries to increase the contribution of fuel and non-fuel products from these refinery firms to the gross domestic product. Consequently, the present dwindling revenues accruing to the country as a result of the fall in oil prices will be drastically changed and Nigeria will become net exporter of refined petroleum products.

Keywords: Private refinery, petroleum product, crude oil, modular refinery, conventional

1.0 Introduction

Nigeria has been one of the world's leading importers of refined petroleum products for over two decades now. This unenviable position has earned the nation a very bad image among the Organization of Petroleum Exporting Countries (OPEC). It is very clear that the absence of functional refineries has multiple negative effects on the nation's economy and it is a big strain on foreign reserves in particular and the economy in general (Alike, 2015). How Nigeria can get out of the problem of importing refined products and become an exporting country of refined petroleum products expected of a big crude oil producer through the establishment of private refineries is the theme of this paper. It is clear that involving the private sector participation in the petroleum refining aspect of the important energy sector of the nation's economy will essentially solve the current problems of available and refined crude oil products for domestic consumption and perhaps for export (Atojoko, 2015). The present scenario whereby one of the worlds's leading exporter of crude oil

is importing premium motor spirit (petrol) is unacceptable. Obviously, the development of private refineries will be the solution to this problem. Undoubtedly, operating functional refineries in the country would not only increase the supply of the following refined petroleum products: Automotive Gas Oil (AGO), Base oil, Bitumen, High Pour Flow Oil (HPFO), Liquidified Petroleum Gas (LPG), Polypropylene, and Premium Motor Spirit (PMS) to the domestic marketers but would also guarantee supplies to neighbouring Economic Community of West African States (ECOWAS). It will create employment for the teeming unemployed youths and bring to an end a fast-encroaching poverty and hunger (Igwe, 2014). Additionally, the huge financial cost to the nation in terms of freight charges, storage and demurrage incurred on late delivery of petroleum products cannot be overemphasized. The design, construction and commissioning of functional private refineries in different locations of Nigeria would bring to an end the petroleum subsidy fund (PSF), price equalization, bridging cost and

other subsidies paid by the government to help oil marketers to import, store and distribute petrol under a regulated economic system (Lukman 2010).

2.0 Problems and Solutions:
Problems
What are the major problems militating against the smooth taking off of private refineries in Nigeria?

Government Regulation: The federal government regulates the prices of the refined petroleum products in Nigeria through the Petroleum Products Pricing and Regulatory Authority (PPPRA). The upstream sector is not regulated. The non-regulation of the upstream sector is not unconnected with the large number of local and foreign investors such as Chevron, Conoil, Mobil, Seplat and Shell found in this sector. However, the midstream and downstream sectors are regulated by the continuous fixing of the prices of petroleum products by PPPRA.

Profit Margin: Private investors are not willing to invest their money where they would sell the refined products at stipulated official price (Ogedegbe, 2009). One of the greatest hurdles to any private investor anywhere in the world is the inability to recover the cost of investment within a stipulated period and make profit. There is no doubt that the total deregulation of the telecommunication industry by the federal government more than a decade ago brought sanity and competition into the sector which was better transformed by multinational telecommunication companies such as Airtel, Etisalat, GLO and MTN. Deregulation of the midstream and downstream sectors of the petroleum industry will encourage local and foreign investors to pump their financial resources into the sector and guarantee full cost recovery for investors. It will also bring about competition among the major investors and increase domestic production of refined products. The fear being nursed by private investors, both local and international, is that they will not be able to recoup their investments in the private

refinery industry if the present regulation policy is not reversed.

Conducive Environment: The regular incidents of attacks on government oil installations across the country, more especially in the Niger Delta areas by pipeline vandals and hostile operating environment is one of the major barriers encountered by licensees of privately owned refineries that borders on the issue of security. The increasing waves of crude oil theft and other criminal activities in the sector will greatly hamper the establishment of privately controlled large and cottage refineries. The security of the refineries and other subsidiary ventures is an important factor to be considered by investors before they set up their industrial outfit in such regions (Ogedegbe, 2009). No investor, whether local or foreign, is ready to put his financial resources in troubled areas.

Lack of Fund: Another problem militating against the establishment of private refineries in Nigeria is the absence of fund. Refinery business is a capital intensive venture that requires a lot of money running into billions of dollars. The local entrepreneur may not be able to source for this huge amount of money alone. He has to go into partnership with local and international oil companies to be able to secure the required capital. Again, the formation of a strong partnership between Nigerian banks and domestic oil and gas firms can guarantee the establishment of functional refineries in Nigeria (Ubah, 2010). Consistent investment infrastructure in the oil sector will eventually end the current challenge of fuel scarcity and ensured an uninterrupted supply of locally refined petroleum products to the Nigerian market and beyond its shores.

Lack of Crude Oil: The failure of 17 investors out of the 18 investors licensed in 2002 to build private refineries in the country has been attributed to lack of crude oil. These investors were not satisfied with the federal government's position that they would buy the country's crude oil at the international market price as this would not guarantee good returns on investment since

they would sell the refined products at stipulated official price (Izeze, 2015).

Solutions: Establishment of Modular Refineries: Long term thoughtful strategy is very important to be able to solve the problem of acute fuel shortages in Nigeria. Looking at the demand and supply schedule of the Nigerian citizens, the most appropriate solution to filling the gap is to build private refineries to complement the four refineries built by the national oil company, the Nigerian National Petroleum Corporation (NNPC) to meet the citizens' demand. Personal primitive acquisition of wealth through importation of petroleum products by few notorious oil cabals is not the solution. There is a two dimensional approach to this issue through the establishment of small scale and large scale conventional private refineries (Ogedegbe, 2009). Modular refineries should be set up at strategic demand locations to solve the product demand requirements. Modular refinery has several advantages which are its cost-effectiveness in remote areas, flexibility, ease and speed of construction, low capital cost and concentrate on the production of one product at a time. That is, a modular refinery specializes in the production of a particular product, for instance diesel, gasoline, kerosene or petrol. It is on like conventional refinery which produces different product mix at once. In addition, the construction and functional operations of modular refinery will provide employment opportunities for the teeming jobless youths. It is necessary to convince and persuade the government of Nigeria on the attendant merits from modular refining methods. Among the OPEC members the most troubled ones have modular processing plants (Igwe, 2014). The crack down on illegal refineries by the government in the Niger Delta region should be turned around towards the development and constructions of modular refineries as legal entities to reduce unemployment and acute shortages of refined petroleum products as well as oil bunkering. Providing an opportunity to engage in modular refinery businesses will turn the oil bunkers into modular refinery businessmen and it will also act as a disincentive to vandalize pipelines thereby turning these oil gangs into useful citizens. The raw skilled manpower used in the illegal refining business can be transformed into modern productive skilled manpower through adequate training on modern distillation processes, specifications, appropriate catalysis, codes and standards among others. Consequently, environmental pollution and degradation will be drastically reduced to the barest minimum. This is because all the refining products poured into streams and rivers will be completely used in some other process plants and can be processed into valuable end products. Thus, we will have safe and good drinking water in our rivers thereby ensuring the good health of our people and that of the aquatic life. During the Nigeria civil war which lasted for 30 months, the secessionist enclave of Biafra was able to drive his economy by producing petroleum fuels for her airplane, buses, cars, cooking machines, tractors and trucks by the utilization of modular refineries.

Establishment of Conventional Private Refineries: Apart from the small scale cottage refineries, big-time businessmen should establish private conventional refineries. Dangote is now building a private refinery at a cost of 9 billion dollars of which 7.5 billion dollars is for the petroleum refinery complex while 1.5 billion dollars is for the fertilizer complex. The Dangote proposed refinery will bring to an end the current importation of refined petroleum products by the time it is commissioned in 2017. It is being constructed with a loan facility of 5.5 billion provided by a consortium of local and international banks and 3.5 billion from Dangote equity. According to Dangote, the plant will further entrench Africa's role on the global map as not only a valued contributor for natural resources, but also a competent manufacturer of refined petroleum products and fertilizer. With the global demand for crude oil projected to keep dropping the way forward is for us to start exporting refined products rather than crude. We

will get far better money value that way (Atojoke, 2015). Dangote refinery would bring more opportunities and encourage other big-time businessmen and multinationals to go into private petroleum refining business. The petroleum marketers and all those involved in the importation of refined petroleum products can pull their resources together to build a private refinery.

Conducive Environment: The investor should be ready to make the host community to be happy by cleaning up the environment as soon as possible if there is any oil spillage or pollution. It can also provide social amenities such as good roads, electricity, pipe-borne water, schools and maternity to his host communities. When the host communities are happy and satisfied with the investor, they will provide the needed security and safety for his oil facilities and the crude oil feedstock supplies to the sites.

Government Regulation: For an effective and competitive domestic petroleum products market to be developed in Nigeria, the downstream sector must be deregulated to encourage investment in refining and marketing infrastructure. This would boost private investment in the sector, create more jobs and enhance the sector's contribution to national output (Lukman, 2010). We believe in free market economy as being sine qua non to a vibrant downstream oil sector that is both profitable and self sustaining (PPPRA, 2010). There is an urgent need to free the petroleum industry of all forms of administrative, social and economic hindrances. Both the potential investors and marketers would favour the total deregulation of the mid-stream and downstream oil industry if they must come in to build private refineries. The smooth takeoff of private refineries in Nigeria can be blamed on the National Assembly for their delay in passing the Petroleum Industry Bill (PIB). The PIB contains mechanisms to completely deregulate the downstream sector to make its market price competitive thereby attracting local and foreign investments. Petroleum market regulation has its

negative effects – it encourages smuggling, hoarding and black markets. It lacks fiscal sustainability and it distorts the market. Above all, it benefits only a few wealthy oil cabals at the expense of the generality of the people. The resources used for oil subsidy can be channeled into other vital areas of the nation's economy.

Mobilization of Fund: The local banks should mobilize funds and bankroll the proposals submitted by indigenous oil firms for private refineries in the country. The local banks can equally assist the local refinery businessman to get foreign credit lines. This was done in Brazil and Venezuela and today these countries have testified that it was the indigenous oil firms that added value to their oil and gas industry and not the foreign firms (OPEC, 2012).

Setting up of Refinery Technical Crew

A technical crew consortium should be set up to oversee the design, construction and turnaround maintenance of the private refineries. No country can develop by solely depending on other countries in terms of investment and development strategies, design, construction and technical rehabilitation of its infrastructures.

Diversification of the Products from Private Refineries

Diversification should be vigorously pursued in the petroleum refinery business as this will result in wealth creation using the hydrocarbon value chain through provision of employment opportunities, gross domestic product growth and import substitution. The diversification of the energy sector from oil to gas, and fuels (such as automotive gas oil, diesel, kerosene, low pour fuel oil, premium motor spirit) to non-fuels (like polypropylene, an important raw material for plastic and fabric products, fertilizer products, asphalt, antifreeze, pesticides, pharmaceuticals, synthetic rubber, plastics, bitumen which is used for road construction, just to mention a few. In this way the contribution of oil to the gross domestic product will increase from its current low value of 13% GDP (NNPC, 2014) and the present dwindling revenues accruing to the

federation as a result of the fall in crude oil prices is drastically changed.

3.0 Conclusion

Modular and Conventional private refineries should be set up in the country to change Nigeria from being an importer to exporter of refined petroleum products. This will get Nigeria out of the problem of importing refined products and then become an exporter of refined petroleum products expected of a big crude oil producer. The current problems of available and refined crude oil products for domestic consumption and perhaps for export will be a thing of the past if private refineries are allowed to operate at full capacity.

4.0 References

Alike, E. (2015): In an article titled 'Department of Petroleum Resources (DPR) Blames Absence of Private Refineries on Lack of Crude Oil in This Day Live of 7 July, 2015.

Atojoko, S. (2015): In an article titled 'Private Investors to the Rescue' in Tell Magazine, May 18, 2015; Volume 20 page 20.

Igwe, G. (2014): In an article titled 'Igwe: Modular Refineries will Address Perennial Shortage of Petroleum Products' on 8 September 2014.

Izeze, I. (2015): In an article titled 'Between Private Refineries and Access to Crude Oil Feedstock' on 2 August 2015.

Lukman, R.(2010): In an article titled 'Fuel Crisis Still Waiting for Private Refineries' in Daily Sun of 12 July, 2010.

NNPC (2014): Nigeria National Corporation Website Publications in June 2014

Ogedengbe, A. O. (2009): 'The Nigeria Petroleum Refineries: History, Problems and Possible Solutions'. A lecture delivered at the Induction Ceremony for New Fellows at the Nigeria Academy of Engineering. June 11, 2009. Pp 1-23

OPEC (2012): Organization of Petroleum Exporting Countries Website Publications in January 2012.

PPPRA (2010): In an article titled 'Fuel Crisis Still Waiting for Private Refineries' in Daily Sun of 12 July, 2010.

Ubah, I. (2010): In an article titled 'Fuel Crisis Still Waiting for Private Refineries' in Daily Sun of 12 July, 2010

P 011

CRUDE OIL SPILLAGE IN THE NIGER DELTA REGION OF NIGERIA – A REVIEW

[1]Odisu, T *., [2]Okieimen, C.O and [3]Ogbeide, S.E

Department of Chemical Engineering, Federal University of Petroleum Resources, Effurun
Department of Chemical Engineering, University of Benin, Benin City
Department of Chemical Engineering, University of Benin, Benin City
*teddyodi2002 @yahoo.com; cookieimen@yahoo.com, seogbeide@gmail.com

Abstract

The role of crude oil as a source of modern day energy and feedstock for production of numerous products particularly petrochemical based has come to stay considering the enormous level of consumption as seen from production and market figures. However, its exploration, production and even transportation processes have continuously left behind most times pains occasioned by its spillage and resultant environmental effects. While this has become a global issue for land and water where any segment of these operations takes place, the mangrove swamp and particularly that of the Nigerian Niger Delta is of particular concern here. This is because of its role, level of dependence, and the unimaginable extent to which it has been degraded. This review thus focused on oil exploration in Nigeria, nature of mangrove swamps, the extent of damage by oil production activities, its effects, the physical/mass transfer processes that drive oil and pseudo component transport in the mangrove swamp, holding capacities and level of persistence or residence time. The paper also identified research gap in oil spill modeling and management and suggested practical steps that can be employed in the modeling of oil spill in this peculiar terrain.
Key words: oil spill, pseudo components, mangrove, Diffusion and Niger Delta

1.0 Introduction

Over the years, crude oil spill (the accidental discharge of oil into the environment) has become a common phenomenon in areas where oil is explored, produced, along the chain of transportation and in some cases as a result of sabotage. The attendant effects of this problem have assumed a global dimension with Nigeria and particularly its Niger Delta area getting a full share of it. Crude oil has been defined as a naturally occurring complex liquid mixture of organic molecules, mostly hydrocarbons. It is composed primarily of five elements: carbon, hydrogen, sulfur, nitrogen, and oxygen. These five elements are present in various combinations within oil. Hydrocarbons are the most abundant compounds found in crude oils, up to 85% of the overall mixture. The major hydrocarbon components include alkanes, aromatics, resins and asphaltenes with several contaminants like sulphur compounds, carbon dioxide, nitrogen compounds, and trace metals, etc (Leila et al, 2011)

Crude oil also called petroleum is recovered through drilling, then refined based on the principle of difference in boiling point (fractional distillation) and separated into a large number of products like petrol (or gasoline), kerosene, asphalt and chemical reagents used to make plastics and pharmaceuticals. It is used directly and indirectly in the manufacturing of a wide variety of materials, with an estimation of a global consumption of over 88 million barrels each day.

In Nigeria, crude oil was first discovered at Oloibiri, a village in Bayelsa state, in its Niger Delta region of with commercial production beginning in 1958. As at today, there are over 606 oil fields in the Niger Delta, of which 360 are on-shore and 246 off-shores. There exist over 3,000 kilometres of pipeline laid across the landscape of the Delta, linking 275 flow stations to various export facilities (Wale, 2001).

According to the Nigerian Senate, Nigeria has experienced the highest number of oil spills incidences among oil producing countries in the World worse than other notoriously impacted regions such as Azerbaijan, Kazakhstan, Siberia and Ecuador.

Fifty years after the discovery of oil in Nigeria's Niger Delta, an independent team of experts from Nigeria, the UK, and the United States convened by the Nigerian Conservation Foundation concluded that the Niger Delta is one of the World's most severely petroleum-impacted ecosystems. This conclusion was reached after a Natural Resource Damage Assessment and Restoration scoping visit to the Niger Delta from May 21 – 29, 2006. The team of experts, with participation by Nigeria's Ministry of Environment, WWF UK and the International Union of Common Wealth Union (IUCN) Commission on Environmental, Economic and Social Policy visited Delta communities and spill-damaged sites in Rivers, Bayelsa and Delta states (Federal ministry of Environment, 2006)

Among the preliminary findings of the independent team were:

1. An estimated 9 – 13 million barrels (1.5 million tons) of oil has spilled in the Niger Delta ecosystem over the past 50 years, representing about 50 times the estimated volume spilled in the popular Exxon Valdez Oil Spill of Alaska in 1989. This amount is equivalent to about one "Exxon Valdez" spill in the Niger Delta each year.
2. The financial valuation of the environmental damage caused by 57 years of oil and gas activities in the region - taking into account the unique and productive character of the ecosystem as well as comparable valuations on other such ecosystems – would be tens of billions of dollars

2.0 Causes and cases of oil spill

A reasonable number of oil spills in Nigeria have been caused by sabotage where some of the citizens of this country in collaboration with people from other countries engage in oil bunkering at different scale and levels. They damage and break oil pipelines in their bid to have access to and steal oil from them funnelling nearly 400,000 barrels per day from our oil and selling it illegally on the international trade market. This led to about 17 percent fall in official sales of the crude in the international market in 2013 with a loss of about $4 billion in January 2001, N7.7 billion in 2002 (Egberongbe et al, 2006). .

Another statistics has it that fifty percent (50%) of oil spills is due to corrosion, twenty eight percent (28%) to sabotage and twenty one percent (21%) to oil production operations. One percent (1%) of oil spills is due to engineering drills, inability to effectively control oil wells, failure of machines, and inadequate care in loading and unloading oil vessels (Nwilo and Badejo, 2005)

Oil spill incidents have occurred in various parts and at different times along our coast. Some major spills in the coastal zone are the GOCON's Escravos spill in 1978 of about 300,000 barrels, SPDC's Forcados Terminal tank failure in 1978 of about 580,000 barrels and Texaco Funiwa-5 blow out in 1980 of about 400,000 barrels (Egberongbe et al, 2006)..

The most publicised of all oil spills in Nigeria occurred on January 17 1980 when a total of 37.0 million litres of crude oil got spilled into the environment. This spill occurred as a result of a blow out at Funiwa 5 offshore station. Another serious spill was the offshore well-blow out in January 1980 when an estimated 200,000 barrels of oil (8.4million US gallons) spilled into the Atlantic Ocean from an oil industry facility and that damaged 340 hectares of mangrove (Nwilo and Badejo, 2005). In 1998, over 40,000 barrels from a Mobil pipeline off the Nigeria coast while in December 2011, over 40,000 barrels spilled from the Shell Bonga off the Nigerian coast (John, 2011)

According to the Department of Petroleum Resources (DPR), between 1976 and 1996 a total of 4,647 incidents resulted in the spill of approximately 2,369,470 barrels of oil into the environment. Of this quantity, an estimated 1,820,410.5 barrels (77%) were lost to the environment.

Oil spillage is categorized into four groups: minor, medium, major and disaster. The minor spills take place when the oil discharge is less than 25 barrels in inland waters or less than 250 barrels on land, offshore or coastal waters that does not pose a threat to the public health or welfare (Ntukepko, 1996).
In the case of the medium, the spill must be 250 barrels or less in the inland water or 250 to 2,500 barrels on land, offshore and coastal water while for the major spill, the discharge to the inland waters is in excess of 250 and 2500 barrels in inland waters and on land, offshore or coastal waters respectively (Ntukepko, 1996).

3.0 Effects of oil spill

Oil spill constitute a great deal of risk and danger to the environment and its direct and indirect habitats as it affects aquatic life, economy, tourism and leisure activities. Though the toxicity of each individual component is known, that of complex mixtures such as crude oils and refined products are extremely difficult to assess because researchers know little about the overall effects of the various mixtures. In addition, the chemical composition of each crude oil and petroleum product varies significantly, and can have diverse effects on different organisms within the same ecosystem (Overton, et al, 1994).
These differences in toxic effects are due to differences both in composition as well as concentration of the chemical constituents. (Kyung-Hwa Baek et al, 2004)
Research have shown that when living things are exposed to crude oil for a long time it poses a great risk and the effect ranges from stinging eyes, rashes, nausea, dizziness, headaches, coughs and other respiratory symptoms to DNA damage (which usually is a first step towards cancer)
Martin Marietta Materials Data Sheet (2007) gave an overview of health effects caused by overexposure to one or more components in Crude Oil depending on the mode of contact. Contact with eyes may cause mild to severe irritation including stinging, watering, redness, and swelling. Mild skin irritation including redness and a burning sensation may follow. Prolonged contact may cause dermatitis, folliculitis, or oil acne.
Liquid may be absorbed through the skin in toxic amounts if large amounts of skin are exposed repeatedly. There have been rare occurrences of precancerous warts on the forearm, back of hands and scrotum from chronic prolonged contact. The major threat of ingestion occurs from the aspiration (breathing) of liquid drops into the lungs. Aspiration may result in chemical pneumonia (fluid in the lungs), severe lung damage, respiratory failure, and

death. Ingestion may cause gastrointestinal disturbances including irritation, nausea, vomiting and diarrheal. (*Martin, 2000*)
.

4.0 Niger Delta Mangrove

Oil spillage can occur in land and water (turbulent, low flowing or calm and non flowing waters). The calm and non- flowing water environment is common in the mangrove areas where we have high vegetation density with large surface area for oil adsorption and possible retention, high sediment load and marshes
Mangrove swamps are predominant in the Niger Delta and are one of the principal places where spilled oil and associated impacts converge. They suffer both lethal and sub lethal effects from oil spill. (Cutler, 2012). Mangrove is home to countless microbial organisms of different diversity which control many biochemical reactions concerned in the mineralization of soil organic matter and in the nutrition of plants particularly agricultural crops whose activity is governed by the soil environment. Therefore, any factor that affects these microbial activities also adversely affects plant growth, as well as detoxification of organic pollutants (Clark and Patrick, 1987).

The term mangrove refers to a non-taxonomic grouping of woody, halophytic permatophytes that occur along low energy coastlines, deltas, estuaries, and embayments throughout the tropics and subtropics (Snedaker et al, 1995). They dominate coastal intertidal areas with marshes that are subject to stranding and trapping of oil due to their sheltered nature. A number of researchers consider mangrove to be the most sensitive of all coastal ecosystem types to oil spill (Hayes and Gundlach, 1980). They grow and develop in sheltered, calm, low energy depositional areas which also tend to be sites where oil accumulates and pollutants removal can be extremely reduced and contain marsh fauna like crabs, molluscs and worms, with some of the species burrowing into the sediments and thus providing biological pathways for oil penetration in the event of a spill (IPIECA, 1994)

5.0 Physical transformation processes and existing models

Several processes govern the fate of spilled crude oil in a mangrove swamp. These include: evaporation, spreading, emulsification, adsorption, diffusion, sedimentation and entrainment. Of these, the most critical ones that control the fate of spilled oil in mangrove area like the Niger Delta are- adsorption, (including phyto-sorption) diffusion, entrainment and sedimentation.
Adsorption is the process of system component redistribution between a bulk mobile phase and a surface layer on a solid phase. Dissolved molecules displace molecules of solvent at the solid interface during the

process of adsorption from solution. Different mechanisms of surface layer formation are possible depending upon the different nature of adsorbed components, their concentrations, morphology of the surface of the adsorbent, and its wettability. It has been established that both the surface and pores of sediment can adsorb molecular oil. So the adsorption of oil by sediment can be classified as two kinds: Surface adsorption due to active ions on the sediment surface and capillary adsorption due to pores.
Based on experimental results, the capacity of surface adsorption can be described by the well known Langmuir adsorption equation Langmuir 1916, while the capacity of capillary adsorption is mainly related to the diameter of sediment particles (Chao et al, 2003).

Sedimentation is defined as adhesion of oil to solid particles in the water column. The significance of sedimentation as an important transport process will depend on the sediment load of the surrounding water, their type and size, salinity of the water, and sulphur content of the oil and oil droplet size, which is directly related to oil viscosity (Payne *et al, 1994)*. For muddy rivers, where the sediment load can be more than 0.5 kglm3, the removal by sedimentation is considerable and exceeds the loss due to normal dispersion (Marcia et al, 2010).

When oil is released in low energy mangrove swamp, it can be transported as micron sized droplets (particulate), component (pseudo component diffusion) or through chemical partitioning mechanisms with suspended sediment. Vertical transport of the oil is then altered due to changes in oil-sediment aggregate size and density (Sterling Jr. et al, 2004). Oil-sediment aggregation effects on released oil transport and fate have been highlighted in a number of crude oil releases (Le Floch et al, 2002). The diffusion of oil components as a mass transfer process from its bulk into an aqueous phase is controlled by several factors like the surface tension, interfacial tension, contact angle, and surface charge. Also, the acid and base, surfactant (surface active materials) contribute a great deal to the process (Kanicky et al, 2001).

All crude oils contained water soluble components within a relatively narrow range of molecular size but different polarity (Andreas et al, 2007). Surfactants have two functional groups namely the hydrophilic (water soluble or polar) and hydrophobic (water insoluble or non polar) group. The hydrophobic group is described as a long hydrocarbon chain (c_8-c_{18}) which may or may not be branched. While the hydrophilic group is formed by moieties such as carboxylates, sulphates, sulfonates (anionic) alcohols, polyoxyethylenated chains (non-ionic)

and quaternary ammonium salts, alcohols and other natural surface-active agents.

When crude oil is brought in contact with water (as in this case), these natural surface agents accumulate at the interface and form an adsorbed film which lowers the interfacial tension of the crude oil/water interface. The key here is that with the presence of surface active materials at the interface, interfacial tension is lowered allowing for the diffusion of certain components from the crude oil bulk into the water.

The adsorption of surface active molecules from a bulk phase to a surface or interface is governed by equilibrium rate constant, and the adsorption occurs at any concentration. Beyond the critical concentration, individual surfactant monomers begin to aggregate with their hydrophilic heads pointing outward towards the solution and the hydrophobic tails pointing inwards away from the water (Mona et al, 2013)

Also, oil can penetrate into the soil, particularly through crustacean burrows and voids formed by dead mangroves roots. Lighter oils tend to penetrate more deeply into mangroves forest than heavier and more weathered oils, but will not persist like heavy oils unless they mix into the soil. Heavy oils and emulsified oils can be trapped in thickets of red mangrove prop roots and black mangrove pneumatophores and are likely to adhere to and coat these surfaces, as well as other organic materials, such as sea grass wrack. Re-oiling from re-suspended oil, particularly as tides rise and fall may further injure plants over time. Where oil persists, sheens may be generated for months or years.

The degree of oil penetration into sediment years after a spill was investigated. Evidence of subsurface oil in middle and intertidal sediments oiled by the Exxon Valdez spill 13 years after the spill were found. Concentrations of dissolved-phase total polyaromatic hydrocarbons (PAHs) averaged 1,200 ng/l ranging from 76ng/l to 4,600ng/l compared to 18ng/l – 27ng/l for reference sites (Payne et al. 2005)

In a literature review conducted on the persistence of oil in subtidal sediments with data analyzed to determine oil decay rates, it was found that the rate of disappearance of subtidal oil fits first-order decay kinetics, and concluded that fine sediments can retain oil longer than coarse sediments.

The type of sediment is important since oil remains longer in soils with higher organic matter and, therefore, has greater impact on resident environment. Some wetland sediment can act as a reservoir absorbing oil and leaching it out into adjacent coastal habitats, causing chronic impacts on biota.

The oil-holding capacity of a shoreline and sediment is dependent on the oil and beach characteristics and consists of two components – maximum surface loading and maximum subsurface loading (Gundlach 1987). The oil-holding capacity was expressed by Cheng et al, (2000) as;

$$M_* = \rho_o [L_t T_m + C_v D_p L_S] \qquad (1)$$

Oil retention was calculated as:

$$\frac{Volume_{oil}}{Volume_{sed}} = \frac{t_o - t_1 . A}{d.A} \qquad (2)$$

Oil in a completely saturated substrate would be represented by:

$$Vol. of oil = [(\tfrac{1}{2} r)^3 \quad (\tfrac{4}{3} \pi r^3)] \qquad (3)$$

And the oil removal coefficients (K_f) and rate were calculated from empirical data using the equation;

$$M_i = M_{io} * e^{-k_f t} \qquad \text{(Gundlach, 1987)}$$

The impact of a heavy fuel oil spill on a marsh area that was dominated by *Spartina, Scirpus*, and *Juncus* vegetation was examined by Baca et al. (1983). Geometric formulae were developed to estimate the amount of oil adhering to the vegetation. For example, the formula for *Spartina* was determined to be:

$$nA_L + N A_s + = A_T \qquad (4)$$
$$A_T M = H \qquad (5)$$

For proper and effective contingency planning, clean up and remediation of crude oil spill irrespective of the processes involved, it is necessary to develop predictive mathematical models for pathway monitoring, pollution distribution for risk assessment, and kinetics. Several types of oil models (besides the above) have been developed and applied to oil spill cases. These are simple trajectory, or particle tracking models, three dimensional trajectory and fate models that include biological effects (Reed, 1999) and continuous source for multi

163

component. These existing models were developed for turbulent and high flowing water environment characterized with waves and tides.

Chao et al presented the development and application of two dimensional and three dimensional oil trajectory and fate models for coastal waters. In the two dimensional model, the spreading, advection, turbulent diffusion, evaporation and dissolution were taken into account to describe the oil slick movement on the water surface. Three dimensional oil fate model was proposed that is based on the mass transport equation to simulate the distribution of oil particles in the water column (Chao, et al, 2001).

$$A = 2270 \left(\frac{\Delta \rho}{\rho_0}\right)^{1/3} V^{2/3} t^{1/2} +$$

$$40 \left(\frac{\Delta \rho}{\rho_0}\right)^{1/3} V^{1/3} U_{wind}^{4/3} t$$

$$\qquad (7)$$

While the advection velocity of each grid point U_d was computed using;

$$\overrightarrow{U d} = K_t \overrightarrow{U t} + K_w \overrightarrow{U w} \qquad (7)$$

The horizontal turbulent diffusion is

$$\Delta S = [R]_0^1 \sqrt{12 D_h \, \Delta t} \qquad (8)$$

The displacement of every grid point at every time step was computed by;

$$L_x(\Delta t) = U_{dx} \Delta t + \Delta S \cos\theta \qquad (9)$$

$$L_y(\Delta t) = U_{dy} \Delta t + \Delta S \sin\theta \qquad (10)$$

The evaporative effect was considered by calculating the evaporative amount of a given component of oil using;

$$M_i = \frac{K_g A t X_i \, P_i^S}{RT} \qquad (11)$$

While the rates of evaporation can be calculated by;

$$S_e = \sum \frac{M_i}{t} = \sum \frac{K_g A X_i \, P_i^S}{RT} \qquad (12)$$

The amount of components lost by dissolution was accounted for by using the formulation;

$$M_{di} = K_d A t X_i \, S_i \qquad (13)$$

And the dissolution rate is calculated using;

$$S_d = \sum \frac{M_d}{t} = \sum K_d \, A \, X_i \, S_i \qquad (14)$$

For vertical dispersion,
The entrainment rate was calculated using;

$$Q(d) = K_{en} \, D_{ba}^{0.57} \, S_{cov} \, F_{wc} \, d^{0.7} \, \Delta d \qquad (15)$$

The rate of vertical dispersion is;

$$S_{vd} = \int_{d_{min}}^{d_{max}} Q(d) \Delta d \qquad (16)$$

Finally for the 2-dimensional modelling, shoreline deposition is;

$$C_{max} = L_s W_s D_s \epsilon_{eff} \qquad (17)$$

The governing equation of a 3-D tidal flows as well as oil concentration and distribution in coastal waters are as follows:

Continuity equation:

$$\frac{\partial U}{\partial x} + \frac{\partial V}{\partial y} + \frac{\partial W}{\partial z} = 0 \qquad (18)$$

Momentum equation in the x and y directions:

$$\frac{\partial U}{dt} + U\frac{\partial U}{\partial x} + V\frac{\partial U}{\partial z} = \frac{1}{\rho}\frac{\partial P}{\partial x} + \frac{\partial}{\partial x}\left(V_h \frac{\partial U}{\partial x}\right) + \frac{\partial}{\partial y}\left(V_h \frac{\partial U}{\partial y}\right) + \frac{1}{\rho}\frac{\partial(\tau_x)}{\partial z}) + \Omega V$$

$$\qquad (19)$$

$$\frac{\partial V}{\partial t} + U\frac{\partial V}{\partial x} + U\frac{\partial V}{\partial y} + w\frac{\partial V}{\partial z} = \frac{1}{\rho}\frac{\partial P}{\partial y} + \frac{\partial}{\partial y}\left(V_h \frac{\partial V}{\partial x}\right) + \frac{\partial}{\partial y}\left(V_h \frac{\partial V}{\partial y}\right) + \frac{1}{\rho}\frac{\partial(\tau_x)}{\partial z}) - \Omega U$$

$$\qquad (20)$$

164

Hydrostatic pressure equation;

$$\frac{\partial P}{\partial z} + \rho g = 0 \qquad (21)$$

Oil particle transport equation:

$$\frac{\partial C}{\partial t} + \frac{\partial (UC)}{\partial x} + \frac{\partial (VC)}{\partial y} + \frac{\partial (WC)}{\partial z} =$$
$$\frac{\partial}{\partial x}\left(D_x \frac{\partial C}{\partial x}\right) + \frac{\partial}{\partial y}\left(D_y \frac{\partial C}{\partial y}\right) + \frac{\partial}{\partial z}\left(D_z \frac{\partial C}{\partial z}\right) +$$
$$\frac{\partial (\omega C)}{\partial z} + \sum S$$
$$(22)$$

Wang et al., developed a three dimensional model for transport of oil spills in seas to investigate the vertical dispersion/ motion of the spilled oil slick which simulates the motion of oil spill more realistic. Furthermore, this model includes the processor hydrolysis, photo oxidation and biodegradation (Wang et al, 2008). The model shows that the drift velocity of the surface oil is the result of the combined action of the wave, current and waves and can be written as follows;

$$\langle u \rangle = \alpha_w D u_w + \alpha_c u_c + u_{wave}$$
$$\langle v \rangle = \alpha_w D v_w + \alpha_c v_c + u_{wave}$$
$$\langle w \rangle = w_c \qquad (23)$$

$$D = \begin{Bmatrix} \cos\theta & \sin\theta \\ -\sin\theta & \cos\theta \end{Bmatrix}, \text{ where } \theta = 40^o$$
$$-8\sqrt[4]{u^2_w + v^2_w} \text{ when } 0 \leq \sqrt{u^2_w + v^2_w}$$
$$\leq 25m/s$$

And $\theta = 0$ when $\sqrt{u^2_w + v^2_w} > 25$

Where the drift velocity of the oil droplets in the water column is the result of the combined action of the current and wave and can be calculated as;

$$\langle u \rangle = u_c + u_{wave}, \ \langle v \rangle = v_c + u_{wave},$$
$$\langle w \rangle = w_c \qquad (24)$$

The model gave the net current speed due to wave to be;

$$u_{wave} = \frac{k_w H^2_s}{8 \sin h^2 (kh)} \cosh(2kz_o) \qquad (25)$$

The turbulent diffusion is given as;

$$u' = R_n \sqrt{4K_\alpha / \Delta t} \cos(\emptyset) \ ,$$
$$v' = R_n \sqrt{4K_\alpha / \Delta t} \sin(\emptyset), \ , \ w' = R_n \sqrt{2K_z / \Delta t}$$
$$(26)$$

And the vertical mixing is calculated as;

$$d_c = \frac{9.52 v^{2/8}}{g^{1/8} \left(1 - (\rho_o / \rho_w)^{1/8}\right)} \qquad (27)$$

However, there seem to be a relative scarcity of information on pathway and model equations for non-flowing water bodies found in mangrove swamps. Therefore, the need to consider the development of such models most importantly for the Nigerian Niger Delta is undoubtedly important. Modelling the fate of oil spill in such water environment can be achieved using the empirical/statistical approach or the analytical approach as did for the models above.
The empirical/statistical modelling may involve the following steps

- Design of experiment using any of the experimental design tools available like the design expert with consideration to variables like the concentration or volume of oil spilled, sediment load of water, sampling depth, time or age of spill, and water temperature with most times as a function of season. Also, the type of vegetation, pore size of the leaves, available total surface area, and leaf thickness.
- Simulate or access a spill site where the variables mentioned above can determine and monitored.
- Take samples of water, vegetation and soil (from water bed and shorelines using the appropriate sampling tools like the auger for soil sampling and the depth sampler for water depth sampling.
- Carry out hydrocarbon evaluation analysis using the appropriate analytical equipment like the GC/MS to get the

amount of hydrocarbon contained and their group in the samples collected.

- Use the experimental design software to develop an appropriate empirical model for the different physical processes.
- Fit the value of the measured variables to the model to get the calculated values
- Compare the calculated with the experimental
  Carry out appropriate statistical analysis on the result to determine the – reproducibility of data, significance of model, adequacy of model, and model accuracy.

While modelling oil spill in non-flowing terrain analytically may involve the following consideration:

- Identify probable operating physical processes in the system –adsorption of whole oil and components on suspended sediments both on the surface of water and water column, diffusion of oil components from the bulk of oil across the oil-water interface, diffusion of oil components from the interface into the bulk of the water and down the sediment bed, and sedimentation of the whole oil-sediment with density equal and above that of water down to the bed, settling of emulsified oil, interaction of oil with available vegetations.
- Developing an overall material balance equation with the assumption that there is no continuous inlet flow (that is inlet is zero). That is, a batch system.
- Get the necessary transport /mass transfer equations considering the immiscible nature of the fluids, multiple phases (oil, water and base sediment)
- The option of thermodynamic term if one is considering the changes in temperature due to variation in season (non isothermal) or a constant

temperature system (isothermal). While the isothermal consideration may make the modelling easier, it really may not capture the true state of the environmental condition in the water, and the consideration that the diffusivity of liquids is strongly a function of temperature.

- Source for the necessary constants based on the selected process equations.
- Solve the ensuing equation using any mathematical tool
- Validate the final models to see their validity comparing with the experimental results.

The benefits of this research area though seemly tedious are numerous. These may include:

- Proper evaluation of the class and amount of residual lost/ transported hydrocarbon from the bulk before and after a clean-up operation.
- Residual hydrocarbon residence time
- Evaluation of real time effect of an spill on its victim environment
- Determination of proper close out time for a clean-up operation
- Evaluation of adequate compensation for oil spill impacted environment dependants.

Conclusion

Oil spill has become a global environmental issue which has cost us so much in terms of money, time, energy and even intellectual ability not to mention the losses in environmental serenity and life. Though, lots of work has been done in prediction, monitoring and management in high flowing water and land, not much has been done for non flowing water like those in the Nigerian Niger Delta swamps. Therefore, due to the peculiar and intricate nature of the swamps and the potential to retain oil either in whole or as components there is need to

engage research for the development of valid models that can be useful in contingency planning of oil spill management.

References
Andreas Hannisdal, Robert Orr and Johan Sjoblom (2007). Viscoelastic Properties of Crude Oil Components at Oil-Water Interfaces. 1. The Effect of Dilution. Journal of Dispersion Science and Technology, 28, pp. 81-93

Baca, B.J., Michel, J., Kana, T.W. and Maynard, N.G. (1983). Cape Fear River Oil Spill (North Carolina): Determining oil quantity from Marsh Surface Area. In: *Proceedings of the 1983 Oil Spill Conference, pp.* 419 – 422

Chao, X. B., Shankar, N. J., and Wang, S. S. Y (2003). Development and Application of Oil Spill Model for Singapore Coastal Waters. *Journal of Hydraulic Engineering*, 129(7), pp. 495-503

Chao, X., Shankar, N.J. and Cheong, H.F. (2001). Two –and Three- Dimensional Oil Spill Model for Coastal Waters. *Ocean Engineering,* 28, pp. 1557- 1573

Clark, J.R and Patrick, J.M Jr (1987). Toxicity of Sediment Incorporated Drilling Fluids. Marine Pollution Bulletin, 18 (11), pp. 600-603

Cutler Cleveland, (2012). Oil Spill in Mangroves'', Encyclopaedia of Earth, Edited by Cuttler .J. Cleveland (Washington, D.C. Environmental information Coalition, National Council for Science and the Environment), www.eoearth.org/article/oil_spill _in _ mangroves

Egberongbe, F.A.O., Nwilo, P.C. and Badejo, O.T. (2006). *Oil Spill Disaster along Nigerian Coastlines. In:Proceedings of* 5th Regional Conference on Promoting Land Administration and Good Governance, Accra, Ghana

Federal Ministry of Environment, Abuja, Nigeria Conservation Foundation, Lagos and WWF UK , CEESP- IUCN Commission on Environmental, Economic, and Social Policy (2006). Niger Delta *Natural Resource Damage Assessment and Restoration* Project. Niger Delta, Phase 1 scoping Report, May 31, pp 1-13

Gundlach, E.R. (1987). Oil-holding Capacities and Removal Coefficients for Different Shoreline Types to Computer Simulate Spills in Coastal Waters. In: Proceedings *of the 1987 International Oil Spill Conference, Pp* 451 – 457

Hayes, M.O., Gundlach, E.R. and Getter, C.D. (1980). Sensitivity Ranking of Energy-Port Shorelines. In: *Proceedings of Ports conference, American Society of Civil Engineers, Norfolk, Virginia: Pp* 697 – 707

IPIECA report series (1994). Biological Impacts of Oil Pollution: Salt marshes. 6, pp 36-40

John Vidal (2011). BP Oil Spill. Environment editor, guardian.co.uk, Thursday 22 December

Kyung-Hwa Baek, Hee-sik kim, Hee-Mock oh, Byung-Dae Yoon, Jaisoo Kim, and Insook Lee (2004). Effects of Crude Oil, Oil Components and Bioremediation on Plant Growth. Journal of Environmental Science and Health, Part A- Toxic/ Hazardous substance and environmental engineering, A39 (9), pp 2465-2472

Le Floch, S., Guyomarch, J., Merlin, F. X., Stoffyn-Egli, P., Dixon, J., and Lee, K. (2002). The Influence of salinity on Oil-Mineral Aggregate Formation. *Spill Science and Technology Bulletin,* 8(1), pp 65-71

Leila Mohajeri, Hamidi Abdul Aziz, Mohammad Ali Zahed, Soraya Mahajeri, Shamsul Rahman Mohamed Kutty and Mohamed Hasnam Isa (2011). Response Surface Analysis and Modelling of n-Alkanes Removal through

167

Bioremediation of Weathered Crude Oil. Water Science and Technology 63 (4), pp 618-626

Martin Marietta Materials. Materials Safety Data Sheet. 2710 Wycliff Road, Raleigh, North Carolina, 27602-3303 (919) pp 781-4550

Mona Eftekhardadkhad, Pieter Reynders and Gisle Øye, (2013). Dynamic Adsorption of Water Soluble Crude Oil Components at Air Bubbles. Journal of Chemical Engineering Science, Elsevier, 101, page 359-365
Ntukekpo D.S. (1996). Spillage: Bane of Petroleum. Ultimate Water Technology and Environment

Nwilo, P.C. and Badejo, O.T. (2005). Oil Spill Problems and Management in the Niger Delta. In: Proceedings of International Oil Spill Conference, Miami, Florida, USA

Overton, E.B, Sharp, W.D, and Roberts, P.(1994). Toxicity of Petroleum. In: , Cockerman, C.G. Shane, B.S, Eds, C.R.C Press, Boca Raton, F.L. Basic Environmental Toxicology, 10, pp 133-156

Payne, J.R., (1994). Use of Oil Spill Weathering Data in Toxicity Studies for Chemically and Naturally Disposed Oil Slicks. Section 4.0 In: J.H Kukick (ed), Proceedings of the First Meeting of the Chemical Response Corporation, Ecological Effect of Research forum, Marine Spill Response Corporation, Washington, D.C, MRSC Technical Report series, 94-017, pp 87

Payne, J.R., Lindberg, M.R., Fournier, M., Larsen, M.L., Short, J.W., Rice, S.D., Driskell, W.D. and Janka, D. (2005). Dissolved- and Particulate-Phase Hydrocarbon in Interstitial Water from Prince William Sound Intertidal Beaches Containing Buried Oil Thirteen Years after the Exxon Valdez Oil Spill. In: *Proceedings of the 2005 International Oil Spill Conference: pp* 83 – 88.

Reed, M., Johansen, O., Brandvik, P.J., Daling, P., Lewis, A., Fiocco, R.,Mackay, D. and Prentki, R. (1999). Oil Spill Modeling towards the Close` of 20th Century: Overview of the State of the Art. *Spill Science and Technology Bulletin*, 5 (1), pp 3-16

Snedaker, S. C., Biber, P.D. and Rafael J. A. (1995). Oil Spills and Mangroves: An Overview. In: Workshop Convened August at McNeese State University, Prepared under Cooperative Agreement 14-35-0001-30690 by Louisiana Environmental Research Center , McNeese State University Lake Charles, Louisiana 70609

Wale Adabanwi (2001). Nigeria: Shell of a State'', Dollas and Sence magazine, July/August, pp 2

Wang, S-D., Shen, Y-M., Guo, Y-K., and Tang, J. (2008). Three –Nimensional Numerical Simulation for Transport of Oil Spills in Seas'', *Ocean Engineering,* 35, pp 503-510

P 012

PLASMA TREATMENT OF INCINERATOR ASHES: A REVIEW

Ali, A.M., Shehu, M.S. and *Nyam, T.

Department of Chemical Engineering, Kaduna Polytechnic

*tobiasnyam@yahoo.com; habsan2002@gmail.com

Abstract:

This paper is a review of studies reported on treatment or vitrification of incinerator ashes. Owing to the fact that incineration is the method most readily used for handling of the ever increasing municipal waste tragedy; a further challenge is posed by the increase in the ashes generated and their toxicity from this waste reduction method. The expanse of reported incinerator ash type in modern times covered by studies has been captured alongside the plasma technology used for the vitrification processes. Analytical techniques deployed for pre and post vitrification of ashes were reviewed; as well as the results on chemical composition and leachability of heavy metals from slag. Evidently, the results show that the process not only reduces considerably the volume in ashes, it also checks leachable toxic components threat. The process is to a large extent possible, safe though with cost implications at set up. Some of the studies reviewed recommended possible uses for the resulting glass-ceramics whose mechanical and chemical properties have also been tested. There is also the need for further studies in various regards of concern.

Keywords: plasma treatment, incinerator ashes, glass ceramic, vitrification, slag

1.0 Introduction

Solid waste globally is increasing at an alarming rate and along with it are the challenges of handling and treatment. Studies show that governments in various countries have proffered measures aimed at curbing the alarming growth of solid waste which range from provision of landfill through incineration, (Zhao, Ni, Jiang, Chen, Chen, & Meng, 2010; Pan and Xie, 2014 and Cheng, Tu, Ko, & Ueng, 2011).

Incineration has been lauded as a treatment process that reduces the volume of solid waste by up to 80%. Secondary pollution however results in the process and its products are usually fly ash and bottom ash. These products, which contain hazardous substances, are also calling for treatment and disposal (consolidation) attention as they increase in volume (Cheng *et al.*, 2011). In some plants, the electricity required for vitrification is generated as thermal energy recovery process from the incineration plants, (Katou, Asou, Kurauchi, & Sameshima, 2000; Colombo, *et al.*, NA and Chen, *et al.*, 2009)

Thermal plasma is being adopted at various levels as a means of vitrification of ashes from incineration plants. The some of the merits the technology has are that, thus far its product (slag) is capable of safely immobilizing some heavy metals in a stable form. At the same time persistant organic pollutants such as dioxins and furans are completely checked by the process. The energy source of plasma systems is electricity which is independent of the waste being destroyed. Furthermore the system can be small but possessing high temperature and energy densities that encourage chemical reactions within short residence time. Cheng *et al.*, (2011) and Pan and Xie, (2014) reported that the technology has been used in the treatment of various hazardous wastes with satisfactory results.

Some studies have been devoted to the characterisation and applications of the vitrification process products namely: molten slag, molten metal (ingot) recoverable at the bottom and off gas Colombo *et al.,* (NA); Cheng *et al.,* (2011); Chen *et al.*, (2009); Pan and Xie (2014); Zhao *et al.*, (2010); Katou *et al.*, (2001) and Karoly *et al.*, (2007) These studies and more report significant increase in the densities of the products which translate to 60-70% reduction of volume; according to Katou *et al.*, (2000), reducing incineration ashes to slag can effectively prolong landfill life. The studies on glass-ceramics nature of slag are of no less importance either.

In this paper we seek to review the thermal plasma technology so far in use for the treatment of incinerator residue and fly ash. We are also viewing analytical techniques deployed in raw materials and product analysis hence the chemical composition and TCLP data respectively.

2.0 Thermal Plasma Application

2.1 Types of Incineration Ash

Thermal plasma has been applied to vitrification of various ashes at laboratory scale and industrial scale as reported in Japan (Katou *et al.*, 2000) and Taiwan (Cheng et al., 2007). However, it is clear that incinerators serve various types of waste categories and could be specialised. These researchers also took cognisance of the peculiarity of ashes available as residue or fly ash as depicted in Table 1. The incinerator ashes were from municipal solid waste incinerator (MSWI), medical waste incinerator (MWI) and laboratory waste (LWI).

Table 1 Incinerator Ash

Type of Incinerator	Ash	Additive	References
MSWI	Bottom & Fly ashes	Fluorescent lamps	Colombo *et al.,* NA
MSWI	Fly ash & Incinerator scrubber ash		Cheng *et al.,* 2011
MSWI	Fly ash & Bottom ash	Colouring agents	Cheng *et al.,* 2007
MSWI	Not indicated		Cheng *et al.,* 2002
MSWI	Fly ash		Cheng *et al.,* 2009
MWI & MSWI	Fly ash		Pan & Xie, 2014
MSWI	Fly ash		Zhao *et al.,* 2010
MSWI	Wet Bottom ash		Katou *et al.,* 2001
MSWI		With and without Lime	Karoly *et al.,* 2006
MWI	Fly ash		Pan *et al.,* 2013
LWI	Bottom ash, Fly ash	Sludge, activated carbon and cullet	Kuo *et al.,* 2010
Not stated	Fly ash		Stockholm, 2011
MSWI	Fly ash	Silica & Alumina	Rani *et al.,* 2008
MSWI	Fly ash	Pulp & paper boiler ash	Carrabin & Gagnon, 2007
MSWI	Bottom ash & fly ash		Colombo *et al.,* NA

2.2 Thermal Plasma Generator

According to Huang and Tang, (2007) thermal plasma generation is achievable by use of direct current (DC), alternating current (AC), microwave discharge (MW) or radio frequency (RF) induction. They further reported that the arc plasma generators are categorised into transferred arc torch and non-transferred arc torch. The thermal plasma generator employed for gasification and vitrification of incinerator ashes by some workers are shown in Tables 2 and 3. Some studies were at laboratory scale while others were either at pilot plant or industrial scale as depicted in the Tables. The generators generally, generate high temperature alongside ultra-violet radiations. The inert gas and high temperature atmosphere employed in the process suppress the generation of NO_x, SO_x and HCl (Huang and Tang, 2007; Rani *et al.,* 2008).

Table 2 Thermal Plasma Generators used for Melting of Incinerator Ashes (Lab Scale)

	Electric Power source/ Ash Throughput	Working Gas/ Flow rate	Electrodes		Crucible bed shape	reference
			Cathode	**Anode**		
RF	30kW 100kW NT	Ar Ar	Graphite			Colombo *et al.,* Cheng *et al.,* 2002 2011
DC	1 ton/ day	N	Graphite			Chen *et al.,* 2009
DC	Double arc 20-30V/100A 50-60V/100A	Ar/ 12-14L/Min				Pan & Xie, 2014
DC	100kW/ 100kg/h	N / 12L/Min	Graphite		Cone	Zhao *et al.,* 2010

Table 3 Thermal Plasma Generators used for Melting of Incinerator Ashes (industrial)

	Electric power / Ash Throughput	Working Gas/s Flow rate	Electrodes		Crucible bed shape	reference
			Cathode	**Anode**		
DC	1710kW/ 16 tons/day	N	Graphite	Counter electrode	Flat	Katou *et al.,* 2001
DC	1200kW NT/ 250kg/h					Cheng *et al.,* 2011

3.0 Analytical Methods

Table 4 shows the analytical technique used by most of the reviewed researchers. It reflects mostly a common stand point with some variance. In some cases, instruments could detect very small quantities of substance whereas other workers reported not detected.

Table 4 Analytical Methods

Material	Purpose of analysis	Method	References
Raw materials Fly Ash, Bottom Ash, Sludge & Activated Carbon	Chemical composition of Ashes	XRF	6, 2, 15
		SEM-EDS	12, 1
	Leachability	TCLP(USEPA, method 1311)	5, 4, 11, 12
	Crystal structure	XRD	11
		SEM	12
	Elemental composition	EDS	11
	Heavy metal		11
	Concentration of solids	ICP-MS	10
	Concentration of PCDDs/Fs	HRGC/ HRMS	12
Slag	Chemical composition	EDS	3
		SEM-EDS	6, 10
		ICP-AES	8
	Micro-structural characteristics	SEM-EDX	8
		SEM	5, 4, 11, 12, 3
	Leachability	TCLP(USEPA, method 1311)	5, 4, 15, 12, 11, 1, 3
	Crystal Structure	XRD	10, 11
	Concentration of metal	AFS & GFAAS during TCLP	15
	Concentration of solids	ICP-MS	10
	Nature of glass	XRD	6
Glass	Determination of crystal structure	XRD	3, 2, 4, 8, 10, 11, 15
	Conductivity	-	14
	Bending strength & compressive strength	Electronic Tensile Tester	4
	Porosity, Water absorption, physical/ mechanical properties	-	3, 5, 4, 14
Ingot	Micro-structure of solids	SEM-EDS	10

3.1 Raw Material Analysis

The studies as seen from Table 5 shows, expectedly, that the composition (%) of the constituent chemicals or elements varies with type and source of ash and chemical reagents used for various functions e.g. removal of acid, adsorption of volatized metals, etc. Fly ash (FA) alone will not form glass without the addition glass formers, consequently some additives such as industries waste output serve to improve silica content (Carabin and Gagnon, 2007 and Rani *et al.,* 2008). Accordingly, the makeup of the ashes is also predicated upon the scrubber solution (lime CaO or NaOH) or adsorbent (Activated Carbon) effect especially where fly ash is involved (Pan and Xie, 2014, Pan *et al.,* 2013 and Kuo *et al.,* 2010). Specifically for lime enables the development of crystal structure at lower temperatures (Karoly *et al.,* 2007); in contrast high chlorine content together with low basicity in raw ash according to Pan and Xie, (2014) can be detrimental to solidification of heavy metals. MWI Ash has higher organic components as compared with MSWI ash thus Pan *et al.,* (2013) reported dioxins concentration in raw material as well as flue gas. Though not shown here, PCDD/Fs proportion in the waste ashes is higher in incinerated MWI than MSWI.

Table 6 shows metal concentrations as reported by various workers. Zinc, lead and copper are the dominant metals in most of the ashes analysed. The sources of the ashes especially FA include from the cyclone part of Air Pollution Cleaning (APC) device, bag (bag house) filters of kilns (Pan *et al.,* 2013 and Rani *et al.,* 2008).

Table 5 **Raw Material Analysis**

Group	Ca	O	Na	K	Si	Al	S	Zn	Fe	Cl	Cu	Pb	Cr	Cd	Mn	Ni	Ba	P	Mg	C	LOI	As	Sr	Te	Ag	Hg	Ti	Mo	Ref
Fly Ash — Elemental composition wt%	22.95	30.86	2.26	2.79	7.50	3.59	3.58		2.15	11.96								1.12	2.61	8.69	7.17								11
	7.89	33.15	1.29	1.44	13.87	8.89	0.99		3.24	1.26								0.73	1.23	25.35	10.3								11
	21.66	23.90	1.75	1.50	6.17	4.28	1.51		0.56	17.23								0.63	1.75	13.54	18.2								11*
	21.7	23.9	1.75	1.50	6.17	4.28				17.2									3.01	13.5									12
	8.55	35.5	0.95	1.56	14.4	8.95			1.28										1.03	25.4									12
Fly Ash — Chemical composition wt% *(sub-header)*	Ca	O	Na	K	Se	Al	V	Zn	Fe	Co	Cu	Pb	Cr	Cd	Mn	Ni	Ba	P	Mg	C	LOI	As	Sr	Te	Ag	Hg	Ti	Mo	Ref
	8.5		49.4	77.2	2.0	10.9	12.2	24.4	17.5	0.6	5.5	4.3	8.6	32.1	19.6	12	3.3		8.6			46.2	5.4	20.1	34.9	32.8	3.5	67.3	10
Scrubber ash — Chemical composition wt% *(sub-header)*	CaO		Na_2O	K_2O	Si_2O	Al_2O_3	SO_3	ZnO	Fe_2O_3	Cl	CuO	PbO	Cr_2O_3	CdO	MnO	NiO	BaO	P_2O_5	MgO	ZrO_2	SnO_2	Br	SrO		$NaCl$	Y_2O_3	TiO_2		Ref
	26.84		3.45	9.79	16.01	4.39	13.72	1.31	3.49	14.54	0.15	0.46	0.08		0.18	0.01	0.1	2.06	1.76	0.04	0.15	0.11	0.1				1.24		2
	28.04		4.55	4.43	21.6	8.6	8.31	1.26	2.45	9.8	0.1	0.22	0.13	0.14	0.19	0.02		3.07	2.87	<0.01	0.26						2.0		5
	26.84			9.79	16.01	4.39	13.72	1.31	3.489	14.54	0.15	0.46	0.08		0.18		0.1	2.06	1.76	0.04	0.15		0.1		3.45	ND	1.25		15
	25.4		6.9	3.1	23.9	15.8		2.1	5.1	3.1								5.6	2.4								2.9		1
	26.6		10.5	3.8	18.1	13.3		4.0	3.0	8.5			0.2		3.0			3.1	2.0										1
	42.57		4.83	4.64	2.05	0.45	3.79	1.47	0.27	31.5	0.13	0.47	0.01	0.47	0.02	<0.01		0.37	0.98	<0.01			0.15				0.09		5
Bottom Ash — Chemical composition *(sub-header)*	CaO		Na_2O	K_2O	Si_2O	Al_2O_3	SO_3	ZnO	Fe_2O_3	Cl	CuO	PbO	Cr_2O_3	CdO	MnO	NiO	BaO	P_2O_5	MgO	ZrO_2	SnO_2	Br	SrO		$NaCl$	Y_2O_3	TiO_2		Ref
	17.69		**6.46**	**1.08**	**55.14**	**8.25**	**0.275**		**5.88**		**0.164**						**0.246**	**0.933**	**2.53**								**0.714**		6
(sub-header)	CaO	O	Na	K	Si_2O	Al_2O_3	S	ZnO	Fe_2O_3	Cl	Cu	PbO	Cr_2O_3	CdO	MnO	NiO	BaO	P_2O_5	MgO	T-C	SnO_2	Br	SrO		$NaCl$	Y_2O_3	TiO_2		Ref
	13.1		1.12	0.38	39.8	10.3	0.17		18.9	0.47	0.29								2.21	2.4									9
AC *(sub-header)*	Ca	O	Na	K	Se	Al	V	Zn	Fe	Co	Cu	Pb	Cr	Cd	Mn	Ni	Ba	P	Mg	C	LOI	As	Sr	Te	Ag	Hg	Ti	Mo	Ref
	45.9		18.3	22.2	94.1	50.2	42	12.1	37.4	63.8	69.3	0.6	31.4	25.7	26.3	43	89.3		39.2			15.5	68.4	42.3	10.3	18.5	89.4	8.8	*10
	18.0	14.3	0.3	2.0	23.6	29.9		21.9	19.4	14.4	0.7	93.6	3.8	3.6	25.7	1.7	4.4		39.9			3.0	2.7	37.5	13.4	17.5	6.5	0.4	10

AC – Activated Carbon

* Medical waste incinerator ash

* Mass distribution of input materials (%)

Table 6   Metals in Raw Material Analysis

					Heavy Metal Concentration (mg/kg)				
		Pb	Cu	Cd	Cr	Zn	Ni	As	Hg	Ref.
		2055	888	193	181	-	68.69	79.6	1.23	Chen *et al.* (2009)
Fly Ash		2943.5	465.2	142.2	74.3	9743.8	74.9	-	-	Pan & Xie, (2014)
		1964.2	542.7	68.4	93.7	7512.5	69.2	-	-	Pan & Xie, (2014)
		1237.4	227.7	74.7	117.3	8053.4	55.9	-	-	~Pan & Xie, (2014)
		2100	-	172	182	8100	-	81	1.11	Zhao *et al.* (2010)
		1444	243	88	153	8720	82.4	-	-	Pan *et al.* (2013)
		1174	157	31.9	32.1	4614	21.2	-	-	Pan *et al.* (2013)
Bottom Ash		Pb	Se	Cd	T-Cr	Zn	-	As	T-Hg	
		3000	3	<0.2	1200	5100	-	<1	0.4	Katou *et al.* (2000)

~ Medical Waste Incinerator ash

4.0 Products
4.1 Products Treatment

The products derivable from plasma treatment are flue gases, slag and ingot. The slag can be cooled variously as seen from Table 7. Water cooling gives a more amorphous structure while air cooling results a more crystallized structure (Kuo *et al.,* 2010 and Zhao *et al.,* 2010). However, Carabin & Gagnon, (2007) opined that quick cooling results in amorphous structure where the silicate molecules matrix locks in the contaminants; on the other hand slow cooling results in crystalline structure. Describing the surface characteristics as affected by quenching method, Zhao *et al.,* (2010) indicated that water-cooled slag manifests less physical hardness and much porosity as compared to air-cooled or composite-cooled slag which also have better vitreous appearance.

Table 7   Product Treatment Analysis

Raw Material Processing Temp.	Slag Treatment	Gas out of Plasma Furnace	Reference
>1300°C	Water quenched	Promptly cooled below 250°C	Chen *et al.* (2009)
Maintained at > 1500°C for 1h at 7°C/min	Lab-scale slag was Air cooled Pilot-scale was water quenched		Cheng *et al.* (2011)
>1700K	Water quenched, air cooled, "composite cooling"		Zhao *et al.* (2010)
NA	Water chilled and crushed		Katou *et al.* (2000)
1600°C	Cooled, annealed at 600°C for 2 h slow cooling to room temp. Crystallization Heat Treatment (CHT) at 850, 900, 950, 1000 & 1050°C for 2 h and cooling 5°C/min		Karoly *et al.* (2007)
>1400°C for 1h	Water quenched, drying, grinding. CHT at 1000-1100°C for 2 h Addition of colour pigments: TiO_2, MnO, Fe_2O_3 & CP-236 (cobalt aluminum oxide)		Cheng *et al.* (2007)
1350°C	Maintained 1350°C for 10 min cooled 10°C/min. CHT at 1150, 1050, 950, & 850°C for 2 h then cooled to room temp		Cheng *et al.* (2002)

4.2 Products Characteristics
4.2.1 Slag (Glass-ceramics)

Generally it is established that the major product, slag (glass-ceramics), that results from the melting process is amorphous, its nature is dependent on the ash-SiO_2 ratio among other factors (Pan and Xie, 2014 and Rani *et al.,* 2008). The amorphous slag is speculated by Kuo *et al.*, (2010) to have some crystals on the surface and the major crystalline phases are calcium silicate (Ca_2SiO_4) and soda melilite ($NaCaAlSi_2O_7$). The success reported by Cheng *et al.,* (2007) shows the transformational effects of additives

173

on slag which not only manifest in appearance but impacted on mechanical and chemical properties as well.

In looking at microstructure of glass-ceramics, Table 8 shows the major phases reported by some workers. Karoly *et al.,* (2007), reported a contrast in findings as compared to Cheng *et al.,* (2002), they disagree with the formation of diopside with increasing temperature submitting further that the presence or lack of MgO in raw material content can bring this about. They suggested that addition of lime affects crystallisation.

Table 8 **Glass Product Characterization**

		Major phases in slags						Ref
S1 (SA+FA in ratio 3:1)	Mayenite $(Ca_{12}Al_{14}O_{33})$							5
S2 (SA+FA in ratio 1:3)	gehlenite $(Ca_2Al_2SiO_7)$	Calcium magnesium chloride silicate $(Ca_8Mg(SiO_4)_4Cl_2)$						5
Quenched slag (1:3)	gehlenite $(Ca_2Al_2SiO_7)$	Diopside $(Ca(Mg,Al)(Si,Al)_2)_6)$						5
S3					Wadalite	Rondorfite		1 1
	gehlenite $(Ca_2Al_2SiO_7)$		Anorthite $(CaAl_2Si_2O_8)$	Wollastonite $(CaSiO_3)$				8
	gehlenite $(Ca_2Al_2SiO_7)$		åkermanite $(Ca_2MgSi_2O_7)$					3
Slag without colour agents	gehlenite $(Ca_2Al_2SiO_7)$	grossular $(Ca_3Al_2(SiO_4)_3)$		Wollastonite $(CaSiO_3)$				4
Slag + 10-20 wt% TiO₂	gehlenite $(Ca_2Al_2SiO_7)$		Anorthite $(CaAl_2Si_2O_8)$	Wollastonite $(CaSiO_3)$	Perovkite $(CaTiO_3)$			4
Slag + 5-15 wt% MnO₂	Mayenite $(Ca_{12}Al_{14}O_{33})$	gehlenite $(Ca_2Al_2SiO_7)$				hausmannite (Mn_3O_4)	pyroxmangite $[(Mn, Fe)SiO_3]$	4
Slag + 10-15 wt% Fe₂O₃	gehlenite $(Ca_2Al_2SiO_7)$			Wollastonite $(CaSiO_3)$			hematite (Fe_2O_3)	4
Slag +10-15 wt% CP-236	gehlenite $(Ca_2Al_2SiO_7)$	Cobalt aluminum Oxide $(CoAl_2O_4)$		Wollastonite $(CaSiO_3)$			augite $(CaAl_2O_4)$	4

4.2.2 Ingot

According to Kuo *et al.,* (2010), the ingot major components are Fe, Cu, Na, Ca, and Al. In their (Kuo *et al.,* 2010) words metals with high boiling point and high specific weights constitute the ingot while the ones with low boiling point form part of the flue gas. Pan and Xie, (2014) however report an iron composition which is 30-40% less than other studies. Because of these metals in the flue gas, they opined that secondary APC need be put in place to 'catch volatile metals'. Furthermore, they posit that the ingot requires further processing while its quality can be improved by input material classification.

4.2.3 Leachability of Heavy Metals

The data from the various studies on concentrations of heavy metals in leachates (Table 9) shows the vitrification as one which reduces the heavy metal concentrations to low level, 15 times in some cases less than regulated limits. Some other workers reported chemical compositions of

slag e.g. Colombo *et al.,* (NA). TCLP characteristics were also reported by Pan *et al.,* (2013) to the effects reported earlier; they went further to report low or near no concentrations of PCDD/Fs in slag and off-gas. For Katou *et al.,* (2001) however, PCDD/Fs were not detected in the slag from their study; there were traces in dust from melting and bag house. Though the impact of additives on slag is far reaching Cheng *et al.,* (2007) reported that coloured glass-ceramics retarded the leachability characteristics for most heavy metals as even detected metals are at level lower regulatory limits.

The quenching method has been shown by Zhao *et al.,* (2010) to affect some heavy metals concentration. Their studies show that leachates from air-cooled slag had higher concentrations of these metals than water-cooled and composite-cooled, put in other words composite and water cooling of slag lowers the degree of leaching.

A concern is the non regulated metals and substances; they according to Kuo *et al.,* (2010) may require further treatment/ stabilization. Of note too, is the variance in regulatory limits from country to country.

Table 9   TCLP Results for Slags

Elements (mg/L)	Zn	Cd	Pb	Cu	Ni	Hg	Cr	As	Se	T-Hg	Ag	Ba	Mn	Si	Al	Na	B	Ref
Slag-I	<0.1	<0.1	0.4	<0.1														5
Slag-II	<0.1	<0.1	0.3	<0.1														5
Quenched Slag	ND	ND	0.3	<0.1														5
TCLP Limit (Taiwan)	25	1.0	5.0	15.0														5
	-	<0.005	<0.05	<0.03	<0.05	3×10^{-5}	<0.05	2.48×10^{-3}										2
TCLP Limit (China)		1	5	100	5	0.1	15	5										2
S1	5.94	0.0865	0.0243	1.533	0.0504		BDL											11
S2	0.084	BDL	BDL	0.2972	0.308		BDL											
S3	0.054	0.0559	0.4946	0.0544	0.0763		0.1067											
TCLP Limit (China)	50	0.3	3	50	-		10											
Air – cooled	0.02262	0.00146	0.104	-	-	<0.0005	0.00217	0.0055										15
Water-cooled	0.02660	0.00113	0.0229	-	-	<0.0005	0.00081	0.0006										
Composite-cooled	0.03165	0.0002	0.0315	-	-	NA	0.00026	NA										
TCLP upper Limit (China)	100	1	5	-	-	0.1	5	5										
Slag		<0.01	<0.01				<0.05	<0.01	<0.01	<0.0005								9
Dust from melting		<0.01	0.02				<0.05	0.03	0.85	0.0025								9
Limits in Japan	-	-	-	-	-	-	-	-	-	-								9
	0.003	<0.0	<0.0	<0.0	<0.0	<0.0	<0.0	<0.0	<0.0		<0.0	0.0						10

| | | 01 | 01 | 01 | 01 | 01 | 01 | 01 | 01 | | 01 | 43 | | | | | | 10 |
	-	1	5	15	-	0.2	5	5	1		5	100						6
Slag from BA(ppm)	0.150			4.54	0.88		0.026	0.019				0.304	0.185	0.72	5.27	12.1		6
Slag from FA (ppm)	0.075			0.366	0.032		0.051	0.061				2.170	0.29	4.14	21.1	31.2		6
WAC (Italy) (ppm)	5			5	1		1	0.2				10	-	-	-	-		6
Pilot plant		ND	0.2				ND	ND	ND			ND					ND	1
Sample 1		ND	0.34				ND	ND	ND			ND					ND	1
Sample 2		ND	0.29				ND	ND	ND			ND					ND	1
Sample 3		ND	0.36				ND	ND	ND			ND					ND	1
Province of Quebec Canada		0.5	5.0				5.0	5.0	1.0			100					500	1
Slag (mg/kg)	0.2	<0.0025	<0.007	0.076	0.023	0.0031	<0.016	<0.007				0.053						13
Inert landfill WAC (London)	4	0.04	0.5	2	0.4	0.01	0.5	0.5				20						13

BDL –Below Detection Limit
NA – Not Available
ND- Not Detected
- Not Stated
WAC – Waste Acceptance Criteria

5.0 Conclusion

Plasma treatment of incinerator waste offers a way of alleviating the challenges posed by ashes generated from incineration and the danger they pose. The process can use heat from the incinerator for its energy source as energy conservation process, its products glass ceramics can be used in construction, char can be improved for use as absorbent, super capacitor, etc while the ingot can also be improved for use in industries. The flue gas can be derided of dioxins and furans. This process not only makes waste harmless but is capable of generating wealth and raw material for the construction industry among others; however more work needs to be done in the aspects of regulation, product characterisation and application to wet processes. None of the workers herein reported looked at incinerator waste from oil and gas processes; it is worth considering the use of thermal plasma technology for treatment of gaseous and solid waste from the petroleum industry.

References

1. Carabin P. & Gagnon J. (2007). Plasma Gasification and Vitrification of Ash-Conversion of Ash into Glass-like Products and Syngas. World of Coal Ash; Available at http://www.flyash.info/2007/148carabin.pdf

2. Chen M., Meng Y., Shi J., Kuang J., Ni G., Liu W. and Jiang Y. (2009). DC Arc

Plasma Furnace Melting of Waste Incinerator Fly Ash. J Plasma Science and Technology 11(1):62-65;

3. Cheng T.W., Chu J.P., Tzeng C.C. & Chen Y.S. (2002). Treatment and Recycling of Incinerated Ash using Thermal Plasma Technology 22: 485-490.

4. Cheng T.W., Huang M.Z., Tzeng C.C., Cheng K.B. & Ueng T.H. (2007). Production of Coloured Glass-ceramics from Incinerator Ash using Thermal Plasma Technology. J Chemosphere 68:1937-1945;

5. Cheng T.W., Tu C.C., Ko M.S. and Ueng T.H. (2011). Production of Glass-ceramics from Incinerator Ash using Lab-scale and Pilot-scale Thermal Plasma Systems. J Ceramics International 37:2437-2444;

6. Colombo V, Concetti A, Ghedini E, Gherardi M, Sanibondi P, Vazquez B, Barbieri L and Lancellotti (NA). Rf Thermal Plasma Vitrification of Incinerator Bottom and Fly Ashes with Waste Glasses from Fluorescent Lamps. Paper presented at International Plasma Chemistry Society (ISPC) 20 Conference in Philadelphia USA; also available at http://www.ispc-conference.org/ispcproc/ispc20/401.pdf

7. Huang H & Tang L. (2007). Treatment of Organic Waste using Thermal Plasma Pyrolysis Technology. J Energy Conversion and Management 48:1331-1337;

8. Karoly Z., Mohai I., Toth M., Weber F. & Szepvolgyi J. (2007). Production of Glass-ceramics from Fly Ash using Arc Plasma. Journal of the European Ceramic Society 27: 1721-1725;

9. Katou K., Asou T., Kurauchi Y. & Sameshima R. (2001). Melting Municipal Solid Waste Incineration Residue by Plasma Melting Furnace with a Graphite Electrode. J Thin Solid Films 386:183-188;

10. Kuo Y., Chang J., Chang K., Chao C.C., Tuan Y. & Chang-Chien P. (2010). Stabilisation of Residues Obtained from the Treatment of Laboratory Waste. Part 1-Treatment Path of Metals in a Plasma Melting System 60(4):429-438;

11. Pan X. & Xie Z. (2014). Characteristics of Melting Incinerator Ashes Using a Direct C Plasma Torch. J Environmental & Analytical Toxicology 4(3); available at http://dx.doi.org/10.4172/2161-0525.1000212;

12. Pan X., Yan J. & Xie Z. (2013). Detoxifying PCDD/Fs and Heavy Metals in Fly Ash from Medical Waste Incinerators with a DC Double Arc Plasma Torch. J Environmental Science 25(7):1362-1367;

13. Rani D.A., Gomez E., Boccaccini A.R., Hao L., Deegan D. & Cheeseman C.R. (2008). Plasma Treatment of Air Pollution Control Residues. J Waste Management 28(7): 1254-1262;

14. Stockholm (2011). Plasma Torch and its Application to Waste Destruction. Available at https://intra.ees.kth.se/polopoly_fs/1.254025!/Menu/general/column-content/attachment/report03.pdf

15. Zhao P., Ni G., Jiang Y., Chen L., Chen M. & Meng Y. (2010). Destruction of Inorganic Municipal Solid Waste Incinerator Fly Ash in a DC Plasma Furnace. J Hazardous Materials 181.

176

P 013

SYNTHESIS AND CHARACTERIZATION OF ZEOLITE Y VIA MICROWAVE IRRADIATION

[1]*A.S. Kovo, [2]M.O. Edoga, [3]Ahmed Shehu, [4]Mohammed Aris Ibrahim, [5]A.S. Abdulkareem, [6]Ahmed A.F

[1,3,4,5]Department of Chemical Engineering Federal University of Technology, Minna, Nigeria.

[2]Department of Chemical Engineering, Federal University, Ndufi, Ebonyi State, Nigeria

[6] Department of Environmental Management , Bayero University Kano

*kovo@futminna.edu.ng, kovoabdulsalami@gmail.com

Abstract:

This paper reports the work carried out on the synthesis of Zeolite Y using sol-gel hydrothermal technique but with the application of microwave power irradiation providing the heat. Zeolite Y samples were formed from clear homogenous colloidal solution with batch composition $4.62Na_2O:AlO3:10SiO_2:180H_2O$ and the effects of varying microwave power were investigated at constant crystallization temperature. The XRD analysis showed that the zeolite Y phase synthesized had similar characteristics pattern when compared with commercial zeolite Y and this was obtained after only 5 minutes at microwave power of 800W and crystallization temperature of 120oC. The morphology of the Zeolite Y sample was monitored with the aid of SEM and it showed that, the zeolite Y sample has hexagonal shape and average crystal size of 23.44 μm. The results obtained showed that with Microwave irradiation, Zeolite Y with similar characteristic as the commercial type can be synthesized within a short crystallization time

Keywords: Synthesis, Characterization, Zeolite, Microwave, Irradiation, hydrothermal, Crystals

1.0 Introduction

Zeolites are large class of alumina silicate mineral containing aluminium and silicon combined with oxygen in their structure whether natural or synthetic. They are three dimensional, micro porous, crystalline solid with defined regular frame work structure in which silicon and aluminium atoms are tetrahedrally connected to each other through the shared oxygen atoms. The frame of every zeolite is therefore constructed from tetrahedral building blocks, TO4 where T is a tetrahedral coordinate atom (Szostak, 1992,Kovo, 2011). It is generally believed that no two AlO_4 can be linked directly by sharing their Conner in the Zeolite frame work. The frame work which is the ratio Si to Al of a Zeolite is therefore always greater than one.

There are about 40 natural Zeolites which have been identified during the last 200 years and more than 150 Zeolites have been synthesized (Mayowa, 2014). The common examples of natural Zeolite are phillipsite, chabazite; clinoptilolite, analcine, erionite and mordenite whileexample of synthetic Zeolites include Zeolites A, X, Y and ZSM-5. Both natural and synthetics Zeolites are used commercially because of their unique characteristics likeadsorption, ion-exchange, molecular sieve and catalytic properties (Breck 1974).However, synthetic Zeolites like Zeolite Y hold some advantages over their natural analogues. The synthetic Zeolite comes in a uniform phase-pure state unlike the natural Zeolites that have some varying degree of contaminants like quartz, Fe2+, SO42- and amorphous glass. It is possible to synthesize Zeolite of desirable structure which does not appear naturally such as Zeolite Y. It requires significantly less time than the natural zeolites, the principal raw materials used are among the abundant mineral components on earth. Zeolite Y synthesis involve the hydrothermal crystallization of reactive alumina silicate gel or solution in a basic environment (Breck, 1974) these gels are formed upon mixing silica and aluminates solution in the presence of alkali hydroxide and/or organic bases. The gel is crystallized in a closed hydrothermal system at elevated temperature (usually 100-2000C) and the pressure is generally autogenous. The time required for crystallization varies from a few hours to several days.

Zeolite Y is very important material and this makes its synthesis very justifiable. Zeolite Y is widely used as a catalyst especially in petroleum refining because the physical separation process of crude oil into its various fractions alone cannot satisfy the market demand, so there is need for chemical conversion process such as catalytic cracking, catalytic reforming, isomerization, alkylation and polymerization. Furthermore, during catalytic cracking processes, the catalyst that is normally employed is the Zeolite Y, hence there is a compelling need to apply faster synthesis technique such as application of microwave irradiation to produce zeolite Y. This is will ultimately solve the problem of conventional hydrothermal synthesis method which longer crystallization time to produce zeolite Y.

2.0 Materials and Methods:

2.1 Seed preparation:

The seed gel was produced based on the overall composition as $(4.62Na_2O:Al_2O_3:10SiO_2:180H_2O)$. 19.95g of water ($H_2O$) was firstly weighed into a 500ml plastic beaker, then 4.07g of sodium hydroxide pellets (NaOH)

was weighed and poured into another the 500ml beaker containing water. Thereafter 2.09g of sodium aluminates solid (2NaAl (OH)$_4$) was added into the plastic beaker and the mixture was stirred until it dissolved.

22.72g of sodium silicate solution (Na$_2$SiO$_3$.9H$_2$O) was weighed and poured into a second 500ml plastic beaker. The content of the second beaker was slowly poured into the first beaker, while stirring moderately for at least 10 minutes. After stirring, the beaker was capped and allowed to age at room temperature for one day (24 hours).

2.2 Preparation of feedstock gel:

During the preparation of the feedstock, 130.97g of water was weighed and poured into a 500ml plastic beaker, 0.14g of sodium hydroxide pellet and 13.09g of sodium aluminate solid was added and stirred until dissolved. 142.43g of sodium silicate solution was added to the mixture above in ablender, and the overall content in the blender was vigorously stirred until the gel appears somewhat smooth. The blender was covered until the addition of seed gel.

2.3 Preparation of overall gel:

The overall gel was prepared by using 16.50g of seed gel prepared earlier and was slowly added to the feedstock gel in the blender and agitated (up to 20 minutes) under high shear, the blender was shaken during mixing to ensure the entire gel volume encounter the high shear from the turbine.

2.4 Crystallization of overall gel:

2.4.1 Micro wave irradiation hydrothermal treatment:

Three samples were prepared for crystallization at different microwave power and constant temperature of 120 0C. The first sample (gel) in the blender was poured into a microwave plastic with cover, and was hydrothermally treated in the micro wave chamber at 1200C for two minutes at constant heating power of 800W. The second at 120 0C for three minutes at 600W, and the third was at 1200C for five minutes at 400W. After micro wave irradiation hydrothermal treatment, the gel separated out into a solid that settled at the bottom and a clear supernatant liquid indicating complete crystallization. The product were cooled, and filtered by washing with de-ionized water until a pH of less than 9 was obtained and dried in a hot air oven at 600C for 3 hours.

3.0 Results and Discussions:

The XRD diffractogram of the prepared zeolite Y using microwave irradiation alongside the reference XRD obtained from commercial Zeolite Y (Zeolyst International, Netherland) are represented in Figures 1 to 4. The XRD result enables the determination of the crystalline structure of the Zeolite samples. It is clearly evident that the diffractogram of the three samples of Zeolite Y prepared at the three different microwave power rating at 400, 600 and 800 W showed a characteristic peak of Zeolite Y at 2 theta angle at 6.2^{o}. The diffractogram of

the three samples prepared using microwaves also compared well with XRD pattern of commercial zeolite used as reference (figure 4) . However the intensity of the main characteristic at 6.1^{o}, 10.1^{o} 12°, 14.3^{o}, 17.5^{o} increased as the microwave power and the highest intensity of about 8000 count was obtained at the maximum microwave power studied in this experiment. The gradual increase observed as the power rating of the microwave increased could be attributed to the rapid nucleation caused by the application of microwave power which was to facilitate rapid heating (Wenyaun*et al* 2013) and this in turn aided and catalysed the crystal growth. To further corroborate the formation of Zeolite Y at the three different power rating studied, SEM analysis of the sample were carried out and the results obtained are shown in Figures 4 to 6. Close examination of the micrograph reveal formation of crystalline phase with well define hexagonal shape of various sizes especially at power rating of 800W along with other not well defined shape at other power rating studied i.e. 400 and 600W. It was clear that crystalline material was formed following the crystallization phase and this tend lay credence that zeolite Y was actually synthesised at the conditions of the crystallization which in this case is at temperature of 120°C and time of 6 min. The particle size analysis of the synthesised sample was also carried out for the sample produced at 800W and average crystal size of 23.44 μm was obtained and this is within reasonable level of commercial Zeolite Y sample (Not Shown) used in this work as reference material.
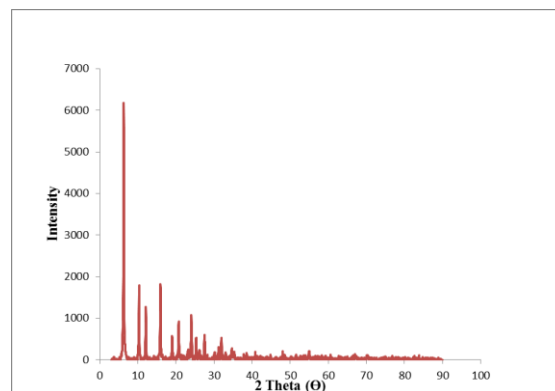
Figure 1:XRD image of synthesized Zeolite Y at 400W microwave power
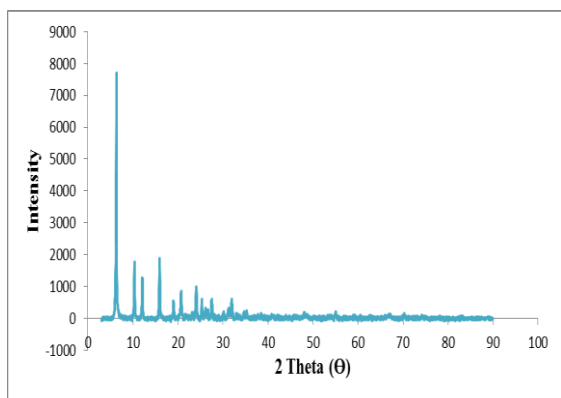
Figure 2: XRD image of Zeolite Y at 600W microwave power

179
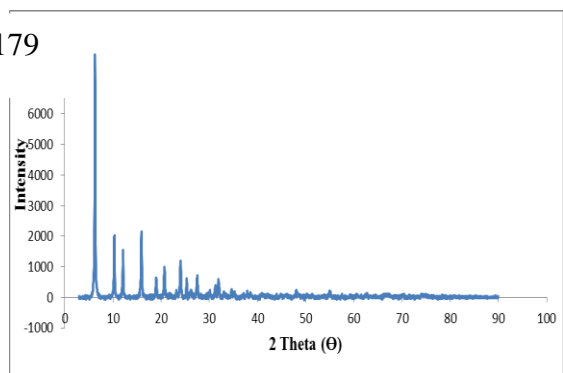
Figure 3: XRD image of synthesized Zeolite Y at 800 W microwave powers.
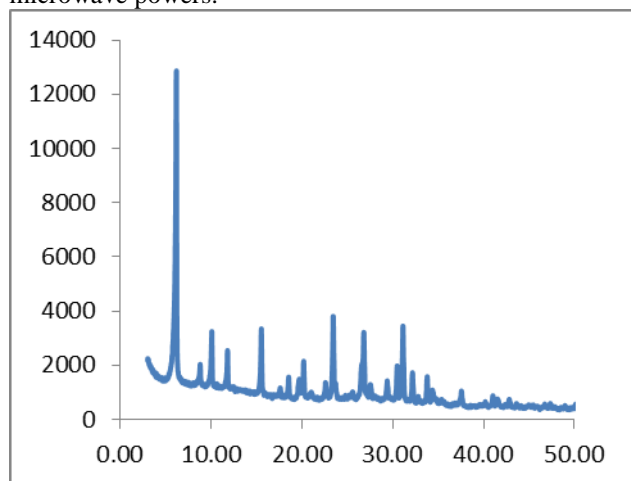
Figure 4: XRD image of commercial Zeolite Y obtained from Zeoyst Netherland
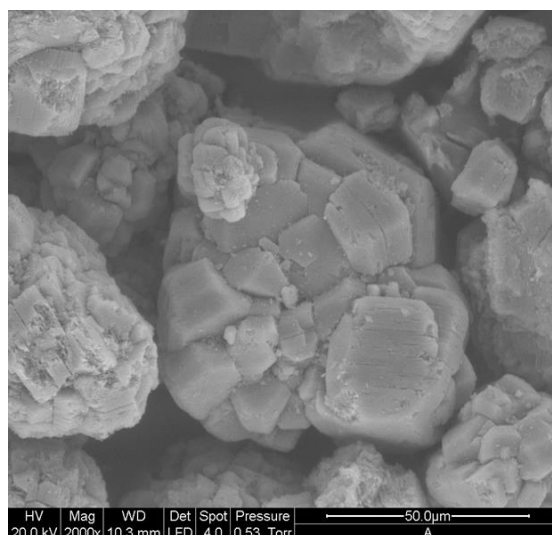
Figure 5 SEM image at 400 W microwave powers

180
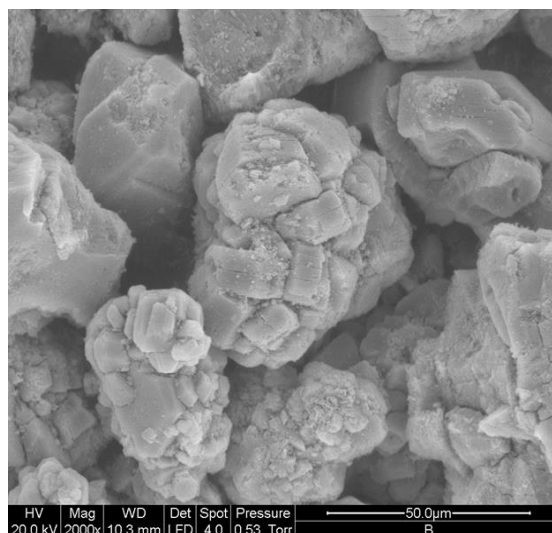
Figure 6: SEM image at 600 W microwave powers.
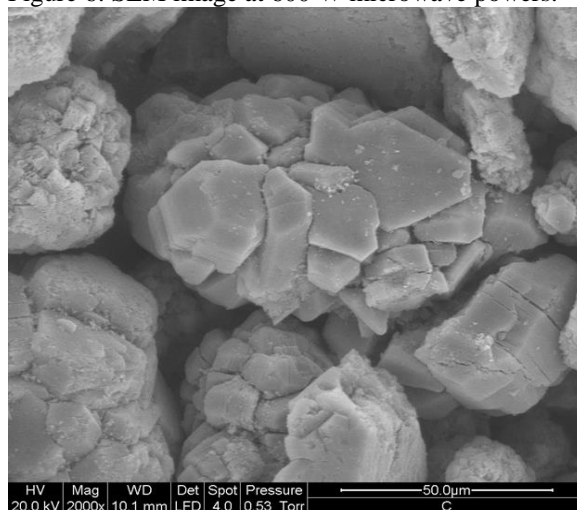
Figure 7: SEM image of synthesized zeolite Y at 800 W microwave powers.

4.0 Conclusions:

Zeolite Y was successfully synthesized following the application of microwave irradiation as source of heat rather conventional hydrothermal method. Both the XRD and SEM analysis of the three sample of zeolite Y prepared revealed the formation of crystalline phase within a period of 5 min which far lower that 3-9 hours at usual reported crystallization temperature of 100oC reported for conventional hydrothermal method of zeolite Y synthesis.

4.0 References

Adeyemi Mayowa David (2014). Synthesis and characterisation of zeolite A using sol-gel hydrothermal method.

Breck, D.W (1974) Zeolite and Molecular Sieve, Structure, Chemistry and Use," New York: John Wiley and Sons. Bogdal, D., Penzek, J.,

Kovo, A. S., (2011). 'Development of zeolites and zeolite membranes from Ahoko Nigerian Kaolin.'Pp. 88-156

Szostak, R (1992) "Molecular sieves, science and technology. Weikamp, J J (Ed) springer, berlin.

Wenyaun Wu, Chunwei Shi, BianXue, Bai Yuting, (2013), Microwave radiation hydrothermal synthesis and charcaterization of micro-and mesoporous composite molecular sieve Y/SBA-15, Arabian Journal of Chemistry, In press

Xianchun, W.U. (2003). " Acidity and Catalytic Activity of Zeolite Catalyst Bound with Silica and Alumina". Ph. D Dissertation. Texas A and M University. China.

P 014

A LINEAR PREDICTIVE MODEL FOR DEBUTANISER PRODUCTS COMPOSITION

Obekpa, R.G. and *Alabi, S.B.
Department of Chemical and Petroleum Engineering, Faculty of Engineering,
University of Uyo, Uyo, Akwa Ibom State, Nigeria
*sundayalabi@uniuyo.edu.ng; roseline261@gmail.com

Abstract:
Debutaniser is an important distillation column in a natural gas processing plant. Due to lack of real time hardware debutaniser products composition sensor, in this study, a linear model was developed for the purposes of online prediction of the debutaniser top and bottom products composition. With the aid of HYSYS 3.2 process simulator, data which cover practical ranges of operating conditions of debutaniser were obtained. Using MINITAB 14 software, the obtained data were used to build and analyse the performance of the proposed model, using percentage mean relative error (PMRE) and R-squared statistic (R^2) as criteria. The model, consisting of five first degree linear regression equations, was found to estimate the compositions of the top and bottom products accurately, with the exception of the equation for the bottom total butane. The minimum R^2 for the four accurate regression equations is 0.905 while the maximum PMRE is 5.66%. Worst-case PMRE, less than 6%, was obtained from the model interpolative test, which indicates high generalisation ability for the four accurate regression equations. Therefore, it is concluded that the proposed model can be considered for real time simultaneous estimation of debutaniser products compositions.

Keywords: *Natural gas liquids, Debutaniser, Predictive model, Real time prediction.*

1.0 INTRODUCTION

Natural gas processing plant purifies raw natural gas from underground gas fields and from well heads with associated gas (Baker, 2002). The natural gas liquids (NGLs) are separated into its individual components at a fractionation plant which consists of a series of fractionation (distillation) columns. Demethaniser, de-ethaniser, depropaniser and debutaniser are examples of distillation columns that can be found in the natural gas processing units (NGPUs) for separating methane, ethane, propane, and butane, respectively, from a feed stream of natural gas liquids (NGLs) (Ahmad et al., 2011). Although butane and propane can be mixed to form liquefied petroleum gas (LPG), there are situations where they are required individually not as a mixture. Butane has about 12 percent more energy than propane by volume and burns more clearly, but propane is a better choice for situations in which temperatures may drop below freezing point (Owen, 2015). Propane is used as a feedstock to make ethylene and propylene petrochemicals through the steam cracking process. Butane is used as a propellant in aerosols; it is also used to make butadiene, a major component of synthetic rubber. Pentane plus on the other hand is used as gasoline blend and petrochemical feedstock. All these account for the need to separate these natural gas liquids into various fractions. There is a need to produce high quality gas, to reduce product rejection rates and to comply with prevailing laws of environmental and occupational safety.
This study focuses on debutaniser. Butane product (distillate) from the debutaniser is allowed to contain a maximum composition of 2.5% mole of propane,

minimum of 95% mole butane and a maximum of 3.0% mole pentane while the maximum allowable butane in the bottom product is 1.5% mole (Ahmad et al., 2011). Too much of propane in butane reduces the latter's energy content and shortens the duration of heat supply. Pentane, if present in excess of the required specification in butane reduces butane's flammability and as such deters its application as heating gas. These constraints are rarely met. Therefore, online monitoring and control of debutaniser products composition are essential. The composition measurement carried out either by offline sample analysis in the laboratories using gas chromatograph or online analyzers are often unsafe, expensive and require frequent and high cost of maintenance (Ramli et al., 2014). Furthermore, the discontinuity and significant delays associated with laboratory analysis or slowly processed quality measurements of online analyzers coupled with the other challenges can reduce the effectiveness of control strategy (Patil and Nigam, 2009). The use of an inferential sensor (also known as soft sensor) is an attractive alternative to hardware sensors in providing real time estimates of the relevant process variables for implementing effective control strategies. According to Huang (2011), soft sensor is a mathematical model, which correlates difficult-to-measure quality variables with the frequently and easily measured process variables.
Therefore, in this study, a linear regression model which is capable of simultaneous estimation of the composition of

the top and bottom products of debutaniser over a wide range of operating conditions is developed.

2.0 METHODOLOGY
2.1 Variables Selection
process manuals that were available to the authors. The variables which affect the composition of the products of the debutaniser column, as well as the relevant output

Sahraie et al (2013) gave a list of parameters needed to describe the application and corresponding characteristics of a debutaniser column. Other useful pieces of information were also obtained from the natural gas

variables are as shown in Table 1. These input variables are assigned letters A-J.

Table 1: Selected Input and Output Variables for Modelling

Symbols	Input variables	Top output variables (mol %)	Bottom output variables (mol %)
A	Feed flow rate (kg/hr)	Total propane concentration	Total butane concentration
B	Feed temperature (^{o}C)	Total butane concentration	Total pentane concentration
C	Feed pressure (kPa)	Total pentane concentration	
D	Reflux flow rate (kg/hr)		
E	Bottom flow rate (kg/hr)		
F	Top pressure (kPa)		
G	Total number of trays		
H	Feed tray		
I	Bottom temperature (^{o}C)		
J	Top temperature (^{o}C)		

Having selected the ten (10) input variables, unique operating points for eight (8) of these variables were obtained from literature (Patil and Nigam, 2009) and the relevant process manuals. These eight (8) variables were the required input variables for simulation using HYSYS software.

The highest and the lowest operating points of these variables were selected and their averages were used as basis for data generation. The corresponding operating points for the remaining two (2) variables (bottom and top temperatures) were obtained via simulation as they are a part of the outputs from the HYSYS.

2.2 Design of Experiments
Three sets (modelling, interpolation and extrapolation) of experimental designs were conducted using Minitab software, version 14.13. In the design of experiment for modelling data generation, the lower and upper limits of the input variables were set at 80% and 120% respectively, of the average values of the input variables. This was done so as to achieve a model which can be applied over a wide range of operating conditions. The upper and lower limits of input variables for the design of experiment for model development are given in Table 2. Full factorial design approach was adopted, using 2-level factorial (default generators) for the eight (8) variables.

Table 2: Upper and lower limit of input variables for the design of experiment for model development

S/No.	Symbols	Variables	Average	Lower limit	Upper Limit
1	A	feed flow rate (kg/hr)	56080	44864	67296
2	B	feed temperature (^{o}C)	93.6	74.88	112.32
3	C	feed pressure (kPa)	634.3	507.44	761.16
4	D	reflux flow rate (kg/hr)	54340	43472	65208
5	E	bottom flow rate (kg/hr)	8735	6988	10482

6	F	top pressure (kPa)	623.3	498.64	747.96
7	G	total No. of trays	35	28	42
8	H	feed tray	18	14	22

The result of the experiment which was designed was used for model data generation via simulation. For the interpolation, 90% of the average values of the input variables were used as the lower limits while 110% were used as the upper limits. This was done so as to obtain a set of data within the range of the modelling data. The lower and upper limits for the extrapolation data were set at 70% and 130%, respectively, of the average values of the input variables.

2.3 Response Variables Data Generation
A model of the debutaniser column was built using HYSYS 3.2 software. Simulation was carried out to generate data from the developed HYSYS model which is shown in figure 1.
This simulation was performed based on the designed experiments described in section 2.2. The originally unavailable input variables (bottom and top temperatures) and the output variables (top and bottom products compositions) required for the model development, interpolation and extrapolation tests were obtained.
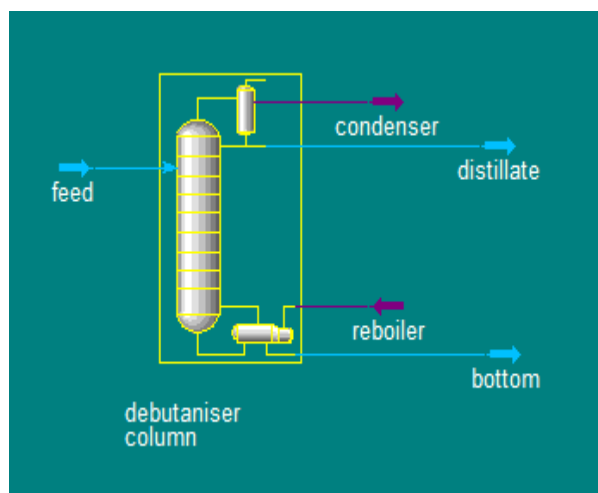
Figure 1: Debutaniser Model.

In an attempt to reduce the number of the input variables and obtain general-purpose model, dimensionless variables were introduced. This was achieved by taking the ratios of the input variables given in Table 1. The input variables were reduced from 10 to 6 while the output variables remain the same. Linear regression equations were then fitted (with the aid of Minitab software) to the modeling data using these six (6) dimensionless input variables. The reduced dimensionless variables denoted by letters K-P are: K= reflux flow/feed flow, L= bottom flow/feed flow, M=bottom temp/feed temp, N=top temp/feed temp, O=feed plate/total plate, P=top pressure/feed pressure. Interpolation and extrapolative tests were carried out using MS Excel Spreadsheet.

2.4 Performance Evaluation Criteria
The performance of the model developed in this work was evaluated based on percentage mean relative error (PMRE) and R-squared statistic. PMRE is a measure of accuracy defined as the average of absolute prediction errors. It is used to indicate the overall prediction performance in terms of both accuracy and reliability (Draper and Smith, 1998). The expression for PMRE is given by equation (1).

$$\text{PMRE} = \frac{\sum_{i=0}^{n}(\text{Actual}-\text{Fit})}{\text{Actual}} \times 100 \qquad (1)$$

Where: Actual = the simulated data, Fit = the predicted results obtained from the developed model, n = the number of observations. R-squared is a statistical measure of how close the data are to the fitted regression line. It provides a measure of how well the observed outcomes are replicated by the model, as the proportion of total variation of outcomes explained by the model (Colin et al., 1997).

3.0 RESULTS AND DISCUSSION
Following the steps outlined in section 2, a model which consists of a set of five (5) linear equations were obtained and is shown in a matrix form in equation (2). The performance indices are given in Table 3. It can be seen from Table 3 that the equations have very high values of R^2 except the regression equation for the total bottom butane which has an R^2 value of 0.347.
The equations with high R^2 show that the observed outcomes are well replicated by the equations, thus indicating high accuracy. However, the R^2 value of 0.347 for total bottom butane equation indicates that the data are not very close to the fitted regression equation and as such the prediction accuracy level is low.

Table 3: Performance Indices of the Developed Model

Predicted outputs	R^2	Percentage mean relative error (%)
Top total propane	0.991	0.15
Top total butane	0.994	0.27
Top total pentane	0.994	3.19

Bottom total butane	0.347	2701.0
Bottom total pentane	0.905	5.66

Similarly, the percentage mean relative errors, as shown in Table 3, are very low with the exception of that of the total bottom butane. These low values indicate that the predictions obtained from those equations are very close to the actual (simulated) data thereby pointing to the high accuracy of the equations. Conversely, the percentage mean relative error of 2701% shows that the total bottom butane equation cannot predict the actual total bottom butane correctly.

The interpolative (generalisation) and extrapolative abilities of the developed model were evaluated using the interpolated and extrapolated data obtained. The resulting performance indices of the models in terms of PMREs are as summarised in Table 4 while the R-squared statistics for the interpolative test are shown in figure 2. Similar trend was obtained for the extrapolation test.

From the results shown in Table 4 and Figure 2, it is observed that irrespective of the verification approach adopted, the errors obtained from the interpolation tests are smaller than those from the corresponding extrapolation tests except for the bottom total butane which has been shown to have failed right from the modelling stage. This shows that the proposed model can perform well with high prediction accuracy and reliability if the output variables to be predicted are within the range of data used for the modelling.

Nevertheless, this model can be used to predict debutaniser products compositions (with the exemption of bottom total butane) outside the range of data used for the modelling, as the extrapolation errors(less than 22%) are deemed reasonable for practical application.

Table 4: Interpolative and Extrapolative Performance Indices of the Developed Model

Predicted outputs	Percentage mean relative error (%)	
	Interpolation	Extrapolation
Total top propane	0.35	0.41
Total top butane	0.091	0.53
Total top pentane	0.75	21.3
Total bottom butane	7645.0	688.0
Total bottom pentane	5.38	21.79
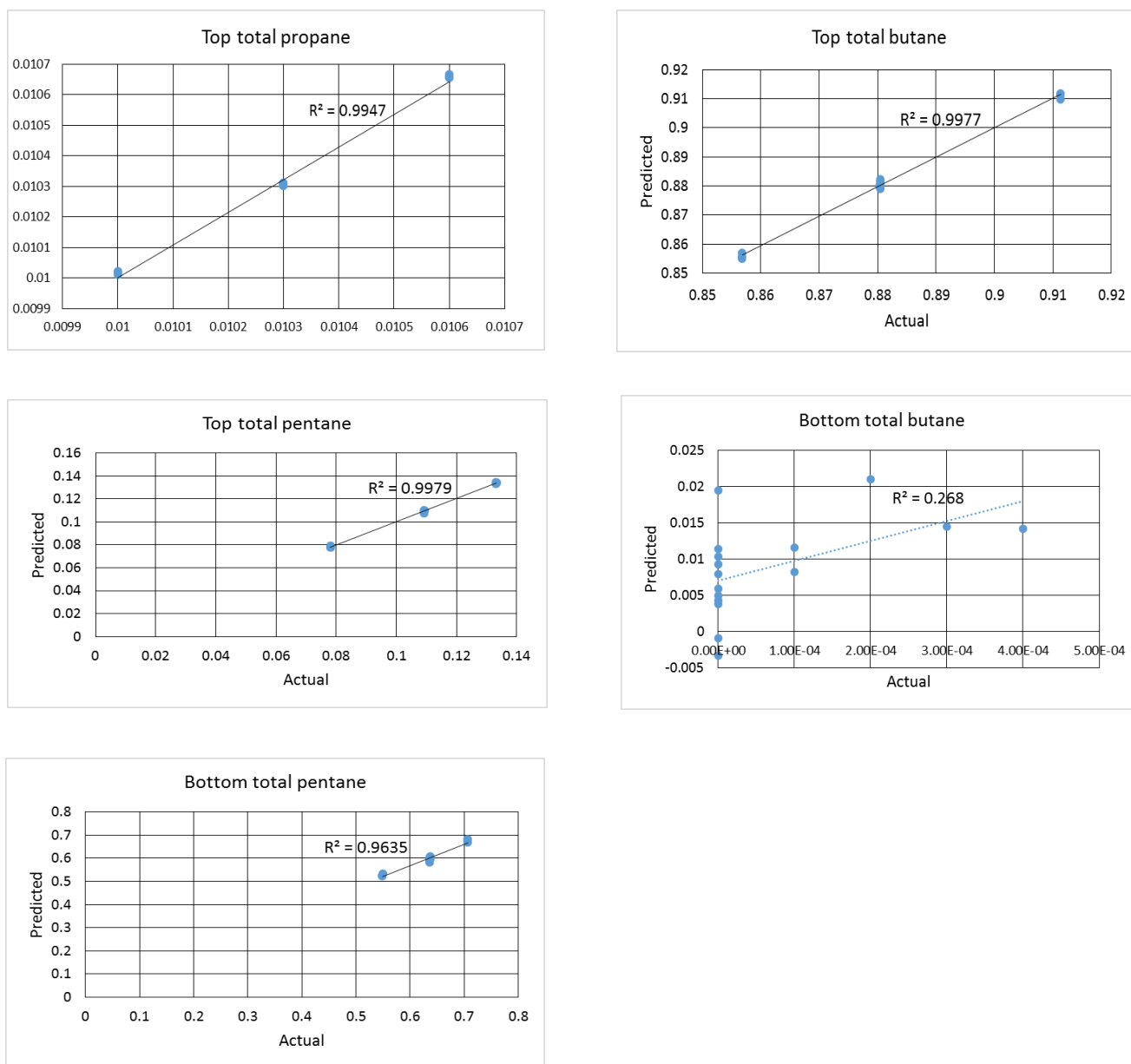
Figure 2: Graphical representation of interpolation ability of the developed model.

4.0 CONCLUSIONS

In this work, a linear regression model having the potentials for application as an inferential sensor for debutaniser products compositions was developed. With the exception of bottom total butane prediction, the various forms of performance evaluation criteria adopted showed that the equations for top total propane, top total butane, top total pentane and bottom total pentane have high accuracies and generalisation abilities (minimum R^2 of 0. 905 and maximum PMRE of 5.66%). Moreover, although with caution, the proposed model can be used outside the range of data used for model development, as the resulting extrapolation errors (of less than 22%) are deemed reasonable for practical applications. However, the performance of the linear regression equation for the bottom total butane is very poor.

5.0 REFERENCES

Ahmad, R., Malla, M., Hladky, M., Shadman, F. and Usman, M. (2011). *Fractionation of Natural Gas Liquids*

to produce LPG. Norwegian University of Science and Technology. Page 6-23.

Baker, R. (2002). *Future Directions of Membrane Gas Separation Technology Ind*. Volume 41, Eng. Chem. Res. Pages 3-9.

Colin, A., Windmeijer, G., Gramajo, H., Cane, E. and Khosla, C. (1997). *An R-squared measure of goodness of fit for some common nonlinear regression models*. Journal of Econometrics 77 (2): 1790–2.doi:10.1016/S0304-4076(96)01818-0.PMID 11230695.

Draper, R. and Smith, H. (1998). *Applied Regression Analysis. Wiley-Interscience.* ISBN 0-471-17082-8.

Huang, B. (2011). Improve Measurement with Soft Sensors for Process Industries. Presentation at ISA Fort McMurray, 18 April, 2011.

Owen, P. (2015). *Propane Vs. Butane Stove*. Available at www.livestrong.com. Accessed 26th February, 2015.

Patil, R. and Nigam, M. (2009). *Soft sensor for multicomponent distillation column using neural network and genetic algorithm based techniques.* International Journal of Computational Intelligence Research. ISSN: 0973-1873. Page 1- 6.

Ramli, N., Hussain, M., Jan, B. and Abdullah, B. (2014). *Composition Prediction of a Debutaniser Column using Equation Based Artificial Neural Network Model.* Neurocomputing limited, Malaysia. Page 62-74.

Sahraie, H., Salehi, G., Ghaffari, A. and Amidpour, M. (2013). *Distillation Column Identification Using Artificial Neural Network.* Gas Processing Journal. ISSN: 2322-3251 Vol.1. Page 31-38.

P 015

DEVELOPMENT OF Pt-Zn/Al₂O₃ CATALYST FOR NAPTHA REFORMING

[1]Oloworishe F. J., [2]Atta, A. [1]Mukhtar B. and [3]Aderemi* B. O.

[1&3]Department of Chemical Engineering, Ahmadu Bello University, Zaria, Nigeria
[2]National Research Institute for Chemical Technology, Bassawa – Zaria, Nigeria

*Corresponding author's e-mail: benjaminaderemi@gmail.com; GSM: 2348033844528

Abstract:
Various platinum and zinc gamma-alumina supported catalysts were formulated and developed in this investigation following the conventional impregnation method. Five of the catalysts consist of 1.0% wt of zinc (Zn) and varying amounts of platinum (Pt) in the range of 0 - 2.0 wt%, while chlorinated gamma-alumina, served as the control sample. The catalysts were characterized using X-ray diffractometer (XRD), BET, and Scanning electron microscope (SEM). The catalytic performances of these catalysts were as well evaluated with respect to n-octane reforming in a packed tubular reactor. The textural and morphological characterization results conformed to literature. The catalytic performances of the catalysts for n-octane reforming were determined at varying reactor temperatures (430°C - 530°C). The yield of reformate from n-octane depends largely on the catalyst's composition and the reactor's operating temperature. Chlorinated γ-alumina was found to produce reformate low in aromatic content. The incorporation of zinc (Zn/Al₂O₃) enhanced the reforming process to acceptable reformate's aromatic constituent (≥ 70%), but at a more severe operating temperature range (505°C to 530°C) when compared to that of Pt doped matrices (Pt-Zn/Al₂O₃), which was at 480°C.

1.0 Introduction

In the past decades, several octane number boosters or additives had been attempted. Such additives include methylbenzene (MTBE), ethylbenzene (ETBE), isooctane, toluene and tetraethyllead (TEL) (Gary and Handwerk, 1984). Nigerian refineries were in the 1980s making use of TEL to boost the quality of her gasoline, but had since phased-out such practice in conformity with global health and environmental regulations. Although there are serious campaigns against the use of aromatics as gasoline octane number enhancer due to its known carcinogenic effects, naphtha catalytic reforming technology for reformate production has continued to enjoy global patronage and enlargement partly due to its supply of the highly needed petrochemical feedstock (Huebner, 1999). The vast knowledge available on the chemistry of naphtha conversion: dehydrogenation of naphthenes to aromatics, isomerization of non-branched or partly-branched hydrocarbon to produce isoparaffin or an isomer of the base ring compound, dehydrogenation and aromatization of paraffin compounds to aromatics, hydrocracking, ring isomerization, dehydroisomerization of alkylcyclopentanes to aromatics and dealkylation of alkylbenzene coupled with increased understanding of the role of acidic sites on catalyst support in promoting isomerization reactions and metallic sites to promote dehydrogenation reactions thereby enhancing aromatization reactions enable specialized catalyst design to favour either isoparaffin production (as octane number enhancer) or to selectively promote aromatics formation for petrochemical industry (Burgazli, 2013, Aboul-Gheit and Cosyns, 2007, Delmon et al., 2005, Gary and Handwerk, 1984 and Huebner, 1999).

Modern reforming catalysts in use today contain platinum (Pt) supported on a silica, silica-aluminum, or alumina base. In most cases, rhenium (Re) is combined with platinum to form a more stable catalyst that permits operation at lower pressures. The cost of Pt poses economic challenges to its sole usage as an active metal in a catalyst (Gary and Handwerk, 1984). It is equally obvious that the current vogue in experimental catalysis lean more towards bifunctional and multifunctional sites to modify one property or the other for particular product selectivity, process condition or economic viability of the entire process (Luciene et al. 2012, Kao and Ramsey, 2011, Pierre-Yves et al., 2012 and Meitzner et al., 1996). Hence, the incorporation of Zn to supplement the Pt (as in Pt-Zn/Al₂O₃ catalyst) in this investigation was a cost saving approach and also to enhance the catalyst stability.

2.0 Materials and Methods

2.1 Development of Monometallic Catalyst:
An aqueous zinc chloride solution was prepared by dissolving 0.2161 g of ZnCl₂ salt in 100 ml of distilled water and the mixture well stirred. In a separate beaker, 10 g of gamma-alumina was immersed in 15 ml of 0.2 M HCl solution and the aqueous solution of ZnCl₂ was added. After stirring the admixture for 1hour the solvent was slowly evaporated by heating at 70°C, while stirring gently. The catalyst was then dried at 120°C for 10 hours. The dried sample was thereafter calcined in a furnace at 500°C for 4 hours, and further reduced under hydrogen flow for 4 hours at 500°C. This same procedure was repeated five times to yield identical samples equivalent to 1.0% Zn/Al₂O₃ catalysts (Meitzner et al., 1996).

2.2 Development of Bimetallic Catalyst:
Varying weights of hexachloroplatonic, H_2PtCl_6 (0.1042, 0.2083, 0.3125, and 0.3750 g) were dissolved in four beakers, each containing 100ml of distilled water, and stirred properly to form aqueous solutions. Four of the prepared monometallic catalysts (8g, 8g, 8g, and 7g) were added to the aqueous solutions of H_2PtCl_6. After proper stirring these were dried, calcined and reduced under hydrogen flow as enumerated for the preparation of the monometallic catalysts. XRD, and BET analyses were carried out on the various catalyst samples prepared (Abdullah et al., 1996, Zhang et al., 2012 and Meitzner et al., 1996)

2.3 Catalysts' Reformation Performance Evaluation
In a typical run, a measured quantity of the catalyst sample was packed (loaded) halfway within a tubular reactor; the reactor's temperature was steadily increased to the desired reaction temperature prior to the admission of the substrate. The n-octane (as a representative of straight run naphtha) was preheated to boil via a heating mantle and its vapour was channeled downstream into the reactor. The vapour outlet from the reaction zone was condensed and collected as product. This procedure was repeated for five different reaction temperatures (430, 455, 480, 505, and 530°C) for each of the catalyst samples developed. The composition of reformate obtained in each case was determined with the aid of a GC-MS machine

3.0 Results and Discussion
In Figure 1(a-f), the low intensity counts and the broad peaks that characterized the diffractograms of the support (γ-Al_2O_3) averred to the fact that the gamma-alumina is amorphous. The Zn/Al_2O_3 catalyst and the sets of Pt-Zn/Al_2O_3 catalysts have closely related bragg angles ($2\theta_s$)

with those of the support, but with different intensity counts. The bragg angles obtained for γ-Al_2O_3 exist at: 37°, 39°, 46°, 60°, and 66° (Fig. 1(a)), which agrees with those (37°, 39°, 46°, 60°, 67°) cited from the works of Hosseini et al. (2011), Mandana et al. (2011), Aderemi and Hameed (2012), and Bawa (2012)

The XRD patterns for the Pt-Zn/Al_2O_3 catalysts (Fig 1 (c-f)) have braggs angles (37°, 40°, 46°, 67°) which nearly coincide with those of the Zn/Al_2O_3 catalyst: (38, 39, 46, and 67°, (Fig. 1(b)). Though, platinum shows a distinct peak at 40° and 46°; the steady rise in the peak intensity at 40^0 and concurrent reduction in peak width indicates increase in crystallinity with increase in the Pt content from 0.5% to 2.0%. At 46°, the peaks of Pt-Zn/Al_2O_3 displayed characteristic trough and crest features which are absent in those of the support or Zn/Al_2O_3 catalyst. The works of Yasuharu et al (2007) also corroborated the fact of XRD pattern of platinum having Bragg angles of 17°, 40°, 46°, and 67°.

Figures 2-7 show the reformate yield patterns with variation in temperature for each catalyst. As depicted in Figures 2 and 3, the acidified alumina (support) and monometallic (Zn-alumina) catalysts, showed regular pattern of increase in reformate yield with temperature and attained maxima at 505°C and 530°C respectively. However, Figures 4 -7 revealed that the presence of Pt in the bimetallic catalysts exhibit increase in the rate of reformate yield with temperature increase attaining its peak value at temperature of 480°C. After the temperature of 480°C the reformate yield pattern became unpredictable possibly due to negative interaction effect between the duo metals at such elevated temperatures. The average conversion value of 84 $\pm$ 1% agrees with 82.44 reported by Axens group (2010) for freshly regenerated catalyst, while the catalyst produced in this work is superior to that in terms of its selectivity towards aromatics.
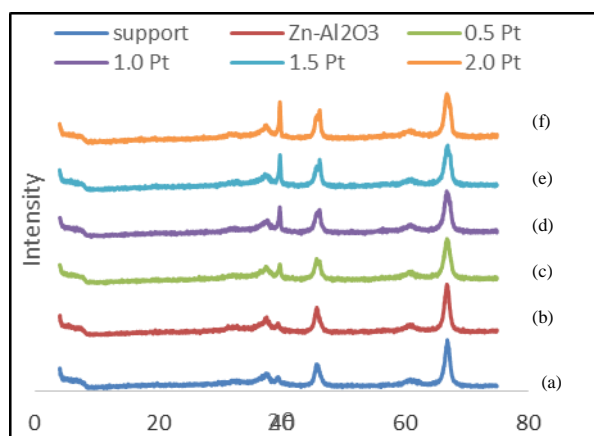
Fig 1: (a-f): Variation of XRD patterns with metal content
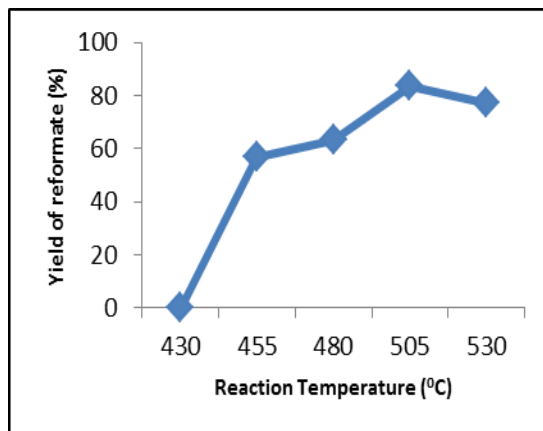
On the alumina support
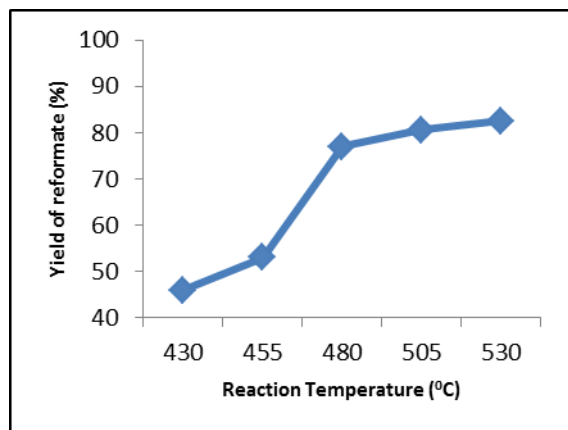
Fig 3: Variation of reformate yield with reaction temperature for the reactor packed with Zn/Al_2O_3 catalyst
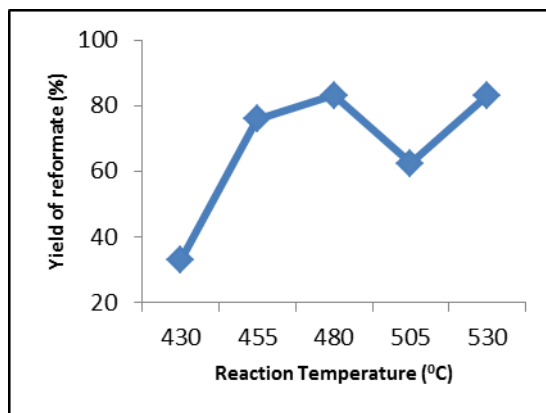
Fig 4: Variation of reformate yield with reaction temperature for the reactor packed with 0.50wt% $Pt-Zn/Al_2O_3$ catalyst
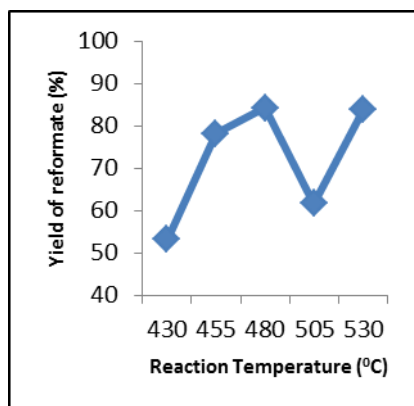
Fig 5: Variation of reformate yield with reaction temperature for reactor packed with 1.0wt% $Pt-Zn/Al_2O_3$ catalyst
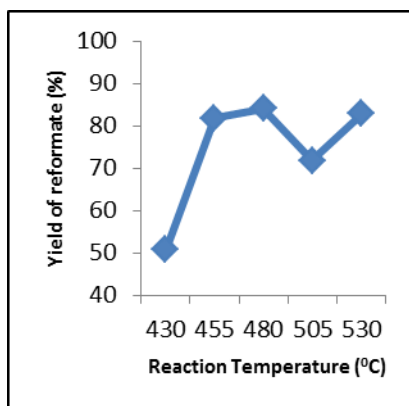
Fig 6: Variation of reformate yield with reaction temperature for reactor packed with 1.5wt% $Pt-Zn/Al_2O_3$ catalyst
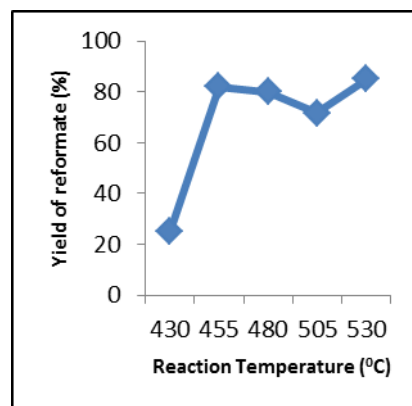
Fig 7: Variation of reformate yield with reaction temperature for reactor packed with 2.0wt% $Pt-Zn/Al_2O_3$ catalyst

Table 1: summary of the n-octane reforming processes

S/N	Reactor packed with	Max yield attained (%)	Temp range from min to max yield (°C)	Quality of product
1	Chlorinatedγ-Al_2O_3	83	455 - 505	Less than 64% of aromatics
2	Zn/Al_2O_3	83	430 - 530	Up-to 73% aromatics
3	0.5% $Pt-Zn/Al_2O_3$	83	430 - 480	Up-to 73% aromatics
4	1.0% $Pt-Zn/Al_2O_3$	84	430 - 480	Up-to 73% aromatics
5	1.5% $Pt-Zn/Al_2O_3$	84	430 - 480	Up-to 78% aromatics
6	2.0% $Pt-Zn/Al_2O_3$	85	430 - 530	Up-to 82% aromatics

5.0 Conclusion

The importance of metal doped catalysts in naphtha reformation process is affirmed in this investigation. Sole chlorinated γ-Al₂O₃ gave reformate with about 64% aromatics content, which fell below the minimum specified standard of 70% by API. The incorporation of zinc (Zn/Al₂O₃) enhances the reforming process, but at a more severe operating temperature range when compared to those of Pt doped matrices (Pt-Zn/Al₂O₃). Since a CRU plant is often designed to operate at high product quality, and narrower temperature range, with minima occurrences of sintering, then the inclusion of Pt is vital to a reforming catalyst. However, for obvious economic expediency, the proportion of Pt required can be made minima if Pt is complimented with zinc as demonstrated in this study.

References

Abdullah, Y., Mat, F. A.., Sufi, M. Mahat A., S. Kasim, R and Abdullah, N.(1996). *Synthesis and Characterization of Platinum Supported on Alumina doped with Cerium Catalyst*, a Research Thesis, Malaysian Institute for Nuclear Technology Research (Mint) Bangi, 43000 Kajang , Malaysia

Aboul-Gheit A.K. and Cosyns, J. (2007). Activation of platinum-alumina catalysts for the hydrogenation of aromatic hydrocarbons: *Journal of Applied Chemistry and Biotechnology*, 26 (1), pp. 15–22. John Wiley & Sons, Ltd

Antos G. J. and Abdullahi M. A. (2005), Catalytic Naphtha Reforming, 2nd Edition, Marcel Dekker Inc., New York, NY 10016, U.S.A

API-American Petroleum Institute (1994), Research Project 65, Sixteenth Annual Report.

Axens Catalyst Handbook for regeneration of reforming catalyst (2010). Axens IFP Group Technologies, Rueil-Malmaison, Paris, France.

Calvin, B. (2001) Journey of Applied Catalysis-Mechanism of catalyst deactivation. Department of Chemical Eng, Brigham Young University, Provo, UT84602, USA. pp. 17-60

Cody, I A. Dumfries, D. H. Neal, A. H. and Riley, K L. (1994). High porosity, high surface area isomerization catalyst and its use (United States Patent 5290426). http://googleads.g.doubleclick.net/pa

Delmon, B. Grange, P. Jacobs, P. A. and Poncelet, G. (2005). 'Preparation of Catalysts II', Elsevier, Amsterdam, deremi, B.O. and Hameed, B.H. (2012). Characterization of kaolin dealumination products. *Nig. J. of Eng*. 19(1), pp.72-77

Gary, J.H. and Handwerk, G.E. (1984). *Petroleum Refining Technology and Economics* 2nd Edition ed., Marcel Dekker Inc

Hosseini, S. A. Aligholi, N. and Dariush S. (2011). Production of γ-Al2O3 from Kaolin; *Open Journal of Physical Chem.,* 1, 23-27, Dept of Applied Chem., University of Tabriz, Tabriz, Iran, (http://www.SciRP.org/journal/ojpc).

Huebner, A. L. (1999) "Tutorial: Fundamentals of Naphtha Reforming," AIChE Spring Meeting 1999, Houston, TX, 14–18

Kalra S. K. (2009), Essentials of Refinery Processes; Indian Oil Corporation Ltd Panipat Refinery. (Cited online at petrofed.winwinhosting.net on 11:00AM on June 25, 2014)

Kao J.L. and Ramsey S. A. (2011). Naphtha reforming catalyst and process, United States Patent (patents.com),

Luciene, S. C. Karla, C. S. Conceica, V. A. Mazzieri, P. Reyes, C. L. Pieck, M. C. and Rangel (2012). Pt-Re-Ge/Al₂O₃ catalyst for n-octane reforming: Influence of the order of addition of metal precursors: *Applied Catalysis A: General* 419-420, pp. 156-163

Meitzner, G. Migone, R.. Mykytka, W. (1996). Noble metal/Zn-A1203 reforming catalysts with enhanced reforming performance (C-2714), United States Patent 5482615

Pierre-Yves L.G. R. and Jay, L. J. (2012). Redefining reforming catalyst performance: High Selectivity and stability. sited online at www. Hydrocarbonprocessing.com on March 27, 2014 by 09:30AM

Selcan, A. (2011). Oxidation of ethanol and carbon monoxide on alumina - supported metal/metal oxide xerogel catalysts. Chem. Eng. Dept, School of Eng and Sciences of İzmir Institute of Technology.

Zhang Y., Y. Zhou, J. Shi, X. Sheng, Y. Duan, S. Zhou, Z. Zhang (2012). Effect of Zinc addition on catalystic properties of PtSnK/γ-Al₂O₃ catalyst for isobutane dehydrogenation: Original Research Article; *Fuel Processing Technology*, *Volume 96*, pp. *220-227*

P 016

THE MITIGATING EFFECTS OF CARBON TO NITROGEN RATIO ON FOAMING POTENTIAL IN MESOPHILIC FOOD WASTE ANAEROBIC DIGESTION

[1]Musa Idris Tanimu*, [2]Tinia Idaty Mohd Ghazi, [2]Mohd Razif Harun [2]Idris Azni

[1]Mohammed Baba Buhari

[1]Department of Chemical Engineering, Kaduna Polytechnic, PMB 2021, Kaduna, Kaduna state, Nigeria. [2]Department of Chemical and Environmental Engineering, Faculty of Engineering, Universiti Putra Malaysia, 43400 Serdang, Selangor, Malaysia.
*musandadrisu@gmail.com; tinia@upm.edu.my,

Abstract:

Foaming problem which occurs occasionally during food waste (FW) anaerobic digestion (AD) was investigated by stepwise increase in organic loading (OL) from 0.5 to 7.5 g VS/L. The FW feedstock with carbon to nitrogen (C/N) ratio of 17 was upgraded to C/N ratio of 26 and 30 by mixing with other wastes from fruits, vegetables and chicken meat. The digestion which was carried out at 37ᵒC in 1L batch reactors showed that foam formation was initiated at an OL of 1.5g VS/L and was further increased as the OL of feedstock was increased. The digestion foaming reached its maximum level at an OL of 5.5 g VS/L and did not increase further even when OL was increased to 7.5 g VS /L. The Increase in the C/N ratio of the feedstock significantly enhanced the microbial degradation activity, leading to better removal of foam causing intermediates and reduced foaming in the reactor by up to 60%.

Keywords: organic loading, anaerobic digestion, foaming, carbon to nitrogen ratio, biogas methane.

1.0 Introduction

Anaerobic digestion (AD) has been widely accepted as an economic treatment option for FW and other high moisture content (MC) organic wastes (Jiang et al., 2012). This is because of its energy recovery benefits in the form of biogas methane yield. However, biologically mediated foaming during AD could result in environmental pollution, poor digestion performance and colossal damage to the reactor, pipeline, pump and other plant equipment. The exact mechanism of foam initiation and its stability is still not well known (Frayer et al., 2011; Heard et al., 2008). In the past, almost every foaming event in the industry has been linked to the presence of foam causing microbial cells. However, fundamental research carried out on the basic mechanisms of stable foam formation in anaerobic digestion (AD) revealed that the foaming results from the close interactions of three phenomena (Grifiths and Stratton, 2010; Ganidi et al., 2011, 2009; Kougias et al., 2013). These include, firstly, the presence of gas bubbles which could be the biogas produced during AD or air entrained in influents to the anaerobic digesters especially if it is emanating from the secondary treatment unit in an activated sludge process in waste water treatment plants. Secondly, the presence of surface active substances (bio or synthetic surfactants) such as oil, grease, lipids volatile fatty acids, detergents, proteins, glycolipids, lipoproteins, phospholipids, polysaccharide-lipid complexes etc (Kougias et al., 2013; Ganidi et al., 2009). These surface active agents which are both hydrophobic and hydrophilic could be present both in the feedstock or produced as intermediates during AD. The surfactants largely serve as food source to bacteria cells in digester media (Ganidi et al., 2009). The third requirement for foaming is the presence of foam causing bacteria cells in the digester medium such as Microthrix Parvicella or Nicordia etc (Marneri et al., 2009). In conventional digesters such as those treating FW, foaming has been attributed to over feeding or inconsistent feeding (Zhang et al., 2012). This factor borders on the concentration of the organic content or OL of the feedstock being digested. Ganidi et al. (2011) investigated the foaming initiation during the AD of municipal wastewater sludge and found an OL of 2.5 g VS /L as the foam initiation threshold and OL of 5g VS /L resulting in persistent foaming. Similarly, Kougias et al. (2013) investigated the effect of feedstock composition and organic loading rate (OLR) on foaming of cattle manure based feedstock. They observed the formation of foam at an OLR of 4.2 g VS /Ld. They concluded that the OLR and organic composition of the cow manure (such as proteins and lipids content) and the biogas produced during AD were the main contributors to the foaming observed. Experimental evidence on the identification of OL for foam initiation in a conventional food waste AD is unclear. It was established that, balanced microbial activity during AD could enhance the delicate balance between the activities of acidogens and methanogens resulting in rapid utilization of foam enhancing intermediates (Zhang et al., 2012). Therefore,

adequate nutrition to the bacterial cells through co-digestion of the feed with complementary wastes could improve its C/N ratio and enhance the activities of methanogens (Zeshan et al., 2012; Jiang et al., 2012; Zhang et al., 2012). In this study, the influence of increasing the food waste C/N ratio on its foaming potential during AD was studied.

2.0 Materials and method

2.1 Nature of the digested food waste
The main components of the mixed FW feedstock (F1) include chicken meat/beef (5%); rice, bread and noodles (77%); leafy vegetables/salad (6%); soup (5%); sea food, fish, egg and egg shell (7%).

2.2 Feedstock and inoculum preparation
The FW (F1), chicken meat, fruits and vegetable wastes were ground separately using a heavy duty blender (model 39BL11 Waring commercial, USA) and sieved to remove large particles using a 1mm sieve size. They were prepared in bulk and stored at -20°C for later use. Inoculum was sourced from the FW treatment plant digester. The proportion of feed mixture to inoculum was 7:3 by volume (Liu et al., 2009).

2.3 Experimental procedure
Thirty glass bottles, each of 1L capacity with a working volume of 0.8 L were used as the batch digesters. The digestion of F1 was carried out in reactor R1 to R10. F2 digestion was carried out in R11 to R20 and F3 in reactors R21 to R30. Each bottle was filled with the feedstock formulated and diluted with tap water to attain the OL of 0.5, 1.5, 3.5, 5.5 and 7.5g volatile solids (VS)/L respectively. These OL were selected based on the performance data reported for FW in literatures (Jiang et al., 2012; Zhang et al., 2012; Forster-Carneiro et al., 2008; Ganidi et al., 2011; Liu et al., 2009; Zhang et al., 2012; Bolzonella et al., 2005). Each of the five OL mentioned above was prepared in duplicate for each of the three feed types i.e F1, F2 and F3 (see Table 1.0). The bottles were placed in an oven at 37°C and its content was agitated daily after observing the foam formation. Biogas production and other parameters such as TS, VS, COD removal, VS destruction, volatile fatty acids (VFA), ammonia-nitrogen (NH_3-N) and alkalinity were monitored

every other day (APHA, 2005). Potential foaming tests were carried out twice weekly because of limited sample.

Table 1: Feedstock characteristics

Detail	F1 (C/N=17)	F2 (C/N=26)	F3 (C/N=30)
Physical characteristics			
Moisture content (MC) (%)[a]	92.43	95.15	90.63
Total Solid (TS) (%)[a]	7.55	4.82	9.35
Total Solids (TS) (g/L)	15.20	12.80	19.64
Volatile Solids (VS) (g/L)[a]	14.64	12.19	18.58
VS/TS (%)	96.30	95.20	94.60
Chemical characteristics			
C (% TS)	33.53	44.55	43.50
K (% TS)	0.48	3.33	0.44
N (%TS)	2.02	1.73	1.45
Na (%TS)	1.06	0.05	0.17
P (%TS)	0.66	0.39	1.57
C/N	16.60	25.75	30.00
Chemical Oxygen Demand (COD) (g/L)	273	282	294
pH	4.40	4.83	5.14
Lipids (%TS)	28.18	13.13	34.49
Lignin (%TS)	26.81	19.31	12.30
Feed Composition			
FW (%)[a]	100.00	50.00	77.30
Fruit waste (%)[a]		40.00	
Vegetable waste (%)[a]		10.00	.
Chicken meat waste (%)[a]			22.70

[a] based on percentage of wet weight

Digestion was carried out for 30 days. The characteristics of the feedstock and inoculum are presented in Tables 1 and 2 respectively.

Table 2: Inoculum characteristics

Parameter	Unit	Value
Moisture content	%	82.57
TS	mg/L	19.27
TS	%	17.43
VS	mg/L	17.80
VS/TS	%	92.37
NH_3-N	mg/L	625
pH		7.3

2.4 Foaming tests

Foaming tendency of the digestion medium was determined by the method of aeration using a bubble column apparatus. The apparatus consists of a 60mm diameter glass cylinder of 1L capacity with a galvanized wire placed at the bottom of the cylinder as air diffuser. A 50 mL sample was obtained from the reactor medium into the apparatus. The maximum foaming height and volume obtained after aeration of the sample sludge for 10 minutes at 60mL/min was recorded (Kougias et al., 2013; Ganidi et al., 2011; Deshpande and Barigou, 2000; Marneri et al., 2009). Foaming potential of the feedstock was evaluated by observing the foam formation in the reactor, the foaming tendency and foam stability. The foaming tendency was obtained by dividing the foam volume (mL) immediately after aeration by the flow rate of air (mL/min). Foam stability was obtained as the percentage of foam persisting after 1h of aeration. Foaming volume in the digester was determined by multiplying the digester surface area by the height of foam observed.

2.5 Analytical methods

Ultimate analysis for carbon and nitrogen were carried out using the CHNS machine (model CHNS 932, Leco Corporation, USA). Portions of the digestion medium were collected and centrifuged with a centrifuging machine (Model 2420, Kubota Corporation, Japan) at 5000 rpm for 15 minutes prior to VFA and NH_3-N tests (Liu et al., (2009). Analysis on alkalinity was performed by titration of 10ml of the sample against 1N H_2SO_4 (APHA, 2005). Ammonia-nitrogen (NH_3-N) was performed by Nessler's method (Ganidi et al., 2011). Volume of biogas collected in the gas bags were measured using the water displacement method (Zeshan and Karthikeyan, 2012). The biogas composition was obtained using a gas chromatograph machine (Agilent 6890N network GC

system) equipped with the carboxen 1010 plot column with dimension 30.0m x 530.0µm x 0.0µm nominal (Supelco 25467, USA). Lignin content was determined using Fibertec 2010 auto fiber analysis system (Foss Analytical, Denmark). Trace elements were measured using the ICP-OES model DV5300 (Perkin-Elmer, USA). Volatile fatty acid (VFA) test was carried out in an Agilent 6890 series gas chromatography using a flame ionization detector and a capillary column type HP-INNOWax polyethylene glycol capillary with dimension 30.0m x 250µm x 0.25µm (Jiang et al., 2012).

3.0 Results and discussion

3.1 Effect of OL variation on feedstock foaming in the reactor

The maximum foaming recorded during the digestion of F1 was at OL of 5.5 and 7.5 g VS/L (Figure1). Comparison of the foaming of feedstock F1 with F2 at the OLs tested showed a decrease in foam formation of 28.57%, 63.63% and 38.46% at OL of 1.5, 3.5 and 5.5g VS/L respectively. A further reduction in foaming of 57.14%, 63.63% and 61.54% was obtained at the same OL when the foaming of F1 was compared with F3. When foaming of F2 was compared with F3, a decrease in foaming of 30 % was observed at OL of 1.5gVS/L and 37.5% at OL of 5.5 and 7.5gVS/L. This means that for the same OL, the potential for foam formation decreases with increase in feedstock C/N ratio. However, within the same feedstock C/N ratio, foaming increased with increase in OL. The correlation between OL and reactor foaming showed a logarithmic trend. The equations 1, 2 and 3 below show the relationship between the two parameters during the digestion of the feedstock at C/N ratio 17, 26, and 30 respectively:
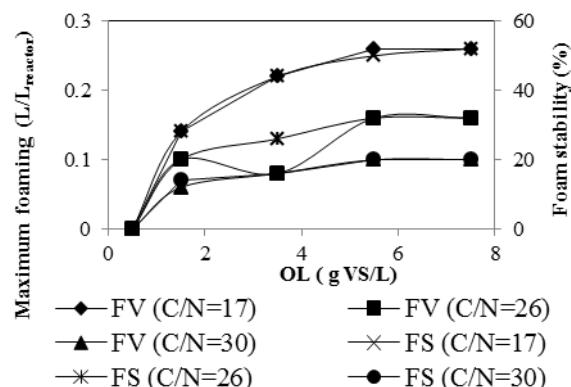
Figure 1: Max foaming (FV) and foam stability (FS) attained during the AD of F1, F2 and F3.

$$Fr = 9.914 \ln (L) + 8.311 \text{ (with } R^2 = 0.98) \ ..... \ (1)$$
$$Fr = 5.582 \ln (L) + 4.769 \text{ (with } R^2 = 0.85) \ ..... \ (2)$$
$$Fr = 3.714 \ln (L) + 3.319 \text{ (with } R^2 = 0.96) \ ..... \ (3)$$

Where Fr = foam formation in the reactor (L/Lreactor) ; L = organic loading of feedstock at 37°C (g VS/L). Foam stability during the digestion of the three feedstocks showed a decreasing trend with increase in C/N ratio (Figure 1). A reduction in foam stability of 50%, 64%, 60% and 62% was obtained during the digestion of F3 at OL of 1.5, 3.5, 5.5 and 7.5 g VS/L respectively when compared with the corresponding values obtained during the digestion of F1. The increase in the feedstock C/N ratio provided adequate buffering for the digestion medium against the accumulation effect of VFA, which is the main source of pH decrease. The range of NH_3-N concentration released during the digestion of F1, F2 and F3 were 65%, 53% and 46% respectively of the inhibiting amount (6000mg/L) reported by Hansen et al. (1998) during the digestion of swine manure. Therefore, F1 was potentially more inhibited than F2 and F3 in that order. Zeshan et al. (2012) attributed the reduction in NH_3-N produced during a similar food waste AD to the reduced protein solubilization rate as the C/N ratio of the feed was increased. Zhang et al. (2012) found that the dilution of feed or biomass waste mixture, as done in this case, could help upgrade its C/N ratio and reduce NH_3-N inhibition. It was observed that the methane yield was higher at low NH_3-N values. For example, F3 at OL of 5.5 g VS/L yielded the highest methane of 0.334 L/g VS and at the same time produced the lowest range of NH_3-N concentration of 1200-2115 mg/L. Although, F3 contained the highest protein content (Table 1), however, it did not lead to the production of high concentration of NH_3-N to inhibiting level. The characteristics of the feed (Table 1) have shown that the protein and lipids content of F1 was higher than F2. It is therefore expected that F1 should contain more of the foam causing surface active bio-surfactants than F2. This may have been responsible for the higher foaming volume recorded during the digestion of F1. The higher NH_3-N content of F1 than F2 is likely due to the higher protein solubilization in F1. In addition, the higher range of VFA released in F1 indicates that the condition during the digestion of F1 was more stressed than F2. It is expected that the digestion of F1 should yield higher theoretical methane than F2 as it contains more lipids content. However, this was not so as a result of the higher stress in F1. Despite having the highest protein content (Table 1), F3 yielded the highest methane (0.334 L/g VS) and the least foam formation range (0.06 – 0.10 L/L$_{reactor}$). This can be attributed to a more balanced and stable microbial activity as evidenced by the improved methanogenic activity (49 – 70% methane content) during its digestion. Removal of chemical oxygen demand (COD) during digestion showed a progressively better removal of organic content with the increase in C/N ratio from 17 to 30 (The results of the COD removal and methane yield are not presented here). This, together with the improved degradation indicates a progressively better acidogenic and methanogenic balance during AD as the feedstock C/N ratio increased. Therefore, the less foam formation observed with increase in C/N ratio during the digestion was likely due to the increasingly better removal or degradation of the foam causing intermediates. Figure 2 shows the correlation between foaming tendency, foam stability and the actual foaming in the reactor. The foaming values considered in each case were the respective maximum values of foam recorded at each of the OLs tested. The foaming tendency showed relatively similar pattern or correlation with the actual foaming produced in the reactors at the OLs tested and in all the feedstock digested. However, there was no clear correlation between the foam stability test and the other foaming parameters in all the feedstock digested. This showed that the foaming tendency test was more reliable in predicting the actual foaming in the reactor than the foam stability test. The foaming parameters show that feedstock F1 was most prone to potential stable foaming incidence (Figure. 2a). Feedstock F3 indicates the highest potential resistance to stable foaming incidence that may occur during the AD (Figure 2c).

3.2 Effect of OL and C/N ratio on methane yield

The maximum yield of CH_4 obtained after 30 days of feedstock digestion were 0.165 L/g VS at OL of 3.5g VS/L for F1; 0.238 L/g VS at OL of 3.5g VS/L for F2 and 0.334 L/g VS at OL of 5.5g VS/L for F3. The feedstock, F3 produced higher methane than F1 and F2 at the same OL. The methane yield obtained is slightly higher than that obtained by Jiang et al. (2012) in a similar AD process. This increase may be due to the higher C/N ratio value of feedstock used in this case. The average range of methane composition obtained during the digestion of F1 was 35-50%. Range of methane composition during F2 and F3 digestions were 38-58% and 40-70% respectively. The range of methane composition demonstrates increasingly better methanogenic activities in F3 than F1 and F2. This could be responsible for obtaining the highest yield of methane as well as the reduced foaming effect observed during the digestion of F3 (Kougias et al., 2013). Better methanogenic activity in this case has contributed to increased methane yield and removal of the foam causing digestion intermediates such as the VFAs. The highest methane yield obtained in this study is about 60% of the theoretically possible (0.572 L/g VS) as proposed by Zhang et al. (2012). The lower yield in this study is likely due to the foam formation and the composition of the feedstock.
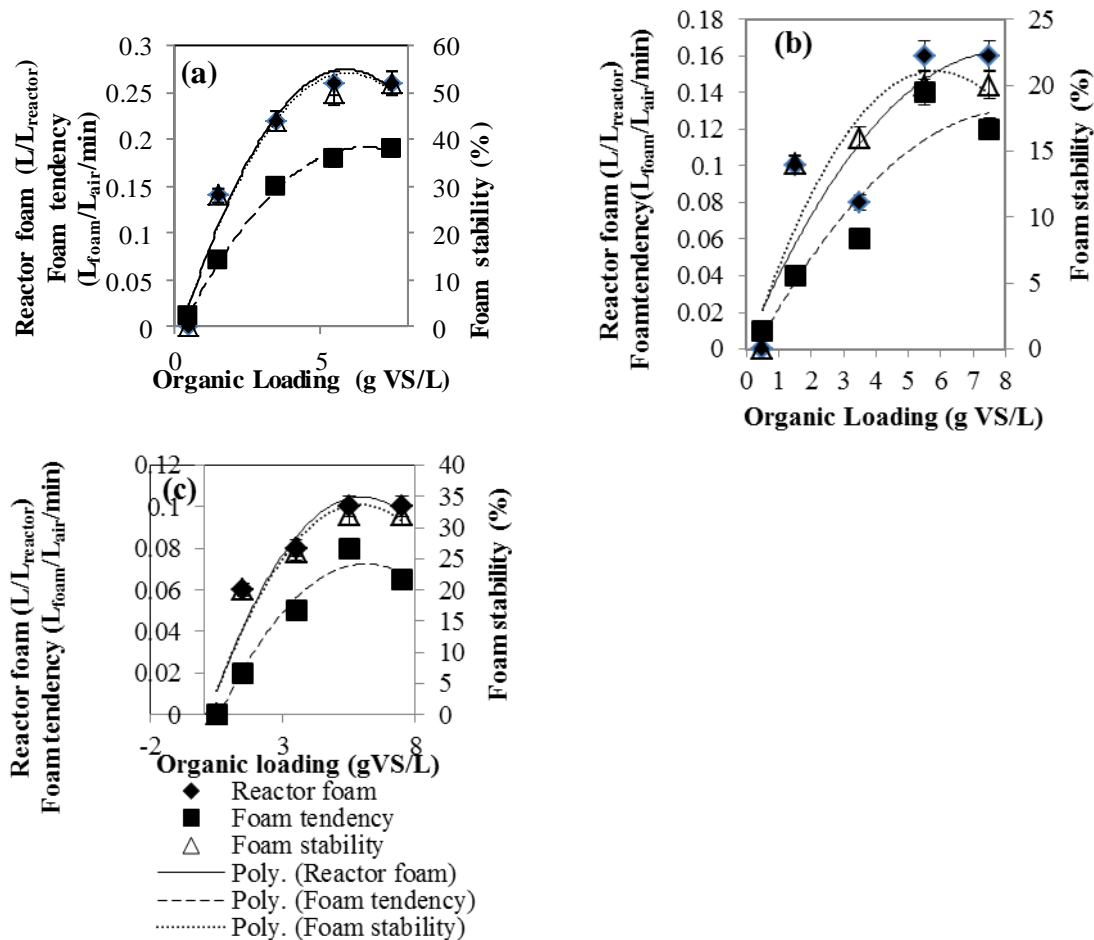
Figure 2: Correlation between foaming tendency, foam stability and the actual foaming in the reactor during the batch mesophilic digestion of feedstock (a) F1 (b) F2 and (c) F3.

4.0 Conclusion

Foaming in each feedstock increased with increase in OL from 1.5 to 5.5g VS/L. At a low OL of 0.5 g VS/L there was no foam formation inspite of comparable biogas production to those of higher OL which resulted to foaming. Therefore, increase in biogas production alone may not cause foaming. Feedstock F1 (C/N=17) was most prone to potential foaming due to the presence of sufficient foam causing intermediate bio-surfactants (e.g. VFAs) during the digestion. However, improved microbial activity due to the increase in feedstock C/N ratio to 30 significantly reduced the foaming by 60%. Increase in C/N ratio of FW feedstock can help mitigate potential foaming effects that may arise during AD.

5.0 References

American Public Health Association (APHA), American Water works Association, Water Environment Federation, (2005). Standard Methods for the Examination of Water and Waste Water, 21st ed., Washington: USA.

Bolzonella, D., Pavan, P., Battistoni, P. and Cecchi, F. (2005). Mesophilic anaerobic digestion of waste activated sludge: Influence of the solid retention time in the waste water treatment process. Process Biochemistry 40, pp. 1453-1460.

Deshpande, N. S. and Barigou, M. (2000). Mechanical suppression of the dynamic foam head in bubble column reactors. Chemical. Engineering. Process 39, pp. 207-217.

Forster-Carneiro, T., Perez, M., and Romero, L. (2008). Influence of total solid and Inoculum contents on performance of anaerobic reactors treating food waste. Bioresource Technology 99,pp. 6994-7002.

Frayer, M., O'Flaherty, E., and Gray, N. F. (2011). Evaluating the measurement of activated sludge foam potential. Water 3, pp. 424-444.

Ganidi, N., Sean, T. and Elise, C. (2011). The effect of organic loading rate on foam initiation during mesophilic anaerobic digestion of municipal wastewater sludge. Bioresource Technology 102, pp. 6637-6643.

Ganidi, N., Sean, T. and Elise, C. (2009). Anaerobic digestion foaming causes-a review. Bioresource. Technology 100, pp. 5546-5554.

Griffiths, P. and Stratton, H. (2010) Foaming organisms in sewage treatment friend or foe: Victim of bad publicity. In: proceedings of the 35th Annual Qld Water Industry Operators Workshop, August 6-8, Rockampton, UK.

Hansen, K. H., Angelidaki, I.and Ahring, B. K. (1998). Anaerobic digestion of swine manure inhibition by ammonia. Water Resources 32, pp. 5-12.

Heard, J., Harvey, E., Johnson, B., Wells, J. and Angove, M. (2008). The effect of filamentous bacteria on foam production and stability. Colloids Surface Biointerference 63, pp. 21-26.

Jiang, Y., Heaven, S. and Banks, C. (2012). Strategies for stable anaerobic digestion of vegetable waste. Renewable Energy 44, pp. 206-214.

Kougias, P. G., Boe, K. and Angelidaki, I. (2013). Effect of organic loading rate and feedstock composition on foaming in manure-based biogas reactors. Bioresource. Technology 144, pp. 1-7.

Liu, G., Zhang, R., El-Mashad, H. M. and Dong, R. (2009). Effect of feed to Inoculum ratio on biogas yields of food and green wastes. Bioresource. Technology 100, pp. 5103-5108.

Marneri, M., Mamais, D. and Koutsiouki, E. (2009). Microthrix parvicella and Gordona amarae in mesophilic and thermophilic anaerobic digestion systems. Environmental. Technology 30, pp. 5-15.

Zeshan, O. and Karthikeyan, C. V. (2012). Effect of C/N ratio and ammonia-N accumulation in a pilot-scale thermophilic dry anaerobic digester. Bioresource Technology 113, pp. 294-302.

Zhang, Y., Heaven, S. and Banks, C. J. (2012). Strategies for stable anaerobic digestion of Vegetable waste. Renewable Energy 44, pp. 206-214.

P 017

STUDYING THE ADSORPTION OF DISPERSED AZO DYES ON RICE HUSK AND MAIZE COB COMPOSITE IN A BATCH SYSTEM

[1]Oneoyekan, E.J. [2]Iyun, O.R.A and [3]Aderemi, B.O*,

[1&3]Department of Chemical Engineering, Ahmadu Bello University,
Zaria, Nigeria.
[2]Department of Chemistry, Ahmadu Bello University,
Zaria, Nigeria.
*Corresponding author,*e-mail address:benjaminaderemi@gmail.com, Tel: +2348033844528;
mrsiyun@yahoo.com, Tel: +2348169363174; Oneoyekanj@gmail.com, Tel: +2348066162241

Abstract:
This work focuses on the determination of the adsorptive capacity of rice husk/maize cob composite of disperse azo dye. Batch adsorption studies were carried out to determine the effect of varying the pH, composite composition, contact time and initial dye concentration on adsorption of the dye. The optimum composite composition was found to be 70% to 30% rice husk/maize cob composite at pH value of 2 within 5minutes of contact time at the initial dye concentration of 40 mg/L..The dye removal process using this low-cost adsorbent from rice husk/maize cob composite is an alternative method worth exploring for the treatment of coloured effluent from industries In addition to its low cost, maximum adsorption within a short time, the preparation technique is also very simple and most importantly, the raw material is readily available in many parts of the country.
Keywords: Rice husk, Maize cob, composite, Disperse Azo dyes, Adsorption

1.0 INTRODUCTION

With the rapid development of modern technologies and industries, the environment has faced more contamination than in the past (Sheela and Arthoba, 2012). Among all the industrial sectors, textile industries are rated as high polluters taking into consideration the volume of discharge and effluent compositions (Cooper, 1995). It was estimated that 10-15% of the dye is lost in the dye effluent, which cause damages to the environment as they significantly affect photosynthetic activity in aquatic life due to reduced light penetration into water and may in consequence distort biological activities of the aquatic life. (Anjaneyulu et al., 2005).

Azo dyes are synthetic organic compounds widely used in textile dyeing, paper printing, and other industrial processes such as the manufacturing of pharmaceutical drugs, toys, and food. This chemical class of dyes, which is characterized by the presence of at least one azo bound (-N=N-) being aromatic rings, dominates the worldwide market of dyestuff with a share of about 70%. In addition azo dyes may degrade to produce carcinogens and toxic products (Shawabkeh, 2007), hence, they have to be removed from the textile effluents before being discharged into the body of waters.

A number of treatment methods for the removal of dyes from aqueous solutions have been reported, namely reduction, ion exchange, electrochemical precipitation, evaporation, chemical coagulation, flocculation, chemical oxidation, photochemical degradation, membrane filtration, including aerobic and anaerobic biological degradation, solvent extraction and adsorption with activated charcoal (Patterson, 1985), but these methods are very costly. Adsorption is a widely-used process for either separation or purification due to its simplicity and easy operational conditions. (Mabrouk et al., 2009).

The adsorbent commonly employed in the conventional adsorption plants is activated carbon, which is a very expensive material. Further research shows that activated carbon can be produced inexpensively from agricultural wastes to successfully replace the commercial one (Mukhtar et al., 2012). The behaviour of the adsorbent (activated carbon)n depend upon the size, porosity, surface chemistry (whether acidic or alkaline), e.t.c. Among the potential adsorbent material are the rice husk and maize cob prepared from agricultural wastes having smaller particle size while it is conventional to convert the source agriculture waste to activated carbon (to enhance the available surface area and ionic charges) before its use (Adefila et al., 2003).

The present work being a preliminary work in this direction, sought to investigate the native capacity of the two selected agro wastes (corn cob and rice-husk) commonly found in abundant quantity in this clime.

2.0 Materials and Methods
2.1 Preparation of 200 mg/L dispersed azo dye solution

Stock solution of dispersed azo dye was prepared by dissolving 0.2 g of the azo dye powder in15ml of dimethyl formaldehyde (DMF). The mixture was stirred thoroughly with a glass rod until it dissolved completely, the glass rod

was then washed inside the beaker with distilled water using wash bottle, and the content was then transferred into one liter volumetric flask. The beaker used was rinsed into the volumetric flask and made up to the level mark with distil water. Thus the above prepared solution was henceforth referred to as the standard stock dye solution (200 mg/L), and any other lower concentrations (working solution) were prepared by serial dilution after which the pH of dye solution was adjusted with 0.1M NaOH or 0.1M H$_2$SO$_4$ using a pH meter. All prepared dye solutions were kept in dark to prevent light degradation,to obtain a working curve the absorbance of the serial solutions were measured using a spectrophotometer and a calibration curve of the absorbance against concentration was plotted.

2.2 Preparation of rice husk-based adsorbents
In this work, Rice husk-based (RH) adsorbent and Maize cob-based (MC) adsorbent composite was used. Rice husk-based adsorbent was prepared using H$_2$SO$_4$ to chemically activate the rice-husk. Here, Rice husk (RH) was sieved and washed with a stream of distilled water to remove dirt, dust, clay particles and any superficial impurities. This was dried in an oven at 100°C for 20 hrs. (Suleiman et al., 2012). The dried RH weighed into a 500 ml clean dry beaker was soaked in 10 M H$_2$SO$_4$ solutions for 20 hrs. The treated rice husk was washed again thoroughly with distilled water and dried (Majid and Majeed, 2013). The dried RH was pyrolyzed in an oxygen atmosphere at 180°C for 5 hours with occasional stirring (El-Shafey, 2007). It was cooled for 30 mins. Acid treated rice husk labeled as RHA.

The corn cob was collected from local agricultural field in the Faculty of Agricultural Science, Ahmadu Bello University Zaria, Nigeria was washed and dried, and subsequently grinded using laboratory pestle and mortal. The grinded powder was sieved and treated with 10M H$_2$SO$_4$ solution at room temperature for 20 hrs and washed with distilled water to remove excess H$_2$SO$_4$. Then it was dried using hot air oven at 100°C for 5 hrs (Rajasekhar, 2014), the so treated maize cob labelled as MC. Now the corn cob absorbents were stored in desiccators.

2.3 Batch Studies
All the batch experiments were carried out in duplicate and the results given are the averages. A control (without sorbent) was simultaneously carried out to ascertain that the sorption was by sorbent and not by the wall of the container. The batch adsorption experiment was carried out in a 250 ml conical flask by mixing 20 ml of 40 mg/L of the standard working solutions of the dispersed azo dye solution with 0.2 g of the composite sorbent (50% RH and 50% MC). The mixture was then stirred thoroughly at room temperature (27 ± 2 ^{0}C) and at constant speed of 150rpm for 20 mins using a magnetic stirrer. After the

equilibrium time, the mixture was filtered immediately using a vacuum pump filter and Whitman filter paper. The absorbance of the filtrate was measured using UV/Visible-spectrophotometer at λ $_{max}$ = 592 nm of the azo dye and pH = 2, after which, the equilibrium concentration was evaluated from the calibration curve and the percentage of the dye adsorbed was consequently calculated from Equation 2.

$$\text{Dye removal (\%)} = \frac{C_o - C_e}{C_o} x100$$

(2)

where *Co* and *Ce* are initial and equilibrium dye concentrations, respectively.
The amount of dye adsorbed per unit weight of adsorbent at equilibrium (*qe*) was calculated as:

$$q_e = (C_o - C_e)\frac{V}{W}$$

(3)

Where *V* is the volume of experimental solution (L) and *W* is the mass of the adsorbent (g) used.

3.0 Result and Discussion

3.1 Effect of Contact Time on Dye Removal
More than 45% removal of the dye concentration occurred in the first 5 seconds of the contact time and the adsorption
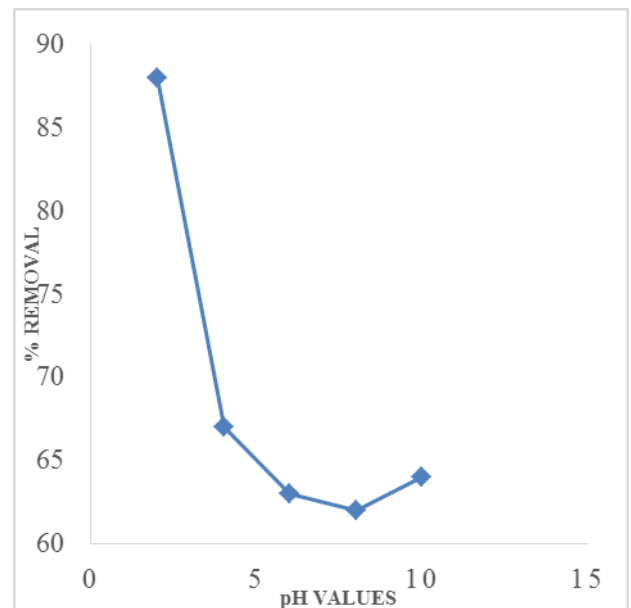
Figure1: Effect of contact time on dye removal capacity after 5 minutes

slowly increased until it reached equilibrium around 5 minutes as shown in Figure 1.

The rapid adsorption is due to the availability of positively charged surface of rice husk/maize cob composite-based adsorbent for adsorption of dispersed azo dye in the solution at pH 2. The results of experiment on contact time shows that percentage of dye removal increases with increasing contact time and optimum time was obtained at 5 minutes. Hence, there was no significant change in adsorption .

Figure 2 presents the result of the effect of pH on dye removal which shows that as pH value increases (from 2 to 10), the absorbance values increases and the percentage removal of dye decreases. Hence the optimum pH was
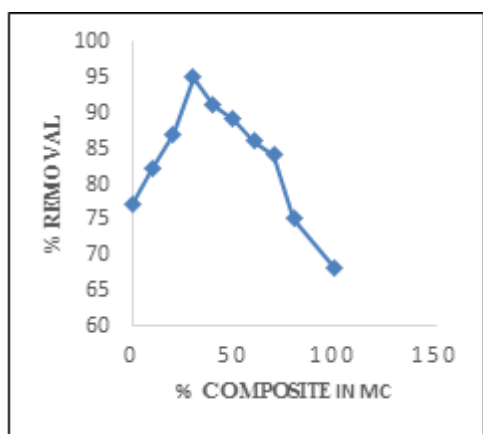
Figure 2: Effect of pH on dye removal
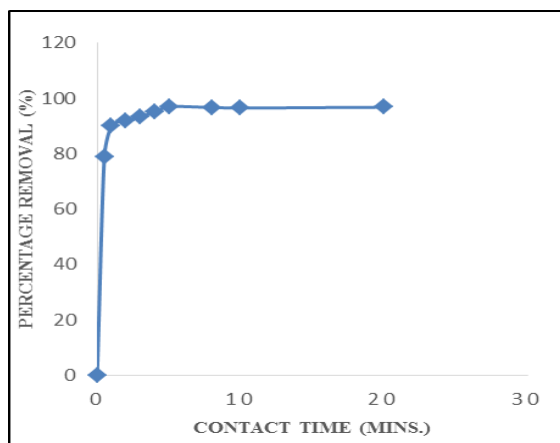
Figure 3: Effect of the adsorbent composite composition on dye removal

obtained at pH value of 2. Therefore, we can say that protonation of the dye solution increases the capacity of the adsorbent to remove the dye.

3.3 Effect of Composite Composition on Dye Removal

Figure 3 shows the effect of the adsorbent composite composition on the percentage of dye removal and it was observed that as the maize cob composition in the composite varies from 0 to 100%, the percentage dye removed increased to about 95% at 30 wt% MC and started to decline thereafter. Hence 30 % maize cob (MC) in rice husk (RH) gave the highest percentage of dye removal. This could possibly be attributed to the increased corn cob
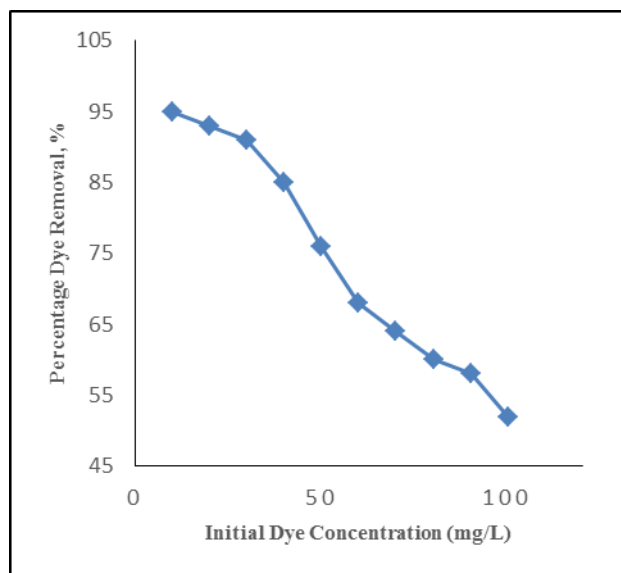
Figure 4: Effect of Initial Dye Concentration on Percentage Dye Removal

powder surface area and availability of more adsorption sites.

3.4 Effect of Initial Dye Concentration on Dye Removal

The falling trend in percentage dye removal could be explained that at lower concentration the ratio of the initial number of dye molecules to the available surface area is low subsequently the fractional adsorption becomes independent of initial concentration. However at higher concentration the available sites of adsorption becomes fewer and hence the percentage removal of dye is dependent upon initial concentrations. Hence, the percentage removal decreases as concentration increases.

CONCLUSIONS

A batch system was applied to study the adsorption of disperse azo dye from aqueous solution
(Synthesized textile industry effluent) by adsorbent obtained from rice husk/maize cob composite. The color removal efficiency of the adsorbent was investigated. The

percentage of color removed increased with increasing contact time, decrease with increasing pH and initial dye concentration. Optimum contact time for equilibrium to be achieved was found to be 5 min with optimum pH of 2. At initial dye concentration of 40 mg/L and composite dosage of 0.20 g 30% maize cob in rice husk/maize cob composite was found to be the optimum composition. Within the limit of experimental error, it can be concluded that the dye removal process by using low-cost adsorbent prepared from rice husk/maize cob composite is worth investigating further it could be an interesting alternative to the conventional method such as coagulation-flocculation, ozonation and photo degradation. In addition to its low cost, the preparation method is also very simple and most importantly, the raw material is readily available in any part of the country.

REFERENCES

Adefila S.S. B.O Aderemi, O.A Ajayi, and D.A Baderin (2003) Nigerian Journal of Engineering 11 (2) 88-95.

Ademiluyi F.T, and David –West E.O (2012) Effect of chemical activation on the Adsorption of heavy metals using activated carbon from waste materials: Nigerian society of chemical Engineers Conference/A.G.M.

Aksu, Z. Application of biosorption for the removal of organic pollutants: a review. *J. Process Biochemistry*. **40** (2005), 997-1002.

Anjaneyulu, Y., Sreedhara Chary, N. and Suman Raj, D.S. (2005). Decolourization of industrial effluents – available methods and emerging technologies – a review. *Reviews in Environmental Science and Biotechnology,* Vol.4, pp.245-273.

Banat, I.M., Nigam, P., Singh, D., Marchant, R. (1996) Microbial decolorization of textile- dye containing effluents: a review. *J. Bioreso. Technol*. **58**, 217- 227.

Cooper, P. (1995). Color in dye house effluent. Society of Dyers and Colorists, West Yorkshire BDI 2JB, England.

Crini, G. (2006). Non-conventional low-cost adsorbent for dye removal: A review. *Bioresource Technology,* Vol.97, pp.1061-1085.

El-Shafey, E.I. (2007). Sorption of Cd (II) and Se (IV) from aqueous solution using modified rice husk. *Journal of Hazardous Materials,* Vol.147, pp. 546-555.

Kant, R (2012). Textile dyeing industry an environmental hazard. *Natural Science*, Vol.4, pp. 22-26.

Mabrouk, E., Ikram, J., Mourad, B. (2009) Adsorption of copper ions on two clays from Tunisia: pH and temperature effects. Applied Clay science 46, 409-413.

Majid Rasheed Majeed Al-palany (2013). "The Use of Fixed Bed Filters Technique for the Removing of Some Heavy Metals from Industrial Waste Water by Plant Waste". A Thesis. University Baghdad, College of Science. 23.

Mukhtar B., A.O.Ameh and L.Tijani (2012) Activated carbon from Almond Nutshell for Tannery Wastewater Treatment: Nigerian society of chemical Engineers Conference/A.G.M.

Patterson, J.W. (1985) Industrial Wastewater Treatment Technology, (2nd edn.) Butterworth-Heinemann, London.

Rajasekhar,K.(2014) *IJECS Volume 3Issue 3 Page No 5083-5087*

Shawabkeh .R.A. (2007), Adsorption of phenol and methylene blue by activated carbon from pear shells ISSN 1061-933x, colloid journal, vol.69, No.3, pp.355-359.

Sheela, T., Arthoba Nayaka, Y. (2012) Kinetics and thermodynamics of cadmium and lead ions adsorption on NiO nanoparticles, Chemical Engineering journal 191, 123-131.

Suleiman Y., A.S Ahmed, J.F Iyun, M.Dauda and S.G Bawa (2012) Preparation of high grade silica from rice husk for zeolite synthesis: Nigerian society of chemical Engineers Conference/A.G.M.

Zaharia C. and Suteu D. (2012). Textile Organic Dyes – Characteristics, Polluting Effects and Separation/Elimination Procedures from Industrial Effluents – A Critical Overview, *Organic Pollutants Ten Years After the Stockholm Convention - Environmental and Analytical Update*, pp.55-86.

P 018

OPTIMIZATION OF THE HYDROLYSIS OF CORN COB HEMICELLULOSE FOR THE PRODUCTION OF XYLITOL

E. A Afolabi, U.G Akpan and A.T Adeosun

Department of Chemical Engineering, Federal University of Technology, Minna, Nigeria
elizamos2001@yahoo.com; ugaekon@yahoo.co.uk

Abstract:

This study was aimed at studying the effects of process variables on the hydrolysis of corn cob hemicellulose for the production of xylitol and the method of conversion of the xylose-rich substrate obtained on the production of xylitol. The result of the hydrolysis study showed that the optimal reaction conditions for the recovery of xylose-rich substrate from corn cob hemicellulose was 2 % sulphuric acid concentration, a solid to liquid ratio of 1:10 and a reaction temperature and time of 130^oC and 20 minutes respectively. The optimal yield of xylitol obtained after hydrogenation and subsequent purification by several runs of ion-exchange chromatography was at solid to liquid ratio 1:10, acid concentration 2%, temperature 130^0C and time 20 minutes.

Keywords: Corn cob, Hydrolysis, Hemicellulose, Xylitol , Xylose,

1.0 Introduction

Corn cobs have always been classified as an agricultural waste and thrown away after the kernels have been eaten. This cause pollution in the environment and also block the water drainage channels. Corn cobs are rich in a chemical called xylitol which can be extracted for human consumption (Ahmed et al; 2004). Xylitol is a sugar-alcohol and a good substitute for other sweeteners because it diminishes tooth decay (Ruth; 2010). Its granules when dissolved, can be used to sweeten cereals, hot beverages and for baking. (Wrolstad, 2012). Its intermediates such as xylan and xylose can be found naturally in the fibres of many vegetables, fruits, berries, corn husks, nuts, oats, sugarcane, mushrooms etc. Xylitol molecule has five carbon atoms in its organic structure instead of six commonly exhibited by other sweeteners such as sucrose and glucose (Parajo et al; 1998).

Marianne (2012) reported that the human body can metabolize xylitol produced from corn cob with about 50 percent of it ingested reaching the bloodstream. The rest makes it to the large intestine where bacteria may digest some and the remainder eliminated as faeces. Apparently, corn cobs can be shredded and used to make industrial chemical compounds and products on a large scale. Therefore, this research is designed to make use of this waste material in the production of xylitol.

Xylitol has a lot of health benefits and this has been the motivation for its production, recovery from the broth, uses and applications. Other sugars such as glucose, fructose, and sorbitol causes tooth decay and increases blood sugar. However, xylitol is different as it prevents the action of microorganisms which causes tooth decay and cavities. Xylitol is usually recommended as supplement in sugary foods for diabetic patient without changes in the physical

and sensory characteristics. In addition, it can be used to diminish the damaging effects of other sweeteners on oral health (David 2010; Gare 2003).

The corn cob contains hemicelluloses known as xylan which undergoes hydrolysis in the presence of an acid and converted to d-xylose. The d-xylose is later reduced by hydrogenation and ion exchange to xylitol (Chaudhary et al; 2013, Anu et al; 2010). In order to selectively obtained xylose as an intermediate in the production of xylitol, it is very important to establish process variables for the hydrolysis step, so as to obtained substrates that are highly rich in xylose with no need for further purification (Rao et al; 2006, Richard; 2000). This study centered on the hydrolysis of the hemicelluloses contained in grinded corn cob using dilute sulphuric acid. In addition, evaluation of the effect of four process variables (solid-liquid ratio, acid concentration, reaction temperature and time) on the dilute acid hydrolysis of the hemicellulose in corn cobs was carried out. Lastly, chromatography technique was employed in analyzing and separating xylitol from other fractions.

2.0 Materials and Method

2.1 Preparation and Production of xylose from corn cob hemicellulosic hydrolysate

Corn cobs were collected from Chinchaga market, Minna, Niger state, dried with sunlight to reduce moisture content. The glass wares and some of the equipments were provided by the Chemical Engineering Department Laboratories of Federal University of Technology, Minna. The corn cob was crushed and sieved to an average particle size diameter of 2 mm. The sieved corn cob sample was then mixed with 40 to 100 ml of 2% (w/v) Sulphuric acid and hydrochloric acid in order to prepare samples of solid

to liquid ratio in between 1:4 to 1:10. The beakers containing the reactants were then placed in an oven at 130°C for a time period between 10 to 60 minutes. The optimum solid to liquid ratio was determined based on the highest concentration of xylose obtained after the hydrolysis step has been completed.

The solids were filtered from the aqueous solution and the filtrate (hemicellulose hydrolysate) concentrated by evaporation for 15 minutes to increase xylose concentration (Rafiqul and Sakinah, 2012; Guo et al; 2006). The filtrate (hemicellulosic fractions) was analysed for solubilised sugars and by-products using a high performance liquid chromatography system. The pH of the filtered substrate was raised to 9 with potassium hydroxide, reduced back to pH 6 with sulphuric acid solution consecutively and then filtered again. The filtrate was concentrated again at 100°C for 15 minutes in order to reduce water content and increase xylose concentration. The xylose in the filtrate was finally converted to xylitol by hydrogenation and purified by several runs of ion exchange chromatographic separation.

2.2 Analytical procedure

The high pressure liquid chromatography (HPLC) system with an Aminex HPX-87H, carbohydrate column (300 x 7.8mm) was used to determine the concentration of the constituents present in the filtrate at 45°C with 0.005 M of H_2SO_4. A consistent flow rate of 1.0 ml/min and a sample volume of 20 µl were maintained for all the samples. The eluate was monitored with an ultra-violet detector and quantified by relating their peak areas with retention times to obtain a calibration curve and then compared with authentic standards (Cailing et al; 2006).

3.0 Results and Discussion

3.1 Effect of solid to liquid ratio on the hydrolysis of corn cob to obtain xylose

As shown in Figure 1, the effect of the solid-liquid ratio of corn cob hemicellulose to dilute acid was plotted against the concentration of xylose recovered from corn cob hemicellulose. At the lowest volume of dilute acid solution of 40 ml of 2% sulphuric acid that reacted with 10 g of the grinded corn cob, xylose concentration of 22.9 g/l was obtained. However, when the volume of dilute sulphuric acid increases to 100 ml at the same weight of sieved corn cob, highest xylose concentration of 68.3 g/l was obtained. This signifies that an increase in the solid to liquid ratio leads to an increase in the concentration of xylose produced. Therefore, the solid-liquid ratio of 1:10 was selected as the optimum yield for further experimental study. This result is in agreement with the work of Preziosi-Belloy *et al.* (1997). They observed that an increased in the solid to liquid ratio led to increase in the concentration of xylose produced at the initial stage and later a decrease.
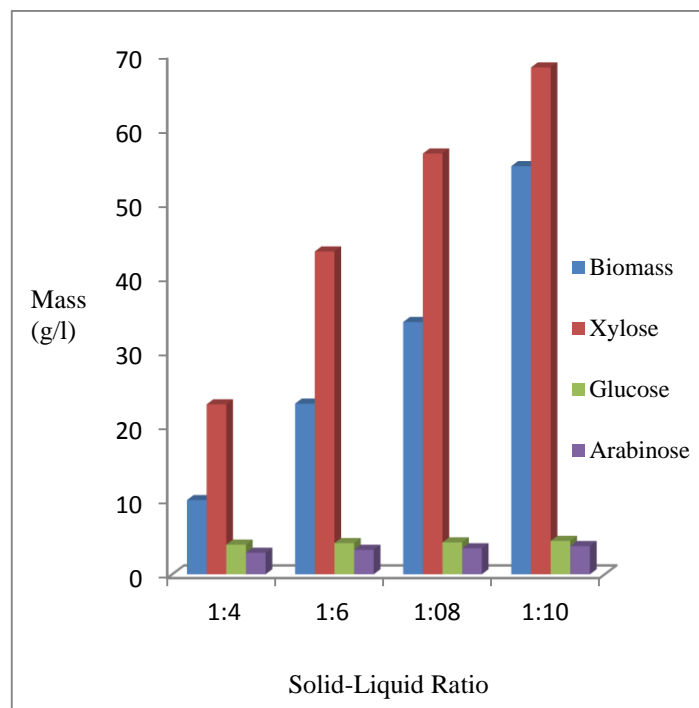
Figure 1: Effect of solid to liquid ratio on the recovery of xylose from corn cob temperature: 130°C, time: 20 min, acid concentration; 2% H_2SO_4.

3.2 Effect of sulphuric acid concentration on the hydrolysis of corn cob to obtain xylose

Figure 2 gives the hydrolysis of the corn cob hemicellulose in which 10 g of the grinded corn cobs reacted with sulphuric acid of varying concentrations ranging from 1% to 4% at a solid to liquid ratio of 1:10 and temperature 130°C for 20 minutes. The highest concentration of xylose of 68.3 g/l was obtained from the reaction mixture with 2% sulphuric acid at 130°C for 20 minutes.

The concentration of the corn cob degrading fractions with the exception of xylose increases gradually with an increased in the concentration of the sulphuric acid. For example, the concentrations of glucose, arabinose, acetic acid, hydroxyl-methylfurfural (HMF) and furfural were 4.0 g/l, 3.6 g/l, 6.3 g/l, 0 g/l and 0 g/l at 1% sulphuric acid concentration and increased to 5.1 g/l, 3.9 g/l, 6.9 g/l, 0.15 g/l and 0.17 g/l at 4% sulphuric acid concentration respectively. The xylose concentration obtained after hydrolysis is 50 g/l and increased to 68 g/l as the sulphuric acid concentration increases from 1% to 2%. Then after, as concentration of sulphuric acid increases from 2%, the concentration of xylose recovered from the hydrolysis of

corn cob decreases. This reduction is probably due to the degradation of xylose by the synergistic effect of the other fractions as reported by Preziosi-Belloy *et al*. (1997). In summary, the amount of xylose increased with acid concentration up to 2% and then after began to decrease. This result is in agreement with the study of Torget *et al.* (1991).
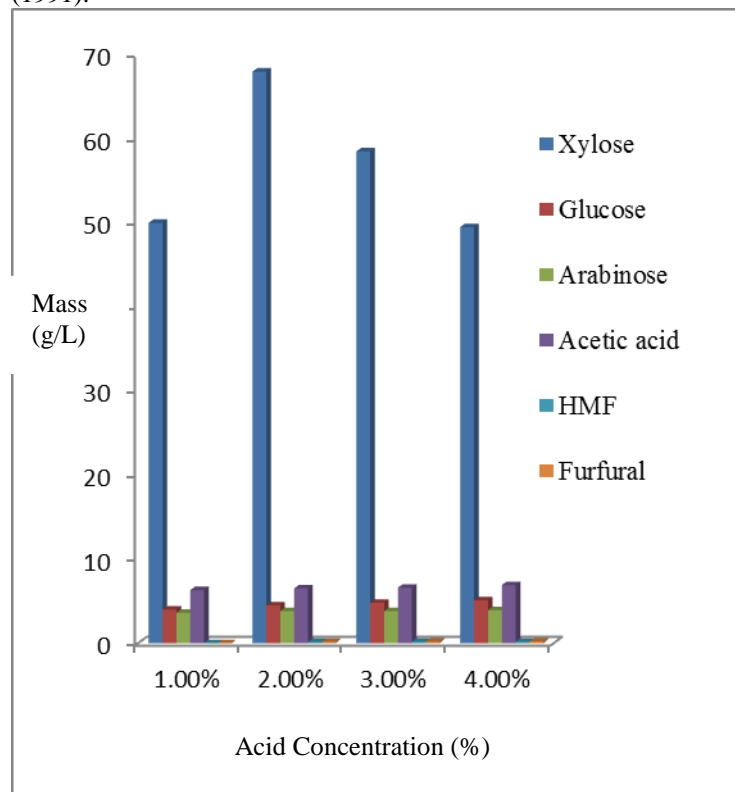

Figure 2: Effect of sulphuric acid concentration on the recovery of xylose on corn cob at temperature 130°C, time: 20 min, acid conc.: solid to liquid ratio 1:10

3.3 Effect of reaction temperature and time on the hydrolysis of corn cob to obtain xylose

The effects of reaction time and temperature for the hydrolysis of corn cob hemicellulose are presented in Figures 3 and 4 respectively. The concentration of xylose in the substrate increases from 54.3 to 58.9 g/l as the reacting time increases from 20 minutes, to 60 minutes respectively. However, it can be concluded that the reacting time has less significant effect on the hydrolysis of corn cob as an increased in time from 20 – 60 minutes is not commensurate with the concentration of xylose obtained.
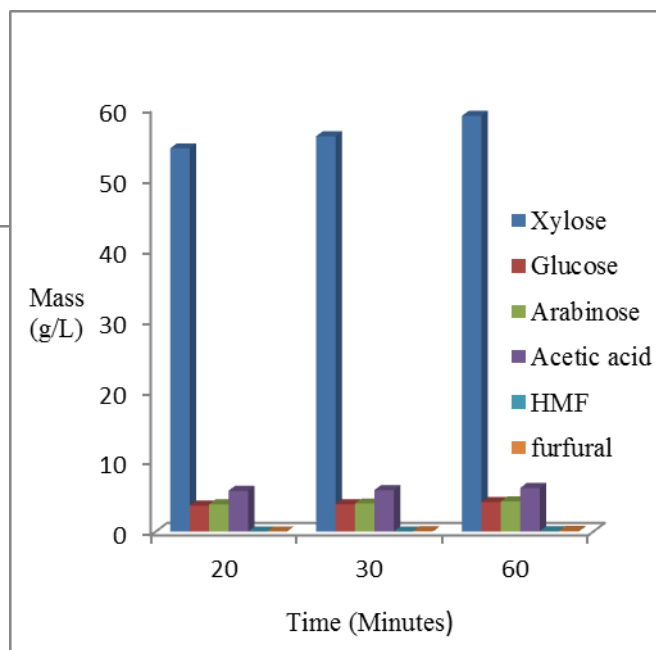
Figure 3: Effect of reaction time on the recovery of xylose at temperature 120°C, acid conc. 2%, and solid to liquid ratio 1:10.

As shown in Figure 4, the concentration of xylose increased from 54.3 g/l to 69.4 g/l with an increased in temperature from 120 ^{0}C to 130 ^{0}C at reaction time of 20 minutes. The same pattern is observed at reaction time of 30 minutes. This signified that an optimum reaction temperature of 130°C favoured the production of xylose and as temperature increases from 120 to 130 °C, the concentration of other compounds produced along with xylose gradually increased and will definitely served as inhibitors to the continuous formation of xylose. This result is consistent with previous results published by Jeevan *et al* (2011) who worked on the optimization studies on acid hydrolysis of corn cob.
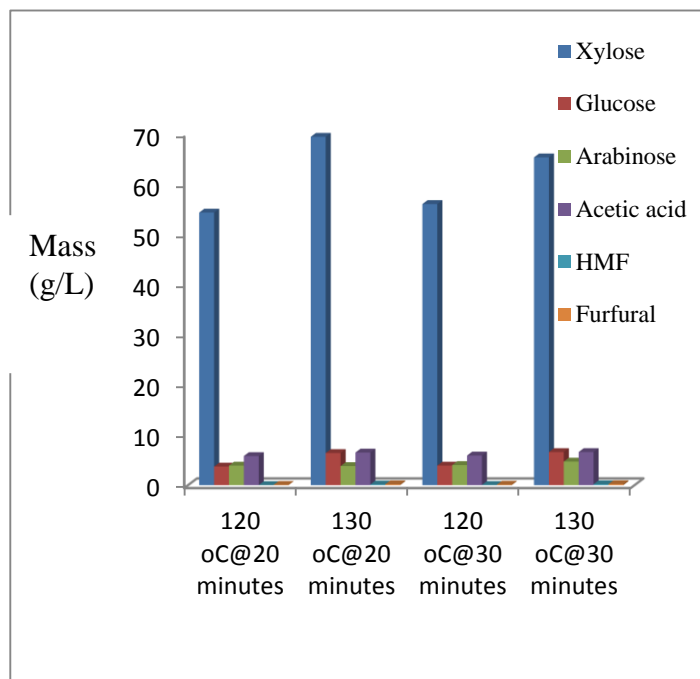
Figure 4: Effect of reaction temperature on the recovery of xylose

3.4 Analysis of the conversion of xylose to xylitol

The conversion of xylose to xylitol was carried out on the sample used to study the effect of sulphuric acid concentration on the hydrolysis of corn cob after the substrate had been detoxified. This was carried out in an aqueous medium by passing hydrogen gas through the xylose substrate with a nickel catalyst at pH of 6, a hydrogen atmosphere of 30 atm, and a temperature of $110^{o}C$ for 4.5 hours. Figure 5 showed the yield of xylitol as obtained after hydrogenation and subsequent purification by several runs of ion-exchange chromatography. At the initial stage, the concentration of xylitol increased from 31.7 to 40.4 g/l with an increased in the concentration of sulphuric acid from 1% to 2%. However, a further increase in concentration of sulphuric acid from 2% to 4% resulted in decreased in concentration of xylitol. The optimal yield of xylitol is obtained at 2% concentration of sulphuric acid.
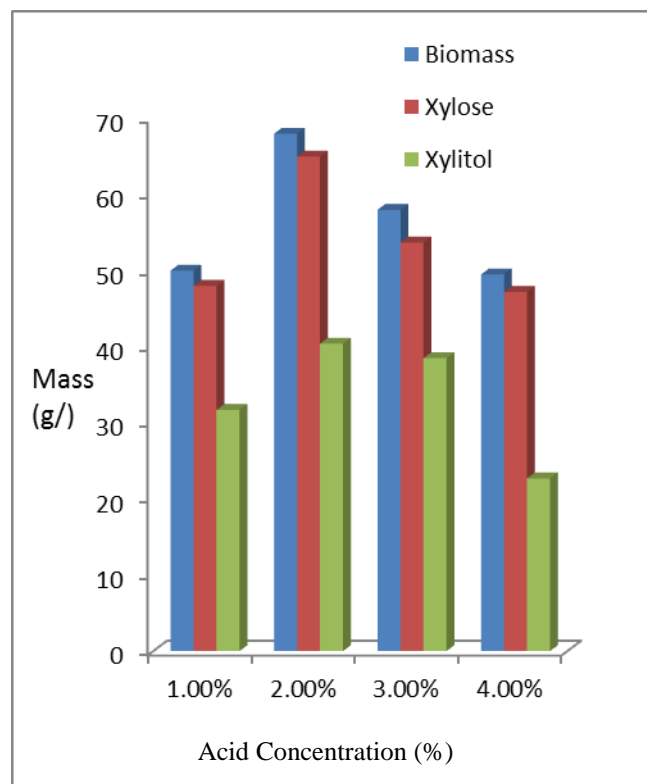
Table 5: Recovery of xylitol from xylose at temperature of 130˚C, time of 20 minutes, solid to liquid ratio of 1:10

5.0 References
Journal articles
Ahmed I., El-baaz, Salwa A. and Khalaf, A (2004). Xylitol Production from Corn cobs Hemicellulosic Hydrolysate by *Candida Tropicalis* Immobilized cells in Hydrogel Copolymer carrier, *Journal of Agriculture and Biology*, Volume 6, pp 1066-1073.

Anuj, K, Chandel, O.V, Singh, L and Venkateswar, R., (2010). Biotechnological Applications of Hemicellulosic Derived Sugars: State-of-the-Art, *Sustainable Biotechnology*. pp 63-81.

Cailing Y., Huayu H., Haixia Z and Mancang, L., (2006). Analysis of Insulin by High Performance Liquid Chromatography Method with Prenoculom Derivatization with 4-Chloro-7-Nitrobenzo-2-oxa-1, 3 Diazole. *Analytical letters*, 39(12), pp 2463-2473.

Chaudhary N., Balomajumder C and Jagati V., (2013). Biological Production of Xylitol from Corn husk and Switch grass by *pichia stiptis*, *Research Journal of Chemical Sciences*, Volume 3, pp 58-64.

Guo C., Zhao C, He P, Lu D, Shen A and Jiang N., (2006). Screening and Characterization of Yeasts for Xylitol Production, *Journal of Applied Microbiology*, 101(1), pp1096-104.

Rafiqul, I.S.M and Sakinah A.M., (2012). Design of Process Parameters for the Production of Xylose from Wood Sawdust, *Chemical Engineering Research and Design Journal,* 19(2), pp 405-408

Jeevan P., Nelson R., Edith and Rena A., (2011). Optimization Studies on Acid hydrolysis of Corn cob Hemicellulosic Hydrolysate for the Microbial Production of Xylitol, *Microbiology and Biotechnology research*, Volume 4, pp 114-123

Parajo, J.C, Dominguez, H.D and Dominguez, J.M., (1998). Biotechnological Production of Xylitol. Part I: Interest of Xylitol and Fundamental of its Biosynthesis, *Bioresource Technology*, Volume 65, pp 191-201.

Preziosi-Belloy, l.V, Nolleau, J.M, and Navarro, F (1997). Enzyme Microbial Technology *Bioresource Technology*, (21) pp 124–129.

Rao, R.S, Jyothi, Pavana Ch, Prakasham, R.S, Sharma, P.N, and Rao, Venkateswar (2006). Xylitol Production from Corn fiber and Sugarcane Bagasse Hydrolysate by *Candida Tropicalis*, *Bioresource Technology*, 97(15): pp1974-1978.

Richard P.A, (2000). Recovery of Xylitol from Fermentation of Hemicellulosic Hydrolysate using Membrane Technology, *Biological Systems Engineering*. pp 4-15

Torget R., Walter P, Himmel M and Grohmann K, (1991). Applications of Biochemistry and Biotechnology, 28/29, pp75-86.

Books
Gare, F, (2003). *The sweet Miracle of Xylitol*, Basic Health Publications, Inc., ISBN 1- 59120-038-5.

Ruth, W, (2010). *A Consumer's Dictionary of Food Additives*, 7th ed; Three Rivers Press, Retrieved from http://www.befoodsmart.com/.../xylitol.php on 29th May, 2010.

Wrolstad, R.E. (2012). *Food Carbohydrate Chemistry*, England; John Wiley and Sons.

Others
David, T., (2010). *Dental Benefits of Xylito*l.Retrieved from http://www,xylitol.org/dental-benefit-of-xylitol on 1st, August 2013.

Elson, H., (2010). Frequently asked Questions on Health Issues. Retrieved from http://www.myhealthwire.com/news/herbs on 30th December, 2013.
Marianne, T., (2012). Xylitol toxicity in Human and Dogs. Retrieved from http://www.vetlearn.com/.../xylitol-toxicity-in-humans-and-dogs on 4th January, 2013

P 019

PROFITABILITY CHALLENGES OF THE ESCRAVOS GTL PLANT

[1]O. E. Onyelucheya*, and [2]E. C. Ibe

Department of Chemical Engineering, Federal University of Technology, Owerri.
*okechukwu.onyelucheya@futo.edu.ng; ibe_zims@yahoo.com

Abstract:

In this work, an economic analysis of the Escravos FT-GTL was done using a template developed on Microsoft Excel to calculate the cash flows. The template provided values for the Net Present value (NPV) and Internal Rate of Return (IRR) of the plant under various scenarios. The impact of variation of the following economic parameters on the NPV and IRR were assessed: the plant capital expenditure (CAPEX), the discount rate, the tax rate, the plant operating expenditure (OPEX), the feed gas cost, the crude oil price, and the product shipping cost. An economic sensitivity analysis of the plants was also carried out using Tornado charts and the results from the sensitivity analysis show that the profitability of the EGTL is most affected by the plant CAPEX followed by the crude oil price. The results of the economic analysis obtained at the base case scenario using the most likely values of the economic input parameters, indicate that the Escravos FT-GTL with a CAPEX of $9.5 billion, has an NPV of -$4.27 billion, and IRR of -2.0%. The analysis also indicated that for the Escravos FT-GTL to be profitable, the crude oil price has to be at least $150/barrel.

Keywords: Gas-to-liquid, Net Present Value, Capital Expenditure, Discounted Cash Flow, Sensitivity Analysis

1.0 Introduction

Natural gas has played an important role in the supply of daily energy requirements for industrial and domestic use. The total global annual gas consumption is forecasted to rise to 2.9 trillion cubic meters by 2015 accounting for approximately 27% of the total primary energy supply; and will further rise to 4.59 trillion cubic meters by 2020 with an annual increase rate of 3.2%, and could rise by more than 50% by 2035, from 2010 levels (Nwaoha and Iyoke, 2013).

Nigeria loses about 1.79 billion USD annually on gas flaring. The need to meet its flare down targets and promote production and use of environmentally friendly fuels serves as a drive for investment in the gas sector of the Nigerian economy. Also, with the global depletion of existing oil reserves, there is a drive towards finding the most economically viable way of commercializing our abundant gas reserves. This twin need of reducing gas flaring and utilizing our abundant gas reserves in economically, technologically and environmentally sustainable manner serves as a justification for this study.

The options for utilization of these significant quantities of Natural Gas reserves include Liquefied Natural Gas (LNG) and Gas-To-Liquid (GTL) technologies.

LNG is essentially a physical change process converting natural gas to liquid for ease of transportation while GTL is a chemical change process yielding naphtha, transportation fuels and specialty chemicals such as lubes and base stocks (Patel, 2005).

Until recently the viability of GTL did not look promising when compared to alternative transportation fuels production from crude oil refining. Developments in GTL technology and stringent environmental specifications for transportation of fuel oils have paved the way for GTL projects. In addition to its favourable emission qualities, the low sulphur content of GTL diesel offers improved engine wear, reduces engine noise and enables greater lubricant longevity (Black, 2010). The use of GTL technology spearheaded by Qatar has the potential for becoming a prominent alternative for stranded gas monetization in the next two decades.

2.0 Financial and economic analysis of the Escravos GTL

The major aspect of this economic evaluation was done by using a Microsoft Excel template developed for this purpose and shown in the procedure below. This template took into account the various variables that affect the viability of the projects such as plant life, construction period, CAPEX, tax, depreciation schedule, etc. Economides (2005) has also shown that the profitability of a GTL plant is also dependent on the crude oil price.

The financial and economic analysis was carried out using the technique of discounted cash flow (DCF) analysis. The DCF analysis yielded project performance criteria such as net present value (NPV) and internal rate of return (IRR) which were obtained from the cash flow of the projects under consideration. Sensitivity analyses were then carried out by varying the values of some of the economic parameters and determining their impacts on the project performance criteria within predetermined ranges. The essence of a sensitivity analysis is to determine the economic parameter which has the most profound impact on the project economics.

2.1 Measures of profitability

There are a number of criteria that can be used to appraise the economic profitability of a project. Some of these measures of profitability are defined below as given by Black (1984), Mott (1989), Peters et al(2003), Ross et al(1996), and Sinnot (2005).

2.1.1 Net present value (NPV)

The Net Present Value of a proposed investment is the sum of all the cash flow (both positive and negative) discounted to its present value. It is obtained by summing the discounted cash flows for each year for the life span of the project. A project is regarded as economically desirable if the NPV is positive. This implies that the project can bear the cost of capital (i.e. the interest rate) and still generate a surplus or profit. If the NPV is negative, the project should not be pursued because the cash flow will also be negative and the project will not be profitable. If other measures of valuation are held constant, a project with the highest NPV value will be preferred when projects are being ranked.

2.1.2 Internal rate of return (IRR) or discounted cash-flow rate of return (DCFRR)

The IRR or DCFRR is the interest rate at which the cumulative NPV at the end of the project is zero. It is a measure of the interest rate the project can pay and still break even by the end of the project life. A project is judged to be worthwhile in economic terms if the IRR is greater than the cost of capital, otherwise it should be rejected. The general criterion used for economic evaluation of an investment by means of IRR is to compare the obtained IRR with a required rate of return known as the hurdle rate or discount rate. A discount rate of 10% is usually assumed for projects such as the one under consideration (Gradassi, 2001).

2.2 Estimation of economic terms used

2.2.1 Total capital investment

The total capital investment for a project comprises the fixed capital investment (total cost of plant ready for start-up) and the working capital (additional investment needed over and above the fixed capital to start up the plant and operate it to the point where income is earned) (Sinnot, 2005, Creese and Adithan, 1992).

The capital expenditure for the Escravos GTL (EGTL) is $9.5 billion and the plant processes 340 MMSCFD to 34000 bbl. /d of products. It is worthy of note that the EGTL was initially scheduled to be completed in 2008 with a CAPEX of $1.7 billion but was only realised in 2014 with a CAPEX of $9.5 billion (Uzuegbunam, 2014). The ORYX GTL plant in Qatar which has the same capacity and operates on the same technology as the Escravos GTL came on stream in 2006 and was realised with a CAPEX of $1.2 billion (Halstead, 2006).

The economic parameters used in this study were obtained from the works of (Patel, 2005; Gradassi, 2001; Avellant et al, 1996; Chang, 2001; Halstead, 2006; Economides et al, 2005; Nwankwo, 2008) and their summary is as shown in the tables below:

Table 1: Summary of Parameter Assumptions used

PARAMETER	VALUE
Plant life	20 years
Plant construction period	3 years
Plant construction spending per year	25%, 35%, and 40%
Depreciation	5-year MACRS
Tax rate	35%
Plant Operating Time	330 days/annum
Feed Gas Cost	$ 0.50/MMBTU
Discount Rate	10%
OPEX	FT-GTL:$5/bbl
Product Sipping Cost	FT-GTL:$1.20/bbl
Crude Oil Price	$45.00/bbl
FT-GTL Diesel Premium	$5.00/bbl
FT-GTL Naphtha Premium	$3.00/bbl

Table 2: Parameter values used for FT-GTL sensitivity analysis

PARAMETER	Most Likely Value	Minimum Expected Value	Maximum Expected Value
Crude Oil Price ($/bbl)	45	30	60
Feed Gas Cost ($/MMBTU)	0.50	0.25	1.00
CAPEX Factor	1	0.7	1.3
OPEX ($/bbl)	5	3.5	6.5
Shipping Cost ($/bbl)	1.2	0.8	1.6
Discount Rate (%)	10	8	12
Tax Rate	35	20	50
GTL Diesel Premium ($/bbl)	5	3.5	6.5
GTL Naphtha Premium ($/bbl)	3	2	4

3.0 Results of the economic analysis of the Escravos FT-GTL

The CAPEX for the FT-GTL is $9.5 billion. From the economic analysis using the "most likely values" shown in table 2, the Internal Rate of Return (IRR) for this plant is -2.0% and the Net Present Value (NPV) is -$4,272,702,681 at a discount rate of 10%.

The following paragraphs show the impact of the various parameter values on the economic analysis.

3.1   Impact of varying feed gas cost, crude oil price and CAPEX

Figure 1 shows the effect of varying feed gas cost on the NPV of EGTL when the other parameters are held constant at their base/most likely values. Figure 2 shows the impact of varying plant CAPEX on the NPV of the EGTL when the other parameters are held constant at their base/most likely values. Figure 3 shows the impact of varying crude oil price on the NPV of the EGTL when the other parameters are held constant at their base/most likely values. Economic analysis of GTL plants is specifically tied to crude oil price as its products are forms of refinery products whose costs depend on the crude oil price.
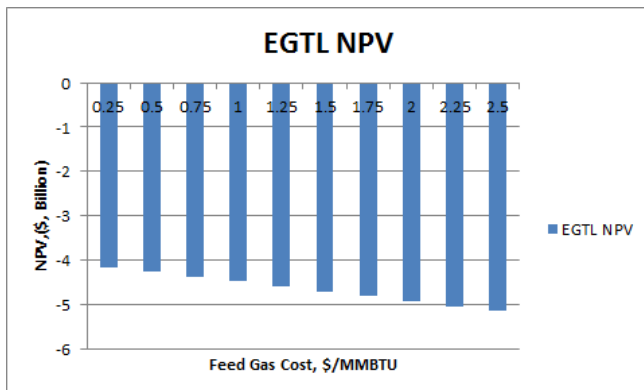
Figure 1: Effect of varying Feed Gas Cost on the NPV of EGTL
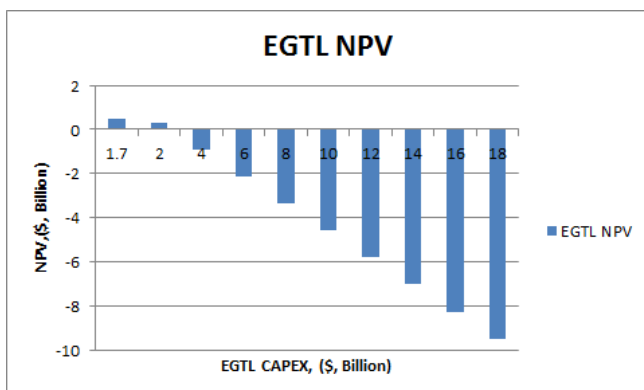
Figure 2: Effect of varying CAPEX on the NPV of EGTL
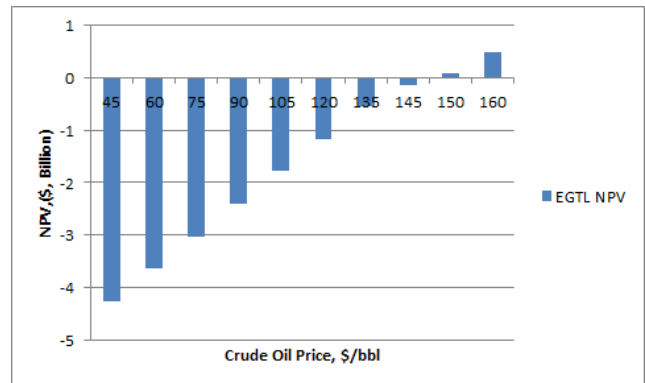
Figure 3: Effect of varying crude oil price on the NPV of EGTL

3.2   Escravos GTL sensitivity analysis

Sensitivity analysis is a way of examining the effects of uncertainties in the forecasts on the viability of a project by giving decision makers a quick overview of the risks involved. To carry out the test, the values of the chosen criteria are first calculated at most probable values to obtain the base case for the analysis. Other values are then obtained for the test criteria at the maximum and minimum expected values to provide the high and low case scenarios. The sensitivity analysis on the EGTL plant was done with the aid of tornado diagrams which serve as a standard tool for sensitivity analysis.

Tornado charts are modified versions of bar charts where the largest bar appears at the top of the chart followed by the second largest and so on. They are so named because the final chart visually resembles one half of or a complete tornado. The change in NPV between the base values and the maximum/minimum expected values is used as our test criteria. The parameter with the longest bar has the greatest effect on the NPV while the one with the shortest has the least effect on the NPV. The base case, high and low values used for this analysis are as given in table 2 while the sensitivity plot is given in figure 4.
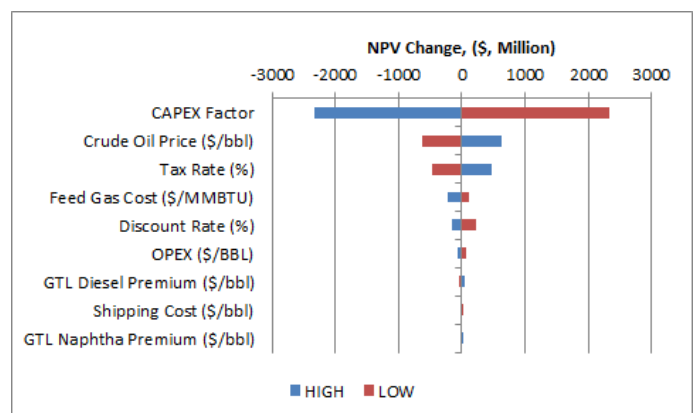
Figure 4: Tornado Plot for EGTL Sensitivity Analysis.

Figure 1 shows the effect of varying feed gas cost on the NPV of EGTL. It can be observed from this figure that the NPV remains negative irrespective of the feed gas cost and will still be negative even if the gas is gotten completely free. Figure 2 shows the effect of varying CAPEX on the NPV of EGTL. It can be observed that the lower the CAPEX values, the higher the NPV for the plant. At CAPEX values of $1.7 billion and $2.0 billion, the NPV of the EGTL would be $0.514 billion and $0.33billion respectively with the other economic parameters at their most probable values. This is indeed a very desirable scenario and it is also observed that the NPV reduces as the CAPEX increases.

Figure 3 shows the effect of varying crude oil price on the NPV of the EGTL. From the figure, it can be seen that the NPV of the EGTL is negative below crude oil price of $150 /barrel and rises to $0.5 billion at crude oil price of $160/barrel. The EGTL plant therefore will not be profitable at the prevailing crude oil price levels of about $50/barrel as the NPV is negative at this price.

Figure 4 shows the Tornado plot for the EGTL. The profitability of the plant is most sensitive to the change in CAPEX factor as this has the longest bar in the Tornado chart shown in figure 4 followed by the crude oil price. The other factors like the discount rate, feed gas cost, tax rate and OPEX do not have an appreciable impact on profitability of the plant as indicated by the length of their bars in the Tornado chart of figure 4.

4.0 Conclusion

The need to find the most economically viable option for monetisation of gas reserves will remain a priority as long as there are untapped gas reserves waiting to be utilised. From the results of the analysis done in this work, the Escravos GTL would not be profitable at the most likely values used in the base case scenarios analysis because of its negative NPV and IRR values. The major reason for this is the unusually high CAPEX of the EGTL plant as discussed in a previous section. For the EGTL plant to operate profitably even with its high CAPEX, it will require a crude oil price above $150 / barrel when the other economic parameters are at their base case scenario values.

From the sensitivity analysis as given by the Tornado charts, the profitability of the EGTL plant is most sensitive to the plant CAPEX followed by the crude oil price

5.0 References

Avellant, R. A., Thomas, C. P., Robertson, E. P.,(1996), *"Options for Alaska North Slope Natural Gas Utilisation"*, SPE 35702, Paper Presented at the SPE Western Regional Meeting in Anchorage, Alaska USA, May 22-24, 1996. Texas Society of Petroleum Engineers. P 531-543.

Black, B. G. (2010), *"Monetizing Stranded Gas: Economic Valuation of GTL and LNG Projects"* MA Thesis, University of Texas at Austin, p 6.

Black, J. H. (1984), *"Cost Engineering Planning Techniques for Management"*, CRC press New York, pp. 105, 230.

Chang, S. (2001), *"Comparing Exploitation and Transportation Technologies for Monetization of Offshore Stranded Gas"*, SPE 68680 Paper presented at the SPE Asia Pacific Oil and Gas Conference and Exhibition in Jakarta, Indonesia, 17-19 April 2001. Texas Society of Petroleum Engineers, p7.

Creese, R. and Adithan, M. (1992), *"Estimating and Costing for the Metal Manufacturing Industry"*, CRC press, New York, p. 241.

Economides, M.J., Aguirre, M., Morales, A., Naha, S., Tijani, H., and Vargas, L. (2005). *"The Economics of Gas to Liquids Compared to Liquefied Natural Gas"*, World Energy, 8(1): 136-140.

Gradassi, J. M. (2001), *"Gas-To-Liquid R & D: Setting Cost Reduction Targets"*, Elsevier Science B.V, p 7.

Halstead, K. (2006), *"Oryx GTL - A Case Study"*, Foster Wheeler available at http ://www.tcetoday.com, accessed December 25, 2014.

Mott, G. (1984), *"Investment Appraisal"*, Pitman London, p 196.

Nwankwo, J. E. (2008), *"Gas Utilization in Nigeria - an Economic Comparison of Gas-to-Liquid and Liquefied Natural Gas Technologies"*, M.Sc. Thesis, North-West University, South Africa.

Nwaoha, C. and Iyoke, U. J. (2013), *"A Review on Natural Gas Utilization and Cutting Carbon Emissions: How Viable is Compressed Natural Gas for Road Vehicle Fuel?"*, Journal of Energy Technologies and Policy, Vol.3, No.5.

Peters, M. S., Timmerhaus, K. D., and West, R. E. (2003), *"Plant Design and Economics for Chemical Engineers"*, McGrawhill New York, 5ᵗʰ edition, p 973.

Patel, B. (2005), *"Gas Monetisation: A Techno-Economic Comparison of Gas-to-Liquid and LNG"*, Foster Wheeler Energy Ltd, Reading UK, Paper Presented at the 7ᵗʰ World Congress of Chemical Engineers in Glasgow, pp. 1-11

Ross, S. A., Westerfield, R. W., and Jordan, B. D., (1996), *"Essentials of Corporate Finance"*, McGraw-Hill Chicago, p 490.

Sinnot, R. K. (2005), *"Chemical Engineering Design:*

Chemical Engineering Volume 6", Butterworth-Heinemann, p 244.

Uzuegbunam, F. (2014), *"Chevron Escravos GTL Project Finally Gets Off Ground"*, Accessed at http://businessdayonline.com/2014/09/chevrons-escravos-gtl-project-finally-gets-off-ground

P 020

COMPARISON OF SOME OPTIMIZATION TECHNIQUES IN ROBUST PROCESS CONTROL DESIGN

Adeyemo, S. O. and Taiwo*, O.
Process Systems Engineering Laboratory, Obafemi Awolowo University, Ile-Ife, Nigeria
*femtaiwo@yahoo.com; adeyesam@yahoo.com

Abstract:
*The paper compares the relative efficiency of four major optimization techniques that can be employed in the design of robust control systems. In quantifying system uncertainties, we consider three scenarios: when uncertainties originate from changes in operating conditions, when some parameters in the linearized models are only known approximately and when unmodelled dynamics are envisaged. Decentralized controllers were designed using Internal Model Control (IMC) tuning relations (or SIMULINK auto-tuning facility) and fixed-structure H_∞ design strategy. The former was optimized using Method of Inequalities (MoI), and MATLAB **fmincon** command individually. Optimal centralized controllers were also designed using H_∞ and µ synthesis strategies. The performance of each controller was assessed by calculating the Structured Singular Value for robust stability and performance, the IAE values during unit step changes and other transient response characteristics. For the examples considered, the ease of attaining desired performance with each technique was found to be largely a function of system complexity (variation in behavior at different operating points, interactions and presence of delay terms) and number of parameters to be optimized. Also, it may be necessary to specify different bandwidth requirement for a system with the different optimization techniques considered.*

Keywords: Nominal plant, process uncertainty, robust stability, robust performance, optimization

1.0 Introduction

A typical control engineering problem entails the design of a control system subject to closed-loop stability and certain performance requirements (Oloomi and Shafai, 2011). The requirements may include the figures of merit such as gain/phase margin, bandwidth, and tracking error to a reference command. The robust control theory attempts to address the question of stability and performance of multivariable systems in the face of modelling errors and unknown disturbances (Zhou *et al.*, 1996).

Un-modelled dynamics, non linearity of systems and the existence of disturbances are largely responsible for the inability of linear control systems theory to reach the ideal solution. For this, Fard *et al* (2013) identified several targets that are often demanded in a control system namely: robust stability, nominal performance, robust performance, operating limitation on controlling signal and minimized disturbance effect.

In robust control theory, the question concerning the achievable performance limits is generally posed as an optimization problem in an appropriate mathematical setting. A major benefit of this approach is that it provides a means to optimize the system performance by trading off various stringent, and often conflicting, specifications against each other.

Gu and co-workers (2005) synthesized robust controllers for some physical and chemical systems using H∞ synthesis, H∞ Loop-shaping Design Procedures (LSDP), and µ synthesis. Oloomi and Shafai (2011) specifically worked on optimizing the tracking performance in robust process control by deriving expressions relating the tracking error specifications to various parameters of the weighting functions used in the mixed Sensitivity/Complementary Sensitivity (S/T) design.

In some other works, different optimization procedures have been combined to obtain a single robust controller. For instance, Fard and co-workers (2013) carried out a combination of two methods: µ and H_2/H_∞. Similarly McKernan *et al* (2009) combined MoI with McFarlane and Glover's H_∞ LSDP in a mixed-optimization approach.

In this work we considered situations in which controller parameters are optimized using MoI and MATLAB optimization toolbox. We do this for when only controller parameters are optimized and also for situations where the performance weight parameter ω_B^* was optimized alongside the controller parameters. We also employed H∞ and µ controller synthesis strategies to obtain optimal controllers.

In section 2, we give a brief background description of the optimization techniques compared in this work while applications of these methods to typical multivariable systems are presented in section 3. The performances of the resulting control systems were compared based on the structured singular values for robust stability, robust performance and servo and regulatory performances. A discussion of the results and conclusions from the work are presented in section 4.

2.0 Methodology

2.1 Uncertainty modelling:

CASE I: We consider the average plant (going by the Nyquist plots of different operating points) as the nominal model. Then the deviation of the models of the other operating points from this nominal model was plotted as a function of frequency and the upper bounds of these deviations were captured by curve fitting to give the relation for the uncertainty weight.

CASE II: The models of plants with single operating points are taken as the nominal models in which we may have uncertain parameters. These parameters are varied between considered limits and the deviations of the frequency behaviours from those of the unperturbed plants are treated as in Case I.

CASE III: Certain magnitudes of uncertainties that could result from unmodelled/neglected dynamics at low and high frequencies are modelled for systems with single operating point and no uncertain parameters.

2.2 Controller design and optimization:

The IMC tuning relations and fixed structure H∞ strategies were engaged in designing multiloop controllers in which case the former was optimized using MoI and *fmincon*. Optimal centralized controllers were also designed using the H∞ and μ synthesis strategies

2.2.1 Method of Inequalities (MoI)

The method of inequalities (Zakian and Al-Naib, 1973, Zakian, 1979), is a general multi-objective optimization method that requires the formulation of design problems as a set of inequalities:

$$\varphi i(p) \le Ci, \quad i = 1, 2, ..., m, \quad (1)$$

where $p \in R^n$ is the design parameter vector, φ_i represent performance measures or physical properties of the system, and the bounds C_i are the supremal values of $\varphi i(p)$ that can be tolerated. Any point p satisfying (1) is an acceptable design solution.

For control system design, the functions $\varphi i(p)$ may be functionals of the system step response, for example the rise-time, overshoot or the integral absolute error, or functionals of the frequency response, such as the bandwidth. They can also represent measures of the system stability and robustness, such as the maximum real part of the closed-loop poles. Additional inequalities which arise from the physical constraints of the system can also be included, to restrict for example, the maximum control signal. The design parameter, p, may parameterize a controller with a particular structure. Alternatively, p may

parameterize the weighting functions required by analytical optimisation methods to provide a mixed optimisation approach.

2.2.2 MATLAB Optimization Toolbox

The MATLAB Optimization Toolbox is a collection of functions that extend the capability of the MATLAB® numeric computing environment (Coleman *et al*, 1999). The toolbox includes routines for many types of optimization including: unconstrained nonlinear minimization, constrained nonlinear minimization, quadratic and linear programming, nonlinear least squares and curve-fitting, nonlinear system of equation solving and constrained linear least squares.

In this work, our focus is on constrained nonlinear minimization in which we employ the MATLAB command **fmincon**.

2.2.3 H∞ synthesis

The design is based on minimizing the infinity norm of transfer function between some set of exogenous inputs (disturbance, noise) and output errors. Such transfer function is what is referred to as cost functions and this strategy is targeted at obtaining a stabilizing controller that maintains the infinity norm of the cost function below a value of 1 at all frequencies e.g.

$$\left\| \begin{array}{c} W_P S \\ W_u KS \end{array} \right\|_\infty \le 1 \quad (2)$$

For this case, the objective is to achieve good disturbance rejection and set point tracking (error minimization). This transfer function matrix is the Lower Linear Fractional Transformation of the generalized plant without uncertainty, P and the controller, K as shown below.
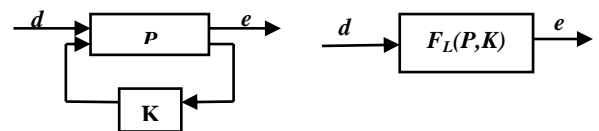
Figure 1: Configuration for H-infinity Controller Synthesis

2.2.4 μ synthesis

In Figure 2, we show a general representation of an uncertain system in which P is the generalized plant (i.e. the nominal plant G interconnected with the various weights) and is a matrix form that is partitioned to be compatible with the controller matrix K; e and d are vectors of all exogenous outputs and exogenous inputs

respectively. *e* constitutes a set of error signals to be minimized with weight W_p specifying the performance requirements.
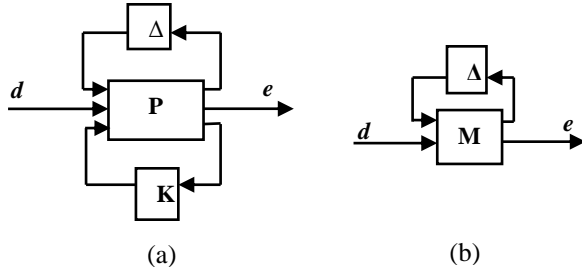

(a)   (b)

Figure 2: (a) General Representation of an Uncertain System (b) Δ-M Structure for Controller Analysis

M is a matrix whose dimension conforms with those of *Δ*. It is related to *P* and *K* by the Lower Fractional Transformation rule:

$$M = F_l(P,K) = P_{11} + P_{12} K (I - P_{22}K)^{-1} P_{21} \quad (3)$$

given $\quad P = \begin{bmatrix} P_{11} & P_{12} \\ P_{21} & P_{22} \end{bmatrix}$ and $\quad M = \begin{bmatrix} M_{11} & M_{12} \\ M_{21} & M_{22} \end{bmatrix}$

The uncertainty closed-loop transfer function, *F* from *d* to *e* is related to *M* and *Δ* by the upper Linear Fractional Transformation:

$$F = F_u(M,\Delta) = M_{22} + M_{21}\Delta(I - M_{11}\Delta)^{-1}M_{12} \quad (4)$$

The Structured Singular Value, μ is defined as

$$\mu = \frac{1}{\bar{\sigma}(N)} \quad (5)$$

where $\bar{\sigma}(N)$ is the smallest level of perturbation, *Δ* that will cause instability in *N*. For robust stability analysis, *N* is M_{11}; for nominal performance, *N* is M_{22} and for robust performance, *N* is *M* as described above.

The aim of μ-synthesis is to find a stabilizing controller *K*, such that for each frequency $\omega \in [0, \infty]$ the structured singular value is to satisfy the condition

$$\mu_{\Delta P} [F_L(P,K)(j\omega)] < 1 \quad (6)$$

Remark: In this work, optimization with MoI and *fmincon* were carried out by setting bounds on functionals such as rise-time, settling time, interactions and Structured Singular Values for robust stability and performance.

3.0 Illustrative Examples

3.1   Example 1: Two CSTR in Series with Recycle

The process consists of two continuously stirred tank reactors with recycle as shown in Figure 3 (Scali and Ferrari, 1999). The state variable model for this process in deviation variables at the given operating point takes the form:

$$\begin{bmatrix} x_1' \\ x_2' \end{bmatrix} = \begin{bmatrix} -12.5 & 0 \\ 1.05 & 1.6 \end{bmatrix}\begin{bmatrix} x_1(t) \\ x_2(t) \end{bmatrix} + \begin{bmatrix} 0 & 10 \\ 0 & 0 \end{bmatrix}\begin{bmatrix} x_1(t) \\ x_2(t-2) \end{bmatrix} + \quad (7)$$
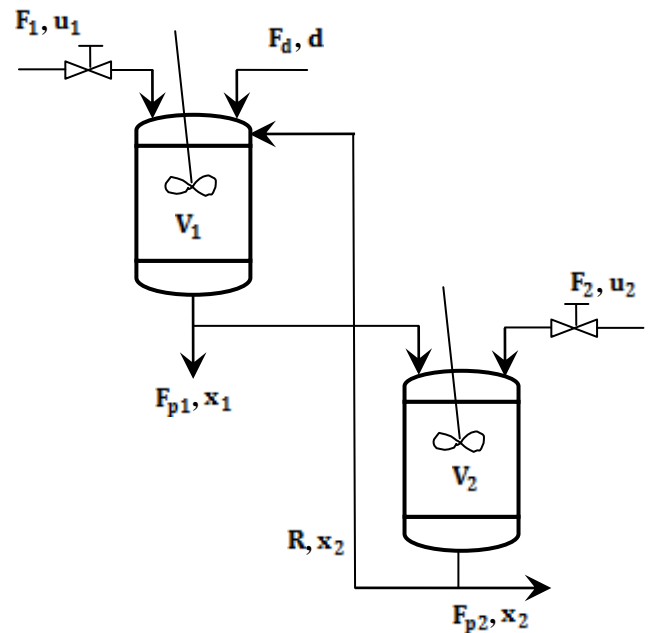
Figure 3: Two CSTR in series with recycle

Taiwo and co-workers (2014) show that the controllers designed for recycle compensated plants (see Taiwo, 1985 for details) often perform well on the uncompensated system even above those designed directly from the uncompensated plants. Hence for this example we take the recycle compensated plant as our nominal model for which we model an uncertainty weight to cover up for unmodelled dynamics in the plant. The compensated plant has the following transfer function:

$$G(s) = \begin{bmatrix} \dfrac{0.08e^{-s}}{0.08s+1} & 0 \\ \dfrac{1.05e^{-s}}{(s+12.5)(s+1.6)} & \dfrac{0.03125e^{-s}}{0.625s+1} \end{bmatrix} \quad (8)$$

The modelled input uncertainty weight is given by

$$W_i = diag(w_i, w_i); \qquad w_i(s) = 0.2\frac{0.2s+1}{0.02s+1}$$

(9)

which permits 20% uncertainty at low frequencies and 200% at high frequencies but attaining 100% uncertainty at a frequency of about 30rad/min. the performance weight for controller analyses is also given by

$$W_P = diag(w_p, w_p) \qquad w_p(s) = \frac{s/Ms + \omega_B^*}{s}$$

(10)

in which we have specified Ms=2.5 (with an implication that $GM \geq 1.67$ and $PM \geq 23.07^0$), $\omega_B^* = 0.1$rad/min.

Controller Design and Optimization

The calculated RGA for the system $\begin{pmatrix} 1 & 0 \\ 0 & 1 \end{pmatrix}$ suggests diagonal pairing for decentralized control. The initial IMC tuned parameters were optimized alongside the performance weight parameter ω_B^*. Both initial and optimized parameters are presented in Table 1 together with the fixed-structure H_∞ controller.

Table 1: Controller Parameters for Two CSTR in Series with Recycle, $K(s) = P + \frac{1}{s}I$

Controller	k_{11}		k_{22}		ω_B^*
	P	I	P	I	
Initial Parameters	0.7350	9.1875	4.7520	7.6032	0.1000
MoI Optimized	1.8605	5.5125	15.8375	20.9207	0.1102
fmincon Optimized	0.8872	6.7112	14.0879	19.9736	0.1001
Fixed-structure H_∞	0.6900	7.0600	11.4000	16.8000	0.1102

6th order centralized H_∞ controller and 12th order μ controller were obtained for the system. The order of the μ controller was successfully reduced to 2 whereas order reduction for the H_∞ controller did not yield a controller with satisfactory performance.

Table 2 summarizes the performance indices of the different controllers for the system and Figure 4 displays their relative performance as regards response to unit step changes and disturbance rejection. Note that the robust performance index μ_{RP} was calculated using the strictest ω_B^* requirement obtained after optimization.

Table 2: Performance and Robustness Indices for Two CSTR in Series with Recycle

Controller	IAE for step in y_1	IAE for step in y_2	Total IAE	μ_{RP} ($\omega_B^* = 0.1102$)
Initial Parameters	4.957	4.203	**9.160**	1.0964
MoI Optimized	3.271	1.954	**5.225**	0.9628
fmincon	3.261	1.995	**5.256**	1.0031
Optimized Centralized H_∞	2.582	2.385	**4.967**	0.7403
Centralized μ	2.430	2.449	**4.879**	0.7343
Fixed-structure H_∞	3.500	2.060	**5.560**	0.9812

From the performance indices and simulation plots, we observe that the centralized controllers (H_∞ and μ) have the least IAE values followed by the MoI and *fmincon* controllers. All the controllers tend to have approximately the same settling time. It should however be noted that we arrive at such speed with the centralized H_∞ and μ

controllers by raising the ω_B^* specification in W_P to 0.35rad/min during synthesis, otherwise the resulting controllers were much slower in their responses.
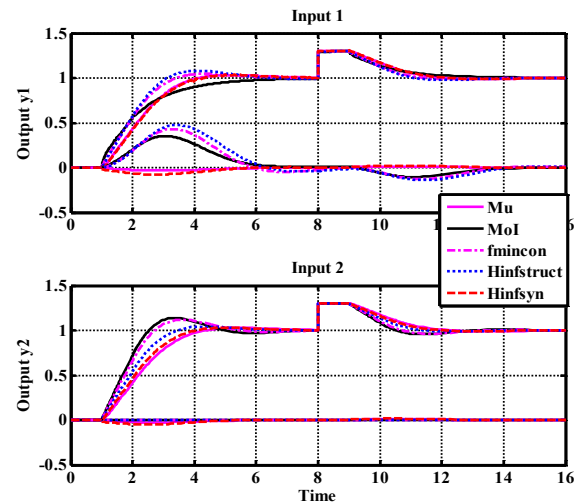
Figure 4: Servo and Regulatory Responses for CSTR with Different Controllers

3.2 Example 2: Three-Tank System

The three-tank plant is as shown in Figure 5. It is a combination of three transparent calibrated cylindrical tanks of equal dimensions (See Amira, 2002 for detailed description). The controlled variables are the levels, h_1 and h_2 inside tanks 1 and 2. The level h_3, in tank 3, though not being controlled is to be maintained not to overflow or run dry.

The mathematical model for this system is gotten from the following transient balance equations for all the tanks:

$$A\frac{dh_1}{dt} = q_1 - q_{13} - d_1$$
$$A\frac{dh_2}{dt} = q_2 + q_{32} - q_{20} - d_3$$
$$A\frac{dh_3}{dt} = q_{13} - q_{32} - d_2 \qquad (11)$$

where d_1, d_2 and d_3 represent leaks from tanks 1, 2 and 3 respectively, A represents the cross-sectional area of the tanks, and q_{13}, q_{32} and q_{20} are flow rates across pipes connecting, respectively, tanks 1 and 3, tanks 3 and 2, and tanks 2 and the water reservoir and are given by the Torricelli rule;

$$q_{13} = \mu_1.S_p.sgn(h_1 - h_3).\sqrt{2g|h_1 - h_2|}$$
$$q_{32} = \mu_3.S_p.sgn(h_3 - h_2).\sqrt{2g|h_3 - h_2|}$$
$$q_{20} = \mu_2.S_p.\sqrt{2g\,h_2} \qquad (12)$$

In this work, we consider three (3) different operating points (see Tables 3 & 4) around which the above system models are linearized to have
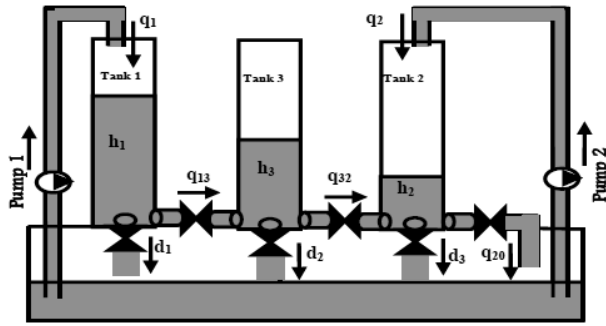
Figure 5: Schematic Diagram of Three-tank System

$$\begin{bmatrix} dh_1 \\ dh_2 \\ dh_3 \end{bmatrix} = A_i \begin{bmatrix} h_1 \\ h_2 \\ h_3 \end{bmatrix} + \begin{bmatrix} 0.00671 & 0 \\ 0 & 0.00671 \\ 0 & 0 \end{bmatrix} \begin{bmatrix} q_1 \\ q_2 \end{bmatrix} \quad i = 1,2,3$$

$$\begin{bmatrix} h_1 \\ h_2 \end{bmatrix} = \begin{bmatrix} 1 & 0 & 0 \\ 0 & 1 & 0 \end{bmatrix} \begin{bmatrix} h_1 \\ h_2 \\ h_3 \end{bmatrix}$$

$$(13)$$

OP 1
$$A_1 = \begin{bmatrix} -0.00797 & 0 & 0.00797 \\ 0 & -0.0211 & 0.00726 \\ 0.00797 & 0.00726 & -0.0152 \end{bmatrix}$$

OP 2
$$A_2 = \begin{bmatrix} -0.00995 & 0 & 0.00995 \\ 0 & -0.0257 & 0.00909 \\ 0.00995 & 0.00909 & -0.019 \end{bmatrix}$$

OP 3
$$A_3 = \begin{bmatrix} -0.01065 & 0 & 0.01065 \\ 0 & -0.0257 & 0.00909 \\ 0.01065 & 0.00968 & -0.0203 \end{bmatrix}$$

Table 3: Process parameters for three-tank system

Outflow coefficients: μ_1, μ_2, μ_3	0.44, 0.87, 0.42
Area of tank: A_1, A_2, A_3 (cm^2)	149

Area of connecting pipes: S_p (cm^2)	0.5

Table 4: Operating conditions for three-tank system

	OP1	OP2	OP3
Q_{1s} (cm^3)	40	32	30
Q_{2s} (cm^3)	50	43	40
H_{1s} (cm)	57.16	37.8	33.08
H_{2s} (cm)	21.82	15.2	13.20
H_{3s} (cm)	40.31	26.97	23.60

Uncertainty modelling for this system is a sort of combination of Cases I , II and III of section 2.2.1 in that we consider the relative deviations of the operating points

(1, 2 and 3) with parametric uncertainties ($\pm10\%$ in μ_2 and

μ_3) from the nominal operating point 2 which is about the average plant going by the Nyquist plots. This yields us uncertainty as high as 50% at low frequencies but drops to about 1% at high frequencies. To give room for other sources of uncertainty such as unmodelled dynamics, we consider an uncertainty which increases in magnitude from 50% at low frequency to 80% at high frequency. For this we obtain

$$W_i = diag(w_i, w_i); \quad w_i(s) = \frac{0.7964(s+0.0045)(s+0.0490)}{(s+0.0601)(s+0.0058)}$$
$$(14)$$

The performance weight for controller analyses is also given by

$$W_p = diag(w_p, w_p) \qquad w_p(s) = \frac{s/2 + 0.015}{s} \qquad (15)$$

in which we have specified Ms=2 (with an implication that $GM \geq 2$ and $PM \geq 28.96^0$), $\omega_B^* = 0.015$rad/min.

Controller Design and Optimization

The nominal model RGA $\begin{pmatrix} 1.2865 & -0.2865 \\ -0.2865 & 1.2865 \end{pmatrix}$ suggests diagonal pairing for multiloop control. Initial multiloop controller parameters were obtained using SIMULINK auto-tuning facility. These parameters alongside the optimised parameters and fixed-structure H_∞ controller parameters are presented in Table 5. 5th order centralized H_∞ controller and 15th order µ controller were obtained for the system. Order reduction to 3 and 5 respectively were successful but the H_∞ controller lost its robustness in the process. Table 6 summarizes the performance indices of the different controllers for the system and Figure 6 displays their relative performance at OP2 as regards response to unit step changes and disturbance rejection. Note that the responses were found to be similar for the other operating points.

216

Table 5: Controller Parameters for Three-Tank System, $K = P + I/s$

Controller	k_{11}		k_{22}	
	P	I	P	I
Initial Parameters	2.3652	0.0537	1.3647	0.1108
MoI Optimized	18.6200	0.1990	14.6300	0.4050
fmincon Optimized	16.2821	0.5370	13.6470	0.8834
Fixed-structure $H\infty$	10.3000	0.115	9.9500	0.3190

Table 6: Performance and Robustness Indices for Three-Tank System

Controller	IAE for step in y_1	IAE for step in y_2	Total IAE	μ_{RP}
Initial Parameters	71.25	66.91	**138.16**	1.5863
MoI Optimized	13.13	14.44	**27.17**	0.8487
fmincon Optimized	13.43	12.66	**26.09**	0.9338
Fixed-structure H_∞	17.68	15.61	**33.24**	0.8946
Centralized H_∞	12.50	12.50	**25.00**	0.8404
Centralized μ	10.60	11.37	**21.97**	0.8790
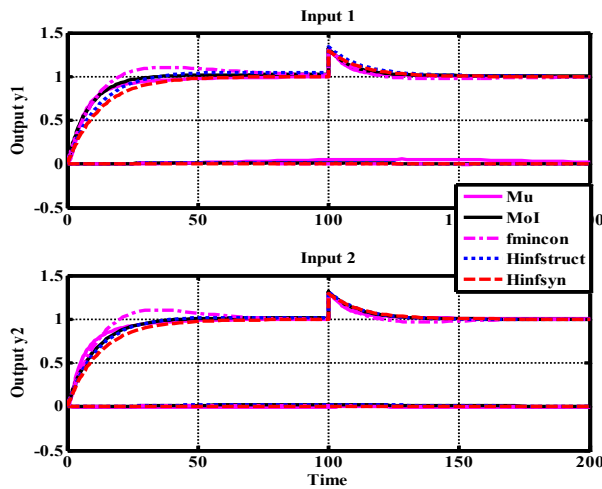
Figure 6: Servo and Regulatory Responses for Three-Tank System with Different Controllers

From the above analyses, centralized μ controller is observed to have the least IAE value followed by the centralized H_∞, decentralized *fmincon*, MoI and fixed-structure H_∞, controllers in that order. All optimized controllers attained good robust performance but just as in

the case of the previous example, the ω_B^* specification in

W_P was raised to 0.04rad/min during H_∞, and μ syntheses, otherwise the resulting controllers were much slower in their responses.

3.3 Example 3: Six-Spherical Tank System

The six-spherical tank system (Figure 7) is a theoretical case study that was posited by Escobar and Trierweiler (2013)
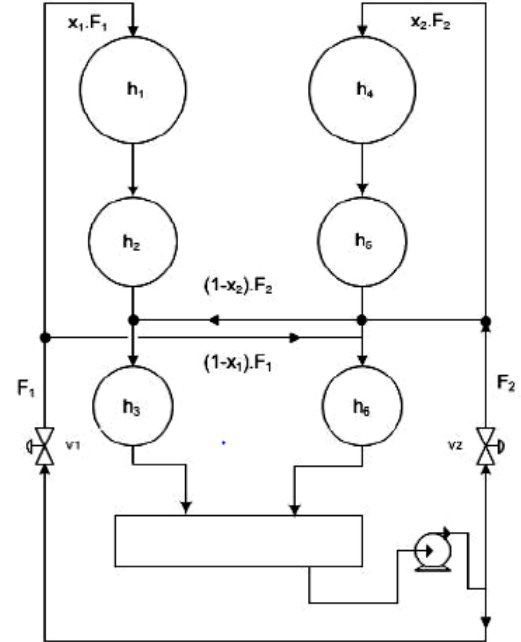
Figure 7: Schematic Diagram of Six-Tank System

The control objective is to maintain the lower levels h_3 and h_6 at their reference values (set-points) by manipulating the opening of the two valves (x_1, x_2), with $0 \leq x_1, x_2 \leq 1$, and defining the flow rates as F_1 and F_2.

The following set of differential equations was derived as model describing the system:

$$A_1 \frac{dh_1}{dt} = f_1 = x_1 F_1 - R_1\sqrt{h_1}$$
$$A_2 \frac{dh_2}{dt} = f_2 = R_1\sqrt{h_1} - R_2\sqrt{h_2}$$
$$A_3 \frac{dh_3}{dt} = f_3 = (1 - x_2)F_2 + R_2\sqrt{h_2} - R_3\sqrt{h_3}$$
$$A_4 \frac{dh_4}{dt} = f_4 = x_2 F_2 - R_4\sqrt{h_4}$$
$$A_5 \frac{dh_5}{dt} = f_5 = R_4\sqrt{h_4} - R_5\sqrt{h_5}$$
$$A_6 \frac{dh_6}{dt} = f_6 = (1 - x_1)F_1 + R_5\sqrt{h_5} - R_6\sqrt{h_6} \quad (16)$$

where A_i denotes the tank i cross-sectional area, g is the acceleration due to gravity, R_i is the tank i discharge coefficient, a_i is the cross-sectional area of the tank i discharge pipe, and D_i is the tank i diameter.

$$A_i = \pi(D_i h_i - h_i^2) \quad \text{and} \quad R_i = a_i\sqrt{2g}$$

Four operating conditions are considered (Table7 & 8). Linearization of the above equations about these operating points was done. The following general form of the linearized model given by Escobar and Trierweiler (2013) contains delay terms introduced to the system to capture dynamics not reflected in the differential equations.

Table 7: Process Parameters for Six-tank System

Parameters	Value
$D_1\ D_4$ [cm]	35
$D_2\ D_5$ [cm]	30
$D_3\ D_6$ [cm]	25
$R_1\ R_4$ [cm$^{2.5}$min^{-1}]	1690
$R_2\ R_5$ [cm$^{2.5}$min^{-1}]	1830
$R_3\ R_6$ [cm$^{2.5}$min^{-1}]	2000

Table 8: Operating Points of Six-tank System

Variables	OP1	OP2	OP3	OP4
$h_{1s}[cm]$	2.7450	9.6504	2.7450	9.6504
$h_{2s}[cm]$	2.3411	3.2303	2.3411	8.2303
$h_{3s}[cm]$	4.8400	17.0156	8.4100	11.7306
$h_{4s}[cm]$	2.0167	7.0901	7.0901	2.0167
$h_{5s}[cm]$	1.7200	6.0468	6.0468	1.7200
$h_{6s}[cm]$	3.2400	11.3906	8.1225	5.4056
$F_{1s}\ [L\ min^{-1}]$	4	7.5	4	7.5
$F_{2s}\ [L\ min^{-1}]$	4	7.5	7.5	4
x_1, x_2	0.7, 0.6	0.7, 0.6	0.7, 0.6	0.7, 0.6

$$\begin{bmatrix} h_3(s) \\ h_6(s) \end{bmatrix} = \begin{bmatrix} \dfrac{x_1 c_1 e^{-0.9s}}{\prod_{i=1}^{3}(\tau_i s+1)} & \dfrac{(1-x_2)c_1 e^{-0.3s}}{(\tau_3 s+1)} \\ \dfrac{(1-x_1)c_2 e^{-0.3s}}{(\tau_6 s+1)} & \dfrac{x_1 c_1 e^{-0.9s}}{\prod_{i=4}^{6}(\tau_i s+1)} \end{bmatrix} \begin{bmatrix} F_1(s) \\ F_2(s) \end{bmatrix} \quad (17)$$

where $\quad c_1 = \dfrac{2\sqrt{h_{3s}}}{R_3}, \quad c_2 = \dfrac{2\sqrt{h_{6s}}}{R_6} \quad$ and $\quad \tau_i = \dfrac{2A_i\sqrt{h_{is}}}{R_i}$

The nominal model considered for controller design and optimization is given as

$$G_{nom} = \begin{bmatrix} \dfrac{2.215(1-0.9s)}{(0.5454s+1)(0.0883s+1)(2.3s+1)} & \dfrac{1.265(1-0.3s)}{(1.2175s+1)} \\ \dfrac{0.77625(1-0.3s)}{(1.0211s+1)} & \dfrac{1.5525(1-0.9s)}{(0.0712s+1)(1.2227s+1)(1.20s+1)} \end{bmatrix}$$

$$(18)$$

In Figure 8, we show how well this plant represents the average plant of the four operating points. The multiplicative input uncertainty modelled for this system to cover for all the operating points is given by:

$$W_i = \text{diag}(w_i, w_i); \quad w_i(s) = \frac{1.7395(s+0.0422)(s+0.2550)}{(s+0.4816)(s+0.1268)} \quad (19)$$

W_I increases from a magnitude of about 30% at low frequencies to approximately 175% at high frequency reaching 100% uncertainty at about 0.25rad/min

8(a) Element (1,1)
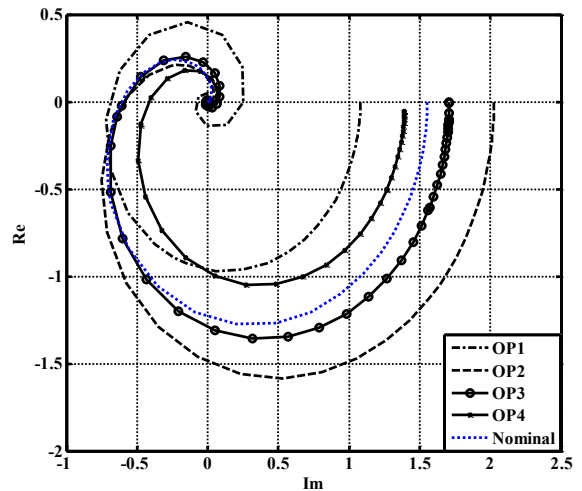
8(b) Element (2,2)

Figure 8: Nyquist Plots of diagonal elements of different Ops for six-tank system

Controller Design and Optimization

RGA was calculated for the above approximated transfer function and we obtained $\begin{pmatrix} 1.3997 & -0.3997 \\ -0.3997 & 1.3997 \end{pmatrix}$. This

suggests a diagonal pairing. IMC tuning relation was employed to obtain the initial controller parameters In Table 9 we present the initial IMC controller parameters and final values obtained after optimization using MoI and MATLAB Optimization Toolbox command, *fmincon*. We also present the parameters for the fixed-structure H_∞ controller in this table.

Table 9: Controller Parameters for Six-Tank System, $K(s) = P + \frac{1}{s}I$

Controller	Loop 1		Loop 2	
	P	I	P	I
Initial Parameters	0.1672	0.0456	0.2449	0.0840
MoI Optimized	0.2936	0.0570	0.0649	0.0576
fmincon Optimized	0.2880	0.0778	0.0752	0.0580
fixed-structure H_∞ controller	0.2380	0.0741	0.1130	0.0665

For centralized control system, 10th order centralized H_∞ controller and 22nd order μ controllers were also synthesized. The order of the latter was successfully reduced to 2 while for the H_∞ controller, attempt to obtain lower order controller that retains the stability and performance of the initial controller was not successful.

For robust performance analyses, we consider the performance weight

$$W_p = daig(w_p, w_p) \qquad w_p = \frac{0.4s + 0.03}{s} \qquad (20)$$

With this, we have specified Ms=2.5 (with an implication that $GM \geq 1.67$ and $PM \geq 23.07°$) and $\omega_B^* = 0.03$rad/s.

Table 10 contains the robustness and performance indices of the different controllers while Figures 9 and 10 respectively show the simulation response at the nominal and most challenging operating point, OP2.

A major challenge in the design of a robust controller for this system is the large variation in the dynamics of the system which makes it difficult for the speeds at different operating points to meet a common ω_B^* requirement. The results show that the fixed structure H_∞ controller has the minimum IAE value but also the highest μ_{RP} value and interactions among the optimized controllers. Generally, we observe that μ_{RP} is inversely proportional to the calculated IAE values. This is a pointer to the compromise reached between attainable robust performance and speed of the control system.

Table 10: Performance and Robustness Indices for Six-Tank System

	IAE for step in y_1	IAE for step in y_2	Total IAE	μ_{RS}	μ_{RP}
Initial Parameters	17.61	22.02	**39.63**	0.6016	1.0406
MoI Optimized	16.56	24.64	**41.20**	0.5570	1.0000
fmincon Optimized	13.58	22.16	**35.74**	0.3490	1.0001
Fixed-structure H_∞	13.29	20.51	**33.80**	0.3489	1.0020
Centralized H_∞	18.58	20.38	**38.96**	0.2798	0.9521
Centralized μ	17.08	20.25	**37.33**	0.2455	0.9502
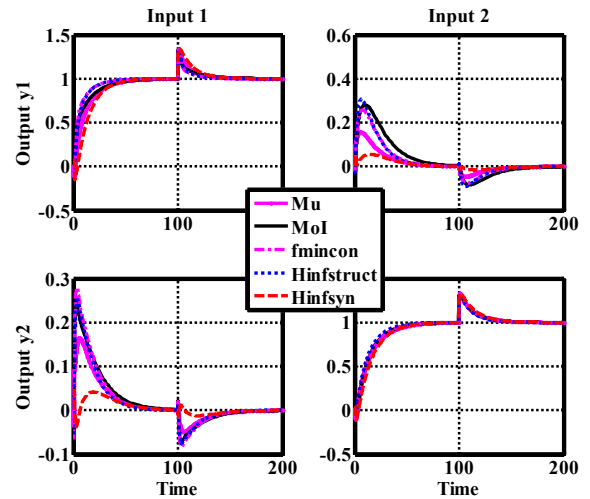
Figure 9: Process Outputs and Interactions for Unit Set-point Change (Nominal Model)
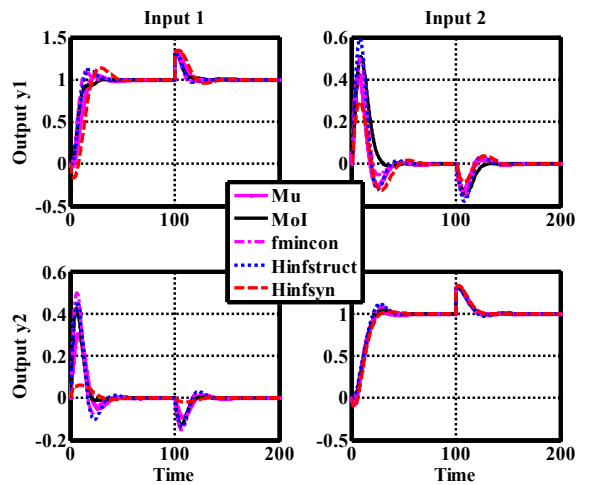
Figure 10: Process Outputs and Interactions for Unit Set-point Change (OP2)

The centralized controllers which have $\mu_{RP} < 1$ and minimum interactions have slightly higher IAE values consequent upon the marginally slower response to unit set-point change and disturbance rejection.

3.4 Example 4: Quadruple Tank System

The quadruple tank system (Figure 11) is a multivariable laboratory process of four interconnected water tanks (Johansson, 2000).
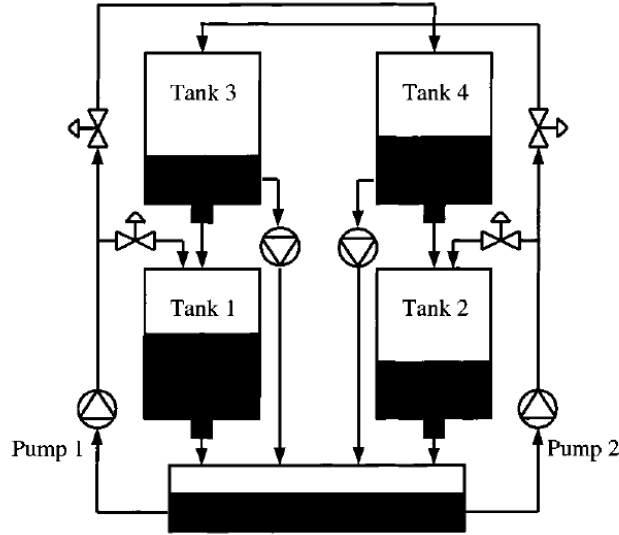
Figure 11: Schematic Diagram of Quadruple Tank System

The differential equations representing the mass balances in this four-tank system are

$$\frac{dh_1}{dt} = -\frac{a_1}{A_1}\sqrt{2gh_1} + \frac{a_3}{A_1}\sqrt{2gh_3} + \frac{\gamma_1 k_1}{A_1}v_1$$

$$\frac{dh_2}{dt} = -\frac{a_2}{A_2}\sqrt{2gh_2} + \frac{a_4}{A_2}\sqrt{2gh_4} + \frac{\gamma_2 k_2}{A_2}v_2$$

$$\frac{dh_3}{dt} = -\frac{a_3}{A_3}\sqrt{2gh_3} + \frac{(1-\gamma_2)k_2}{A_1}v_2 - \frac{k_{d1}d_1}{A_3}$$

$$\frac{dh_4}{dt} = -\frac{a_4}{A_4}\sqrt{2gh_4} + \frac{(1-\gamma_1)k_1}{A_4}v_1 - \frac{k_{d2}d_2}{A_4} \qquad (21)$$

where hi is the liquid level in tank i; a_i is the outlet cross-sectional area of tank i; A_i is the cross-sectional area of tank i; v_j is the speed setting of pump j, with the corresponding gain k_j; γ_j is the portion of the flow that goes into the upper tank from pump j; and d_1 and d_2 are flow disturbances from tank 3 and tank 4, respectively, with corresponding gains k_{d1} and k_{d2}. The process manipulated inputs are v_1 and v_2 (speed settings to the pumps), and the measured outputs are $y1$ and $y2$ (voltages from level measurement devices).

The process transfer function under the operating conditions described in Table 9 is given as

$$G(s) = \begin{pmatrix} \dfrac{0.199}{65s+1} & \dfrac{0.3787}{(65s+1)(34s+1)} \\ \dfrac{0.4643}{(54.1s+1)(45.3s+1)} & \dfrac{0.1623}{54.1s+1} \end{pmatrix} \qquad (22)$$

Table 9: Operating Conditions for Quadruple Tank System

Symbol	State/Parameters	Value
h^0(cm)	nominal levels	16.3, 13.7, 6.0, 8.1
v^0(%)	nominal pump settings	50, 50
a_i(cm²⁾	area of the drain in tank i	2.05, 2.26, 2.37, 2.07
A_i(cm²⁾	areas of the tanks	730
γ_1	ratio of flow in tank 1 to flow in tank 4	0.3
γ_2	ratio of flow in tank 1 to flow in tank 4	0.3
k_j(cm³/s %)	pump proportionality constants	7.45, 7.30
k_{dj}	disturbance gains	0.049, 0.049
T_i(s)	time constants in the linearized model	65, 54.1, 34, 45.3
g(cm/s²)	gravitation constant	981

According to Vadigepalli *et al* (2001) the quadruple tank system under consideration exhibits similar dynamics when operated at different steady-state levels in each of the minimum phase and non-minimum-phase regimes. Hence uncertainty modelling for this plant is obtained numerically

by varying the parameters γ_2, γ_1, k_1, and k_2 by $\pm10\%$ of the corresponding nominal value. This yields us uncertainty as high as 28% at low frequencies but drops to about 22% at high frequencies. To give room for other sources of uncertainty such as unmodelled dynamics, we consider an uncertainty which increases in magnitude from 40% at low frequency to 130% at high frequency. For this we obtain

$$W_i = \text{diag}(w_i, w_i); \quad w_i = \frac{1.3s + 0.03666}{s + 0.0926} \qquad (23)$$

The performance weight for controller analyses is also given by

$$W_P = diag(w_p, w_p) \quad w_p(s) = \frac{s/2.5 + 0.003}{s} \qquad (24)$$

With this, we have specified Ms=2.5 (with an implication that $GM \geq 1.67$ and $PM \geq 23.07^o$) and $\omega_B^\bullet = 0.003$rad/s

Controller Design and Optimization

The nominal model RGA $\begin{pmatrix} -0.2250 & 1.2250 \\ 1.2250 & -0.2250 \end{pmatrix}$ suggests an anti-diagonal pairing for multiloop control. Initial multiloop controller was obtained using IMC tuning relations. These parameters were optimised alongside with

the performance weight parameter, ω_B^*. Both initial and optimised parameters together with the fixed-structure H_∞ controller parameters are presented in Table 12.

6th order centralized H_∞ controller and 16th order μ controller were obtained for the system. In both cases, attempted order reduction did not yield lower order controllers with satisfactory performance.

Table 13 summarizes the performance indices of the different controllers for the system and Figure 12 displays their relative performance as regards response to unit step changes and disturbance rejection.

Table 12: Controller Parameters for Quadruple Tank System, $K = P + \dfrac{I}{s}$

Controller	k_{21}			k_{12}			ω_B^*
	P	I	D	P	I	D	
Initial Parameters	4.49	0.05	100.19	5.38	0.05	132.78	0.0030
MoI Optimized	4.77	0.05	73.11	4.88	0.05	80.08	0.0046
fmincon Optimized	5.84	0.06	118.63	2.15	0.07	53.11	0.0026
Fixed-structure H_∞	3.50	0.03	-	3.25	0.04	-	0.0046

Table 13: Performance and Robustness Indices for Quadruple Tank System
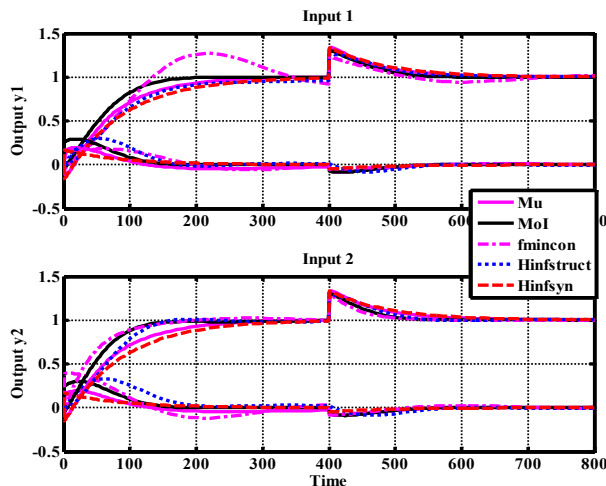
Figure 12: Servo and Regulatory Responses for Quadruple Tank System with Different Controllers

For this particular example, we have used the same ω_B^* specification in W_P for multiloop MoI and *fmincon* optimization and H_∞, and μ syntheses. This brings to bare the relatively slow speed of response of the synthesized centralized controllers under this condition. Of all the optimized controllers for this example, only the *fmincon* controller did not perfectly meet the robust performance condition.

4.0 Discussion

It is important to first note that MoI and *fmincon* optimizations require starting parameters to proceed unlike H_∞ and μ syntheses strategies which can proceed on declaration of the system and desired performance. The results show that *fmincon* which works better with more parameters may rather appear "aggressive" on simple systems with few parameters to be optimized unlike MoI which optimizes rather progressively. Centralized H_∞ and μ syntheses are observed to be reliable strategies for obtaining robust controllers even for complex systems (systems of large dimensions, high order, great interactions and/or delay terms) but may often result in controllers of high order, and in some cases, desirable properties of the controller may be lost on order reduction.

Also, we observe that the performance requirement of the

system in terms of ω_B^* can be better tightened in the course of optimization with MoI than with *fmincon*.

Finally, with the same specified ω_B^* for controller optimization, H_∞ and μ synthesized controllers often

Controller	IAE for step in y_1	IAE for step in y_2	Total IAE	μ_{RP} ($\omega_B^* = 0.0046$)
Initial Parameters	35.16	36.01	**71.17**	1.3175
MoI Optimized	35.22	34.81	**70.03**	0.9134
fmincon Optimized	33.48	34.90	**68.38**	1.0257
Fixed-structure H_∞	32.29	32.31	**64.60**	0.9644
H_∞ Controller	33.84	34.18	**68.02**	0.9656
μ Controller	34.49	35.00	**69.49**	0.9260

appear relatively slower than MoI and *fmincon* optimized controllers which also meet the stated performance requirements.

5.0 Conclusions

Optimal ω_B^* requirement for a control system can be easily obtained with MoI. It may be necessary to specify higher

values of ω_B^* when employing H_∞ and μ synthesis strategies as compared to MoI and *fmincon* optimization. Also, the H_∞ and μ syntheses may be reserved for complex systems for which multiloop MoI and *fmincon* optimization fail to attain desired performance. The fixed-structure H_∞ design strategy can be a good substitute in many cases for centralized H_∞ and μ syntheses although its robustness may be slightly less than that of the centralized H_∞ and μ.

6.0 References

Amira (2002). *Laboratory Setup three-tank-system.* Amira GmbH.

Coleman, T., Branch, M.A. and Grace, A. (1999). *Optimization toolbox for use with MATLAB.* The MAthworks Inc, Natick, MA.

Escobar, M., and Trierweiler, J. O. (2013). Multivariable PID controller design for chemical processes by frequency response approximation. *Chemical Engineering Science* 88, 1–15

Fard, J. M., Nekoui, M. A., Sedigh, A. K. and Amjadifard, R. (2013). Robust Controller Design by Multi-Objective Optimization With H$_2$/H∞/μ Combination. *International Journal of Computer Science And Technology* Vol. 4, Issue 1.

Gu, W. D., Petkov, P. H. and Konstantinov, M. M. (2005). *Robust Control Design with MATLAB.* British Library Catalogue.

Johansson, K. H. (2000). The Quadruple-Tank Process: A Multivariable Laboratory Process with an Adjustable Zero. *IEEE Trans. On Control and System Technology*, Vol. 8, No. 3

McKernan, J., Whidborne, J. F. and Papadakis, G. (2009) Poiseuille Flow Controller Design via the Method of Inequalities. *Int. J. Automation & Comp.* 6, 23-30

Oloomi, H. and Shafai, B. (2011). 'Optimizing The Tracking Performance In Robust Control Systems'. Recent Advances In Robust Control – Theory And Applications In Robotics And Electromechanics. Andreas Mueller. (Ed), ISBN: 978-953-307-421-4, InTech, 103-114. Available from: http://www.intechopen.com/books/recentadvances-in-robust-control-theory-and-applications-in-robotics-and-electromechanics/optimizing-the-trackingperformance-in-robust-control-systems

Scali, C and Ferrari,F. (1999). Performance of control systems based on recycle compensators in integrated plants. *Journal of Process Control.* 425-437.

Taiwo, O. (1985). The Dynamics and Control of Plants with Recycle, *J. Nig. Soc. Chem. Eng.* (4):96 - 107.

Taiwo, O., Bamimore, A., Adeyemo, S. and King, R. (2014). On Robust Control System Design for Plants with Recycle.

Preprints of the 19th World Congress, The International Federation of Automatic Control, Cape Town, South Africa.

Vadigepalli, R., Gatzke, E. P. and Doyle, F. J. (2001). Robust Control of a Multivariable Experimental Four-Tank System. *Ind. Eng. Chem. Res.*, 40, 1916-1927

Zakian, V. (1979). New formulation for the method of inequalities. *Proceedings of the Institution of Electrical Engineers*, 126(6):579–584.

Zakian, V. and Al-Naib, U. (1973). Design of dynamical and control systems by the method of inequalities. *Proceedings of the Institution of Electrical Engineers*, 120(11):1421–1427.

Zhou, K., Doyle, J. C. and Glover, K. (1996). *Robust and Optimal Control.* Prentice Hall, Englewood Cliffs, New Jersey.

7.0 Appendix: Synthesized Controllers

$$K = \frac{\begin{bmatrix} num_{11} & num_{12} \\ num_{21} & num_{22} \end{bmatrix}}{den}$$

A. CSTR H_∞ Controller

$num_{11} = $ -1156 s^6 - 2.775e09 s^5 - 3.477e10 s^4 + 4.942e11 s^3 + 6.971e12 s^2 + 9.764e12 s + 1688

$num_{21} = $ -3.291e10 s^5 - 5.377e11 s^4 - 2.643e12 s^3 - 1.483e13 s^2 - 1.894e13 s - 2516

$num_{12} = $ -1.754e09 s^5 - 4.905e10 s^4 - 4.079e11 s^3 - 9.082e11 s^2 - 5.984e11 s - 2965

$num_{22} = $ -57.8 s^6 - 1.679e10 s^5 + 5.912e11 s^4 + 1.27e13 s^3 + 3.572e13 s^2 + 2.718e13 s + 1.296e05

$den = $ s^6 + 2.935e08 s^5 + 8.996e10 s^4 + 1.216e12 s^3 + 1.717e12 s^2 + 8468 s + 1.427e-06

B. CSTR μ Controller

$num_{11} = $ -0.01039 s^2 + 5.771 s + 2.752e-08

$num_{21} = $ -10.39 s - 4.954e-08

$num_{12} = $ -0.1944 s - 1.944e-11

$num_{22} = $ -0.3993 s^2 + 14.66 s + 1.466e-09

$den = $ s^2 + 4.869e-09 s + 4.769e-19

C. Three-tank H_∞ Controller

$num_{11} = $ 1393 s^2 + 11.76 s + 1.176e-06

$num_{21} = $ 1223 s^2 - 11.76 s - 1.176e-06

$num_{12} = $ 1238 s^2 - 11.76 s - 1.176e-06

$num_{22} = $ 1087 s^2 + 52.92 s + 5.292e-06

$den = $ s^3 + 553.8 s^2 + 0.0001108 s + 5.539e-12

D. Three-tank μ Controller

$num_{11} = $ - 3.556 s^4 + 2.022 s^3 + 0.01042 s^2 + 1.644e05 s + 1.644e-12

$num_{21} = $ -0.3991 s^4 - 0.07677 s^3 - 0.00854 s^2 - 3.03e-05 s - 3.03e-12

$num_{12} = $ -0.2357 s^4 - 0.07591 s^3 - 0.007622 s^2 - 2.92e-05 s - 2.92e-12

$num_{22} = $ 5.712 s^4 + 2.308 s^3 + 0.03778 s^2 + 0.0001055 s + 1.055e-11

$den = $ s^5 + 0.9542 s^4 + 0.2201 s^3 + 0.0002896 s^2 + 5.791e-11 s + 2.896e-18

E. Six-tank H_∞ Controller

$num_{11} =$ 0.03964 s^9 + 1.291 s^8 + 19.56 s^7 + 149 s^6 + 455.9 s^5 + 651.6 s^4 + 465.6 s^3 + 160.3 s^2 + 21.13 s + 9.08e-09

$num_{21} =$ -0.3117 s^10 - 10.04 s^9 - 109.6 s^8 - 496.9 s^7 - 1132 s^6 - 1437 s^5 - 1056 s^4 - 442.7 s^3 - 97.33 s^2 - 8.76 s - 3.765e-09

$num_{12} =$ -0.2281 s^10 - 7.456 s^9 - 83.66 s^8 - 399.4 s^7 - 985.5 s^6 - 1378 s^5 - 1132 s^4 - 538.8 s^3 - 137.2 s^2 - 14.44 s - 1.444e-09

$num_{22} =$ 0.05648 s^9 + 1.788 s^8 + 25.99 s^7 + 207.5 s^6 + 597.4 s^5 + 815.9 s^4 + 578 s^3 + 204.8 s^2 + 28.47 s + 2.847e-09

den = s^10 + 33.74 s^9 + 400.8 s^8 + 2119 s^7 + 5887 s^6 + 9313 s^5 + 8176 s^4 + 3599 s^3 + 599.4 s^2 + 3.176e-07 s + 2.576e-17

F. Six-Tank μ Controller

$num_{11} =$ 0.04198 s + 4.198e-12

$num_{21} =$ -0.02341 s^2 - 0.007167 s - 7.167e-13

$num_{12} =$ -0.03283 s^2 - 0.02115 s - 2.115e-12

$num_{22} =$ 0.05388 s + 5.388e-12

den = s^2 + 2e-10 s + 1e-20

G. Quadruple Tank H_∞ Controller

$num_{11} =$ -1.814e04 s^5 - 3.495e04 s^4 - 2702 s^3 - 64.98 s^2 - 0.4894 s - 4.894e-08

$num_{21} =$ 1.748e04 s^5 + 3.511e04 s^4 + 5917 s^3 + 211.4 s^2 + 1.98 s + 1.98e-07

$num_{12} =$ 1.742e04 s^5 + 3.422e04 s^4 + 5381 s^3 + 176.4 s^2 + 1.635 s + 1.635e-07

$num_{22} =$ -1.678e04 s^5 - 3.303e04 s^4 - 2719 s^3 - 72.58 s^2 - 0.6104 s - 6.104e-08

den = s^6 + 101.1 s^5 + 609.3 s^4 + 820.5 s^3 + 65.67 s^2 + 1.313e-05 s + 6.567e-13

H. Quadruple Tank μ Controller

$num_{11} =$ -71.08 s^15 - 238.4 s^14 - 279.7 s^13 - 136.2 s^12 - 26.16 s^11 - 2.561 s^10 - 0.149 s^9 - 0.00567 s^8 - 0.0001473 s^7 - 2.636e-06 s^6 - 3.215e-08 s^5 - 2.597e-10 s^4 - 1.318e-12 s^3 - 3.767e-15 s^2 - 4.598e-18 s - 4.598e-25

$num_{21} =$ 46.16 s^15 + 188.1 s^14 + 274 s^13 + 169.4 s^12 + 42.65 s^11 + 5.485 s^10 + 0.403 s^9 + 0.01797 s^8 + 0.0005081 s^7 + 9.342e-06 s^6 + 1.125e-07 s^5 + 8.753e-10 s^4 + 4.209e-12 s^3 + 1.131e-14 s^2 + 1.29e-17 s + 1.29e-24

$num_{12} =$ 81.21 s^15 + 287.1 s^14 + 342.4 s^13 + 176.2 s^12 + 41.07 s^11 + 5.067 s^10 + 0.361 s^9 + 0.01568 s^8 + 0.0004337 s^7 + 7.841e-06 s^6 + 9.333e-08 s^5 + 7.204e-10 s^4 + 3.447e-12 s^3 + 9.227e-15 s^2 + 1.051e-17 s + 1.051e-24

$num_{22} =$ -39.53 s^15 - 164.9 s^14 - 229.6 s^13 - 122.7 s^12 - 24.25 s^11 - 2.409 s^10 - 0.1424 s^9 - 0.005549 s^8 - 0.000149 s^7 - 2.772e-06 s^6 3.512e-08 s^5- 2.936e-10 s^4 - 1.532e-12 s^3 - 4.481e-15 s^2 - 5.568e-18 s - 5.567e-25

den = s^16 + 5.882 s^15 + 14.18 s^14 + 17.91 s^13 + 12.42 s^12 + 4.479 s^11 + 0.741 s^10 + 0.06418 s^9 + 0.003132 s^8 + 8.884e-05 s^7 + 1.497e-06 s^6 + 1.502e-08 s^5 + 8.705e-11 s^4 + 2.66e-13 s^3 + 3.289e-16 s^2 + 6.578e-23 s + 3.289e-30

P 021

NUMERICAL PREDICTION OF THE OPTIMAL REACTION TEMPERATURE OF THE RISER OF AN INDUSTRIAL FLUID CATALYTIC CRACKING (FCC) UNIT

[1*]Olanrewaju O. F.   [2]Okonkwo P. C.   [3]Aderemi B. O.

[1]National Agency for Science and Engineering Infrastructure (NASENI), Idu Industrial Area, Abuja, Nigeria.
[2,3]Faculty of Engineering, Department of Chemical Engineering, Ahmadu Bello University (ABU), Kaduna, Nigeria.
[1]*sonictreasure@gmail.com; [2]chemstprom@yahoo.com, [3]benjaminaderemi@gmail.com

Abstract:

A pseudo homogeneous two-dimensional (2D) model of an industrial Fluid Catalytic Cracking (FCC) riser is here presented. The riser models of previous researchers were mostly based on the assumption of negligible mass transfer resistance and 1D plug flow. These assumptions reduce the accuracy of the models by over-predicting the optimum residence time of the riser. In this work the coke content of FCC catalyst was modeled as a function of the reactor temperature with the aim of predicting the operating conditions that will reduce coke on catalyst without drastically reducing the yield of gasoline. Mass transfer resistance was incorporated in the reactor model to enhance the accuracy of the results. The mass transfer coefficient and the catalyst effectiveness factor were estimated from empirical correlations obtained from literature. Data used for the simulation were sourced from an existing plant (KRPC) and from literature. Finite difference scheme was used to discretise the model equation. At the end of the investigation, three different operating temperature regimes were identified from the simulated results for the coking of FCC catalyst (low temperature, optimal temperature and high temperature regimes). An optimum operating temperature range of 786K-788K was predicted for the riser.

Keywords: FCC, Finite difference, Mass transfer resistance, Riser, Catalyst.

1.0 Introduction

Fluid Catalytic Cracking (FCC) is one of the most profitable processes in oil refineries. It is the major producer of gasoline in refineries and as such it is sometimes referred to as the heart of the refinery. FCC converts vacuum gas oils (VGO) and heavy feed stocks (molecular weight > 250) from other refinery operations into high octane gasoline, light fuel oils and gases (Fernandes *et al*. 2003).

FCC unit comprises mainly of the riser, the regenerator and the main fractionators. Among the major process variables of FCC (temperature, pressure and catalyst-to-oil ratio), the reactor temperature is the most sensitive variable that affects feed conversion, product yield and catalyst coking. The optimum reaction temperature in FCC is such that guarantees high yield of the desired product without quenching the reactions or causing over-cracking of the key product.

Fernandes *et al*. (2003) used a 6-lump, 1D model to simulate the riser of an industrial FCCU. Their model predicted a gasoline yield of 48%. The temperature, gas and solid phase velocity profiles were also predicted by the authors. However, the assumption of 1D plug flow and negligible mass transfer resistance by the authors oversimplified their models thereby undermining the accuracy of the predictions. Ahari *et al*. (2008) used a 4-lump, 1D model in their investigation. Their model predicted the temperature drop along the riser and they

predicted a gasoline yield of 45%. The major limitation of their model was the assumption of negligible dispersion. The authors' work did not predict optimum parameters for the process. A 5-lump reaction scheme was used by Alsabei (2011). The author also based his investigation on negligible dispersion which contradicts the basic principles of heterogeneous catalysis especially for porous catalysts such as the FCC Zeolite catalyst. A 4-lump, 1D scheme was also used by Heydari *et al*. (2010) to model an industrial riser. Their model was also oversimplified and they did not predict the optimum reaction temperature.

Models of higher dimensionality have also been used by other authors. Souza *et al*. (2007) used a 2D hydrodynamic, 6-lump model to simulate an industrial riser. They predicted a gasoline yield of 48%. Ahsan (2013) used a 2D, 4-lump riser model to predict gasoline yield and temperature profile of FCC. The author predicted a gasoline yield of 40%. Novia *et al*. (2006) used a 3D riser model to predict the hydrodynamic effect on the operation of the riser. They predicted the flow pattern of solid, the velocity vector of solid phases and the solid volume fraction. Gupta (2006) and Lopes *et al*. (2012) used 3D models in their investigations. Gupta (2006) used a mechanistic approach involving 50 lumps (pseudo species) to model an industrial FCCU. Lopes *et al*. (2012) on the other hand, used a 4-lump reaction scheme to investigate the effects of various exit configurations of the riser on the hydrodynamics of the reactor as well as the yield of gasoline. They found that the T-shape exit configuration

enhanced the yield of gasoline owing to enhanced solid (catalyst) reflux. In all the models aforementioned, the authors did not attempt to predict the optimal reaction temperature for FCCU riser.

A 2D quasi-steady state model of an industrial riser is here presented. A five-lump reaction scheme was used to model the FCC reactions. Finite difference numerical scheme was used to discretise the model equation and a code was written in Matlab to solve the discretised equations. This investigation has advanced the works of the previous researchers in this field by simulating the catalyst coke content with a view to predicting the operating conditions that will minimize the coking of FCC catalyst thereby reducing the cost of regeneration of the coked catalyst.

2.0 Materials and Methodology

The FCCU reactor was modeled in this work using MATLAB (R2009a) on a Compaq HP CQ61 laptop.

The following assumptions were made in the development of the model:

1. Pseudo homogenous two-dimensional transport with axial and radial gradients.
2. The catalyst and gas are at thermal equilibrium
3. Hydrocarbon feed comes into contact with the hot catalyst coming from the regenerator and instantly vaporizes (Gupta, 2006).
4. There is no heat loss from the riser, the temperature of the reaction mixture falls only because of the endothermicity of the cracking reactions (Gupta, 2006).
5. The riser dynamic is fast enough to justify a quasi-steady state model.

Figure 1 depicts the five-lump reaction scheme that was used in this investigation.
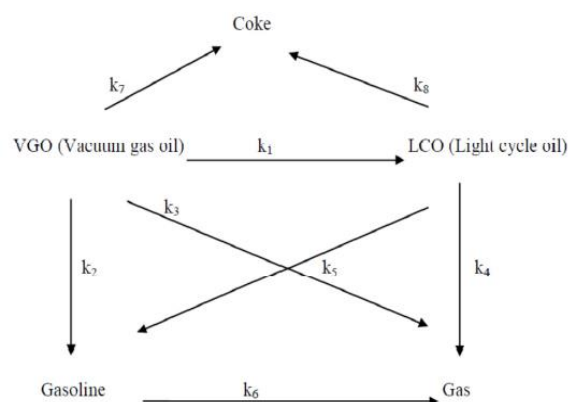
Figure 1: Five-lump model (Den Hollander *et al.* 2003)

In Figure 1, k_j is the rate constant of the jth reaction in s^{-1} where j = 1, 2, …, 8.

2.1 Model rate equation

In the five-lump model given in Figure 1, the eight reactions of the model are taken to follow first order kinetics as follows (mass transfer resistance taken into consideration):

$$r_j = \frac{a\, c_i}{\left(\frac{1}{k_g} + \left(\frac{1}{\eta k_j}\right)\right)} \qquad j = 1, \dots, 8 \qquad (1)$$

$$a = exp(-k_d c_{coke}) \qquad (2)$$

$$k_d = 8.2 \text{ (Den Hollander \emph{et al.} 2003)}$$

$$\eta = \frac{3}{\varphi}\left(\frac{1}{tanh\varphi} - \frac{1}{\varphi}\right) \qquad (3)$$

$$\varphi = R\left(\frac{k_j}{D_e}\right)^{\frac{1}{2}} \qquad (4)$$

c_i = species concentration (weight fraction), k_g = mass transfer coefficient of reactant in m/s, η = particle effectiveness factor, k_j = reaction rate constant in s^{-1}, φ = Thiele modulus and D_e = effective diffusivity in m/s^2. Equation (1) is the model rate equation which incorporates mass transfer resistance terms, k_g and η. Equation (1) reverts to the classical first order rate equation when 1/ k_g = 0, $\eta = 1$. The particle effectiveness factor, η expressed by Equation (3) is the ratio of the reaction rate when there is diffusion resistance to the rate when there is no diffusion resistance. It is a direct measure of the extent to which diffusion resistance reduces the rate of chemical reactions in heterogeneous catalysis and it is a function of Thiele modulus. Thiele modulus, φ is the ratio of intrinsic reaction rate to diffusion rate and as such Equation (4) provides a yardstick for determining the rate determining step in heterogeneous catalysis. Equation (4) holds for spherical particles assumed in this work.

The basic parameters to be determined in Equations (1) to (4) are D_e and k_g. D_e was estimated from empirical correlations in literature (Missen *et al.* 1999) while k_g was

estimated from Sherwood number for gases (Geankoplis 2011).

2.2 Riser model equations

Figure 2 depicts the 2D riser while the control volume that was used in deriving the model equations from Conservation laws is shown in Figure 3 (Missen *et al.* 1999).
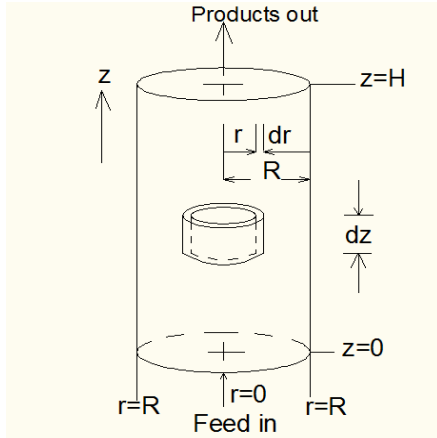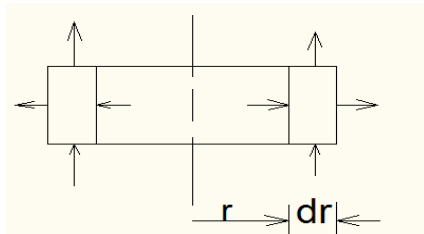

Figure 2: 2D riser reactor (Missen *et al.* 1999)

Figure 3: Control volume (Missen *et al.* 1999)

2.2.1 Continuity equation

The component continuity equation for the model is as given below.

$$D_{zi}\frac{\partial^2 c_i}{\partial z^2} + D_{ri}\left(\frac{\partial^2 c_i}{\partial r^2} + \frac{1}{r}\frac{\partial c_i}{\partial r}\right) - \frac{\partial(uc_i)}{\partial z} - \rho_B(-r_i) = 0$$

$$u = \frac{q}{A_c}, m^3(fluid)\,s^{-1}m^2(vessel) \qquad (6)$$

q is the volumetric flow rate of the gas through interparticle bed voidage, $m^3(fluid)\,s^{-1}$, D_z and D_r are effective diffusivities in $m^3(fluid)\,m^{-1}(vessel)\,s^{-1}$, $(-r_i)$ is in $kg\,species\,kg^{-1}(catalyst)\,s^{-1}$.

2.2.2 Riser hydrodynamic model

The numerical value of the catalyst slip factor (the ratio of the gas interstitial velocity to the average particle velocity) can be predicted from Equation (7) (Ahari *et al.* 2008):

$$\psi = \frac{u_0}{\varepsilon v_p} = 1 + \frac{5.6}{Fr} + 0.47Fr_t^{0.47} \qquad (7)$$

Fr = Froude number and Fr_t = Froude number at terminal velocity.

$$F_r = \frac{u_0}{(gD)^{0.5}} \qquad (8)$$

g = acceleration due to gravity (m²/s).

The average particle velocity in the riser, v_p is given by Equation (9).

$$v_p = \frac{G_s}{\rho_s(1-\varepsilon)} \qquad (9)$$

G_s is the catalyst mass flux.

The expression for the average voidage in terms of the solid mass flux, superficial gas velocity, riser diameter and catalyst physical properties was derived from Equations (7) and (9). Equation (10) gives the average voidage of the reactor.

$$\varepsilon = 1 - \frac{G_s\psi}{u_0\rho_s + G_s\psi} \qquad (10)$$

2.2.3 Energy balance

The model energy balance, Equation (11) is given below.

$$k_z\frac{\partial^2 T}{\partial z^2} + k_r\left(\frac{\partial^2 T}{\partial r^2} + \frac{1}{r}\frac{\partial T}{\partial r}\right) - G_s c_p\frac{\partial T}{\partial z} + \rho_B\sum_{i=1}^{8}(-r_i)(-\Delta H_{Ri}) = 0$$

k_z and k_r are the effective thermal conductivities.

The coupling between the riser and the regenerator is expressed in the model by Equation (12).

$$F_{cat}c_{pcat}(T_0 - T_{cat}) + F_f\,c_{pfl}(T_{vap} - T_f) + F_f\,c_{pfv}(T_0 - T_{vap}) + F_f\,\Delta$$
$$= 0 \qquad (12)$$

The governing equations, Equations (5) and (11) were expressed in a general, normalized form as follows:

$$\alpha\left(\frac{\partial^2\sigma}{\partial r^{*2}} + \frac{1}{r^*}\frac{\partial\sigma}{\partial r^*}\right) + \beta\frac{\partial^2\sigma}{\partial z^{*2}} + \gamma\frac{\partial\sigma}{\partial z^*} + \lambda(-r_i) = 0$$

Equation (14) gives the boundary conditions that were used to solve the riser model equation. (5)

@

$z^* = 0, 0 < r^* < 1\,(inlet): \sigma_{vgo} = \sigma_T = 1,\, \sigma_{lco} = \sigma_{gasoline} = \sigma_{ga}$

$@\, z^* = 1, 0 < r^* < 1\,(outlet): \frac{\partial\sigma}{\partial z^*} = 0$

$@\, r^* = 0, 0 < z^* < 1: \frac{\partial\sigma}{\partial r^*} = 0\,(symmetry)$

$@\, r^* = 1, 0 < z^* < 1: \frac{\partial\sigma}{\partial r^*} = 0 \qquad (14)$

The model equations given above were solved by using finite difference discretization (explicit finite difference scheme). A code was written in Matlab to solve the discretized equations. Grid optimization was carried out by using 10x10, 20x20, 50x50 and 100x100 grids. 20x20 grid mesh was found to give the best convergence.

2.3 Model data

The data used for the simulation are as given in Tables 1 and 2.

Table 1: Kinetic constants for five-lump model

Reaction number	k (s^{-1})
1	1.90
2	7.50
3	1.50
4	0.00
5	1.00
6	0.30
7	0.21
8	0.50

Source: Den Hollander *et al.* 2003

Table 2: Model parameters

S/N	Parameter	Value
1	Reactor inlet temperature, T_0 (K)	791
2	Feed inlet temperature, T_f (K)	613
3	Catalyst inlet temperature, T_{cat} (K)	927
4	Specific heat capacity (liquid feed), cpfl (J/kg-K)	2.67e3 (Ahari *et al.* 2008)
5	Specific heat capacity (vapour feed), cpvf (J/kg-K)	3.30e3 (Ahari *et al.* 2008)
6	Specific heat capacity (catalyst), cpcat (J/kg-K)	1.09e3 (Ahari *et al.* 2008)
7	Feed vaporization temperature, T_{vap} (K)	698
8	Enthalpy of vaporization, delHvap (J/kg)	190e3 (Ahari *et al.* 2008)
9	Density (solid catalyst), ρ_s (kg/m^3)	1250
10	Catalyst velocity, U_c (m/s)	5 (Gupta 2006)
11	Gas superficial velocity, U (m/s)	18
12	Slip factor, psi	2
13	Feed flow rate, F_f (kg/s)	35.5
14	Riser diameter, D_R (m)	1.146
15	Riser height, H (m)	25
16	Pore diameter, P_d (m)	2.00e-9
17	Particle diameter, D_p (m)	60e-6
18	Gas average density ρ_g (kg/m^3)	0.92
19	Gas average viscosity μ_g (Pa.s^{-1})	1.40e-5 (Ahari *et al.* 2008)
20	Riser pressure, P (atm)	2.94
21	Particle tortuosity, τ_p	7 (Missen *et al.*

		1999)

Source: Kaduna Refinery and Petrochemicals Company Ltd (except where otherwise stated)

3.0 Results and discussion

The results obtained at the end of the investigation were presented as shown in Figures 4, 5, 6 and 7. The predicted yields of LCO, gasoline, gas and coke as depicted in Figure 4 are 15.54wt%, 49.70wt%, 18.01wt% and 4.90wt% respectively.
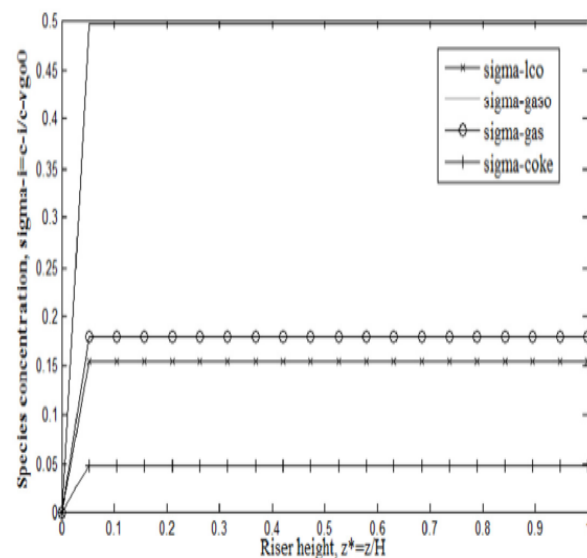
Figure 4: FCC products concentration (wt %) along riser height

FCC reactions are known to occur instantaneously within the first 2-4m of the reactor (Gupta, 2006) because it is within this zone (the reaction zone of the riser) that feed vaporization and feed – catalyst contact occur. Figure 4 predicts that in the FCC riser, products are formed instantaneously within the first 2m of the reactor after which the products yield remain steady through the length of the riser to the exit. In FCC, the riser is operated at an optimum residence time of 2s; the products are quickly withdrawn from the riser and the catalyst is thereafter quickly separated from the product mixture to avoid overcracking of the key product (gasoline) and excessive coking.

Figure 5 presents the predicted conversion of VGO as a function of reactor height while Figure 6 presents the temperature drop along the reactor. A feed stock conversion of 79.28% was predicted by the model. In Figure 5, it can be observed from the feed stock profile that VGO conversion also occurs in the same zone of the riser where the products are formed.
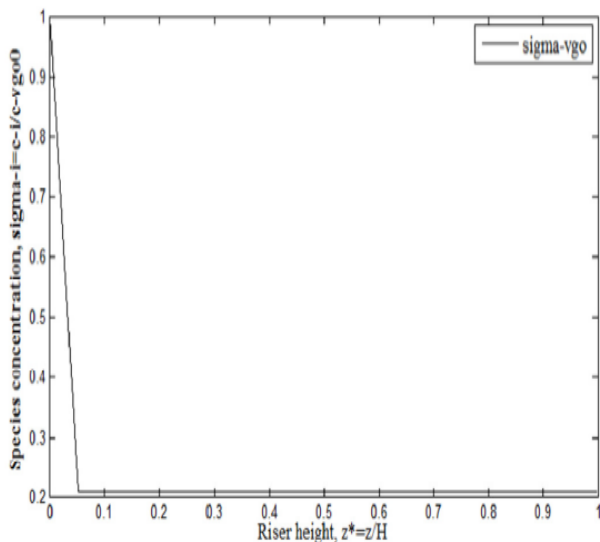
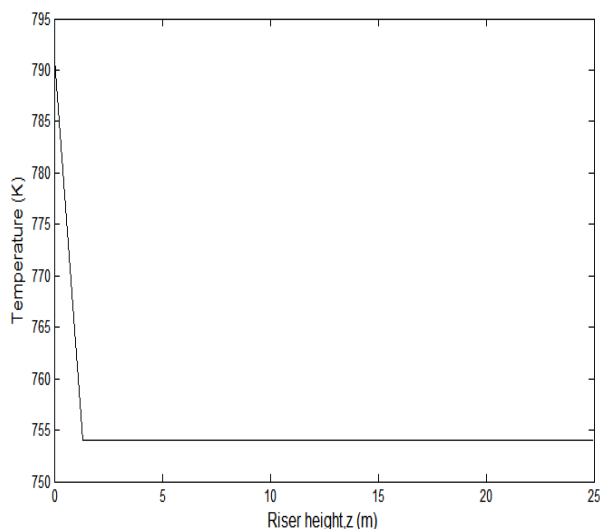Figure 5: Feedstock (VGO) conversion along the height of the riser

Figure 6: Temperature drop along the height of the riser

The model result in Figure 6 predicts a reactor temperature drop of 37^0C (a drop from 791^0C -754^0C). The predicted temperature drop falls within the range predicted in literature for industrial risers; 30-40^0C (Gupta, 2006). The temperature drop is observed to occur in the same zone of the reactor where feed stock conversion occurs. The temperature profile (Figure 6) follows the same trend as the feed stock conversion because FCC reactions are endothermic. Hence, heat transfer between the hot catalyst and the feed (for feed vaporization and initiation of cracking) also occurs in the reaction zone of the riser.

The predicted products yield and feed conversion (Figures 4 and 5) compare favorably well with plant data (Table 3 referred) having percentage deviation value of <5% for all components.

Table 3: Validation of model results with plant data

Species	Conv./Yield, wt% (PDD)	Conv./Yield, wt% *(Model)	% Deviation from Plant data
VGO	80.00	79.28	0.90
LCO	15.15	15.54	2.57
Gasolin-e	50.00	49.70	0.60
Gas	17.88	18.01	0.73
Coke	5.08	4.90	3.54

Key: Conv.: Conversion, PDD: Plant Design Data, VGO: Vacuum Gas Oil, LCO: Light Cycle Oil

The results obtained in this work were also compared with the predictions of previous researchers as shown in Table 4 below. Table 4 shows that the results in this work compare well with the predictions of previous researchers.

Table 4: Comparison of model results with literature values

Species	Conv./Yield, wt% (Fernandes et al., 2003)	Conv./Yield, wt% (Ahari et al., 2008)	Conv./Yield, wt% (Model)
VGO	78.00	78.00	79.28
LCO	10.00	-	15.54
Gasoline	48.00	45.00	49.70
Gas	18.00	-	18.01
Coke	5.00	5.00	4.90

Coke on catalyst was simulated using the validated model. The result was presented as a plot of catalyst coke content as a function of reactor temperature as shown in Figure 7.
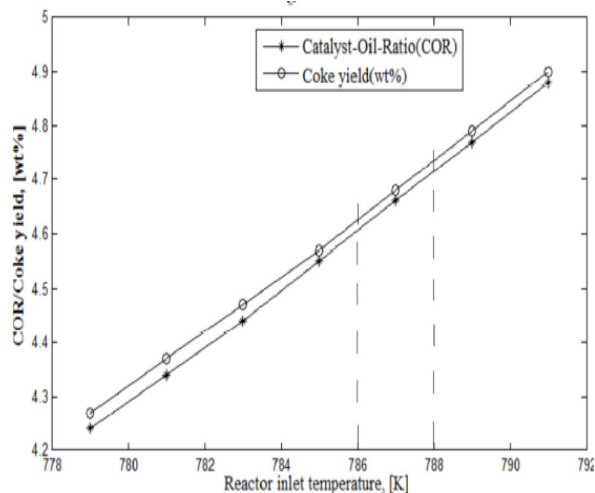
Figure7: Model result for simulation of FCC catalyst coking

The result of the simulation carried out on the riser in this work showed that the yield of coke and catalyst-oil-ratio (COR) increase as the reaction temperature increases. Also, three critical temperature regimes were identified from the plot in Figure 7. These are:

i.   Low operating temperature regime (T<786K): If the riser is operated in this regime (lower region of the graph), the reactions will quench. Hence, operation in this regime is not advisable.

ii.   Optimal operating temperature regime (786K<T<788K): In this temperature range, COR and catalyst coke content profiles taper towards each other as shown in Figure 7. This is the regime of optimal riser operation (without excessive coking).

iii. High operating temperature regime (T>788K): In this temperature zone, the two curves tend to diverge from each other again symbolizing excessive coking of the catalyst. Unit operation in this temperature range is also not advisable because it leads to excessive coking and gas production at the expense of the most economical product (gasoline).

4.0 Conclusions

A 2D pseudo-homogeneous reactor model with a five-lump reaction scheme was used to model the reactions that occur in Fluid Catalytic Cracking (FCC) riser. Mass transfer resistance was incorporated in the model which resulted in the improvement of the accuracy of the model predictions from 89.46% to 98.33%.

The predicted yield of gasoline by the model here presented is 49.70% with VGO conversion of 79.28% and a coke yield of 4.90%. The model results obtained in this work compare favorably well with plant design data (50% gasoline, 80% VGO conversion and 5% coke).

The coking of the FCC catalyst was also simulated for temperatures ranging from 779K to 791K. It can be inferred from the results of this investigation that an operating temperature range of 786K<T<788K is optimal for FCC. The predicted optimal temperature range corresponds to an optimal catalyst-to-oil ratio (COR) of 4.60-4.71.

Nomenclature

a	Catalyst activity for non-coking reactions
c_i	Species concentration (weight fraction)
c_p	Specific heat capacity (J/kg-K)
d_{AB}	Collision diameter (m)
D_{AB}	Molecular diffusivity (m/s^2)
D_e	Effective diffusivity (m/s^2)
D_k	Knudsen diffusivity (m/s^2)
D_p	Particle diameter (m)
$D^\bullet$	Overall diffusivity (m/s^2)
F_i	Flow rate of species i (kg/s)
G_s	Catalyst mass flux (kg/m^2.s)
ΔH_{Ri}	Enthalpy of cracking of species i (kJ/kg)
ΔH_{vap}	Enthalpy of vaporization (kJ/kg)
P	Pressure (atm)
r_e	Average pore radius (m)
r_i	Species reaction rate (kg species (kg catalyst)$^{-1}$s^{-1})
k	Reaction rate constant (s^{-1})
k_r, k_z	Effective thermal conductivity (W/m.K)
k_g	Mass transfer coefficient (m/s)
t	Time (s)
X	Conversion
M_i	Molecular weight species i (kg/Kmol)
m	Node number in the horizontal direction
T	Temperature (K)
R	Radius (m)
Δr	Radial spatial interval (m)
n	Node number in the vertical direction
N_A	Molar flux (kmol/m^2.s)
N_{Re}	Particle Reynolds number
N_{sc}	Schmidt number
N_{sh}	Sherwood number
N_r	Number of divisions in radial direction
N_z	Number of divisions in axial direction
V	Reactor volume (m^3)
v_{ij}	Stoichiometric coefficient
v_p	Average particle velocity (m/s)
H	Reactor height (m)
u	Superficial velocity (m/s)
q	Volumetric flow rate (m^3/s)
A_c	Cross-sectional area (m^2)
F_r	Froude number
Δz	Axial spatial interval (m)

Greek letters:

α'	Decay function rate constant
α	Normalized parameter
β	Normalized parameter

γ	Normalized parameter
δ	Decay function constant
ε	Porosity
η	Particle effectiveness factor
η_0	Particle overall effectiveness factor
λ	Normalized parameter
μ	Viscosity (Pa.s^{-1})
π	Pi
φ	Thiele modulus
ψ	Slip factor
ρ	Density (kg/m^3)
σ	Normalized variable
τ	Tortuosity
Ω_D	Collision integral

Subscripts:

i	Species number
j	Reaction number

Abbreviations:

KRPC   Kaduna Refinery & Petrochemicals Company Ltd

References

Ahari, J.S., Farshi, A. and Forsat, K. (2008). A Mathematical Modeling of the Riser Reactor in Industrial FCC Unit. *Petroleum and Coal,* 50(2), pp. 15-24.

Ahsan, M. (2013). Prediction of Gasoline Yield in a Fluid Catalytic Cracking (FCC) riser using k-epsilon turbulence and 4-lump kinetic models: A Computational Fluid Dynamics (CFD) Approach. *Journal of King Saud University-Engineering Sciences* 2013, pp. 4-5.

Alsabei, R.M. (2011). Model Based Approach for the Plant-wide Economic Control of Fluid Catalytic Cracking Unit. *PhD Thesis*, Loughborough University.

Den Hollander, M.A., Wissink, M., Makkee, M. and Moulijn, J.A. (2003). Fluid Catalytic Cracking. *Appl. Catal. A*, **223**, pp. 103.

Fernandes, J.L., Pinheiro, C.I.C., Oliveira, N. and Bibeiro, F.R. (2003). Modeling and Simulation of an Operating Industrial Fluidized Catalytic Cracking (FCC) Riser. In: Proceedings of the 4th Mercosur Congress on Process Systems Engineering, Coasta Verde, Brazil.

Geankoplis, C.J. (2011). *Transport Processes and Separation Process Principles.* 4th ed., New Jersey: Pearson Education, Inc. pp. 425, 482.

Gupta, R.S. (2006). Modeling and Simulation of Fluid Catalytic Cracking Unit. *PhD Thesis*, Thapar Institute of Engineering and Technology, India.

Heydari, M., Ebrahim, H.A. and Dabir, B. (2010). Modeling of an Industrial Riser in the Fluid Catalytic Cracking Unit. *American Journal of Applied Sciences,* 7 (2), pp. 221-226.

Lopes, G.C., Rosa, L.M., Mori, M., Nunhez, J.R. and Martignoni, W.P. (2012). CFD Study of Industrial FCC Risers: The Effect of Outlet Configurations on Hydrodynamics and Reactions. *International Journal of Chemical Engineering* 2012.

Missen, R.W., Mims, C.A. and Saville, B.A. (1999). *Introduction to Chemical Reaction Engineering and Kinetics*. New York: John Wiley & Sons, Inc. pp. 198-214.

Novia, N., Ray, M.S. and Pareek, V.K. (2006). Unsteady State Simulation of Eulerian-Eulerian Multiphase flow in FCC Riser Reactors. In: Proceedings of the 5th International Conference on CFD in Process Industries, CSIRO, Melbourne, Australia.

Souza, J.A., Vargas, J.V.C., Von Meien, O.F. and Martignoni, W.P. (2007). Modeling and Simulation of Industrial FCC Risers. *Thermal Engineering,* 6(1), pp. 21-24.

P 022

REFINEMENT AND CHARACTERIZATION OF NIGERIAN AHOKO KAOLIN
[1]*A.S. Kovo, [2]M.O. Edoga, [3]Solomon Olu, [4]Mohammed Tatabu, [5]A.S. Abdulkareem, [6]Ahmed A.F

[1,3,4,5]**Department of Chemical Engineering Federal University of Technology, Minna, Nigeria.**
[2]**Department of Chemical engineering, Federal University, Ndufi, Ebonyi State, Nigeria**
[6] **Department of Environmental Management , Bayero University Kano**

*kovo@futminna.edu.ng, kovoabdulsalami@gmail.com

Abstract:

Kaolin has always being recognized as an important mineral with multiple applications in several chemical industries. This study presents the outcome of refinement of Ahoko Nigerian Kaolin to be used as a combined source of Si and Al during the synthesis of different type of Zeolites. The refined kaolin mineral was obtained by the extraction of the fine particle fraction using Stokes' law of free settling and leaving the non-clay mineral mostly quartz as a residue. The results from XRD, XRF,IR, NMR and SEM analysis of the refined kaolin show a well ordered, highly crystallized kaolinite clay with the Si/Al ratio of 1 as required for kaolin used in zeolite synthesis.

Keywords: *Nigerian Ahoko Kaolin (NAK), X-ray diffraction (XRD), X-ray Fluorescence (XRF), Refinement, Characterization, Nuclear Magnetic Resonance (NMR)*

1.0 Introduction

Kaolinite is the primary clay mineral material present in the kaolinite mineral group (Brigatti *et al* 2006). Kaolin is viewed industrially as a term that means clays which is composed mainly of minerals called kaolinite and are amenable to property variation making them useful in the production of series of industrial products (Murray, 1980). Kaolinite is a layered structure material with a general chemical composition of $Al_2Si_2O_5(OH)_4$ (Brindley and Brown, 1980). It can be viewed as a continuous two dimensional structure containing a silica tetrahedral sheet with central cation usually octahedral alumina which is linked to four shared oxygen atoms.

The position of Si, Al and O in the kaolinite structure is well documented but the location of the OH is in some doubt, however the bonding system of OH in the interlayer has been explained by Benco *et al.*(2001). Four different OH groups were identified and two are part of weak bond formation and the remainder do not participate in hydrogen-bonding. The surface of clay mineral generally can be thought to be hydrophobic however in kaolinite, the presence of hydroxyl group and defect sites at the surface introduce hydrophilicity. The defects present can easily be detected with the aid of an X-ray diffraction (XRD). The patterns of ordered kaolin are sharp and narrow in their peaks while disordered show broad and asymmetries peaks (Bergaya and Lagaly, 2006).

Impurities such as quartz, feldspar, and iron are usually found with clay minerals but because they do not exhibit plasticity, they are called non clay or accessory minerals (Bergaya and Lagaly, 2006). . This associated mineral requires removal or reduction because it generally reduces the commercial value of the clay mineral hence purification is very important before usage. However two tests are normally performed to identify the degree of order in a kaolin sample namely Hinckley index range and Weiss index (Bergaya and Lagaly, 2006). Kaolin obtained naturally is usually fractionated to enrich the kaolinite content and reduce other unwanted clay mineral before application in manufacturing materials such as Zeolites synthesis or as a filler in paper production(Chipera Bish 2001, Muller, 1977, Elton *et al* 1994). The most common and simplest method of enriching the kaolin content of raw kaolin sample is fractionation by sedimentation (Bergaya and Lagaly, 2006). The refining process of kaolin is divided into two groups namely removal of foreign material by chemical method and refinement by sedimentation to remove larger impurities especially quartz which is trapped within the mineral aggregates. However addition of chemicals in the treatment process can impair the properties of the parent material, therefore, the use of chemical treatment should be a last resort (Chipera Bish 2001). Even though there are several other methods such as selective flocculation, flotation, delamination, ultrasonic treatment that can be used to process raw kaolin, fractionation by sedimentation is the most common procedure used for kaolin processing to obtain highly pure kaolin at laboratory level (Chipera Bish 2001, Duane and Robert 1997). Sedimentation is based on the principle that a particle with different mass and density will settle at different terminal velocity in a given viscous media (Pabst *et al* 1999). Stokes' law enables the separation based on the clay particle size which is assumed to have a spherical shape (Bergaya and Lagaly, 2006). The largest usage of kaolin is in the paper industry where it is utilized as a filler and coating agent. Other uses of kaolin include additive in the production of paint, processing into catalyst by activation and Production of ceramics, sanitary ware,

electrical porcelain etc there is also growing interest in the use of kaolin as a combined source of silica and alumina (Xu *et al* 2007) for zeolite synthesis. Hence there is the urgent need to develop processes for refinement of raw kaolin deposit.

2. Materials and Methods

NAK representative samples were taken from Ahoko, Kogi State, Nigeria. Initial analyses of the raw sample were carried out with the aid of X-ray diffraction (XRD), Infra-red spectroscopy (IR), Scanning electron microscope/transmission electron microscope SEM/TEM, X-ray fluorescence (XRF), and N_2 Adsorption. This was done to know the constituent mineral and determine the impurities present.WBB, a clay processing company in the UK was obtained and was used as a reference kaolin.

2.1 Refining of Raw NAK

The XRD and XRF analysis along with the other tests of the raw NAK showed that much of the non-clay fraction was quartz. This requires refining, as quartz and many other non-clay minerals can impede the application of kaolin in many industrial processes. Size separation based on differences in particle size and density, as typified by Stokes law of settling particles in solution, is adopted for the purification process. The solution to the well known stokes model was simulated using called Atterberg or Sedigraph (http://sedicalc.sourceforge.net).

The experiment involves the disaggregation of the solid rock in a tumbler and was used to obtain a good sample of kaolin slurry using deionised water. Size separation was achieved by allowing free settling of clay suspension in 24 measuring cylinders of 30 cm height used as settling tubes. A clay suspension was created from a mixture of clay (2 cm) and deionised water (28 ml) and the settling time of the heavier component (quartz) was determined from the Atterberg software based on expected particle sizes of 10, 4 and 2 µm as shown in Table 1.

Table 1: Settling time calculation

Grain Size µm	Days	Hours	minute	Seconds
63	0	0	1	24
40	0	0	3	29
20	0	0	13	57
10	0	0	55	49
6	0	2	35	5
4	0	5	48	57
2	0	23	15	48
1	3	21	3	14
0.6	10	18	28	59
0.4	24	5	35	13
0.2	96	22	20	54

This was based on the density of quartz, temperature of the surrounding environment and the height of the settling tube. At the end of the settling time, the heavier (coarse) component naturally settled and the kaolin sample (lighter fraction) remains as supernatant. The supernatant was decanted into a different measuring cylinder and was allowed to settle for 24 h. A settled clay sample, (the fine fraction, <2 µm) was obtained after decanting the suspended deionised water. This process was repeated in order to obtain enough samples for analysis. The settled fine clay were dried using an Edward freezer dryer for 24 h and then characterized by XRD, XRF, SEM, nuclear magnetic resonance (NMR), IR, N_2 adsorption and mercury porosimetry.WBB kaolin was sourced from UK and served as standard kaolin for comparison with refined NAK.

3.0 Results and Discussion

In order to identify the NAK and verify the existence of impurities, the XRD pattern obtained was compared with WBB kaolin UK which served as reference kaolin.

The XRD pattern of the raw NAK sample figure 1 shows several peaks due to the mineral present in the material. An analysis of the peaks indicate a sharp peak with low intensity at $2\theta = 12.335^o$ (d = 7.15Å). This is the main peak used in the identification of kaolin (Ramaswamy , 2007, Lori *et al* 2007) , Further analysis of the sample by XRD indicates the presence of large quantities of quartz existing at peak position corresponding to $2\theta = 26.37^o$.

Natural kaolin deposit are predominantly an association of kaolinite and quartz (Eva *et al* 2001) and as such the high concentration of quartz in NAK is not unexpected. Other impurities found with kaolin include hydrated mica, and non-crystalline hydroxide of iron. The level of each impurity in individual kaolinite deposit depends on location and geology of the deposit.

However the industrial application of kaolin especially for the synthesis of Zeolites requires that the quartz content be reduce to minimum level.
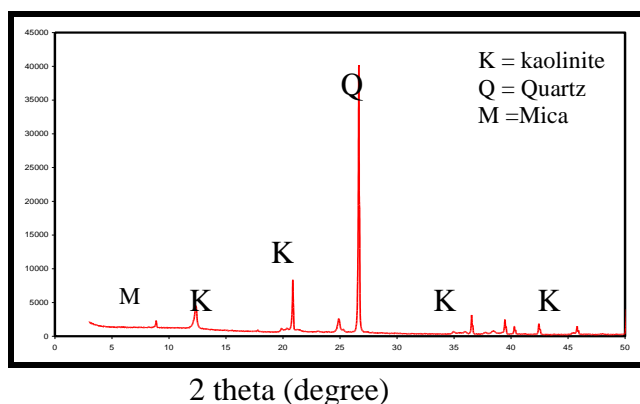
2 theta (degree)

Figure 1: XRD pattern of raw ANK

The XRF shows the chemical composition of the sample (Table 2) and it indicates a high percentage of SiO_2 (with 1-2% margin of error). The high silica content as reflected in the XRF analysis is a clear evidence of the high content of quartz present in the sample. This analysis corroborates the XRD result.

Table 2: XRF analysis of the as-shipped NAK sample

Chemical constituent	Weight %
SiO_2	72.455
Al_2O_3	18.963
Na_2O	0.021
K_2O	0.431
Fe_2O_3	1.0471
MgO	0.132
LOI[a]	6.170

[a] Loss on Ignition

Further analysis by IR (DRIFT) was performed in this work to complement the XRD analysis in the identification and structural analysis of NAK. The bands due to structural OH and Si-O group in the kaolinite mineral are used for the identification. The diffuse reflectance spectra of raw NAK (figure 2) shows a peak at 3618.6 cm^{-1} which has been assigned to inner hydroxyl group, the peak at 3667.2cm^{-1} has also been assigned to out-of-plane stretching vibration of the –OH group. The bands at 1010.8, and 1033.6 cm^{-1} belong to Si-O stretching while the bands at 470.8 cm^{-1} and 434.1 cm^{-1} are all assigned to the deformation vibration of Si-O in the kaolinite structure. The assignment of the key

peaks indicates that the raw sample is kaolin rich but it was difficult to identify the impurities present using the IR.
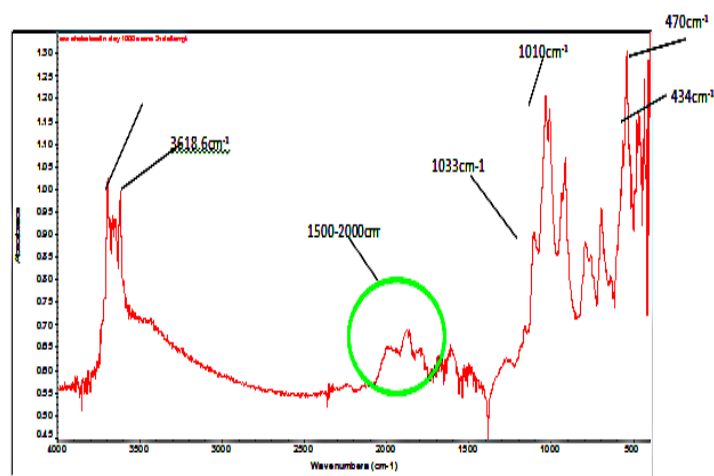
Figure 2: IR spectra of raw NAK sample

The SEM and transmission electron micrscropeTEM were also used to further elucidate the morphology of the raw ANK sample and identify the associated mineral as well. The results are shown in figure 3 and 4. The SEM and TEM images of the sample revealed the existence of kaolinite minerals in association with quartz.
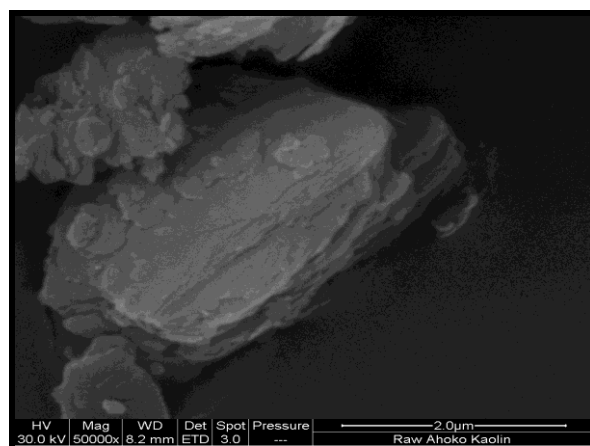
Figure 3: SEM image of the raw NAK sample
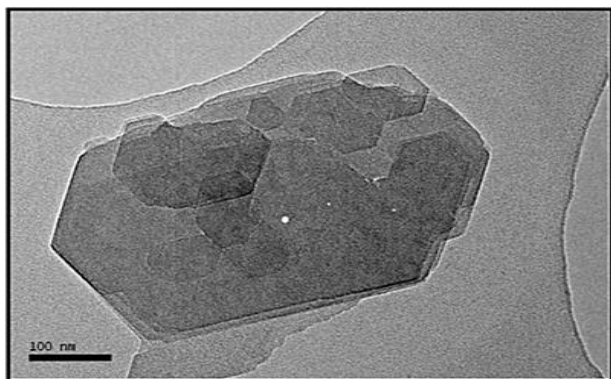
Figure 4: TEM image of raw NAK sample

The SEM and TEM images shows a well crystallized kaolinite particle with a typical pseudo-hexagonal platelet shape as reported for other kaolinite in the literature (Nakagawa et al 2006, Rue et al 1974, Frost *et al 2002*)However the angular orientation of the SEM images depicts the consolidation of quartz with the clay mineral (Nakagawa *et al* 2006). Therefore just like most other naturally occurring minerals, NAK requires purification or enrichment before it can be used especially in the synthesis of Zeolites.

The presence of quartz is not desirable in kaolin (Velho and Gomes, 1991) because it is difficult to dissolve hence it is necessary to eliminate or reduce the amount of quartz before the kaolin is used in the synthesis of Zeolites. A further look at table 2 indicates a low concentration of alumina (18 wt %) in the raw sample, which is in contrast with the theoretical concentration of alumina in kaolin. Generally zeolite synthesis requires a substantial amount of alumina in the kaolin which is within limit provided for kaolin used for zeolite synthesis (Marcelo *et al*, 2007). The combination of a high concentration of quartz and low amount of alumina present in the raw kaolin make enrichment necessary.

There are several techniques used in the purification of crude kaolin and each of the method has its advantages and weak points. The most important factor considered in the choice of purification is the effect of the processing on the microstructure of the kaolinite mineral.

Some of the well known techniques usually used to refine kaolin are selective flocculation (Luz, 2004), high gradient magnetic separation (Ohara *et al* 2001, Yan *et al*, 1994, Yan *et al* 1989), flotation purification (Gorken *et al* 2005) and particle size separation by sedimentation (Michaels and Bolger, 1962, Vie *et al*, 2007, Lau and Krishnappan, 1992, Shimoiizaka *et al* 1962).

The first three methods mentioned have major advantage over the particle size separation by sedimentation mainly because the processes are faster but the techniques are

more expensive and influence the chemical and microstructure of the kaolin sample. The choice of sedimentation technique as a purification procedure is clear. It is cheaper and offers little modification of the microstructure of the parent material especially when dispersant or deflocculant are not used. Particle size of kaolin is major parameter which determine the clay mineral from all the associated non-clay mineral (Bergaya and Lagaly, 2006) hence the particle size of the kaolin sample was deliberately chosen to obtained the purest form of the clay from combining with impurities. Usually there is standard upper or lower limit, but generally particle sizes are set between 1 to10 micron. The separation by particle size by sedimentation have unique advantage of not altering the properties and structure of kaolin even though the method is slow and require carefully control of the concentration of kaolin in the settling cylinder to avoid flocculation.

The settling time for >2 micron fraction (quartz) was determined using the Stokes' model to be 23 h 15 mins. The time of settling was determined using Atterberg software and was based on the density, height of settling tubes, and temperature of the medium. This means that the <2 µm kaolinite phase remained in suspension during settling and the quartz settled out (Duane and Robert 1997).

The analysis of the purified sample was performed using the same technique as the raw sample as well as nuclear magnetic resonance (NMR). The XRD pattern of the refined sample reveals a sharp and narrow peak with a basal reflection at $2\theta = 12.37^\circ$ (d= 7.15 Å). This is similar to the peak position in the raw sample. It is important to note that the peak positions in refined NAK compared well with those of WBB kaolin sourced from UK (figure 5 which was used as standard in this work.
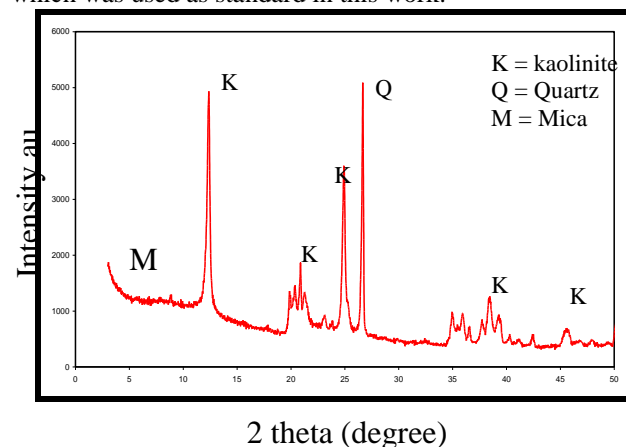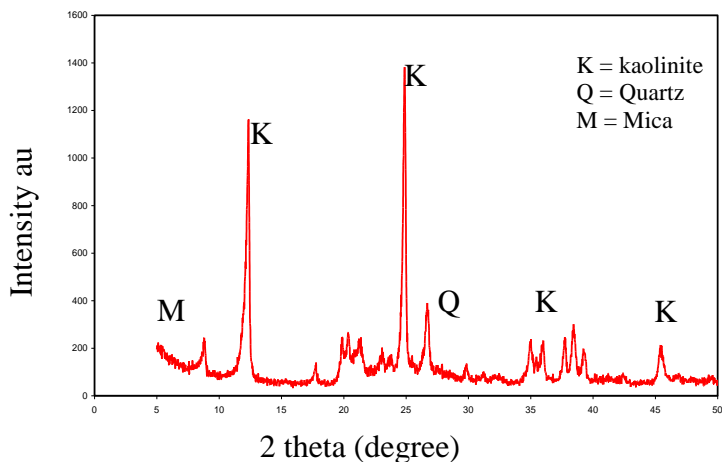

2 theta (degree)

Figure 5: XRD pattern of refined NAK

Figure 6: XRD pattern of WBB Kaolin UK used as a standard

Chemical constituent	Weight %
K_2O	0.537
Fe_2O_3	2.009
MgO	0.177
LOI^a	2.07

The result in table shows a significant reduction in the percentage composition of SiO_2 and corresponding increase in the percentage composition of Al_2O_3 for the refined NAK.

A high percentage of Al_2O_3 (> 30%) in the purified sample also indicates that Ahoko kaolin clay can be classified as kaolinite rich clay. Addition characterization technique using NMR to complement XRD was used to confirm the formation of purified kaolin as shown in figure 6 and 7. The ^{29}Si and ^{27}Al MAS NMR spectra of the refined NAK sample are similar to the NMR spectra of other standard kaolin thereby confirming NAK as a kaolinite mineral. The ^{29}Si NMR chemical shift of silicon tetrahedral is said to vary between -60ppm and -115ppm for the structure between Q^o and Q^4. A chemical shift of -91.07 ppm obtained for NAK is similar to Q^3 structure unit of aluminosilicate kaolinite. The Q^3 structure are associated with silica in association with hydroxyl group $(Si(OSi)_3OH$. Also the ^{27}Al Mas NMR spectra (figure 12) of NAK shows a single, sharp and broad asymmetric peak at -2.8 ppm which is a confirmation of a well crystallized kaolin (Temuujin *et al*, 2001) The NMR result therefore corroborates the XRD which indicate the formation of refined kaolin that is of high crystallinity.
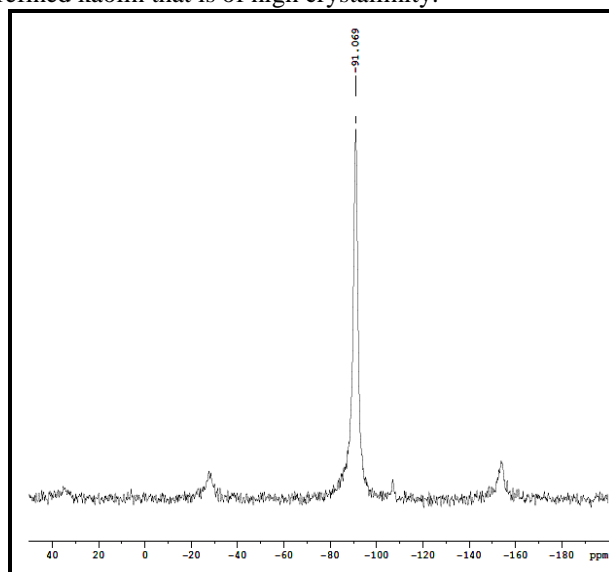
Quantitative analysis of the XRD pattern of the raw, refined NAK samples was also performed using Siroquant software to determine the level of quartz reduction during the refinement process (Table 3). The percentage of kaolin and quartz in the raw sample was determined to be 22.7 and 77.3% respectively, however the refining process resulted in the production of fine product with kaolinite concentration of 97.4% and 2.5 % quartz (with an error margin of 0.46%).

Table 3: Analysis of the kaolin samples by Siroquant software

Sample		Kaolin wt%	Quartz wt%
Raw kaolin	Ahoko	22.7	77.3
Refined kaolin	Ahoko	97.4	2.5
Standard kaolin	WBB	95.4	4.6

Further chemical analysis by XRF (table 4) corroborates the results obtained with the XRD analysis.

Table 4: XRF result of Refined NAK

Chemical constituent	Weight %
SiO_2	54.039
Al_2O_3	40.827
Na_2O	0.109

Figure 6: ^{29}Si NMR spectra of refined NAK kaolin
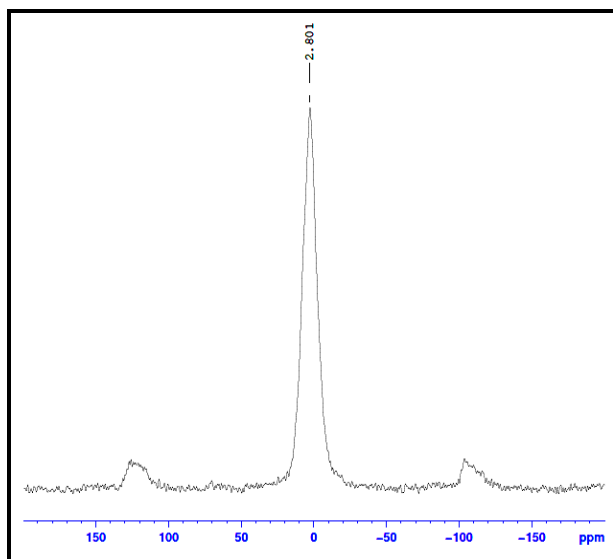
Figur

Figure 7: ^{27}Al NMR spectra of refined NAK kaolin

The surface morphology of both the refined samples was studied by SEM to further confirm the refinement that has taken place. The SEM images of the refined kaolin (figure 8) clearly reveal kaolinite particles with varying sizes. These come with a low aspect (crystal-width to thickness) ratio. Apart from the usual pseudo-hexagonal platelet which is still visible, rough edge are also observed in most of the particles, however the observed platelets show thinness of kaolinite flakes indicating finesse of the kaolin surface. The SEM also reveal highly ordered and crystalline particles.
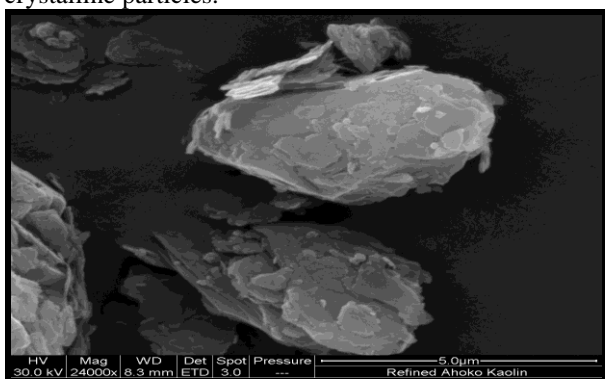
Figure 8 SEM image of refined NAK

It must also be stated again that other processes for kaolin separation methods would have given a higher percentage recovery, but the advantage of the chosen procedure ensure that no chemical is added as a dispersant and all the outcome of the analysis can only be attributed to kaolin as the chemical make-up of the parent material is not altered and the process is cost effective.

Other parameter such as porosity and surface area   of kaolin which is germane to its industrial application was also investigated using (ASAP 2001 micromeritic nitrogen adsorption and Pascal 140/240 system. mercury porosimetry. The result are shown in Table 4

Table 4: Summary of some physical properties of ANK

	Raw Ahoko kaolin	Refined Ahoko kaolin
BET surface area m^2/g	7.424	15.227
Porosity[a]%	3.144	28.818
Total pore volume cm^3/g	0.028	0.052

[a]the porosity values were obtained using the Pascal 140 mercury porosimetry system

The result obtained from both nitrogen adsorption and mercury porosimetry shows changes that took place in the BET surface area and porosity from the raw kaolin and the refined Ahoko kaolin during the refining process. The value obtained for most of the parameters e.g. surface area, and porosity compared well with similar kaolin reported in the literature (Shvarzmana *et al* 2003).

4.0 Conclusions

Simple sedimentation using Stoke's law of free settling clearly prove to be an efficient method of refinement of kaolin with high concentration of quartz as an impurities. The refinement of the raw NAK look like a simple process, however obtaining highly purified kaolin can only be possible if the right amount or concentration of the deionised water/raw kaolin sample mixture is chosen to the settling cylinder and this reduces the attractive forces causing the less dense kaolin particles to remain in suspension as a decantant. These careful controls prevent the use of deflocculant which could have led to chemical modification of the kaolin sample. The quartz content of the raw NAK was successfully reduced to less than 2% using this technique producing a well crystallized and highly ordered, porous kaolin sample with the right concentration of silica and alumina.

References

Bergaya F and G. Lagaly, *Handbook of Clay science* ed. F. Bergaya, B.K.G. Theng, and G. Lagaly. 2006.

Benco, L, D.T., J. Hafner,and H. Lischka, *Upper Limit of the O-H...O Hydrogen Bond. Ab Initio Study of*

the Kaolinite Structure. Journal of phys.Chem., 2001. **105**(44): p. 10812-10817.

Brigatti, M.F., E. Galan, and B.K.G. Theng, *Structure and MIneralogy of Clay Minerals* in *Handbook of Clay Science* 2006, Elservier Amsterdam. p. 1224.

Brindley, G.W. and G. Brown. *Crystal Structures of Clay Minerals and Their X-Ray Identification. Mineralogical Society, .* in *Mineralogical Society London*. 1980. London.

Chipera, S.J. and D.L. Bish, *Baseline Studies of the Clay Minerals Society Source Clays: Powder X-ray Diffraction Analysis* Clays and Clays Minerals 2001. **49**(5): p. 398-409.

Duane, M.M. and C.R. Robert, *X-ray Diffraction and the identification and analysis of Clay Minerals* second edition ed. 1997, Oxford Oxford University Press 378.

Elton, N.J., P.D. Salt, and J.M. Adams, *Determination of quartz in kaolins by x-ray powder diffractometry* Analytica Chimica Acta 1994. **286**: p. 37-47.

Eva Mako, R.L.F., Janos Kristof and Erzsebet Horvath *The effect of Quartz Content on the Mechanochemical Activation of Kaolinite* Journal of Colloid and Interface Science 2001. **244**: p. 359-364.

Frost,R.L.,Marek Zbik, J.T.Velho, , *Characterization of Portuguese kaolin for the paper industry: beneficiation through new delamination techniques* Applied Clay Science, 1991. **6**: p. 155-170.

Gorken, A., W. Perez, and S.A. Ravishankar. *Flotation purification of kaolin clay with hydroxamate collectors*. 2005. Brisbane, QLD, Australia: Australasian Institute of Mining and Metallurgy.

Lau, Y.L. and B.G. Krishnappan, *Size distribution and settling velocity of cohesive sediments during settling*. Journal of Hydraulic Research, 1992. **30**(5): p. 673-684.

Lori, J.A., A.O. Lawal, and E.J. Ekanem, *Characterization and Optimization of Deferration of Kankara Clay* ARPN Journal of Engineering and Applied Science 2007. **2**(5): p. 60-73.

Luz, A.B.D. *Purification of kaolin by selective flocculation* in *Particle Size Enlargement in Mineral Processing* 2004. Canada

Kloprogge, G.N. Paroz *Birdwood kaolinite: a highly ordered kaolinite that is difficult to intercalate an XRD, SEM and Raman spectroscopy study* Applied Clay Science, 2002. **20**: p. 177-187.

Marcelo L. Mignoni, D.I.P., Nadia R.C. Fernandes Machado, Sibele B.C. Pergher *Synthesis of mordenite using kaolin as Si and Al Source* Applied Clay Science, 2007: p. 6.

Michaels, A.S. and J.C. Bolger, *Settling rates and sediment volumes of flocculated kaolin suspensions.* Industrial and Engineering Chemistry -- Fundamentals, 1962. **1**(1): p. 24-33.

Murray, H., *Major Kaolin Processing Developments* International Journal of Mineral Processing, 1980. **7**: p. 263-274.

Muller, L.D., *Laboratory Methods of Mineral Separation* in *Physical Method in Determinative Mineralogy* J. Zussman, Editor. 1977, Academic Press London p. 34.

Nakagawa,M., M.S., S. Yoshikura, M. Miura, T. Fukuda, A. Harada, *Kaolin deposit at Melthonnakkal and Pallipuram within Trivandrum block southern India* Gondwana Research 2006. **9**: p. 530-538.

Pabst, W. K.K., J. Havrda, E. Gregorova *A note on particle size analyses of kaolin and clays* Journal of European Ceramic Society 1999. **20**: p. 1429-1437.
http://sedicalc.sourceforge.net. [cited 19/07/08].

Ramaswamy, S.C.a.S., *Investigation of a gray kaolin from south east India* Applied Clay Science, 2007. **37**: p. 32-46.

Rue, J.W. and W.R. OTT, *Scanning Electron Microscopic Interpretation of the Thermal Analysis of kaolinite* Journal of Thermal Analysis, 1974. **6**: p. 513-519.

Ohara, T., H. Kumakura, and H. Wada, *Magnetic separation using superconducting magnets.* Physica C: Superconductivity and its Applications, 2001. **357-360** (SUPPL. 1): p. 1272-1280.

Shimoiizaka, J., I. Matsuoka, and T. Sato, *Settling characteristics of suspensions of clay minerals.* Mining and Metallurgical Institute of Japan -- Journal, 1962. **78**(892): p. 739-743.

Temuujin, J., et al., *Characterization of porous silica prepared from mechanically amorphized kaolinite by selective leaching* Powder Technology, 2001. **121**: p. 259-262.

Vie, R., et al., *Study of suspension settling: A approach to determine suspension classification and particle interactions.* Colloids and Surfaces A: Physicochemical and Engineering Aspects, 2007. **298**(3): p. 192-200.

Xu, R., et al., *Chemistry of Zeolites and Related Porous Materials: Synthesis and Structure* 2007, Clementi loop Singapore John Wiley 679.

Yan, L.G., et al., *Laboratory test of an industrial superconducting magnetic separator for kaolin clay purification.* IEEE Transactions on Magnetics, 1994. **30**(4 pt 2): p. 2499-2502.

Yan, L.G., et al., *Laboratory superconducting high gradient magnetic separator.* IEEE Transactions on Magnetics, 1989. **25**(2)

Acknowledgment

P 023
KINETIC MODELLING OF COPPER (II) IONS BIOSORPTION ONTO DRIED LUFFA CYLINDRICA *SEEDS AND LEAVES MIXTURE FOR* SOME SELECTED BIOSORPTION FACTORS

[a]Oboh, I. O., [b]Aluyor, E. O. and [c]Okon E. E.
[a]Department of Chemıcal and Petroleum Engıneerıng, Unıversıty of Uyo, Uyo.
[b]Department of Chemıcal Engıneerıng, Unıversıty of Benın, Benın Cıty.
[c]Department of Chemıcal and Petrochemıcal Engıneerıng, Akwa Ibom State Unıversıty, Mkpaden.

Abstract

There is growing interest in using low cost materials for adsorption as alternatives to activated carbon. The biosorption of copper (II) ions onto Luffa cylindrica as sorbent was studied in this work. Luffa cylindrica was characterized by elemental analysis, surface area, pore size distribution, scanning electron microscopy, and Fourier Transform Infra Red (FTIR) spectrometer. Two factors for adsorption namely particle size and agitation speed were considered. The kinetic models fitted were Pseudo-first order, Pseudo-second order and Intra-particle diffusion. Four error functions, namely coefficient of determination (R^2), hybrid fractional error function (HYBRID), average relative error (ARE) and sum of the errors squared (ERRSQ), were used to predict the best kinetic models for Cu^{2+} ions biosorption onto Luffa cylindrica by varying the particle sizes and agitation speed. A coefficient of non-determination, K^2 was explained and was found to be very useful in identifying the best error function while selecting the best kinetic models. The results obtained showed that all the error functions studied were able to select the pseudo second order and the intra-particle diffusion models as the best kinetic models for particle sizes and agitation speeds for this work.

Keywords: coefficient of non-determination, error function, kinetic model, Luffa cylindrica, biosorption

Introduction

Environmental pollution due to the discharge of heavy metals from various industries, especially when tolerance levels are exceeded, is causing significant concern because of their toxicity and particularly, threat to human life (Gupta et al., 2009). The species with the most toxicological relevance found in the industrial effluents are the heavy metals of which copper and others are examples. These species are bio-accumulative and not biodegradable over time (Abdel-Ghani et al., 2009).

Over the last few decades, adsorption has gained importance as an effective purification and separation technique used in water and wastewater treatment. Adsorption is used extensively in industrial processes for many purposes of separation and purification. The removal of metals, coloured and colourless organic pollutants from industrial wastewater are considered an important application of adsorption processes using suitable adsorbents. The most frequently applied adsorbent for the removal of organic pollutants in wastewaters is currently activated carbon. However, activated carbon is an expensive material.

A wide variety of materials have been used in previous studies such as peat, lignite, diatomite, dolomite, bone char, zeolites, peanut hulls and a range of other natural materials (Richard, 2009). Natural materials that are available in large quantities are potential to be used as low cost adsorbents which are widely available and are environment friendly, as they represent unused resources (Goyal et al., 2008).

Copper metal contamination exists in aqueous waste streams from many industries such as electronic and electrical, metal plating, mining, manufacture of computer heat sinks, Copper plumbing, as well as biostatic surface, as a component in ceramic glazing and glass colouring (Tumin et al., 2008). Copper is regularly used in agricultural chemicals for mildew prevention, and as algicides in water treatment of industrial waters. It is also used as a preservative for wood, leather, and fabrics. Workers in, or those living near mines, smelters, metal fabrication and manufacturing plants,

wood treatment plants, phosphate fertilizer plants, and waste water plants may also experience excessive copper exposure (Jolley et al., 2003). Although copper homeostasis plays an important role in the prevention of copper toxicity, exposure to excessive levels of copper can result in a number of adverse health effects including liver and kidney damage, anemia, immunotoxicity, and developmental toxicity. Many of these effects are consistent with oxidative damage to membranes or macromolecules (ATSDR, 2015).

Luffa cylindrica is derived from the cucumber and marrow family and originates from America (Mazali and Alves, 2005). *Luffa* is diploid species with 26 chromosomes and a cross-pollinated crop (Bal et al., 2004). Loofa sponge is a lignocellulosic material composed mainly of cellulose, hemicelluloses and lignin (Rowell et al., 2002). The fibers are composed of 60% cellulose, 30% hemicelluloses and 10% lignin (Mazali and Alves, 2005). The fruits of *L. cylindrica* are smooth and cylindrical shaped (Mazali and Alves, 2005). This study shows the utility of these very low cost and environmentally friendly plant materials as biosorbents for the removal of divalent cations from aqueous solutions as the cellulose, hemicelluloses, pectin and lignin present in the cell wall are the most important sorption sites (Volesky, 2003). The structure of *Luffa cylindrica* for example, is cellulose based (Rowell et al., 2002; Mazali and Alves, 2005), and the surface of cellulose in contact with water is negatively charged. Copper compound used in this study will dissolve to give the cationic metal and this will undergo attraction on approaching the anionic *Luffa cylindrica* structure (Ho et al., 2002). On this basis, it is expected that the copper cation will have a strong sorption affinity for *Luffa cylindrica*.

The coefficient of non-determination is a much more useful measure of the linear or non-linear co-variation of two variables. It is very much useful to come any conclusion about the extent of the relationship between the transformed experimental data and the predicted kinetic models (Kumar et al., 2008).

The aim of this work is to study the error functions by coefficient of non-determination that could predict the best kinectic models under study for particle sizes and agitation speeds during the sorption of Cu^{2+} ion onto *Luffa cylindrica.*

Materials and Methods
Preparation of *Luffa cylindrica*

The seeds and sponges of *L. cylindrica* were gathered into a clean plastic bag. They were dried in the oven at $105^{o}C$ for 24 hours and afterwards ground with a grinding mill. The ground seeds and sponges were sieved and were of particle size 0.3 to 0.6mm. This was to allow for shorter diffusion path, resulting in a higher rate of biosorption (Adeyinka et al., 2007). The ground seed and sponge were mixed at a ratio of 1:1.

Preparation of aqueous solutions

Stock solution of Copper was prepared with distilled water and Copper (II) tetraoxosulphate (VI). All working solutions were obtained by diluting the stock solutions with distilled water. The pH of the solutions was adjusted to a pH of 5. The concentration of metal ion in solution was analyzed by Atomic Absorption Spectrophotometer (model 210 VGP). A duplicate was analyzed for every sample to track experimental error and show reproducibility of results (Marshall and Champagne, 1995).

Scanning Electron Microscope and Elemental analysis

The microstructures, composition, and morphology of *Luffa cylindrica,* the biosorbent material was analysed by means of scanning electron microscopy (SEM). A Philips scanning electron microscope (ESEM XL30) equipped with energy dispersive X-ray spectrometer (EDX) was used to analyse the various elemental composition found in the powders.

Fourier Transform Infra Red analysis

Fourier transform infrared spectroscopy (FTIR) of the adsorbent was done by using an FTIR spectrometer (Model FTIR 2000, Shimadzu, Kyoto, Japan). About 150 mg KBr disks containing approximately 2% of *Luffa cylindrica* sample was prepared shortly before recording the FTIR spectra in the range of 400 – 4000.0 cm^{-1} and with a resolution of 4 cm^{-1}. The resulting spectra were average of 30 scans.

Surface area

The surface area of the *Luffa cylindrica* sample was determined using Flowsorb 2300 manufactured by Micrometrics Instrument Corporation, USA. Krypton gas was used in conducting single-point surface area measurements. Liquid nitrogen was used in setting the adsorption of nitrogen gas by the samples. The *Luffa cylindrica* was degassed at 100°C for 30 minutes and were then cooled to liquid nitrogen temperature. The surface area of the sample under measurement was then read from the display-meter. The value of the surface area recorded was then converted to specific surface area (m^{2}/g) by dividing the reading on the display by the weight of the *Luffa cylindrica* sample.

Biosorption Experiment

The biosorption studies for evaluation of the *Luffa cylindrica* mixture for removal of the selected heavy metals from aqueous solutions was carried-out using the batch biosorption procedure (Brasil et al., 2006; Lima et al., 2007). For these experiments, fixed amount of adsorbents (1000 mg) were placed in a 250 ml conical flasks containing 50 ml of heavy metal solutions, which were agitated for a suitable time (5 to 120 mins) at 25 ^{0}C. Subsequently, in order to separate the adsorbents from the aqueous solutions, the flasks were centrifuged at 2400 rpm for 10 minutes. The final concentrations of the heavy metals remaining in the solution were determined by atomic absorption spectrophotometer (AAS). The amount of the metal ion sorbed and percentage of removal of metal ion by the biosorbent were calculated by applying the Equations (1) and (2), respectively:

$$q = \frac{(C_0 - C_f)}{m}.V$$

(1)

$$\% \text{ Removal} = \frac{(C_0 - C_f)}{C_0}.100$$

(2)

where q is the amount of metal ion sorbed by the biosorbent (mg/g); C_0 is the initial ion concentration put in contact with the biosorbent (mg/L), C_f is the final concentration (mg/L) after the batch biosorption procedure, V is the volume of aqueous solution (L) put in contact with the biosorbent and m is the mass (g) of biosorbent.

A trial and error was used for nonlinear regression using the solver add-in function, Microsoft Excel, Microsoft Corporation.

Kinetic studies

The kinetic equations, which are, pseudo first-order (Largegren, 1898), pseudo-second order (Ho and Mckay, 1999), and intra-particle diffusion model (Weber Jr. and Morris, 1963) are given in Table 1.

Table 1: Kinetic adsorption models

Kinetic model	Equation
Pseudo-first-order	$q_t = q_e . [1 - \exp(- k_p.t)]$
Pseudo-second-order	$\dfrac{t}{q_t} = \dfrac{1}{kq_e^2} + \dfrac{1}{q_e}t$
Intra-particle diffusion	$q_t = k_{id}\sqrt{t} + C$

Results and Discussion

Characterization of *Luffa cylindrica*

Table 2: Physical properties of the *Luffa cylindrica* biosorbent

Specific surface area - BET (m²/g)
0.28
Total Surface area (m²/g)

1.1895

Pore Diameter Range (µm)

1051.309204 to 0.003577

Bulk density (g /cm³)

Table 2 show the bulk density, surface area and pore diameter range for the biosorbent used for this study. The specific surface area using the BET method was 0.28m²/g and the pore diameter range was between 1051.309204 to 0.003577µm. The bulk density was 0.34g/cm³. As observed, the surface area for the seed and sponge mixture of *L. cylindrica* is relatively low, with pore diameter values in agreement with those found for typical mesoporous materials (Hamoudi and Kaliaguine, 2003).

Table 3: Elemental composition of the *Luffa cylindrica* biosorbent

Elements	Weight %t%	Atomic %t%
C	79.33	86.91
O	12.25	10.07
P	00.95	00.40
S	00.75	00.31
Cl	01.58	00.59
K	03.86	01.30
Ca	01.29	00.42

Table 3 gives the elemental composition of *Luffa cylindrica* that was analysed by means of scanning electron microscopy (SEM). The *Luffa cylindrica* sample showed a very high percentage of carbon followed by oxygen and the potassium.
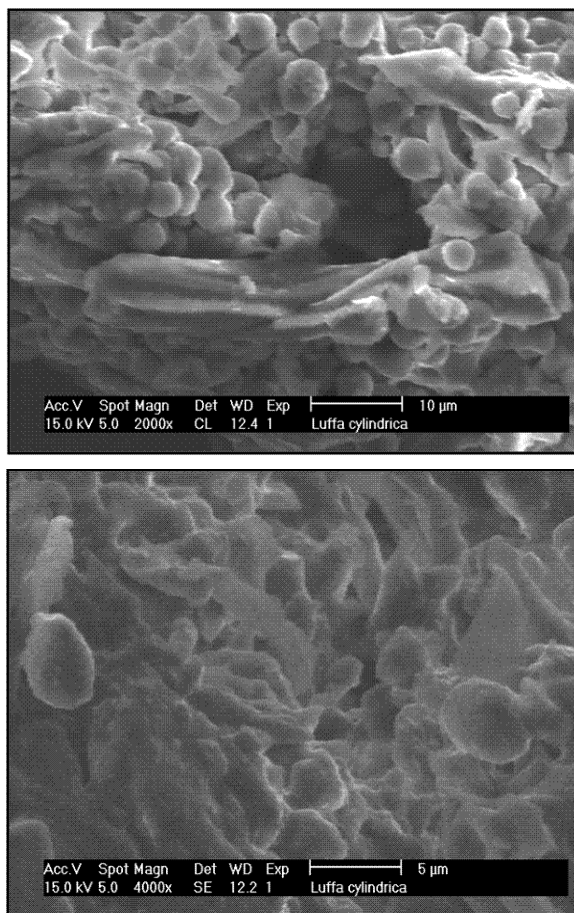
Figure 1: Scanning electron microscopy of *Luffa cylindrica* biosorbent: (A) transversal view of the mixture of seed and sponge 2000×; (B) transversal view of the mixture of seed and sponge 4000×;.

SEM of the *Luffa cylindrica* biosorbent was taken in order to verify the presence of macropores in the structure of the fiber. In the micrographs presented, Figure 1 (A and B) when observed showed the fibrous structure of *Luffa cylindrica*, with some fissures and holes, which indicated the presence of macroporous structure. These, should contribute a little bit to the diffusion of the Cu (II) to the *Luffa cylindrica* biosorbent surface (Passos et al., 2006; Vaghetti et al, 2003; Arenas et al., 2004; Passos et al., 2008). The small number of macroporous structure is confirmed by the low specific surface area of the biosorbent (see Table 1). As the biosorbent material presents few numbers of

macroporous structure, it adsorbed low amount of nitrogen, which led to a low BET surface area (Passos et al., 2006; Vaghetti et al, 2003; Arenas et al., 2004; Passos et al., 2008). Therefore the major contribution of the Cu (II) uptake can be attributed to micro- and mesoporous structures (see Figures 1 A and B)

A   **B**
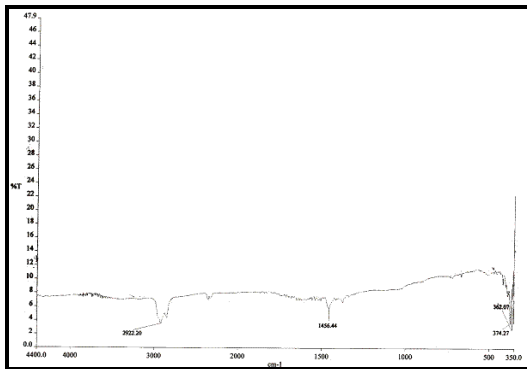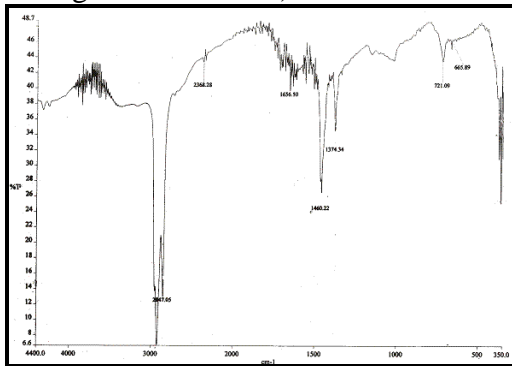
Figure 2: FTIR spectrum of the mixture of seed and sponge of *L. cylindrica* biosorbent- A before biosorption and B after biosorption.

Figures 2 (A and B) show the FTIR spectra for the mixture of seedand sponge of *L. cylindrica* biosorbent before and after. The functional groups on the binding sites were idbiosorptionentified by FTIR spectral comparison of the free biomass with a view to understanding the surface binding mechanisms. The significant bands obtained are shown in Figure 2 A and B. Functional groups found in the structure include carboxylic, alkynes or nitriles and amine groups (Pavia et al., 1996). The stretching vibrations of C-H stretch of -CHO

group shifted from 2847.05 to 2922.20, 2852.58, 2852.46 and 2852.43 cm^{-1} after Cu^{2+} ions biosorption. The assigned bands of the carboxylic, amine groups and alkynes or nitriles vibrations also shifted on biosorption. The shift in the frequency showed that there was biosorption of Cu^{2+} ions on the *L. cylindrica* biosorbent and the carboxylic and amine groups were involved in the sorption of the Cu^{2+} ions (Volesky, 2003).
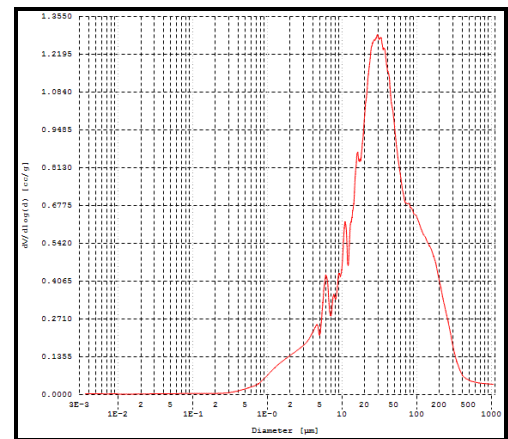
Figure 3: A plot showing the pore size distribution of the biosorbent - *L. cylindrica*

The pore size distribution of the *Luffa cylindrica* sample was obtained by Mercury intrusion method, and it is shown in Figure 3. The distribution of average pore diameter curve presents a maximum with an average pore diameter of about 30 µm. The amount of pores seen in the *Luffa cylindrica* biosorbent; decreases for average pore diameters ranging from 30 to 1000 µm. On the other hand, the amount of average pores ranging from 3 x 10^{-03} to 30 µm is predominant. Therefore, this biosorbent can be considered mixtures of micro- and mesoporous materials (Passos et al., 2006; Vaghetti et al, 2003; Arenas et al., 2004; Passos et al., 2008).

Table 4: Definition of different error functions (Kumar et al., 2008)

Error functions

The coefficient of determination

The sum of the squares of the errors (ERRSQ)

The hybrid error functions (HYBRID)

The average relative error (ARE)

Coefficient of Non determination of Various Error Functions for some Kinetic Models using varied Particle Sizes and Agitation Speeds

Coefficient of non-determination, K^2 was used to check which error function minimizes the error distribution between the experimental and theoretical kinetic models. The coefficient of non-determination, K^2 was defined as:

$$K^2 = \frac{\text{Unexplained variance}}{\text{Total variance}} \qquad (3)$$

The coefficient of non-determination is a much more useful measure of the linear or non-linear co-variation of two variables. The K^2 will be very much useful to come to any conclusion about the extent of the relationship between the transformed experimental data and the predicted kinetic models (Kumar et al., 2008).
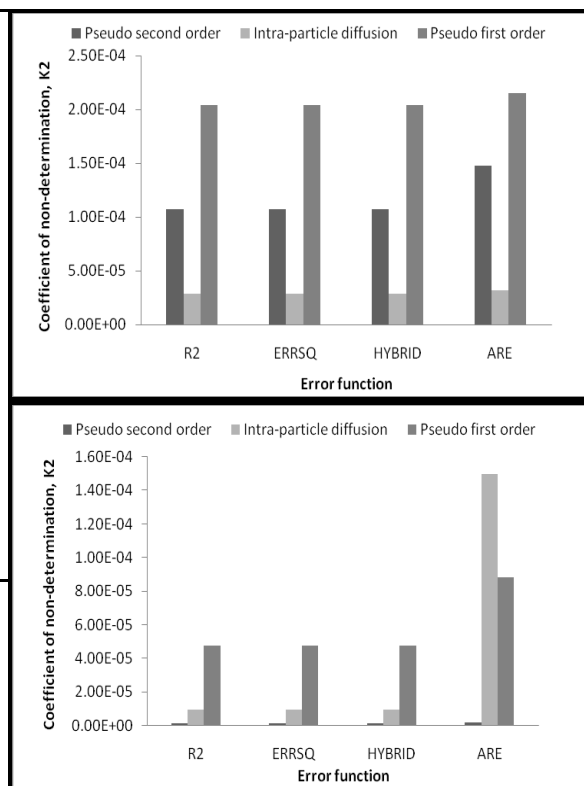
(A)

(B)
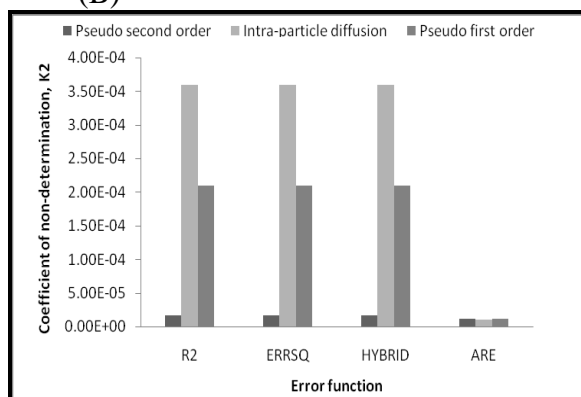
(C)

Figure 4: Coefficient of non-determination for some kinetic models of Cu (II) ions onto *Luffa cylindrica* seeds and sponge mixture at: (A) X100, (B) X200 and (C) X 300.

Figure 4(A–C) show the calculated K^2 values for the kinetic models predicted by minimizing or maximizing the various error functions at X100, X200 and X300 agitation speeds, respectively. From Figure 4A, it was observed that R^2, ERRSQ, ARE and HYBRID functions least
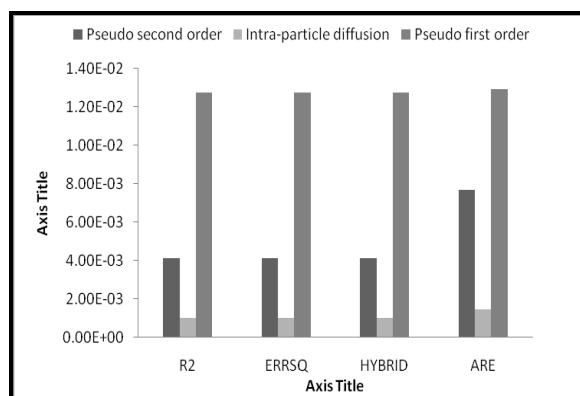
244

unexplained the Intra particle diffusion model suggesting these functions as the best functions to minimize the error distribution between the experimental and predicted Intra particle diffusion model for the biosorption of copper (II) ions. But this was not the case for Figures 4B and 4C where it was observed that the functions R^2, ERRSQ, ARE and HYBRID least unexplained the Pseudo-second order model suggesting these error functions as the best functions to minimize the error distribution between the experimental and predicted Pseudo-second order model for the biosorption of copper (II) ions. In Figure 4c the ARE error function did not least unexplain any kinetic model.
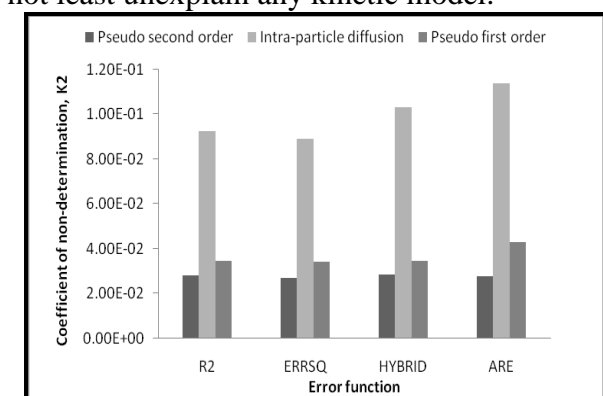
(A)
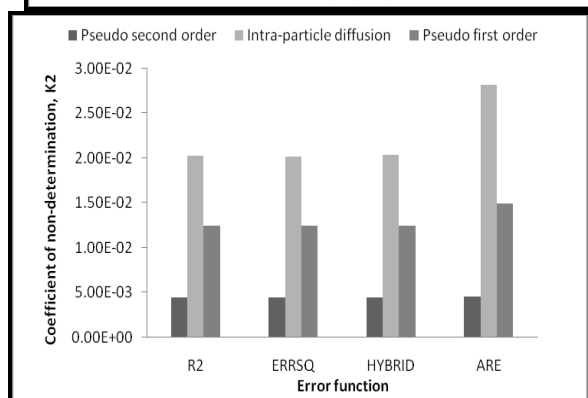
(B)

(C)

Figure 5: Coefficient of non-determination for some kinetic models of Cu (II) ions onto *Luffa cylindrica* seeds and sponge mixture at: (a) 300µm, (b) 425µm and (c) 600µm.

Figures 5 (A–C) show the calculated K^2 values for the kinetic models predicted by minimizing or maximizing the various error functions at 300µm, 425µm and 600µm particle sizes, respectively. From Figures 5A and 5B, it was observed that R^2, ERRSQ, ARE and HYBRID functions least unexplained the Pseudo-second order model suggesting these functions as the best functions to minimize or maximize the error distribution between the experimental and predicted Pseudo-second order model for the biosorption of copper (II) ions onto *Luffa cylindria*. Figure 5C showed that the functions R^2, ERRSQ, ARE and HYBRID least unexplained the Intra particle diffusion models for the biosorption of copper (II) ions.

Conclusion

A kinetic study was carried out and the experimental data fitted into Pseudo-first order, Pseudo-second order and Intra-particle models. The present investigation suggests that the size of error function alone is not a deciding factor to select the best kinetic model. In addition to the size of coefficient of determination, the validation of the theory behind the kinetic model should be verified with the help of experimental data while selecting the best kinetic model. The coefficient of non-determination was found to be a useful statistical term in identifying the best

error function while selecting the best kinetic model. In thıs work ıt was observed that all the error functions studied were able to select the pseudo second order and the intra-particle diffusion kınetıc models as the best kinetic models for particle sizes and agitation speeds.

References

Abdel-Ghani, N.T., Ahmad K. H., El-Chaghaby, G.A. and Lima, E.C. (2009). Factorial experimental design for biosorption of iron and zinc using Typha domingensis phytomass. Desalination 249: 343–347.

Adeyinka A, Liang H, Tina G (2007). Removal of Metal Ion form Waste Water with Natural Waste. School of Engineering and Technology. 1-8(33): 4.

Arenas L.T., Vaghetti J.C.P., Moro C.C., Lima E.C., Benvenutti E.V., Costa T.M.H. (2004). Dabco/silica sol-gel hybrid material. The influence of the morphology on the $CdCl_2$ adsorption capacity. Mater Lett; 58: 895-898.

Bal K. J., Hari B. K. C., Radha K., Ghale G. M., Bhuwon R.S., Madhusudan P.U.(2004) Descriptors for Sponge Gourd [*Luffa cylindrica* (L.) Roem.], NARC, LIBIRD & IPGRI.

Basil JL, Ev RR, Milcharek CD, Martins LC, Pavan FA, dos Santos, Jr. AA, Dias SLP, Dupont J, Noreña CPZ, Lima EC (2006). Statistical Design of Experiments as a tool for optimizing the batch conditions to Cr(VI) biosorption on Araucaria angustifolia wastes. J Hazard Mater; 133: 143-153.

Goyal, P., Sharma, P., Srivastava, S, Srivastava, M. M.(2008). *Saraca indica* leaf powder for decontamination of Pb: removal, recovery, adsorbent characterization and equilibrium modeling, International Journal of Enviornmental Science and Technology, Vol. 5, No. 1, pp. 27-34.

Gupta, N., Prasad, M., Singhal, N. and Kumar, V. (2009). Modeling the Adsorption Kinetics of Divalent Metal Ions onto Pyrophyllite Using the Integral Method. *Ind. Eng. Chem. Res.*, 48 (4), 2125-2128.

Hamoudi, S and Kaliaguine,S. (2003). Sulfonic acid-functionalized periodic mesoporous organosilica. Micropor. Mater. 59, p. 195-204.

Ho, Y.S., Mckay, G.M. (1999).Pseudo-second order model for sorption process, Proc Biochem. 34: 451–465.

Ho, Y.S. Porter, J.F. McKay, G. (2002). Equilibrium isotherm studies for the sorption of divalent metal ions onto peat: copper, nickel and lead single component systems, Water Air Soil Pollution, 141, 1–31. http://www.atsdr.cdc.gov/toxprofiles/tp132-c2.pdf. Toxicological Profile for copper. Assessed September 28th. 2015

Jolley, O.D., O'Brien, G. and Morrison, J. (2003).Evolution of Chemical Contaminant and Toxicology Studies, Part 1 - An Overview, South Pacific Journal of Natural Science, Vol 21, 1-5.

Kumar, K.V., Porkodi, K., Rocha, F. (2008).Isotherms and thermodynamics by linear and non-linear regression analysis for the sorption of methylene blue onto activated carbon: Comparison of various error functions. Journal of Hazardous Materials. 151, 794–804.

Largegren, S.(1898) About the theory of so-called adsorption of soluble substances, Kungliga Suensk Vetenskapsakademiens Handlingar 241: 1–39.

Lima, E. C., Royer, B., Vaghetti, J.C.P., Brasil, J.L., Simon, N.M., dos Santos Jr., A.A., Pavan, F.A., Dias, S.L.P., Benvenutti, E.V. and da Silva, E.A. (2007). Adsorption of Cu(II) on *Araucaria angustifolia*wastes: determination of the optimal conditions by statistic designof experiments, J. Hazard. Mater. 140, 211–220.

Marshall, W. E. and Champagne, T.E. (1995). Agricultural Byproducts as Adsorbents for Metal ions in Laboratory Prepared Solutions

and in Manufacturing Wastewater, Journal of Environmental Science and Health, Part A: Environmental Science and Engineering. Vol. 30, No. 2, 241 – 261.

Mazali I.O. Alves O.L. (2005). Morphosynthesis: high fidelity inorganic replica of the fibrous network of loofa sponge (*Luffa cylindrica*). Anais da Academia Brasileira de Ciências, Vol. 77, No. 1, p. 25-31.

Passos, C.G. Lima, E.C. Arenas, L.T. Simon, N.M. da Cunha, B.M. Brasil, J.L.Costa, T.M.H. Benvenutti, E.V. (2008). Use of 7-amine-4-azahepthylsilica and 10-amine-4-azadecylsilica xerogels as adsorbent for Pb(II). Kinetic and equilibrium study, Colloids Surfaces. A 316; 297–306.

Passos C.G., Ribaski F., Simon N.M., dos Santos Jr. A.A., Vaghetti J.C.P. (2006). Benvenutti EV, Lima, E. C. Use of statistical design of experiments to evaluate the sorption capacity of 7-amine-4-azahepthylsilica and 10-amine- 4-azadecylsilica for Cu(II), Pb(II) and Fe(III) adsorption. J Colloid Interface Sci; 302: 396-407.

Rowell R.M., James S.H., Jeffrey S.R. (2002). Characterization and factors effecting fibre properties, In Frollini E, Leao, AL, Mattoso LHC, (ed.), Natural polymers and agrofibres based composites. Embrapa Instrumentacao Agropecuaria, san Carlos, Brazil pp.115-134.

Tumin, N. D., Chuah, A. L., Zawani, Z., Abdul Rashid, S. (2008) .Adsorption of Copper from aqueous solution by *Elais guineensis* kernel activated carbon. Journal of Engineering Science and Technology Vol. 3, No. 2, 180 – 189.

Vaghetti J. C. P., Zat M., Bentes K.R.S., Ferreira L.S., Benvenutti E.V., Lima E.C. (2003). 4-Phenylenediaminepropylsilica xerogel as a sorbent for copper determination in waters by slurry-sampling ETAAS. J Anal Atom Spectrom; 18: 376-380.

Volesky, B. (2003) *Sorption and Biosorption*. Montreal-St. Lambert, Quebec, Canada, BV Sorbex Inc., 316 p. ISBN 0-9732983-0-8.

Weber Jr., W.J., Morris, J.C. (1963). Kinetics of adsorption on carbon from solution, J. Sanit. Eng. Div. Am. Soc. Civil Eng. 89: 31–59.

P 024

SYNTHESIS AND CHARACTERIZATION OF TRIMETHYLOLPROPANE-BASED BIOLUBRICANTS FROM CASTOR OIL

Musa, U., Mohammed I.A., Sadiq M.M., Aberuagba F., Olurinde A.O.and Obamina R

Department of Chemical Engineering, School of Engineering and Engineering Technology, Federal University of Technology, P.M.B. 65, Minna, Niger State.

Corresponding Author E-mail Address: umar.musa@futminna.edu.ng   Mobile no.: +234(0)8032318723

Abstract:

This paper presents the synthesis and characterization of Trimethylolpropane (TMP) based biolubricant from castor oil seed. Castor Oil Methyl Ester (COME) was synthesized at a temperature of 60 ^{o} C, reaction time of 1 hour, molar ratio of oil to methanol of 1:250 and 1 % wt/wt catalyst via (in situ transesterification) reactive extraction. The TMP ester (Biolubricant) from castor oil was further subsequently synthesized at a temperature of 120 ^{o} C, reaction time of 1 hour, molar ratio of COME to trimethylolpropane (TMP) of 4:1 and catalyst concentration of 0.8 wt%. The TMP ester of castor oil was characterized for its flash point, pour point, viscosity at 40 ^{o} C and at 100 ^{0} C and viscosity index. Fourier Transform Infra-Red (FT-IR) and Gas Chromatography-Mass Spectrophotometer (GC-MS) analysis were carried out on the Biolubricant to confirm the presence of ester group and the composition of the synthesized lubricant. The COME yield was 98.42wt% based on the weight of the oil seed. The transesterification of in situ derived COME with TMP yielded 96.56 wt% of the TMP ester (Biolubricant). The characterization of biolubricant shows favourable lubricating characteristics. The presence of ester group in the resulting biolubricant was confirmed by FT-IR analysis and the percentage of the composition of biolubricant determined by GC-MS analysis revealed a fatty acid composition of 2.88 %, monoester of 0.63 %, diester of 1.70 % and triester (desired end product) of 94.79 %. These FT-IR and GC-MS analysis result shows the effectiveness of the chemical modification of castor oil to biolubricant. The result of characterization of the biolubricant compares favourably with the ISO VG thereby establishing the potential of the biolubricant as gear oil.

Keywords: Biolubricant; in situ transesterification; Trimethylolpropane; Characterization; Methyl ester; Castor oil

1.0 Introduction

Lubricating oils have found wide varieties of application in automobile, refrigeration and compressor (Kamil and Yusup, 2010). A number of lubricant base oils such as petroleum or mineral oil, synthetic oil, re-refined and vegetable oil are used for the manufacturing of lubricating oil (Salimon and Salih, 2009). Synthetic lubricating oils characteristically have great lubricity when compared with petroleum based lubricants (Resul *et al.,* 2001). However, they are four to eight times more expensive than mineral oil based lubricants. Mineral oil based lubricants derived from petroleum are the ones in common use and they have a global market share of 95 % (Resul *et al.,* 2001; Amit and Amit, 2012).

Petroleum reserves are finite (Amit and Amit, 2012). Petroleum products are also very toxic and non biodegradable. Vegetable oil is another example of base oil that can be used for lubricant production. Its advantage over the latter base oil because it can be locally produced,

cheap, renewable and very biodegradable when compared to mineral oil. It has excellent lubricity, low volatility, non-toxic and high viscosity index (Kamil and Yusup, 2010; Salimon and Salih, 2009). The use of vegetable oil as a lubricant base oil has is limited because of low thermo-oxidative stability (Resul *et al.,* 2001), poor corrosion protection and hydrolytic stability (Kamil and Yusup, 2010). The presence of β hydrogen atom in the hydroxyl group of the glycerol is the major cause of low thermal and oxidation stability associated with pure vegetable oil (Resul *et al.,* 2001).

Research has shown that a number of chemical modification techniques such as epoxidation, selective hydrogenation and transesterification of vegetable oil can be used to overcome these limitations. Transesterification of vegetable oil have a more probable possibility for the production of lubricant with better temperature performance and appreciable fluidity (Resul *et al.,* 2001). This techniques help to effectively replace the hydrogen

atom on the β-carbon structure of the oil. This improvement brought about by change in the structure of the oil by conversion into a new ester called the polyol ester (PE). Common polyhydric alcohols used in the transesterification of fatty acids methyl ester are neopentyl glycol (NPG), pentaerythritol (PT) and trimethylolpropane (TMP). TMP is however the most popular alcohol for polyol ester synthesis because the resulting ester are characterized with superior lubricating properties. TMP is known for it high melting point and branched structure which are vital features for biolubricant synthesis (Kamil and Yusup, 2010). Numerous research have been documented on the synthesis of biolubricant from vegetable oil using TMP as a polyol (Kamil and Yusup, 2010; Resul *et al.,* 2001; Uosukainem *et al.,* 1998; Jose, 2011; Arbain and Salimon, 2011; Phani *et al.,* 2013; Mohammed *et al.,* 2011; Ghazi *et al.,* 2010). Nearly in all these studies reported conventional methods of transesterification were used for biodiesel synthesis. This involves various stages: oil extraction, purification and subsequent esterification /transesterification. These multiple biodiesel processing stages constitute greater than 70 % of the total biodiesel production cost if refined oil is used as feedstock (Ponsak *et al.,* 2012) Reactive extraction (*in situ* transesterification) permits the synthesis of biodiesel from oil bearing seed directly without prior extraction. This technique is characterized with the simplification of the biodiesel production technology (Zakaria and Harvey, 2012). The process allows essentially both extraction of oil from its seed and subsequent conversion to take place in a just one single step with the alcohol acting as a solvent for extraction and as a reagent for transesterification (Shuit *et al.*, 2010). Madankar *et al.* (2013) reported the *in situ* transesterification of castor oil seed and stated the methyl ester produced has appreciable potential for biolubricant production.

Castor plant also known as *Ricinus communis* L. belongs to the family *Eurphorbiaceae* and grows mostly in tropical and subtropical areas. Castor plants seed contain castor oil. The seed contains up to 55 % of the oil and can be up to 69 % when released from a peel. Castor seed contains highly poisonous protein (ricin) (ICOA, 2013). Castor oil is soluble in alcohol (Nurbakhit, 2012). Castor oil possesses greater density, viscosity, ethanol solubility and lubricity when compared with other vegetable oils. Castor oil has been used on the manufacturing of more than 800 products, ranging from bullet-proof glasses, contact lenses, lipsticks, metal soaps, special engine and high rotation reactors lubricants, high resistance plastics, and polyurethanes (ICOA, 2013; Nurbakhit, 2012). According to Bugaje and Mohammed (2008) castor plant is known to grow very well across the entire northern states of Nigeria as weed. The

authors are of the opinion that using edible oil for bio energy generation may lead to food crises and uneconomical.

The objective of work is to study the synthesis and characterization of trimethylolpropane ester (TMP ester) of castor oil. To the best of our knowledge this study is one of the very attempts to develop a biolubricant from a typical Nigerian Castor oil seed using an *in situ* transesterification (reactive extraction) for castor methyl ester production.

1. Methodology

1.1. Materials

The castor seed was obtained from a local farm in Minna, Nigeria. The moisture content of the seed was determined to be 4.67 %. The seed was ground to a small particle of 0.5 mm using mortar and pestle. Oil was
Extracted from the seed using sohxlet extractor and the oil content of the seed were determined. n- hexane and potassium hydroxide, methanol obtained from Sigma-Aldrich (St. Louis) and were of analytical grade

1.2. Transesterification of COME and analysis

The COME was initially synthesized according to methods reported by Madankar *et al.,* (2013) and Zakaria and Harvey (2012). The production of Castor oil Biolubricant (COB) was carried out according to the work of Arbian and Salimon (2011). The experimental was conducted in a two-necked round bottom flask equipped with a thermometer and mounted on a magnetic stirrer hot plate. The flask was fitted with Liebig condenser and 1 horse power vacuum pump. A known quantity (20 g) of COME was poured into the round bottom flask and preheated to 60°C, after which 2.3g of TMP and 0.016g of KOH catalyst were added then the temperature increased to 130°C. The molar ratio of methyl ester to TMP was kept at 4: 1; reaction time at 1 hour and catalyst concentration of 0.8 % wt/wt. After the reaction time was completed, the solution was transferred into a separating funnel and washed with warm water containing 0.6 g of ortho-phosphoric acid which corresponds to 10%wt/wt oil. The resulting TMP ester then was dried over a hot plate

Result and Discussion

The sample was analyzed using FT-IR and GC-MS and results tabulated as shown in Table 2 and Table 3. The physio-chemical properties were also determined and compared with other reported work as shown in Table 1

Table 1: Characterization of Biolubricant

Properties	Viscosity at 40°C	Viscosity at 100°C	Viscosity Index	Pour Point (^{o}C)	Flash Point (^{o}C)	Reference
This study	45.3	9.21	191	-8	215	
ISO VG 46	>41.4	>4.1	>90	-10		Bilal *et al.* (2013)
ISO VG 220	>12	>4.1	>50	-6	265	(Nandor *et al.*, 2012)
Mineral Oil based Lube	568	27.8	62	-4		Nandor *et al.*(2012)
Synthetic Lube	9.03	2.70	148	-	204	Nandor *et al.*(2012)
Fusel oil based Lube	6.30	2.28	207	-27	211	Nandor *et al.* (2012)
Canola oil based Lube	40.5	7.8	204	-66		Phani *et al.* (2013)
Jatropha oil based Lube	42.37	9.37	183	-3		Mohammed *et al.* (2011)

The yield of the oil extracted was obtained to be 55.2% based on weight of oil seed used while the optimum methyl ester yield was 98.42 % with a corresponding purity of 90.05 %.The percentage yield of COB was 96.56% at the optimum conditions; COME to TMP ratio of 4:1, temperature 120 ^{o} C, catalyst concentration 0.8 % w/w and reaction time of 60 minutes.

The viscosity of the castor oil based biolubricant was determined to be 45.3 and 9.21 Cst at 40 and 100 ^{o} C respectively as shown in Table 1. This result shows that there was a remarkable improvement in the viscosity of the castor oil methyl ester (11 cst) upon transesterification with TMP. The value obtained shows the biolubricant synthesized met the ISO viscosity grade requirement and consistent with some reported literatures (Nandor *et al.*, 2012; Bilal *et al*., 2013). The variations observed may be attributed to differences in the fatty acid profile of the base oil or the process conditions /catalytic modification techniques used. The finding depict that castor polyol ester (biolubricant) has potential application as a gear oil in automobile as its properties conform to ISO VG 46 and ISO VG 220 requirement for this type of lubricant. There are three standard specification for lubricants of which ISO Viscosity Grade (VG) 46 is one of them and it represents over 80 % of all lubricant consumed (Bilal *et al*., 2013).

Viscosity index (VI) shows the behaviour of the lubricant at different temperature. Castor base oil synthesized lubricant was observed to have a high VI of 191 as shown in Table 1. This exceptionally good VI value obtained was higher than reported values (Mohammed *et al.*, 2011) but lower than the value of Phani (2012). High VI permits lesser wear and lubricant consumption during application. Lubricants with higher VI (>130) find a wide variety of applications (Mohammed *et al.*, 2011). The value observed in this study fulfils the ISO VG 46 and ISO VG220 standard specification for light gear oil. The result indicate that the higher the VI, the less significant the viscosity variation of the synthesized castor base oil lubricant with temperature from ambient temperature when engine components are at rest to high operating temperatures. The quality of the biolubricant synthesized were of comparable standards with commercial lubricants.

Pour point is the property of biolubricant that determines its low temperature usability. The castor derived biolubricant has a pour point of -8 ^{o} C which is an appreciable improvement from - 4 ^{o} C for the COME reacted with the TMP. This improvement is one of the properties imparted on the COME upon reacting it with a branched polyol (TMP). Arbain and Salimon (2011) stated that higher degree of branching of esters leads to higher pour points which are desirable properties of a lubricant. From the result shown in Table 1, the pour point value recorded in this study shows close proximity to the ISO viscosity requirement. The reported value of pour point for the synthesized TMP ester shows its excellent low temperature usability/performance.

Flash point is the lowest temperature at which a lubricant gives off enough vapour to form an ignitable mixture with air. It is used as an assessment for the hazardous potential of a lubricant. The result of the analysis in Table 1 shows that the flash point of ester TMP produced was 215 °C. The high flash point indicates the safety of the resulting ester of TMP. The value also shows appreciable
.

consistency with the reported literature (Nandor *et al.*, 2012)

3.1 FT-IR Analysis

FTIR was used to determine the presence of ester group of TMP ester in the biolubricant produced
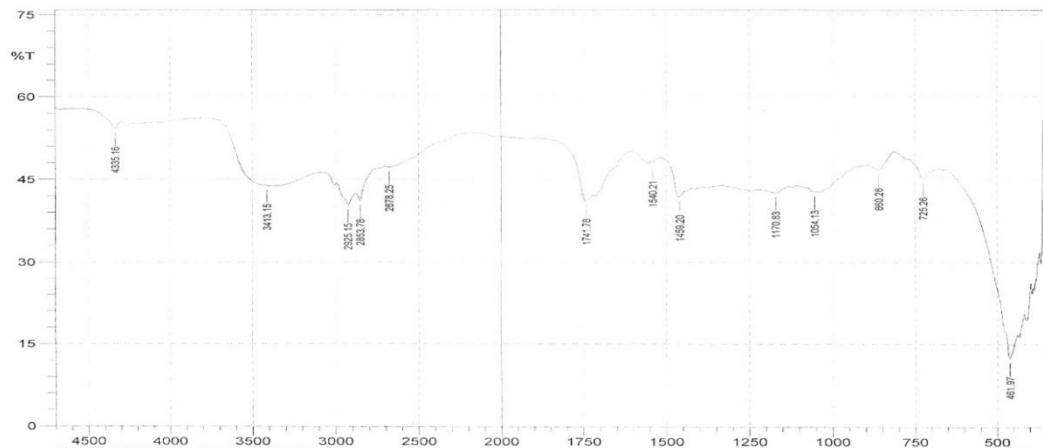
Figure 1.1: FT-IR Result for Castor Oil Biolubricant

Table 2: FT-IR composition of biolubricant

No. of Peaks	Peaks Position	Wave length (cm⁻¹)	Identification
1	461.97	477.40	Polysulfides (S-S Stretch)
2	725.26	770.59	Aromatic C-H
3	860.28	892.11	Vinylidene C-H
4	1054.13	1107.18	Aliphatic fluoro compounds (C-F Stretch)
5	1170.83	1219.05	Aromatic C-H
6	1459.20	1461.13	Carbonate ion
7	1540.21	1543.10	Carboxylate (carboxylic acid salt)
8	1741.78	1742.74	Ester
9	2678.25	2680.18	Aldehyde
10	2853.78	2881.75	Methyl C-H
12	3413.15	3430.51	Hydroxyl group

According to Coates (Coates, 2000) wavelength between 3300 cm⁻¹ - 3100 cm⁻¹ shows the presence of alcohol, the non-appearance of this wavelength in this result as shown in Table 2depicts the absence of alcohol. This is because the OH bond in TMP has effectively reacted with the fatty acid methyl ester to produce TMP ester. There was also an

observed shift in the wavelength of 1543.1 cm⁻¹ for the spectrum of carboxylic acid functional group to 1742.74 cm⁻¹ for the spectrum of TMP ester. This is quite related to the work of Arbain and Salimon (2011).

3. 2 Result of GC analysis

The summary of the fatty acid composition of castor oil biolubricant is shown in Table 3.

Table 3: Composition of castor oil biolubricant

Products	Percentage Composition (%)
Fatty acid	2.88
Monoester	0.63
Diester	1.70
Triester	94.79

The composition of fatty acid in the biolubricant produced was 2.88 % which is higher than that reported by Arbain and Salimon (2011). This may be due to difference in feed stock and variation in experimental conditions. However, the fatty acid consists mainly of ricinoleic acid

which has good lubricating properties and can however improve the properties of the biolubricant. The percentage of monoester (ME) is quite low (0.63) due to rapid reaction that takes place in the conversion of ME to diester (DE). However, the rate of conversion of DE to TE is lower compared to that of ME to DE, thus, the percentage of DE is higher (1.70) than that of ME. As the reaction proceeds DE is converted to Triester (TE) which is the desired product composition in biolubricant. Composition of TE was 94.79 % which is higher than that reported by Ghazi *et al.,* (2010) at 90 % composition of TE and lower than 98.1 % reported by Arbian and Salimon (2011).

Conclusion

This study showed that Castor oil has the potential for the production biodegradable lubricant using reactive extraction. The experimental result of biolubricant produced show that TMP ester exhibit favourable characteristic. FTIR analysis result shows the absence of OH group of TMP and presence of TMP ester. Complimentary GC-MS analysis result shows that high value of triester (94.79 %) was obtained after chemical modification depicting the effectiveness of the conversion process. The TMP esters of castor oil produced shows quantitative agreement with ISO viscosity grade requirement and establish its potential usage as light gear oil. The innovation in this manuscript is that it is one of the very first attempts to study the synthesis of TMP ester of castor oil employing in-situ transesterification for production of COME before subsequent conversion to biolubricant.

Acknowledgements

References

Amit K. J.and Amit S. (2012). Research Approach & Prospects of Non Edible Vegetable Oil as a Potential Resource for Biolubricant - A Review, *Advanced Engineering and Applied Sciences*: An International Journal, pp.23-32, available online at http://www.urpjournals.com

Arbain, N. H. and Salimon J. (2011);Synthesis and characterization of ester trimethylolpropane based *Jatropha curcas* oil as biolubricant base stocks, *Journal of Science and Technology*, 47-58.

Bilal S, Mohammed-Dabo I. A, Nuhu M, Kasim, S. A, Al-mustapha I. H & Yamusa Y. A (2013) Production of biolubricant from *Jatropha curcas* seed oil, *Journal of Chemical Engineering and Materials Science*, 4(6), pp. 72-79,

Bugaje I.M. & Mohammed, I.A (2008) *Biofuel Production Technology.* Science and Technology Forum (STF), 1st Edition, Zaria, Nigeria, pp 1-65.

Coates J. (2000). Interpretation of infrared spectra: A practical approach in encyclopedia of analytical Chemistry, R. A. Meyers (Ed.) John Wiley & Sons, Newtown, USA, 2000, 10815- 10837.

Dormo N., K. Belafi-Bako, L. Bartha, U. Ehrenstein, L. Gubiczaan (2004) Manufacture of an environmental-safe biolubricant from fusel oil by enzymatic esterification in solvent-free system, *Biochemical Engineering Journal,* 22, pp. 229–234

Ghazi, T. I. M., Gunam R. M. F., and Idris A (2010) Production of an improved bio based lubricant from *Jatropha curcas* as renewable source. In: Proceedings of the Third International symposium on Energy from Biomass and waste, Nov. 8-11, Venice, Italy,1-10.

Interntional Castor Oil Association (ICOA) Castor Oil Chemistry It's Derivatives and Their Applications: Technical Bulletin 2013.

José A. C. D (2011). *Biodegradable Lubricants and Their Production Via Chemical Catalysis*, Tribology - Lubricants and Lubrication, Dr. Chang-Hung Kuo (Ed.), InTech. Available from:http://www.intechopen.com/books/tribology-lubricants-and lubrication/biodegradablelubricants-and-their-production-via-chemical-catalysis, pp. 185-200.

Kamil R. N. and Yusup S.(2010). Modeling Kinetics for transesterification of palm- based methyl esters with trimethylolpropane, *Bioresource Technology* 101, pp. 5877-5884.

Madankar, C. S., Subhalaxmi, P., and Naik, S. N. (2013) Parametric study of reactive extraction of castor seed (*Ricinus communis L.*) for Methyl ester production and its potential use as biolubricant, *Industrial crops and Products,* 43, 2283 – 290.

Mohammed F. M. G. R., Ghazi, I. M. T., and Azni, I. (2011); Temperature dependence on the synthesis of *jatropha* biolubricant, In proceedings of IOP conference series: *Materials science and Engineering*, 17, 012032, doi:10.1088/1757-899X/17/1/012032.

Nándor N, Tamás B, Katalin Bélafi-Bakó, László B. and László G. (2012). Biotechnological utilization of fusel oil for biolubricant production, food Industrial Processes - Methods and Equipment, Dr. Benjamin Valdez (Ed.), InTech, Availablefrom:http://www.intechopen.com/books/food-industrial-processes-methods-and equipment/biotechnological-utilisation-of-fusel-oil-for-biolubricant-production.

Nurbakhit I. (2012). Preparation and research on properties of castor oil as a diesel fuel additive, *Applied Technologies & Innovations,* 6(1), Pp.30-37.

Phani S. K. (2013) Comparative tribological property evaluation of trimethylolpropane-based biolubricants derived from methyl oleate and canola biodiesel, *Industrial Crops and Products,* 50, 95– 103. 60.

Ponsak J., Chantaraporn P. and Anurak P. (2012), Single effects of reaction parameters in reactive extraction of palm fruit for biodiesel production, *Chiang Mai J. Sci.*; 40(3), pp 401-407.

Resul G, M. F. M., Mohd. Ghazi, T. I., Muhammad Syam, A., and Idris, A (2001) Synthesis of Biodegradable lubricant from *Jatropha* oil with high content of free fatty acids, Pp 1-6.

Salimon, J. and Salih, N., (2009). Oleic Acid Diesters: synthesis, characterization and low temperature properties, *European Journal of Scientific Research,* 32 (2), pp. 216 – 222.

Shuit, S. H., Lee K. T., Azlina, H. K., and Suzana, Y. (2010); Reactive extraction and *in-situ* esterification of *Jatropha curcas* L. seeds for the production of biodiesel, *Fuel,* 89, 527 – 530.

Uosukainem E., Linko, Y.Y., Lamsa, M., Tervakangas T and Linko P (1998). Trimethylolpropane and rapeseed oil methyl ester to environmentally acceptable lubricants, *Journal of the American Oil Chemist Society*, 75 (11), pp 1557-1563.

Zakaria, R and Harvey, A. P. (2012) Direct production of biodiesel from rapeseed by reactive extraction /*in-situ* trans-esterification, *Fuel processing technology*, 102, 53 –

P 025

EFFECT OF DEREGULATION OF THE OIL SECTOR IN THE DEVELOPMENT OF THE TRANSPORTATION INDUSTRY

[*1]*Offurum, J. C.;* [2]*Undiandeye J.A.;* [1]*Iheme C. S.;* [1]*Chukwu M.M.;* [1]*Nwaozuzu S.C.;*[1]*Mbadike, C.A.*
[1]*Department of Chemical Engineering, Imo State Polytechnic, Umuagwo-Ohaji*
[2]*Department of Chemical Engineering, University of Port-Harcourt, Rivers State*
jullyengine@yahoo.com**; **ihemechigozie2004@gmail.com**; **chuksmorgan@yahoo.com

Abstract:
The present study borders on the effect of government's deregulation policies of the oil sector on transportation. Historically, major petroleum marketers have been the lone suppliers of petroleum products within the territorial boundaries of the Nigerian nation. The companies transported and distributed the products, relying on their distribution networks, and without considering the impacts of this restriction on the major consumers of these products (especially the transportation industry). This has impacted negatively on the common man, who depends on these transporters for movement from one place to another, even though it could be source of higher revenue for the commuters. It, thus, poses a mixed reaction on whether deregulation of the oil sector is actually an advantage or a disadvantage to the transportation sector. Questionnaire method was employed in realizing the research objectives. A sample size of 50 was adopted and the Chi-Square (X^2) was used as the statistical tool to assess the research hypothesis at the degree of freedom of '2' (at 0.05 level of significance). The hypothetical test conducted favours the acceptance of H_1 (as against H_0), which indicates that deregulation of the oil sector is beneficial to the transportation industry.

Keywords: *Effect, Deregulation, Oil Sector, Development, Transportation Industry.*

1.0 INTRODUCTION

Petroleum products supplies have always been an 'analytical test' for successive governments in Nigerian. With the new democratic dispensation, the supply and distribution of petroleum products improved but this was without price stability for almost all the products in the sector (Ojo and Adebusuyi, 1996; Alugbuo, 2004). In this regard, one begins to wonder if there would be any solution to this problem. In different documentations, Adam (2001) and Ozumba (1996) agree that the contemporary passion and tension that usually characterize petroleum discourse is due to inexplicable deprivations and sufferings of Nigerians, amidst plenty and abundance of these products. According to their reports, as supply declines, prices of the products have been on the increase, and successive governments of the federation have continuously searched for the appropriate price schedule.

The combined impacts of inadequate supply and unending price increase have brought untold hardship to the citizenry. And worse still, it has prevented the successful recovery of the lost economic resources as promised by the present democratically elected government of the federation, given that capacity utilization in the manufacturing sector *nose-dives* due to shortages of industrial products. To this effect, many industries have been compelled to close due to non-availability of some of these products. This has, also been partially traced to the deregulation policies of the government.

Deregulation of the downstream sector refers to the reduction or removal of government control, rules and regulations that restrain free operational activities in the sector (Braide, 2003; Igbojekwe, 2002). It means that the roles of government in this sector will be limited mainly to providing regulatory oversight. Thus, the outcome of deregulation has not been encouraging all these years; there has been continuous increase in petroleum prices with persistent scarcity of petroleum products. But, it is expected that deregulation would give room for competition which would transform to price reduction and excellent supply and distribution of network. This study focuses on the effect of deregulation of oil of the Nigerian oil sector on transportation.

However, the present study is motivated by the fact that it will use a market structure performance/framework to analyze the industry, both before and after deregulations, as a means of judging the impact of deregulation in term of petroleum products prices. Also, this study would contribute to existing literature on the subject matter by providing expository analyses on the pattern of regular increases witnessed in prices of oil sector products in Nigeria. This would, eventually enhance policy formulation in the downstream sector with the intention of alleviating the sufferings of the masses.

2.0 MATERIALS AND METHOD

In the present study, questionnaire method was employed to collate opinions from various respondents; personal interviews were also conducted for some selected people. The research equally collated secondary data from works done by different authorities on the subject matter.

2.1 Research Hypothesis

The research hypothesis is usually a two-way statement that guides the researcher towards the realization of the

research goals. For the present study, the hypothesis is given as follows:

H_o: Deregulation of oil sector does not help in transportation industry.

H_1: Deregulation of oil sector helps in transportation industry.

2.2 Sampling Techniques

In order to remove all aspects of bias, probability sampling technique was adopted in administering questionnaires. To this effect, simple random sampling method was adopted during the distribution of the questionnaires.

2.3 Research Sample Size

This is a representation used for the study of a selected part of a given population (Anyanwu, 2000; Echeta and Ojiuko, 2011). Five (5) questionnaires were administered to each of ten (10) different departments in the oil sector, and these form the sample size of fifty (50).

2.4 Research Statistical Tool

To ensure that the present study maintains a scientific standard, chi-square (x^2) was used as a statistical tool in testing the stated hypothesis.

2.5 Method of Data Presentation

All data collated were presented using simple tables, as well as in percentages.

3.0 DATA PRESENTATION AND ANALYSIS

Question 1: Who benefit from the deregulation Of the oil sector?

Table 1:Results for Response to question 1

Response	No. of Respondent	Percentage
Poor	30	60%
Rich	20	40%
Total	50	100%

Question 2: How has the deregulation exercise Impacted on the consumption pattern of Petroleum product in Nigeria?

Table 2: Results for Response to question 2

Response	No. of Respondent	Percentage
Very Good	20	40%
Good	20	40%
Not Good	10	20%
Total	50	100%

Question 3: To what extent has the deregulation of the downstream sector impacted on pricing of petroleum products in Nigeria?

Table 3: Results for Response to question 3

Response	No. of Respondent	Percentage
Normal sells	20	40%
Low sells	10	20%
Booming sells	20	40%
Total	50	100%

Question 4: Why are we still witnessing petroleum products prices increases after deregulation of oil sector?

Table 4: Results for Response to question 4

Response	No. of Respondent	Percentage
Different price	50	100%
Normal prices	-	-
Total	50	100%

Question 5: Do you think that deregulation of soil sector helps in transport sector?

Table 5: Results for Response to question 5

Response	No. of Respondent	Percentage
Yes	20	40%
No	20	40%
Undecided	10	20%
Total	50	100%

4.0 RESULTS AND DISCUSSION

4.1 Data Calculations

$$\frac{Row\ Total - Column\ Total}{Expected\ Grand\ Total} = X2$$

$$C11 = \frac{20 \times 50}{100} = 10$$

So, X^2-calculated = **5.4**

Note:

The degree of freedom is obtained as follows:

$$(r-1)*(c-1) = (2-1)*(3-1) = 1X2 = 2$$

However,

2 = *0.05* level of significance

From the chi-square table, using **0.05** level of significance and the degree of freedom '**2**':

So, X^2-Table = **0.103**

The results obtained from data calculations indicate that there is discrepancy between the calculated Chi-square

(expected frequency) and the table Chi-square value *(observed frequency)*. As reported by Murray and Larry (1998), expected frequencies are usually computed on the basis of H_O (opposing) hypothesis, under which if the computed value is greater than that of the observed frequency, it could be concluded that both of them differ significantly from each other. And on this note, the H_O hypothesis is rejected.

4.2 Hypothetical Analysis

The results of the hypothetical analysis of the collated data at **0.05** level of significance (with degree of freedom '**2**' is presented in Table 6, using the Chi-Square relationship as stated in equation (1) below:

$$x^2 = \sum \frac{(Obs - Exp)^2}{Exp} \qquad (1)$$

From the results, it could be observed that there is Fifty Percent (50%) consent in favour of the proposing hypothesis, H_1. This agrees with the report of Adam (2001) and Montino (1996), which supports the deregulation of the downstream sector of the Petroleum Industry as a way of enhancing tourism development and making the business of commuters very dependable.

Table 6: RESULT OF HYPOTHETICAL TEST

Alternative	Yes	No	Undecided	total
Does not help	$20^{(10)}$	$20^{(10)}$	$10^{(5)}$	50
It helps	$30^{(15)}$	$10^{(5)}$	$10^{(5)}$	50
Total	**50**	**30**	**20**	**100%**

5.0 DECISION RULE

Accept H_1, if $X^2_{CALCULATED} > X^2_{TABLE}$
Otherwise, reject H_1 and accept H_0

5.1 Decision

From the available analytical data, it could be observed that $X^2_{CALCULATED} = 5.4$ is greater than $X^2_{TABLE} = 0.013$ This implies that H_0 is rejected, while H_1 is accepted, which state that: ***"Deregulation of oil sector helps in the transportation industry"***.

6.0 CONCLUSION

Deregulation of the downstream oil sector will improve the efficient use of scarce economic resources, by subjecting decisions in the sector to operations of the forces of Demand and Supply. This will attract new sellers, buyers and investors into the market, thereby increasing competition, promoting overall higher productivity and, consequently, lowering prices over time.

The ultimate effect of this chain of activities is increased gains for the people of Nigeria that would be getting much out of their natural resources. Finally, deregulation of the oil sector encourages more profit, as well as stable market structure; it encourages effective and affordable transportation, especially for tourists.

REFERENCES

Adam, G Aret (2001). *Deregulation of the downstream sector of the Petroleum industry*; Lagos-Nigeria: Post Express Newspaper; August 6.

Alugbuo, C.C. (2004). *Common Concerns of Managers*. Owerri: Achugo Prints.

Anyanwu A. (2000) . *Research Methodology in Business and Social Science.* Mbaise: Canun Publishers Nig. Ltd.

Braide, K.M. (2003). *Deregulation- an Executive Guide*; Nigeria: the Statesman; August 24.

Echeta, D.O. and Ojiuko, A.A. (2011). *Business, Social and Economic Research Methods*; Owerri: Mega Atlas Projects Ltd.

Igbojekwe D.C. (2014). *Effects of Deregulation Policies on Small-scale Businesses*; In: Proceedings of the 4th Annual Conference on Government Policies and Small-Scale Business, Nov 5-7, Owerri-Nigeria.

Montino, L. (1996) . *Tourism Marketing and Management Handbook*; Heemel: Hemstead Prentice Hall.

Murray R.S. and Larry J.S. (1998). *Schaum's Outlines of Theory and Problems of Statistics*, 3rd ed.; New York: McGraw-Hill Companies.

Ojo, M.O. and Adebusuyi, B.S. (1996): *The state of the Nigerian Petroleum Industry*; Owerri: Let-Bez and Co Publishers.

Ozumba, C.C. (1996): *Harnessing the Potential of the Nigeria Oil and Gas for Economic development*; Asaba: Canon Books Nig.

P 026

PRODUCTION AND BLENDING OF SODIUM BASED WATER-RESISTANT LUBRICATING GREASES FROM PETROLEUM AND PETROCHEMICAL BY–PRODUCTS

*Iheme Chigozie S.; *Offurum, Julius C.; Mbadike, C.A.; Nwaozuzu S.C.; Chukwu, M.M.*
Department of Chemical Engineering, Imo State Polytechnic, Umuagwo-Ohaji

jullyengine@yahoo.com; *ihemechigozie2004@gmail.com*; *chuksmorgan@yahoo.com*;

Abstract:
The need to reduce the cost and upgrade the quality of Sodium-based greases available in our local markets motivated the present study. This is realizable by using polypropylene, low-density polyethylene, base-oils, and vegetable oils from Nigerian industries (petroleum and petrochemical industries). The quality of sodium-based greases obtained in the Nigerian market need to be improved. Most of these lubricants contribute to the problems encountered in ball-bearings of heavy-duty equipment, rather than the protection they are meant to provide. Moreover, these products are very expensive, and in most cases, are imported from abroad. At the end, the grease produced from these by-products can compete effectively with the imported sodium and lithium base greases from abroad (USA) cost-wise. Measured quantities of polypropylene were melted separately in a measured quantity of base oil (500N and 650N/BS) by heating to a temperature of about 180^oC. Also sodium–base grease was prepared by a technology bounded by saponification, evaporation, melting of soap formed and blending with calculated quantity of base oil at the temperature ranging from 170^oC to 180^oC. Finally, the two products (melted polypropylene and sodium stearate in base oil) were blended at the temperature of about 100^oC. Quality control analysis was conducted on the product samples. The result obtained from the analysis showed that the product of the blends, when bright- stock and 500N base oils, were used for blending, falls within the American Society for Testing of Materials (ASTM) and National Lubricating Grease Institute (NLGI) standard specifications for ball- bearing grease No.2 and No.3 respectively. The added value to the conventional sodium–base grease was that, the product can resist water up to 80 to 85% or15%-20% water- washout, unlike the conventional sodium grease in the present Nigerian market that mixes readily with water. However, the product of this research is economical in terms of cost and availability of raw materials in Nigeria, when compared with imported grease like Abro–products.
Keywords: *Blending, Sodium base, Water-resistant, Lubricating Grease, Petrochemical.*

INTRODUCTION

Grease is a semisolid lubricant. It generally consists of soap, emulsified with mineral or vegetable oil (Richard, 2002). Greases are applied to mechanism that can only be lubricated infrequently, and where lubricating oil would not stay in position. They also act as sealant to prevent ingress of water and incompressible materials. Grease lubricated bearings have greater frictional characteristics due to their high viscosity (Cowan, 2007). American Society for Testing of Materials (ASTM D288 – 61, 1978) in petroleum terms defines lubricating greases as a "Solid-to-semi fluid" products of dispersion of thickening agent in a liquid lubricant. Grease is used in application where liquid lubricants cannot provide the required protection. It is easy to apply and requires little maintenance. The main properties of grease are that, it stays in place, provides sealing action, and provides extra film thickness.

Grease consists of three main components: thickener, base oil, and additives. Most grease is identified by their thickeners. The most widely used thickeners are: sodium-soap, calcium-soap, lithium-soap, poly-urea, Aluminum complex, polymer, etc. (Noria Corporation, 2009). The need to lubricate various machineries used in manufacturing, automotive engineering and transportation industries has made the provision of various lubricating greases inevitable for their satisfactory end or smooth running. The overall importance of lubricant is to ensure that economic and design life of equipment, machineries and plants are achieved with maximum cost through: maintenance of oil film between moving parts so as to minimize the frictional effect of metal-to-metal contact; removal of dirt from engine parts, thus keeping them clean and efficient; absorbing and dissipating excessive heat generation, thus effecting cooling; and lubricating almost every moving part in the mechanical equipment. The elements of a machine that require lubricants are those in relative motion viz: Gears, Bearings, Slides, Ways, Piston/Cylinders, Cams/Cam followers, Flexible couplings, Pulley/Wire ropes etc. Advanced polymer additives for greases provide superior water wash-off resistance in application that is exposed to high levels of direct or indirect water spray. Grease treated with **Lubrizol-2002** additive reduces the spray-off rate to 14%, in comparison with nearly 100% removal for untreated grease and 96% for competitive products used at comparative treating rates. This additive reacts with the soap thickener and becomes an integral part of the soap structure. Cost efficiency is improved when the thickening efficiency is improved by reducing the amount of soap required to formulate greases (Lubrizol, 2002). Thus, worked penetration rating, as

measured in ASTM D-217 test (in line with NLGI rating), can be achieved with lower soap levels.

However, this study shall focus on the production of sodium-based grease with about 80% water resistant or 20% water wash-off, which is not common in Nigerian auto parts market at the present, and can compete effectively with any other international sodium-based grease at various conditions.

MATERIALS AND METHODS

Grease production involves a batch process which incorporates a technology bounded by saponification, evaporation, melting of thickened soap in a mineral fluid (Base Oil), recycling/cut back, milling or homogenizing and filtration of dispersed thickener in a base oil; this is followed by addition of additives and modifiers to form grease (Noria Corporation, 2009).

SAPONIFICATION AND EVAPORATION STAGE

Saponification is the alkali hydrolysis of fatty matters to form soap. 103 grams of caustic soda solution (prepared by dilution to a concentration of 26%, with the specific gravity of 1.275 at room temperature of about 30^0C) was weighed into a plastic container. Then 206 grams of palm oil was weighed into the reactor in the ratio of (1:2) and was heated to a temperature of 60^0C (saponification temperature), followed by the gradual addition of already weighed caustic soda into the reactor. The mixture of the two reactants was stirred for a period of (5) minutes depending on the mass of the reactants (fatty matter plus caustic soda solution), to saponify and form soap. The soap formed in the process was later heated up to a temperature of about $(120^0C$ to $130^0C)$ (at atmospheric pressure), in other to remove water (by evaporation). This is the temperature at complete saponification, and the soap obtained at this stage is very thick and in a solid state.

GREASE FORMATION AND MILLING OPERATION

After saponification and evaporation at about 130^0C, the thickened soap formed is further heated to a temperature of about 170^0C to 180^0C to melt by adding little quantity of base oil so as to reduce friction or ease the stirring. At the above specified temperature, the thickened soap melts to a liquid state and becomes gummy or sticky on little exposure to air. At this temperature (180^0C), the molten soap was dispersed in base oil by gradual addition and stirring until the grease was formed. Here, reasonable quantity of base oil was added (900m/s for 650N, 800mls for 500N, and 500mls for 150N) in the respective production made and dispersed in each of these base oil samples.

However, before allowing the grease to cool to room temperature, milling operation was performed using locally fabricated grinder at the temperature of 80^0C. Milling is a form of homogenization. This method helped in reducing the particle size of the undispersed thickener in the base oil.

BLENDING OPERATION

Two hundred grams (200g) of dispersed polypropylene product and 200grams of sodium grease from the above were blended together, at the temperature of 100^0C, by heating and stirring the two in a reactor for a period of 10 -15 minutes, based on the quantity of the two products to be blended. At the end of this period, the product of the mixture was allowed to stay for 24hours (one day) to cool. Later on, blending ratios of sodium/polypropylene greases were altered in the form (1:2), (2:3) and (1:3) respectively.

QUALITY CONTROL ANALYSIS

The final product was tested or analyzed for quality. The tests conducted include those of the Dropping point and worked penetration of each of the samples produced.

Worked Penetration (ASTM D217, IP50)

Worked penetration is the penetration of a sample of lubricating grease after it has been brought to 25^0C (77^0F), and then subjected to 60 double strokes in a standard grease worker, and penetrated without delay. This was done following the standard procedure *(ASTM)*.

### Dropping Point of Lubricating Grease (ASTM D566, IP 132)

The ASTM–IP dropping point is the temperature at which a conventional soap–thickened–grease passes from a semi–solid to a liquid state under the conditions of test; this represents the temperature at which certain non–soap–thickened greases rapidly separate oil. This was done following the standard procedure.

RESULT AND DISCUSION
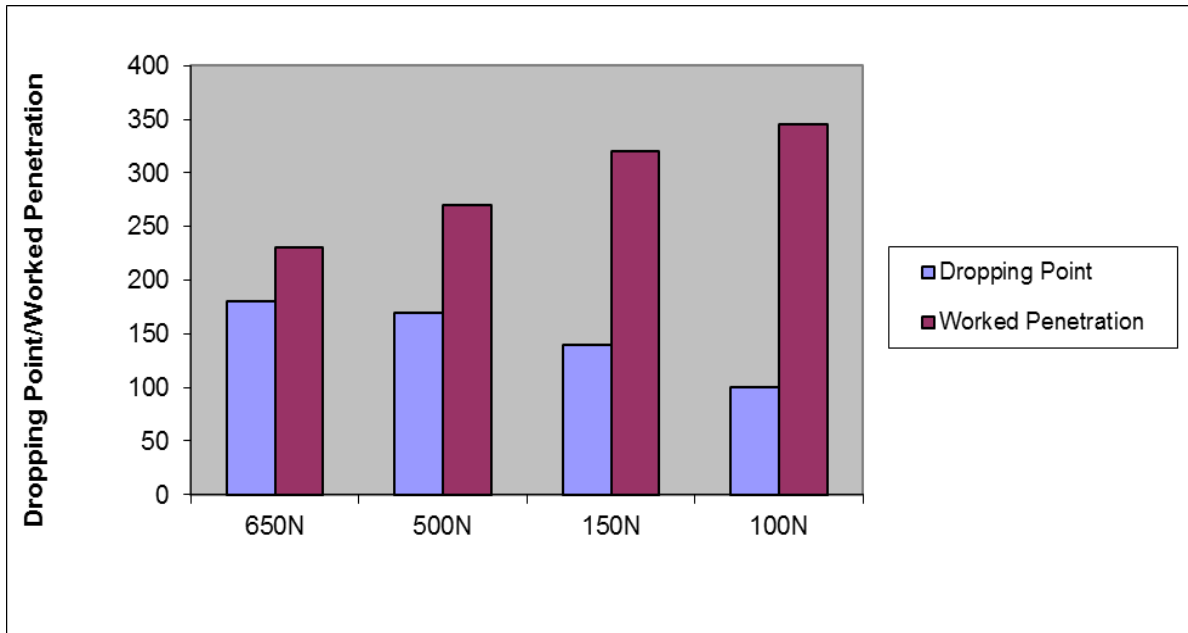
FIGURE 1: Comparative analysis Plot of dropping point versus worked penetration of sodium/polypropylene blended based grease in the ratio of 1:2
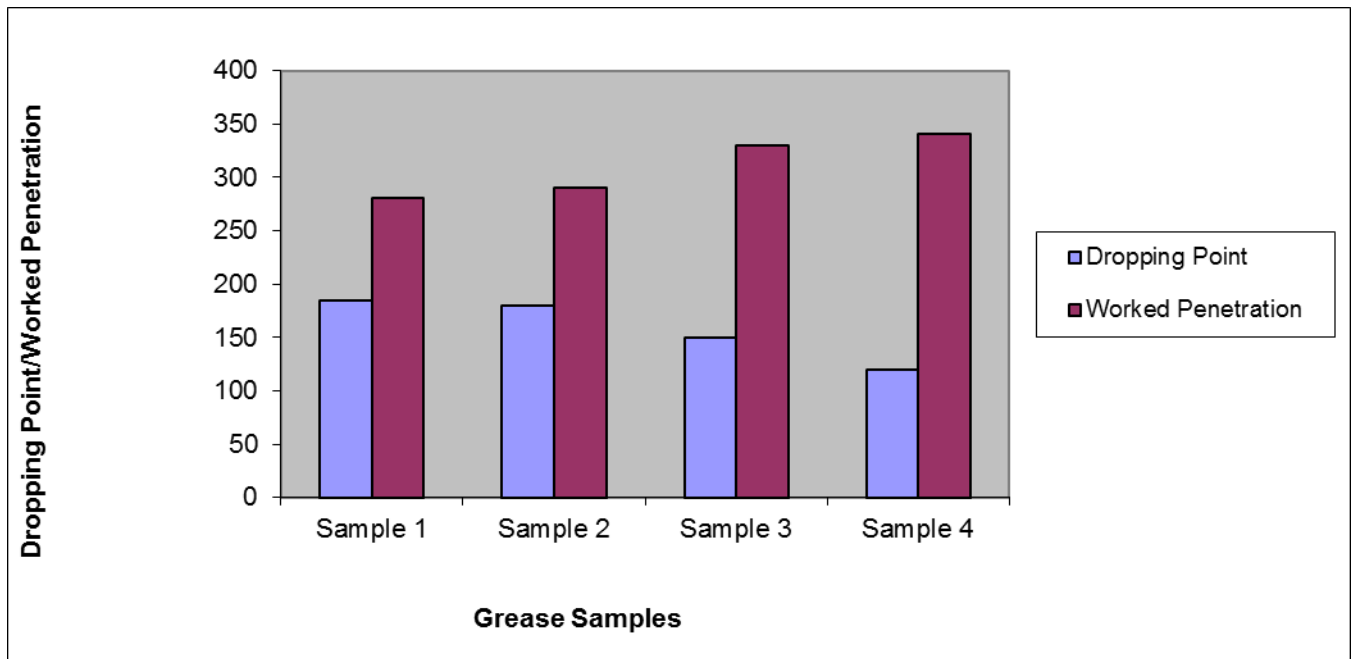
FIGURE 2: Graph of Worked Penetration (10th/mm) Versus Dropping Point(0C) of Polyethylene Greases(where Sample1=600N; 2=500N; 3= 150N; 4=100N)
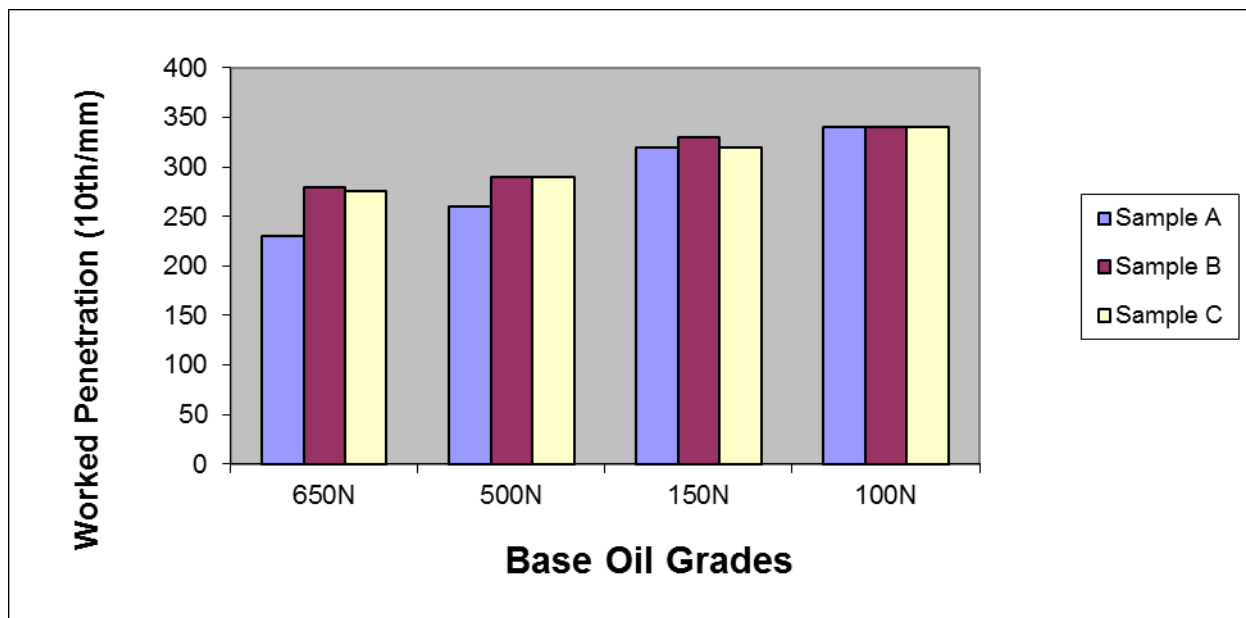
FIGURE 3: Worked Penetration of Samples at Varying Grades of Base Oils.

TABLE 1: RESULT OF ANALYSIS OF SODIUM/POLYPROPYLENE GREASE IN THE RATIO OF   1:1 (SAMPLE A)

Sodium/polypropylene = 1:1	Sodium plus polypropylene Grease with:			
Properties	**650N**	**500N**	**150N**	**100N**
Appearance	Smooth and fibrous	Smooth and fibrous	Buttery and fibrous	Buttery and fibrous
Other Properties	Adhesive and cohesive	Adhesive and cohesive	Adhesive and cohesive	Adhesive and cohesive

TABLE 2: ANALYSIS OF SODIUM/POLYPROPYLENE BLENDED-BASED GREASE IN THE RATIO OF 1:2 (SAMPLE A)

	Sodium plus polypropylene Grease			
PROPERTIES	**650N**	**500N**	**150N**	**100N**
Water resistance	Fair to good	Fair to good	Fair to good	Fair to good
Appearance	Smooth & fibrous	Smooth & fibrous	Smooth & fibrous	Smooth & fibrous
Other properties	Adhesive & cohesive	Adhesive & cohesive	Adhesive & cohesive	Adhesive & cohesive

TABLE 3: RESULT OF ANALYSIS OF POLYETHLENE CO-POLYMER GREASE (SAMPLE B)

	Polyethylene Grease			
PROPERTIES	650N	500N	150N	100N
Appearance	Smooth and buttery	Smooth and buttery	Smooth and soft	Smooth and soft
Other Properties	Cohesive	Cohesive	Cohesive	Cohesive

TABLE 4: NLGI/ASTM GRADE OF SODIUM-BASED AND LOW-DENSITY POLYETHYLENE BASED-GREASED

NLGI COSISTENCY NUMBER	A.S.T.M PENETRATION VALUE (10TH/MM)	DROPPING POINT (^{O}C)	RESULT OF SODIUM-BASED GREASE PRODUCED	RESULT OF LOW DENSITY POLYETHYLENE-BASED GREASE PRODUCED
2	265-295	160 minimum		270-280
3	220-250		230-240	

The results of the analysis are presented in figures 1 – 3, as well as in Tables 1 – 4. The data generated show that worked penetration increases with decrease in dropping point down the capacity (figures 1 and 2). This indicates that the higher the working capacity of the lubricant, the more the flow rate (that is the lesser the viscosity). Also, worked penetration of Sample B is higher than those of Samples **A** and **C** as indicated in figure 3. In agreement with the documentations of the Lubrizol Limited (2012), this implies that Sample B would have a lower penetration point than Samples **A** and **C**, which increases its disadvantages in application. Figures 1 and 2 also indicate that the quality of the grease sample decreases with decrease in the Bright Stock; this is traceable to the effect of the thickener in the high-density base oil (650N or Bright Stock). This agrees with the work of Svaberg (2006), which states that the working capacity determines the strength of lubricant. For this reason, it is undesirable to use grease of lower dropping point on heavy duty equipment. It could be, also, observed that the dispersion of the grease samples were highest at 100N working capacity, as indicated in figure 6. The results of physical analysis in tables 1 to 4, also, indicates that 10% of dispersed polypropylene in 650N (or bright stock) base oil is ideal to fortify sodium grease in the ratio of 1:1, in order to produce water resistance grease suitable for servicing of bearings and other heavy duty equipment.

However, the results obtained from the present study generally show that water-resistant-sodium-based grease and polyethylene (co-polymer) grease, that possess the desired properties (such as good cohesive and adhesive form, smooth/buttery form, as well as fibrous nature) could be produced from petroleum and petrochemical by-products. Also a blend of normal sodium grease and melted polypropylene is an ideal/quality grease that is suitable for ball bearing, based on ASTM/NLGI consistency grading as indicated in Table 4.

CONCLUSION

The present study shows that suitable and ideal concentration of caustic soda, for soap manufacture, is 26% and it corresponds with the specific gravity of 1.275 at the temperature of 30°C. The density of dispersed polyethylene/polypropylene in a fixed volume of base oil increases with increase in the mass of polyethylene/polypropylene dispersed. Also, 10% of dispersed polypropylene in 650N (Bright stock) base oil is ideal to fortify sodium grease in a good ratio (such as 2:1) in order to produce water resistance grease, suitable for servicing bearings and other heavy duty equipment. Caustic Soda, fatty materials, high density base oils (650N / 500N), polypropylene and other additives are reliable raw materials for water resistant sodium-based grease production, while low density polyethylene and polypropylene are recommended for water resistant light grease production. Sodium grease is ball-bearing and heavy duty grease, while polyethylene grease is a multipurpose grease for general servicing of equipment or machines; it could serve as a substitute to imported lithium grease.

REFERENCES

Astrom .H. and Hoglund, E. (1990): **Rheological Properties of Six Greases and their Base Oils**: *Technical report*; Sweden; Lulea University of technology.

Behling,R.D. and Lubrizol corporation, (1996): **Ready Reference for lubricant fuel performance –lubricating oils**; U.S.A.; Tomahawk W.I.,

Cheng, D.C.H (1999): **The Art of Coarse Rheology**;*The British Society of Rheology;32(1), 1-12.*

George T. Austin, (1984): **Shreve's Chemical Process Industries**; New York; McGraw-Hill International Edition.

Gottlieb Hugo E, Kotlyar Vadim, and Nudelman Abraham (1997): **NMR Chemical Shifts of Common Laboratory Solvents as Trace Impurities**; *The Journal of Organic Chemistry*, 62(21), 7512–7515.

Kirk Othmer, (1983): **Encyclopedia of Chemical Technology**; New York;

John Willey and Sons. Lubrizol Limited (2012): **Polymerous Life Science**, Victoria Island-Lagos, Nigeria; Emmyson Nigeria limited.

Noria Cooperation (2009): **Lubricating Grease Guide**; Nigeria; Noria International Limited,.

Totten George E., Westbrook Steven R., and Shah Rajesh J.(2006): **Fuels and Lubricants Handbook Technology, Properties, Performance and Testing;** ASTM manual series, volume 37, Pp 498-560.

Svanberg, I. (2006): **Black slugs (Arion water) as Grease: a Study of Technical Use of Gastropods**; *Journal of Ethnobiology*; 26 (2), 229 – 309.

Vinogradov. G.V., (1989): **Rhelogical and thermophysical properties of Grease**; London; Gordon and Breach Science publications.

Webb, E.T. (1927): **Modern Soap and Glycerine manufacture**; Davis Brothers, London.

P 027

PRODUCTION AND CHARACTERIZATION OF HIBISCUS ESCULENTUS FIBER REINFORCED POLYMER COMPOSITES

E.N. IKEZUE, O.D. ONUKWULI AND ANADEBE C.V.

CHEMICAL ENGINEERING DEPARTMENT
ANAMBRA STATE UNIVERSITY
ULI, NIGERIA

Email: eddikezue@yahoo.com
Cell Phone: +2348037440725

Abstract:
Renewable resources such as fibers in the field of fibre reinforced materials with their range of application represent an important basis in order to fulfill the ecological objectives of creating eco-friendly materials. In view of enormous advantages a study on green composite using hibiscus esculentus fibers as a reinforcing material and polyester resin as a novel matrix has been made. First of all polyester resin synthesized was reinforced with hibiscus esculentus (Okro vegetable) fibre. Reinforcement of the fiber was accomplished in different forms reinforcement, short fiber (10mm) reinforcement and long fiber (50mm) reinforcement. Present work reveals that mechanical properties such as: tensile strength, flexural strength and minimum creep of polyester composite increases to a significant extent when reinforced with hibiscus esculentus fiber which is found in outsized amount in the Nsukka area of Nigeria. These mechanical properties mainly depend upon the dimension of the fiber used and fiber volume fraction and nature of chemical treatment.
Keywords: *Polymer Composites, Reinforcement, Optimization, Mechanical Properties.*

INTRODUCTION

Renewable resources in the field of fiber reinforced polymeric material with their new range of application represent an important basis in order to fulfill the objective of creating eco-friendly materials (Bledzki 1996). Because of their enormous properties such as low density, good mechanical performance, relatively low cost, low weight, less damage to processing equipment, good relative mechanical properties, unlimited availability and problem-free disposal, natural fibers offer a real alternative to the technical reinforcing fibers presently available (Bledzki 1998). An interesting environmentally friendly alternative for the use of synthetic fibers as reinforcement engineering composite are lignocellulosic natural fibers such as flax, *Grewia optiva,* Pine needles, *Hibiscus sabdariffa* etc (Getenpholm 1993). Suitable matrix materials for natural-fiber reinforced polymers are polymer resin systems such

as thermoplastics and thermosetting. Natural fibers like flax, *Hibiscus sabdariffa, Pinus,* Jute, Pineapple leaf fiber, Oil palm fiber have all been proved to be good reinforcements in thermoset and thermoplastic matrices (Maya 2006). Polymer composites can be used in many different forms ranging from structural composites in the construction industry to the high technology composites of the aerospace, space satellite and many other industries.

Hibiscus esculentus (Okro vegetable) fiber collected from higher reaches of Nsukka area Nigeria has been found to contain 53.54% cellulose 28.94% hemicelluose, 18.22% lignin. Literature survey has revealed that no work has been done on utilization of this raw fibrous material as reinforcing agents in polymer composites.

In this paper, synthesis of polyester resin and randomly oriented intimately mixed *hibiscus esculentus* fiber polymer composites by hand lay up technique has been

reported. The effect of fiber reinforcement particularly with 30% weight loading and effect of fiber dimension on the properties of the composites such as compressive strength, tensile strength, and minimum creep behavior has been investigated. Fiber/matrix interaction was analyzed from the mechanical data.

Experimental

Material and Methods

Polyester resin solution and sodium hydroxide supplied by centre for composite research and development Nsukka Nigeria were used in this work. In the present research work we have used thermosetting resin such as polyester as Thermosetting Matrix Polymer.

Hibiscus esculentus fiber was collected from Nsukka area Nigeria. The fibers were washed thoroughly with distilled water and dried in an air oven at 80^0C for 12h and kept in a vacuum oven at 70^0C for 3h before preparation of composites.

1. Long fiber reinforcement

Hibiscus esculentus fibers were chopped into 10mm, 30mm, 50mm sizes and fiber volume fraction were 10%, 30%, and 50% these fibers were used as long fibers.

Instrumentation

Weights of the samples were taken on electronic balance (LIBROR AEG-220). Curing of different samples prepared was done on compression molding machine. Testing of samples for tensile and flexural strengths were done on ASTM made Computerized Universal Testing machine (HOUNSFIELD H25KS), wear testing was done on Wear & Friction Monitor (DUCOM – TR 20L).

Mechanical Characterization

Composites thus prepared were cut into rectangular pieces of dimension 163 x 12.5 x 6mm for the evaluation of tensile and compressive strength. The numbers of specimen used for the determination of mechanical properties were three and the tests were conducted at ambient laboratory conditions.

Results and Discussion

The investigation of mechanical properties of composites is one of the most important techniques in studying the behavior of composite material. it has proved to be the most effective method to study the behaviors of the material under various conditions of tension, compression, stress and phase composition of fiber composites and its role in determining the mechanical properties. Mechanical properties of fiber reinforced composites depend on the nature of the matrix material and the distribution and orientation of the reinforcing fibers, the nature of the fiber-matrix interfaces and of the interfaces region. Even a small change in the physical nature of the fiber for a given matrix may result in prominent changes in the overall mechanical properties of composites. It is well known fact that different degrees of reinforcement effects are achieved by the addition of hydrophilic fiber to different polymers. This may be due to different adhesion strength between matrix and fibers. The adhesion is usually the strongest in polar polymers capable of forming hydrogen bonds with hydroxyl groups available on the natural fiber surface.

Tensile Strength

Tensile strength of polyester matrix (Figure 1) has been found to increase on reinforcement. It has been found that with fiber reinforcement, tensile strength increase to a greater extent as compared to other reinforcement (short and long fiber reinforcement).
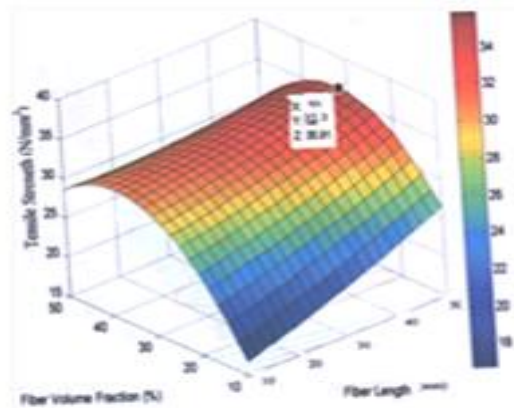
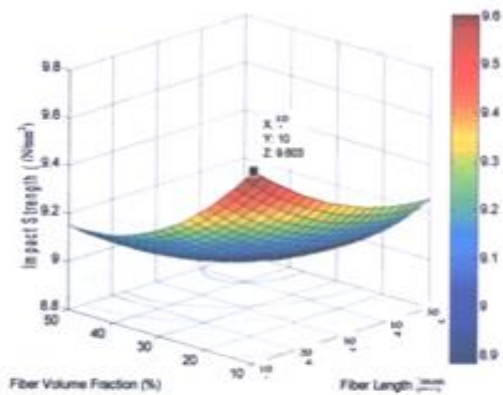Fig. 1: Surface Response plot for Tensile Strength (TS)

Fig. 3: Surface response plot for Impact Strength

Flexural Strength

It has been observed that composites with short fiber reinforcement showed more flexural strength (Figure 2) which was followed by thin fiber and continuous fiber reinforcement composites as well as increased impact resistance (Figure 3).
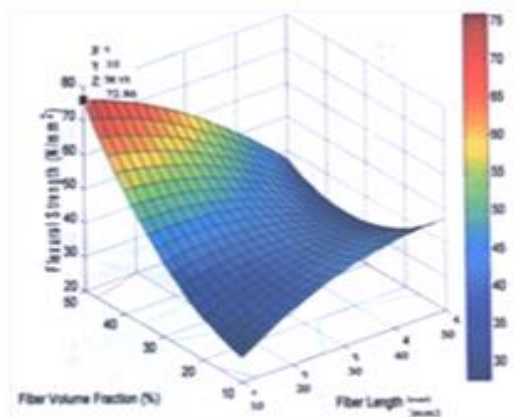

Fig. 2: Surface Response plot for Flexural Strength (FS)

Conclusions

Various test methods were adapted for complete mechanical characterization of natural fiber reinforced composites. In case of mechanical behavior fiber reinforcement of the polyester resin has been found to be more effective as compared to short and long fiber reinforcement. This could be due to more matrix-particle interfacial interaction as compared to short fiber/continuous fiber-matrix interfacial interaction. These results suggest that *hibiscus esculentus* fiber is a potential candidate for reinforcement in polymer composites.

REFERENCES

Bledzki A.K and Gassan J., *Prog. Polym Sci.,* **24,** 221-274.

Bledzki A.K, Reihmane S. and Gassan *J., Polym Plast Technol Eng.,* 1998, **37** (4), 451-68.

Bledzki A.K. Refihmane S. and Gassan *J.J., Appl Polym Sci.,* 1996, **59** (8), 1329-1336.

Gatenpholm P, Bertilsson H. and Mathiasson A, *J. Appl. Polym Sci.,* 1993, **49** (2), 197-208.

Kaith B.S., Singha A.S., Susheel Kumar and Misra B.N, *J. Polym Mater.,* 2005, **22,** 425-432.

Kaith BS, Singha AS, Sanjeev Kumar and Susheel Kalia, *Int. J. Polym Mater.,* 2008, 57(1), 54-72.

Maldas D. and Kokta B.V, *Trends Polym Sci.,* 1993, **1 (6),** 174-8.

Maya J, Bejoy F., Sabu T. and Varughese KT, *Polymer Composites,* 2006, **27** (6), 671-680.

Nabi Saheb D. and Jog J.P, *Adv. Polym Technol* 1999, **18 (4),** 351-63.

Panthapulakkal, S., Zereshkian A. and Sain M, *Bioresource Technol.,* 2006, **97,** 265-72.

Sahib Nabi and Jog JP, *Advances in Polymer Technology,* 1999, **18** (4) 351-363.

Singh B., Verma A. and Gupta M., *J. Appl Polym Sci.,* 1998, **70,** 1847-1858.

Singha A.S, Kaith B.S. and Sarwade B.D, *Hungarian Journal of Industrial Chemistry,* 2002, **30,** 289-293.

Singha A.S., Kumar S. and Kaith B.S., *Int. J. Plast. Tech.,* 2005, **9,** 427.

P 028

COMPARISON OF TWO FLOW IMPROVERS IN A WAXY CRUDE OIL

[*1]Oyedeko K.F.K., [2]Shomuyiwa O.Q., [3]Alagbe E.E

[1, 2] Lagos State University

[3]Federal Institute of Industrial research Oshodi

[*]kfkoyedeko@yahoo.com; edithalagbe@yahoo.co.uk

Abstract

Transportation of crude oil near or below its pour point requires a deep understanding of crude oil chemistry, its rheological properties, and operating conditions. Out of all the methods available for pumping waxy crude oil, use of pour point depressant (PPD) is preferred economically. Optimization of PPD dosages can affect cost savings. The present study deals with the comparison of flow improvers such as Styrene-Maleic and Triethanolamine in a waxy crude oil. The resulting copolymers were esterified with two moles of fatty alcohol ($C_{19}H_{36}O_3$). These polymeric diesters were evaluated for their efficiency as pour point depressants and flow improvers on crude oil from the Niger Delta region of Nigeria. The additives of polymeric diesters of oleic acid series (DO series) were evaluated as PPD and rheological modifiers. The rheological properties of the crude oil such as viscosity, pour point, American Petroleum Index gravity (APIg). Different doses (100, 500, and 1000 ppm) of synthesized polymeric additives were examined at different temperatures with the crude oil to evaluate pour point depressants and to study the dependence of shear rate on its shear stress and viscosity. The polymeric diesters of oleic acid series were found to be more effective and depress the pour point of the crude oil up to 9 ^{o}C with 500 ppm of doses.

KEY WORDS: Crude Oil, Triethanolamine, Styrene-Maleic, Waxy, Improver, Pour point, Viscosity.

1. Introduction

Crude oil having high wax content causes many problems during production, storage and transportation. At low temperatures, waxes separate out from the crude oil and deposit on the wall of pipelines. Due to this, the effective diameter for flow of the crude oil through pipelines becomes less. Therefore, pressure drop between the two ends of the pipeline increases. This results into the reduction of flow and extra burden on the pumping system (Mistra *et al*., 1995,Soni *et al*.2006.). Another major problem during the handling of waxy crude oil is the reusing of the pipeline after prolonged shut down period; the cooled oil slowly develops gel structure which results into high yield stress.(Soni, *et al*.2006, Castro. *et al*.,2011) Pour point is the temperature at which the crude oil is just able to flow and below which there's complete absence of flow in it. Cloud point is defined as the temperature at which the first wax crystal separates out from the crude oil. Below the cloud point crude oil containing high amount of wax possesses high pour point and exhibit non-Newtonian viscosity behavior. As temperature decreases, the abrupt rise in crude oil viscosity depends upon the quantity as well as type of wax present in it.

Polymeric additives known as flow improvers or pour point depressants (PPD) are generally chemical additives used to lower the pour point viscosity and yield stress of crude oil. In pipeline transportation, these additives improve the fluidity of waxy crude and reduce the extra pumping cost (Jun. *et al*., 2011, Atta. *et al*., 2011, AI-Shafey. *et al*., 2014). Any additive to behave as a flow improver should have the following three main characteristics: a wax like paraffin part, typically mixture of linear alkyl chain of 14-25 carbon atoms long that co-crystallize with oil's wax forming component; a polar component typically acrylates or acetates that limit the degree of co-crystallization; polymers that when adsorbed on the growing wax crystals statically hindered their growth, resulting into small crystal.

Any additive which is effective as a PPD may be ineffective to reduce viscosity and yield stress and enhance the flow. The factors that play an important role in the efficiency of flow improvers and pour point depressants have been reported by many workers; the effect of chain length of alkyl groups of the polymer on its efficiency as flow improver and pour point depressant (Al-Sabagh, *et al.,* 2007). Polymeric additives of different types were synthesized in the laboratory and evaluated as pour point depressants and flow improvers for crude oil from oil fields. (Pedersen, 2003, Soni *et al*., 2005)

In this respect, the present work aims; to compare the two types of flow improvers on waxy crude oil and to evaluate the effect of the flow improvers in the waxy crude oil and

to determine the relationship between the two (2) flow improvers. The crude oil samples used for this project were obtained from the Niger Delta region of Nigeria. The rheological properties considered were pour point, APIg (American Petroleum Institute gravity) and viscosity.

2.0 Materials and Methods

The two crude oil samples used for this research work were obtained from the Niger Delta region of Nigeria. The chemicals used for the treatment of wax deposition problem are; Triethanolamine and Styrene-maleic. Other material used for this experiment is Water.

Equipment used are: Density Bottle, Weighing Balance, Beakers, Thermometers, Burette, Film Cans, Retort Stand, Rotational Viscometer, Thermo stated water bath.

2.1 Determination of APIg (American Petroleum Institute gravity) for Triethanolamine and Styrene Maleic Anhydride Copolymer Esters.

This was determined using the test procedure following ASTM D97. The specific gravity (relative density) of the oil: S.G was determined and then used to determine APIg using the following equation:

$$^{\circ}API = \frac{141.5}{S.G \ AT \ 15^{\circ}C} - 131.5$$

This procedure was reported when the crude oil sample was mixed with 0.5ml, 1.0ml, 1.5ml and 2.0ml of triethalonamine and styrene- maleic respectively and the APIg were recorded.

2.2 Determination of Pour Point (Triethanolamine)

The ASTM D97 pour point measurement procedure was used. In this procedure, pour points of sample were obtained by heating each sample to $35^{\circ}C$ and then placed in the pour point test apparatus where it underwent steady cooling. The sample was checked at regular intervals until flow ceased. For flow that did not occur after 5 secs when the test tube was tipped horizontally, the temperature was taken and recorded to give the pour point. The procedure was carried out on the crude oil sample with and without the triethanolamine and styrene-maleic (ASTM Standard, 1998)

2.3 Determination of Viscosity (Triethanolamine)

The equipment used for determining viscosity was a rotational viscometer (Fann model 35). In this procedure, a recently agitated sample of each crude oil was placed in the sample cup, and the instrument head tilted into the sample at $28^{0}C$. The head was adjusted with the knurled knob until the rotor sleeve was immersed to the scribed line. The sample was stirred for about 15 seconds at different speed from (600RPM to 3RPM). The corresponding shear stresses of the samples at these shear rate were read and recorded.

This procedure was repeated for each sample at low temperature range of $1^{0}C$, $5^{0}C$, $10^{0}C$, $20^{0}C$, $22^{0}C$, $25^{\circ}C$ and $30^{\circ}C$. The apparent viscosity (μ_{A}) in mPas of each sample at each shear rate (γ) in rpm was then determined using the procedure describe by Baroid, (2004)'

The procedure was carried out for each pure crude oil sample, crude oil samples mixed with triethanolamine at $5^{0}C$ in the range of 1ml (0.05%), 2ml (0.10%), 3ml (0.15%), and 4ml (0.2%).

2.4 Determination of Dynamic Viscosity (Styrene-Maleic)

A viscometer model was utilized to measure the dynamic viscosity for untreated and treated crude oil with some selected pour point depressants at different concentrations (1, 2, 4, 6, 8, and $10x10^{3}$ ppm). Yield point, and apparent viscosity values were determined. Shear-rate, shear-stress, and viscosity can be calculated (El Gamal I.M., 1998).

Pour Point Measurements (ASTM, D97-96) (Styrene-Maleic)

Solutions of oil soluble samples PPD1-PPPD4 in xylene, contain 10% active material, are prepared. According to ASTM, D 97-96 method, different concentrations of PPD solutions were injected into the waxy crude oil and tested as pour point depressants. The pour points is set at $2.8^{\circ}C$ ($5^{\circ}C$) above the temperature at which the oil became solid.

3.0 Results and Discussion

The results of the APIg determined for the pure samples and samples mixed with triethanolamine are shown in Table 1. The results of the pour point determined for the pure samples and the mixed with triethanolamine are shown in Table 2

Table 1: APIg Values for the Samples (Triethanolamine)

Samples	APIg for Sample A	APIg for Sample B
Pure Samples	20.07	30.62
Sample+0.5ml TEA	20.27	30.69
Sample+1.0ml TEA	19.25	30.07
Sample+1.5ml TEA	19.12	29.68
Sample+2.0ml TEA	19.12	29.68

Table 2: Pour Points of Samples (Triethanolamine)

Samples	Pour Point for Sample A	Pour Point for Sample B

Pure Samples	+6	-9
Sample+0.5ml TEA	+3	-10
Sample+1.0ml TEA	+2.5	-10
Sample+1.5ml TEA	+2.5	-10
Sample+2.0ml TEA	+2.5	-10

Table 3: Physicochemical properties of the used crude oil

Specification	Results
Specific gravity at (60/60°F)	0.8427
APIg at 60°F	36.4
Kinematic Viscosity at 40°C	12.98
Asphaltene Content, %wt	0.25
Pour Point °C	27
Water Content, %Vol.	0.3

Table 4: APIg Values for the Samples (Styrene-Maleic)

Samples	APIg for Sample A	APIg for Sample B
Pure Samples	20.07	30.62
Sample+0.5 PSMA	36.4	30.66
Sample +1.0 PSMA	35.9	30.61
Sample + 1.5 PSMA	35.5	29.77
Sample + 2.0 PSMA	35.5	29.77

Table 5: Pour Point for the Samples (Styrene-Maleic)

Samples	Pour Point for Sample A	Pour Point for Sample B
Pure Samples	+8	-9
Sample + 0.5 PSMA	+6	-6
Sample + 1.0 PSMA	+6	-6
Sample + 1.5 PSMA	+3	-6
Sample + 2.0 PSMA	+3	-6

Table 6: Viscosity Measurement at Styrene-Maleic

Temperatures	Shear rate, sec⁻¹	Shear stress, Pa
30°C	100	3
	300	4
	600	6

	1200	14
25°C	100	3.5
	300	4.7
	600	6.3
	1200	15
20°C	100	4
	300	5.1
	600	8.4
	1200	20
15°C	100	5
	300	6
	600	11
	1200	25

Table 7: Viscosity Measurement for Triethanolamine

Temperatures	Shear Stress	Shear rate
1°C	20	2
	40	3
	60	5
	120	10
5°C	20	2.5
	40	3.5
	60	6
	120	11
10°C	20	3
	40	4
	60	6.4
	120	13
15°C	20	4
	40	5
	60	7
	120	18
20°C	20	5
	40	5.5
	60	10
	120	24

The effect of variation on temperature on the viscosity of Sample A at low temperatures is shown in Figure 1 and the effect of addition of triethanolamine on Sample A at 5°C is shown in Figure 2. The effect of variation of temperature on the viscosity of Sample B is shown in Figure 3 and effect of addition of triethanolamine on Sample B at 5°C is shown in Figure 4
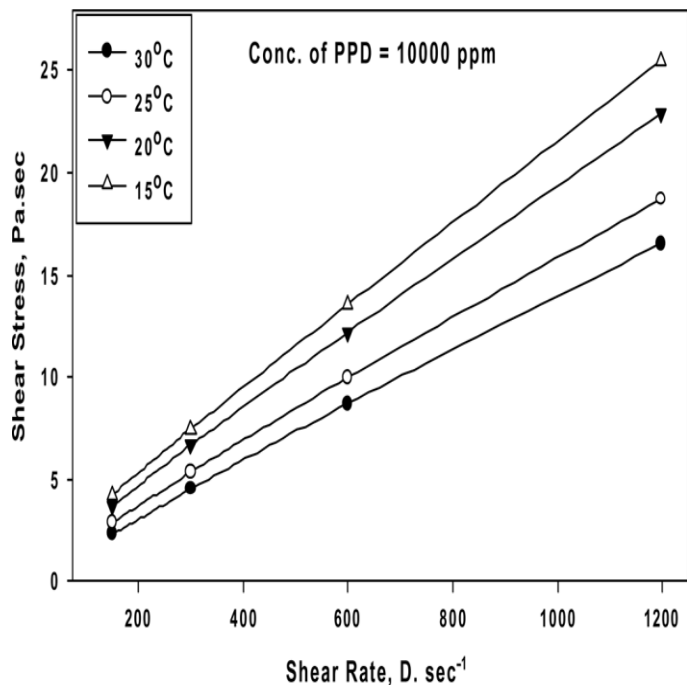
Figure 1 The relation of shear rate against shear stress of the waxy crude oil

Figure 2 the relation between shear rate and dynamic viscosity of crude oil

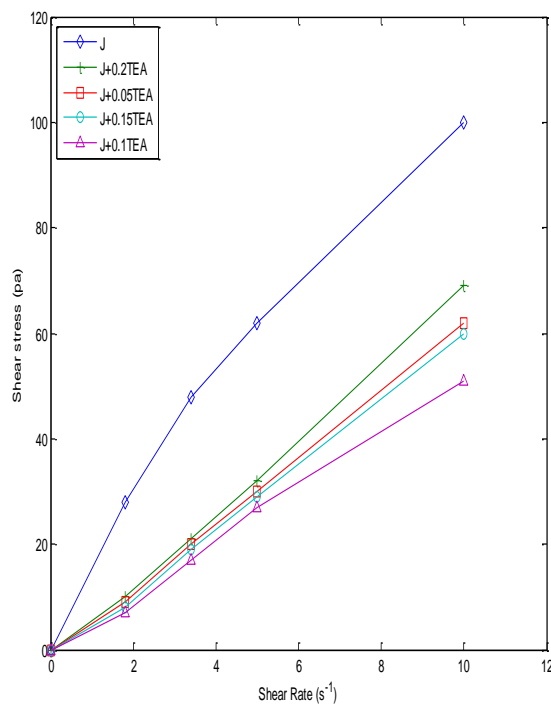Figure 3 Effect of Shear Stress against Shear Rate of Crude Oil

Figure 4 Effect of Triethanolamine on Addition of Crude Oil Samples

270

For Triethanolamine, the API gravity values of the samples tested increased slightly with the addition of small quantity of the additive. Further addition of TEA tends to reduce the APIg values which means their specific gravity increase; this may be justified by the fact that the density of the additive (TEA) is much greater than 1.0. The pour points of the samples tested are affected by the small quantities of triethanolamine, especially sample ranges from 20.10^o to 30.45^o. Sample B has higher API gravity while Sample A has a lower API gravity value.

Sample A has a gravity value below 27^oC and its regarded as Nigerian "medium heavy" on American Bureau Mines rating while Sample B is regarded as Nigerian "medium light" which indicates that Sample B is lighter than Sample A. It is also observed that apparent viscosity of the pure samples decreases with respect to increase in temperature for the two samples tested which is a typical characteristic of a Newtonian fluid.

But for Styrene- Maleic, the above representations explain that the shear stress increases linearly with increase of shear rate at all temperature which is a typical behavior of non-Newtonian fluid. This corroborate the findings of Guozhong and Gang , 2010).)

On the other hand, the relation between shear rate and dynamic viscosity shows a decrease of the dynamic viscosity with respect to an increasing shear rate reaching a limiting value at high shear rate.

This behavior is explained through the following reasons; at temperatures around the pour point of waxy crude oils, at low shear rates, the energy exerted by shear and dissipated energy in the matrix tends to break down the wax crystals partially. Viscosity also decreases with increasing shear rate until the agglomerates are broken into the basic particles. So the waxy crude system shows a non-Newtonian characteristic. (Soni, *et al*.2006, Castro. *et al*.,2011,AI-Shafey. *et al*., 2014)

4.0 Conclusions

In a search for effective chemical additives for improving the flow of waxy crude oil, two major additives were synthesized and characterized in the laboratory and their effects on pour point and rheological properties of the crude oil were investigated. The additives satisfy most of the requirements to act as a pour point depressant and flow improvers. As the two additives have potential to improve the flow behaviour of Nigerian crude oil significantly. Viscosities of waxy crude oil tend to decrease as the temperature rises. Thus flow of waxy crude oil becomes easier at high temperatures. The additives used in carrying out the work definitely affect the rheological properties of the crude oil. Additives of triethanolamine and styrene maleic series are differing by number.

After much ado on knowing a better flow improver, it came to realization and conclusion that Styrene-maleic can serve as better flow improvers in crude oil transportation.

1.   Styrene-maleic should be used other than triethanolamine to ease the flow of waxy crude oil in a pipeline because it   quickly breaks down wax crystals faster than triethanolamine.   2. Oil companies should transport crude oil at temperatures far above the pour points to avoid wax deposition.

3.   Rheology of crude oil should be manipulated via bending with other known crude since it's physical properties of fluid are known to be possibly improved by mixing.

5.0 Reference

Al-Sabagh A. M., Nasser N. M., Khamis E. A (2012). Demulsification of Crude Oil Emulsions Using Ethoxylated Aliphatic Amine Polyesters as Novel Demulsifiers *International Journal of Science and Research*: 2319-7064

A l-Shafey,H.I, A.I. Hashem, R. S. Abdel Hameed, E. A. Dawood,(2011) Studies on the Influence of Long Chain Acrylic Esters Co-Polymers Grafted With Vinyl Acetate as Flow Improver Additives of Crude Oils, *Advances in Applied Science Research,* 2 (5), 476-489.

Al-Shafey, H.I,. Abdel Hameed, R.S. Ismail, E.A. El Azabawy O.E,(2014) Studies of poly ethylene acrylic acid derivatives as pour point depressants of waxy crude oils, Organic Chemistry: *An Indian Journal*, 10(8), 308-314.

ASTM D2500-98 (1998). Annual book of   ASTM Standards Vol. 05.01

Castro V.L, A. Eugenio Flores and Flavio Vazquez,(2011) Terpolymers as Flow Improvers for Mexican Crude Oils, *Energy Fuels,* 25, 539–544.

Dirand M., Chevallier V., Prevost E., Bouroukba M.Petitjean D., Multicomponent paraffin waxes and petroleum solid deposits: Structural and thermodynamic state, *Fuel*, 77, 1253-1260, 1998.

El Gamal, I.M., Khidr, T.T., and Guiba, F.M. (1998) Fuel, 77(5): 375–385.

Garcia,M.C, Carbognani, L,Urbina, A and Orea,M,(1998) Paraffin depositon in oil production. Oil composition and paraffin inhibitors activity. *J.Petrol. Sci. Technol.*, 16(9), 1001.

Guozhong, Z. and Gang, L. (2010). Study on the wax deposition of waxy crude in pipelinesand its application. *Journal of Petroleum Science and Engineering*, 70, 1–9

Jun Xu, Huiqin Qian, Shili Xing, Li Li, and Xuhong Guo, (2011)Synthesis of Poly(maleic acid alkylamide-co-r-o lefin-co-styrene) Co-polymers and Their Effect on the Yield Stress and Morphology of Waxy Gels with Asphaltenes, *Energy Fuels*, 25, 573–579

Li, C., Pan, X., Hua C., Su J., and Tian, H. (2003) Eur. Polym. J., 39(6): 1091– 1097.

Manka, J.S. and Ziegler, K.L. (2001) Society of Petroleum Engineers International Symposium; SPE 67326, SPE Inc.

Misra S., Baruah S., Singh K., Paraffin problems in crude oil production and transportation, SPE., 28181, 50-54, 1995.

Sifferman T.R., Flow properties of difficult-to-handle waxy crude oils, *J. Pet. Technol*., 8, 1042-1050, 1979

Son A.J., Graugnard R.B., Chai B.J., The effect of structure on performance of maleic anhydride copolymers as flow improvers of paraffinic crude oil Proc. SPE. Int. Symp. on Oil Field Chemistry., New Orleans, U.S.A., 25186, 351-362, 1993.

Tanveer S., Sharma U.C., Prasad R., Rheology of multigrade engine oils, *Ind Chem. Technol*., 13,180-184, 2006.

Soni H.P., Bharambe D.P., Nagar A., Kiranbala, Synthesis of chemical additives and their effect on Akholjuni crude oil (Gujarat, India), *Ind. J. Chem. Technol*., 12, 55-61,2005.

Van Wazer J.R., Lyons J.W., Kim K.Y., Colwell R.E., *Viscosity and Flow Measurements*, Wiley Interscience, New York, Ch. 3, 1963.

Vora R.A., Bharambe D.P., Polymeric flow improvers, *Ind. J. Technol.,* 31, 633-635, 1993.

Yuping Song, Tianhui Rena, Xisheng Fu, Xiaohong Xu,(2005) Study on the relationship between the structure and activities of alkyl methacrylate–maleic anhydride polymers as cold flow improvers in diesel fuels, *Fuel Processing Technology,* 86, 641– 650

P 029

STUDY OF THE CONTRIBUTION OF CARBON IV AND CARBON II OXIDES IN METHANOL SYNTHESIS

[1]Minister E. Obonukut and [2]Etim N. Bassey*

[1]Department of Chemical and Petroleum Engineering, University of Uyo, P.M.B. 1017, Uyo, Nigeria
[2]Department of Chemical/Petrochemical Engineering, Akwa Ibom State University, Ikot Akpaden, Nigeria
*enbassey@yahoo.co.uk; minister024life@yahoo.com

Abstract:

The objective of this work was the simulation of methanol production process using a modified kinetic model to study the effect of reaction conditions on the relative contribution of Carbon II and Carbon IV oxides in methanol synthesis. The results showed that Carbon II oxide hydrogenation decreased as percentage of Carbon IV oxide increased and vice-versa. However it was observed that no generalizations could be made regarding the main carbon source in methanol but that the pathway of contribution from CO/CO$_2$ hydrogenation depends on process/reaction conditions. It is recommended that for improved process design, there is the need to carefully interpret experimental data and extrapolate results from low pressure/low conversion to high pressure/high conversion laboratory conditions.

Keywords: Methanol, Natural gas, Kinetic Models, Modified Model, Simulation,

1.0 Introduction

A number of kinetic models for methanol synthesis have been proposed in the literature (Natta, *et al*., 1955, Bakemeier, *et al.,* 1970, Leonov, *et al*., 1973, Klier, *et al*.,1982, Villa, *et al*., 1985, Graaf, *et al*., 1988, McNeil, *et al.,* 1989, Skrzypek *et al.*, 1991, Askgaard, *et al.,*1995, Bussche, *et al*., 1996, Kubota, *et al*., 2001, Setinc and Levec, 2001, Rozovskii and Lin, 2003, Lim, *et al*., 2009). One of the major concerns has been the role of CO and CO$_2$ in methanol production. Initial kinetic studies on methanol synthesis by Natta *et al*. (1955) and Leonov, *et al*.(1973) considered only CO and H$_2$ as the main reactants and neglected any contribution from CO$_2$. Later, Klier, *et al*. (1982) showed that methanol was mainly formed from CO and H$_2$ that adsorbed on the catalyst and CO$_2$ acted only as a promoter and not as a main reactant. They also suggested that methanol production rate was maximum at a CO$_2$/CO ratio of 2:28 which was governed by a balance between the promoting effect of CO$_2$ and the retarding effect due to strong adsorption of CO$_2$. In another study, Liu *et al*. (1985) conducted initial rate experiments in a batch reactor to determine the effect of feed composition on methanol production rate and obtained conflicting results.

Furthermore, Sahibzada, *et al*.(1998) showed that the intrinsic rate of CO$_2$ hydrogenation was twenty times faster than CO hydrogenation and at CO$_2$ greater than 1%, it was the main source of methanol production. They reported that methanol formation rate increased linearly with increase in CO$_2$ concentration in the absence of products. Establishing the role of CO$_2$ in methanol production, Ostrovskii, (2002) studied methanol synthesis mechanism on Cu/Zn containing catalyst under a wide range of experimental conditions and showed that CO$_2$ was the principal source of methanol production.

Lim *et al*. (2009) conducted a comprehensive study using Cu/ZnO with the view that CO and CO$_2$ adsorb on different Cu sites while water adsorbs on a ZnO site. They found that CO$_2$ hydrogenation rate was slower than CO hydrogenation rate which decreased methanol formation rate but since CO$_2$ decreases Water Gas Shift (WGS) reaction rate, it, therefore decreases the production of Dimethyl Ether, a byproduct from methanol. It was therefore, concluded that methanol production rate can be indirectly enhanced by finding an optimum CO$_2$ concentration. Lim, et al., (2009) claimed to be the first to report the role of CO$_2$ in methanol synthesis, suggesting a kinetic mechanism relating CO and CO$_2$ hydrogenation reactions. In a more recent study by the same authors, they have used the developed kinetic model to evaluate the effect of carbon dioxide fraction on the methanol yield, and have also devised an optimization strategy to maximize methanol production rate taking CO$_2$ fraction and temperature profile into account (Lim, *et al*, 2010). However, the controversies regarding the carbon source in methanol and the nature of active sites still remain unsolved.

The simulation of methanol process is based on the model proposed in this work which is considered to adequately describe some features and resolve questions related to methanol synthesis kinetics. An effort, therefore, was reported by the authors in previous work (Obonukut, *et al*., 2015) of a modified model that can adequately describe

some features and resolve questions related to methanol synthesis kinetics. The proposed model is based on the fact that CO and CO_2 hydrogenation both contribute to overall methanol production and when tested it fits better to the experimental data than others. Further, the issue regarding the main source of carbon in methanol was investigated to see its dependence on reaction conditions like conversion, pressure, relative amount of CO and CO_2, as well as hydrogen content in the feed.

In order to observe the contribution of CO and CO_2 in methanol synthesis, the investigation was carried out using Hysys simulation software on the basis of the modified model. The modified model is simply the combined rate expression obtained by adding Graaf's (CO Hydrogenation) model to Kubota's (CO_2 hydrogenation) model. In carrying the simulation process the modified model was used together with some hypothetical reactors.

2.0 METHODOLOGY

The conventional method of producing methanol from steam reforming of natural gas was simulated using Aspen HYSYS version 3.2 and the process flow diagram is as shown in Figure 1. The feedstocks, natural gas and air were fed into the Oxidation reactor to produce synthesis gas which in turn is fed together with steam into Reactor E for water-shift reaction to take place. The product from reactor E - during the investigation for CO and CO_2 contribution, the reactor was a stirred-tank (see Figure 2), and the reaction was designed using modified kinetic parameters (Obonukut, *et al.,* 2015). It was compressed and heated to the required temperature of 500K for methanol synthesis to take place.
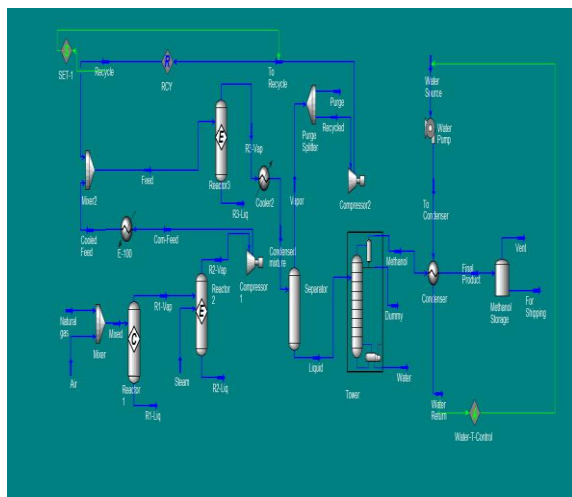
Figure 1: Simulation of Methanol Production Process

The methanol produced was condensed and ejected into a separator where the unreacted feedstocks were separated and the splitter purge the unwanted part and sent the useful part to the compressor which sent it back to the reactor for recycling.
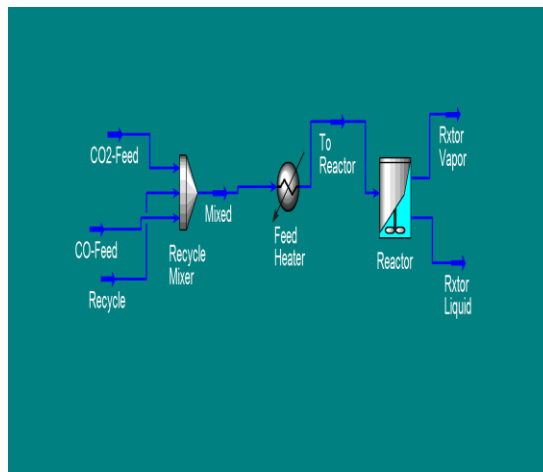
Figure 2: Reactor Simulation of Methanol Production Process using Modified Kinetic Model

Meanwhile, the methanol (Liquid from the separator) was sent to the Tower (distillation column) for purification. The final step in the process was to condense the methanol product and prepare it for storage. Before the condenser is put to use, a source of cooling water is required. It was taken from a storage tank (Water source) and pumped to the required pressure. Initially, the flow rate was set at 100,000 kg/hr to ensure that enough cooling water is pumped for the heat exchanger to condense the product. During the heat exchanger design, this was reduced to 50,000kg/hr. The cooling water's exit temperature is 200K (and need to be adjusted) because of the high flow rate. HYSYS has a unit called an adjust (A for Water-T-Controller). It is like a process controller in a plant, but it manipulates the model, not the process. It tells nothing about the dynamics of the process. Like a controller, it changes the value of one parameter in order to bring another parameter to a specified value. In this case, the cooling water flow is manipulated while the outlet water temperature is controlled. Finally, a tank was designed to store the final product which is a two phase mixture containing some vapor (mostly CO_2 and H_2) which has to be vented from the tank and the liquid methanol is stored for shipping.

The results obtained from the simulation were used to analyze the trends and other aspects related to methanol synthesis. The analysis will mainly concentrate on the

effect of different reaction conditions on the relative contribution of CO and CO_2 to producing methanol.

3.0 RESULTS AND DISCUSSION

The effect of CO_2 and CO hydrogenation on methanol production rate was studied by varying the reaction conditions to see their effect on Methanol production process. The modified kinetic model was incorporated into reactor simulation using its parameters for the methanol production as in Figure 2, which then aided the study of the relative contribution of CO and CO_2 to the hydrogenation process during methanol synthesis. The results as obtained from the simulation study are discussed under the following conditions: Conversion, Hydrogen content in the feed, Pressure and CO/CO_2 content in the feed

3.1 Conversion

Figure 3 shows the Gibb's free energy change of hydrogenation of CO and CO_2 to methanol as a function of temperature. It can be observed that CO_2 hydrogenation has more negative Gibb's free energy change (ΔG) and thus a higher driving force at very low conversions whereas CO hydrogenation is more likely to occur at higher conversions at a temperature of 558 K (Grabow, *et al.*, 2011). These results from thermodynamics prove that conversion levels can affect the extent to which CO and CO_2 hydrogenation will contribute in producing methanol. The study could not show the same behaviour using our results since not enough data points were available at a constant feed composition and the conversions did not change much in order of magnitude. A similar result was reported by Liu, *et al.* (1985) in their study in which they showed that hydrogenation of CO_2 was the primary reaction in producing methanol at low conversion.
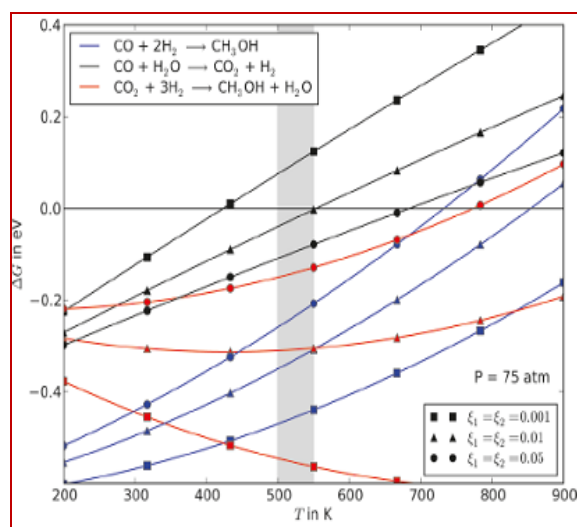
Figure 3: Gibb's free Energy change, ΔG, for CO and CO_2 Hydrogenation to CH_3OH and the WGS reaction at P = 75 atm and three different conversion levels as a function of temperature
 Source: Grabow, *et al.*, 2011

3.2: Hydrogen Content in Feed
 Grabow and Mavrikakis (2011) have reported that hydrogen content in the feed can have a marked effect on methanol production rates for CO rich feeds. Methanol production rate decreases almost linearly with increasing CO_2 content in the feed when the feed is lean in H_2 (< 50 %).
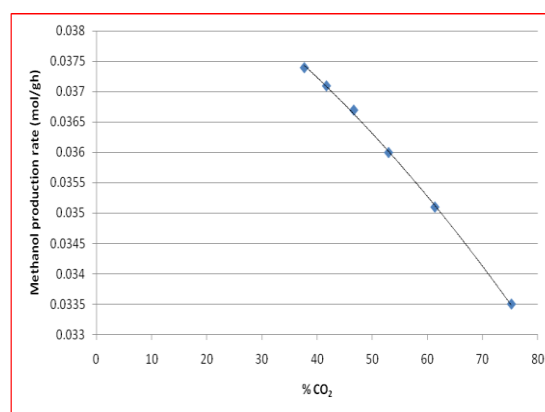
Figure 4: Methanol synthesis rate and % CO_2 in the feed under lean H_2 conditions

A similar trend was predicted by our model and the simulated result confirmed it as shown in Figure 4 which shows a plot of methanol synthesis rate and % CO_2 in the feed under lean H_2 conditions. It was observed that the rate decreased linearly as CO_2 content in the feed increased. This behavior can be attributed to the fact that hydrogenation of one mole of CO to methanol needs two moles of H_2 compared to CO_2 which needs three moles of H_2 to form methanol. Therefore, under lean hydrogen conditions, CO hydrogenation activity is increased. However, as percentage of CO_2 in the feed increased, the overall rate decreased since CO hydrogenation was inhibited by increased amounts of CO_2 in the feed. Also, since there was no water in the feed in the beginning, CO_2 participated competitively in methanol synthesis as well as Water Gas Shift Reaction (RWGS) resulting in lower methanol production. At a pressure of 5066kpa (50 atm), when hydrogen in the feed was increased slightly, the overall rate showed a maximum value at CO_2/ (CO+CO_2) = 0.046 (asterisk in Figure 5) as predicted by the model developed in this study.
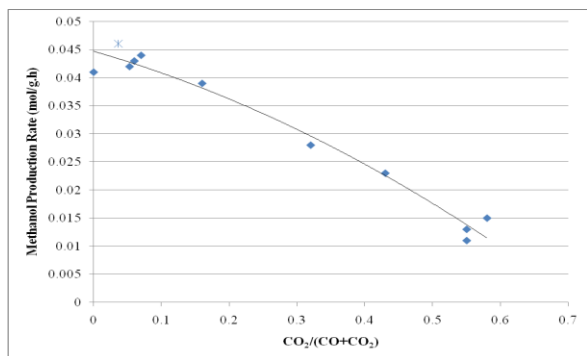
Figure 5: Overall Rate as Function of % CO_2

Calverley (1989) reported similar results in their study. However, they observed the maxima when $0.05 < CO_2/(CO+CO_2) < 0.2$. In this study, hydrogen content in the feed never increased beyond 60%. But at lower pressures (50 atm in our case), less hydrogen may be needed in the feed for the rate to increase with increasing CO_2 amounts. Figure 4.9 shows the overall rate plotted as a function of CO_2 % at a pressure of 50 atm. Therefore, at 50 atm and H_2 content of around 56% in the feed, overall methanol synthesis rate showed an increase in value as % CO_2 increased but it decreased again. This behavior showing maximum rate a particular value of CO_2 % has been reported by other authors as well like Rahman, Klier, *et al.* McNeil, *et al.*, and Lim, *et al.* (Rahman, 2012, Klier, *et al.*,1982, Lim, *et al.,* 2009 and McNeil, *et al.*, 1989).

3.3: Pressure
Total pressure also affects the relative contribution from CO and CO_2in producing methanol. Figure 6 shows the relative contribution of CO and CO_2 at a pressure of 50 atm calculated using the results from the modified model.
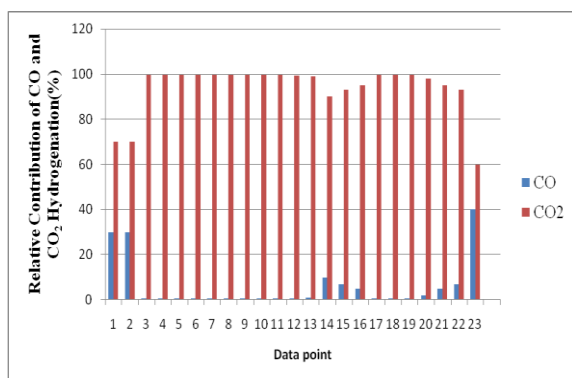
Figure 6: Relative Contribution of CO and CO_2

The plot clearly shows that CO_2 contributed more than CO to methanol production at a low pressure of 50 atm. The effect of pressure on the relative contribution of CO/CO_2 hydrogenation to methanol synthesis can be explained using Le Chatelier-Braun's principle. This principle states

that "whenever stress is imposed on any system (in the form of a change in concentration, temperature, volume or pressure) in a state of equilibrium, the system will always react in a direction which will tend to overcome the imposed stress" (Onuchukwu, 2004). During CO hydrogenation, three moles of CO react to form one mole of product, whereas, during CO_2 hydrogenation, four moles of CO_2 react to form two moles of product. When the pressure was high, CO hydrogenation was favored since it is the pathway which results in lower compression.

CO/CO_2 Content in the Feed
Figure 7 shows overall rate plotted as a function of % CO in the feed in the absence of CO_2.
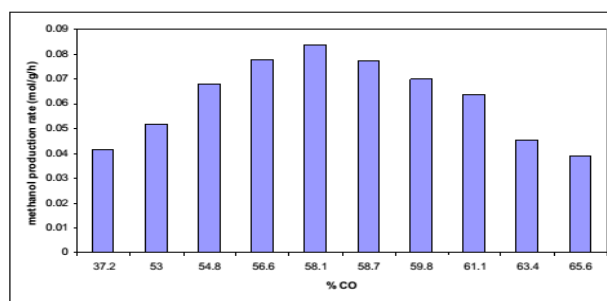

Figure 7: Plot of Overall Methanol Synthesis Rate as a Function of % CO in Feed when % CO_2 in Feed is Low

The rate increased as CO amount in the feed increased, while it decreased when % CO increased beyond 58 %. The increasing trend has also been shown by other authors, for example, McNeil *et al.* (McNeil, *et al.* 1989), as shown in Figure 8. The decreasing trend can be explained by using the fact that in the absence of CO_2, catalyst deactivation occurs via the Boudouard reaction resulting in carbon deposition and, therefore, decreasing methanol synthesis rate. As amount of CO increased, the reaction proceeded in the forward direction at a faster rate leading to more carbon deposition and fouling of the catalyst, and therefore, reducing methanol production rates.
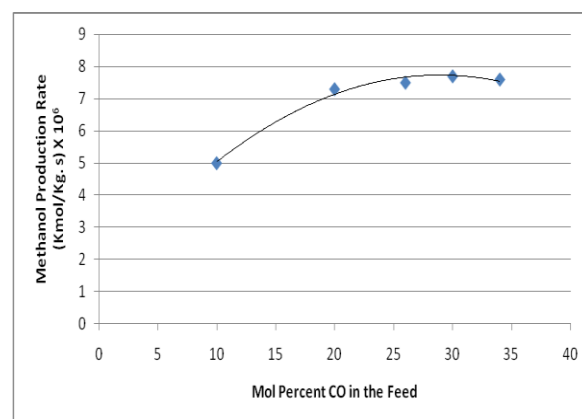
Figure 8: Methanol Production Rate versus Mole Percent Carbon monoxide in the Feed at 513 K and 2.89/4.38 MPa
**Source:** McNeil, *et al*., 1989

The volcanic shape of the plot shown in Figures 7 - 8 has also been reported by Grabow and Mavrikakis (Grabow, *et al.*, 2011). They observed a volcano-shaped curve when methanol production was plotted as a function of $CO_2/(CO+CO_2)$ feed ratio for CO- rich feeds.

Another trend predicted by the modified model is that the contribution from CO hydrogenation to forming methanol decreased as % CO_2 increased (see Figure 9).
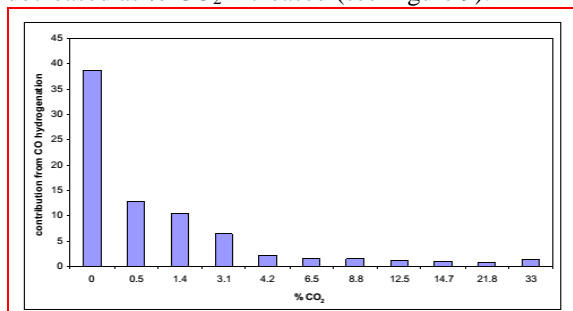
Figure 9: Plot of Relative Contribution of CO Hydrogenation versus %CO_2 in the Feed

The relative contribution from CO hydrogenation in synthesizing methanol plotted as a function of % CO_2 is shown in Figure 10. The plot shows the expected behavior since a high CO_2 content can lead to inhibition of CO hydrogenation due to the strong adsorption of CO_2 on active Cu sites necessary for CO activation. The major fraction of methanol resulted from CO_2 hydrogenation is shown in Figure 10. It is obvious that the intrinsic rate of CO_2 hydrogenation was twenty times faster than CO hydrogenation and at $CO_2 > 1\%$, it was the main source of methanol production. This trend is similar to what Sahibzada, *et al*. reported (Sahibzada, *et al*., 1998).
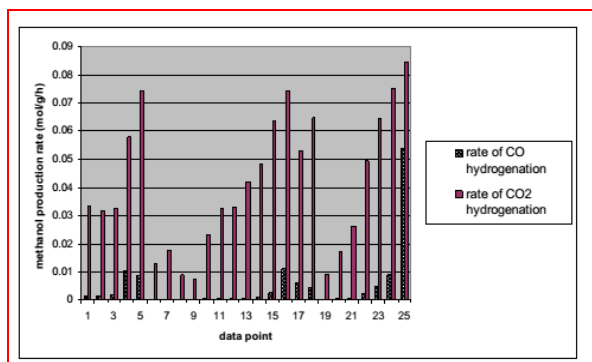
Figure 10: CO versus CO_2 Hydrogenation Rate

This aspect was also studied by Grabow and Mavrikakis who showed that larger fraction of methanol was formed from CO_2. However, they used a different feed composition (Grabow, *et al*., 2011).

4.0: CONCLUSION
Based on the simulation results, the modified model successfully explains the trends related to methanol synthesis kinetics. The results suggest that no generalization can be made regarding a more dominant reaction pathway. Instead, the contribution from each hydrogenation pathway depends on reaction conditions like conversion, pressure, CO/CO_2, and hydrogen content in the feed. Methanol production can be maximized by optimizing these conditions. Thus for improved process design it is necessary to carefully interpret experimental data and extrapolate results from low pressure/low conversion to high pressure/ high conversion laboratory conditions.

5.0 References
Askgaard, T. S., Norskov, J. K., Ovesen, C V and Stoltze P.(1995). A Kinetic Model of methanol synthesis, *Journal of Catalysis* 156, 229- 242.

Bakemeier, H., Laurer, P.R. and Schroder, W.(1970). Kinetic Studies of Methanol Synthesis *Chem.Eng. Prog. Symp. Ser.* 66 (98), 1

Bussche, K. M. V. and Froment, G. F.(1996). A Steady-State Kinetic Model for Methanol Synthesis and the Water Gas Shift Reaction on a Commercial Cu/ZnO/Al$_2$O$_3$ Catalyst. *Journal of Catalysis* 161, pp. 1-10

Calverley, E.M., (1989). A Study of the Mechanism and Kinetics of the Synthesis of Methanol and Higher Alcohols over Alkali Promoted Copper/Zinc Oxide/Chromia Catalysts. Open Access Dissertation and Theses Paper 1913

Graaf, G. H, Stamhuis, E. J. and Beenackers, A. A. C. (1988). Kinetics of Low Pressure Methanol Synthesis. *Chem. Eng. Sci.* 43 (12), pp. 3185-3195

Grabow, I.C and Mavrikakis, J. P. (2011). Mechanism of Methanol Synthesis on Cu through CO_2 and CO hydrogenation. *ACS Catal.*, 1, pp. 365-384

Klier, K., Chatikavanij, V., Herman, R. G. and Simons, G. W. (1982) Catalytic Synthesis of Methanol from CO/H$_2$: IV Effects of Carbon dioxide. *Journal of Catalysis*, 74, pp. 343-360

Kubota, T., Hayakawa, I., Mabuse, H., Mori, K., Ushikoshi, K. Watanabe, T. and Saito, M. (2001). Kinetic

Study of Methanol Synthesis from Carbon dioxide and Hydrogen. *Appl. Organometal. Chem.,* 15, pp. 121-126.

Leonov, V. E., Karavaev, M. M., Tsybina, E. N. and Petrischeva, G. S. (1973). *Kinetics Katal*. 14: 848

Lim, H. W., Jun, H., Park, M., Kim, H., Ha, K., Chae, H., Bae, J. W. and Jun, K. (2010). Optimization of Methanol Synthesis Reaction on Cu/ZnO/Al$_2$O$_3$/ZrO$_2$ Catalyst using Genetic Algorithm: Maximization of the Synergetic Effect by the Optimal CO$_2$ Fraction. *Korean J. Chem. Eng.*, 27(6), pp. 1760-1767.

Lim, H. W., Park, M., Kang, S., Chae, H., Bae, J and Jun, K.,(2009).Modelingofthekineticsformethanolsynthesis using Cu/ZnO/Al$_2$O$_3$/ZrO$_2$ catalyst: Influence of carbon dioxide
 during hydrogenation, *Ind. Eng. Chem. Res.,* 48(23), pp. 10448-10455

Liu, G., Wilcox, D., Garland, M. and Kung, H. H. (1985). The Role of CO$_2$ in Methanol Synthesis on Cu-ZnO: An Isotope Labeling Study, *J. Catalysis*, 96: 251 – 260.

McNeil, M. A., Schack, C. J., Rinker, R. G. (1989). Methanol Synthesis from Hydrogen, Carbon monoxide and Cabon dioxide over a CuO/ZnO/Al$_2$O$_3$ Catalyst II: Development of a Phenomenological Rate Expression. *Applied Catalysis* 50(1), pp.265-285

Natta, G. (1955). Direct Catalytic Synthesis of Higher Alcohols from CO and H$_2$. *Catalysis*. (P. H.Emmett, Ed.) New York: Reinhold, pp. 131-114, 349.

Obonukut, M. E., Bassey, E. N. and Benjamin, B. R. (2015). Kinetic Model Evaluation in Methanol Production for Improved Process Design. *International Journal of Innovative Research and Development*, October Issue, 2015 (Accepted for publication)

Onuchukwu, A. I. (2004). *Chemical Thermodynamics* 3rd Edition Owerri, Nigeria: Academic Publishers.

Ostrovskii, V.E. (2002). Mechanisms of Methanol Synthesis from Hydrogen and Carbon Oxides at Cu-Zn Containing Catalysts in the Context of some Fundamental Problems of Heterogenous Catalysis. *Catalysis Today*, 77, pp. 141-160.

Rahman, Daaniya (2012). Kinetics Modeling of Methanol Synthesis from Carbon monoxide, Carbondioxide and Hydrogen over a Cu/ZnO/Cr$_2$O$_3$ Catalyst. Master's Thesis, San Jose State University.

Rozovskii, A. Y. and Lin, G. I. (2003). Fundamentals of Methanol Synthesis and Decomposition. *Topics in Catalysis* Vol. 22 pp.137-150.

Sahibzada, M., Metcalfe, I. S. and Chadwick, D. (1998). Methanol Synthesis from CO/CO$_2$/H$_2$ over Cu/ZnO/Al$_2$O$_4$ at Differential and Finite Conversions, *Journal of Catalysis* 174, pp. 111-118

 Setinc, M. and Levec, J. (2001). Dynamics of Mixed Slurry Reactor for the Three-Phase Methanol Synthesis. *Chem. Eng. Sci*. 56: 6081-6087

Skryzpek, J., Lachowska, M. and Moroz, H. (1991) Kinetics of Methanol Synthesis over Commercial Copper/Zinc Oxide/Alumina Catalyst. *Chem. Eng. Sci.* 46(11):2809-2813.

Villa, P., Forzatti, P., Buzzi-Ferraris, G., Garone, G. and Pasquon, I. (1985) *Ind. Eng. Chem. Process Des. Dev.* 24: 12

P 030

PERFORMANCE EVALUATION OF BIODIESEL PRODUCED FROM RUBBER SEED OIL USING THE TD-212 SMALL ENGINE TEST SET OF TECQUIPMENT

Dowhodema A.E.*, Onoji E.S. , Aremu A.E., Hassan A., Awoyale A.A., Zakariyya M.A.

Department of Petroleum and Natural Gas Processing Engineering, Petroleum Training Institute, Effurun, Delta State.

Edwarda951@gmail.com*; oluyale@yahoo.com; samonoji@yahoo.co.uk;

Abstract:

The world has experienced negative effect from the fossil fuel such as global warming and acid rain etc. With the increase in consumption of biodiesel, its impact on environment has raised a discussion around the world.. It is produced domestically which helps to reduce costly petroleum imports, it is biodegradable, nontoxic, contains low aromatics and sulphur and hence, is environment friendly. An experimental investigation has been carried out to examine the performance parameters and exhaust emission of the TD-212 small engine test set of TecQuipment filled with conventional diesel and a rubber seed oil biodiesel. The conventional diesel, biodiesel and its blends were ran on the engine to determine the engine speed, torque, power, brake specific fuel consumption and brake thermal efficiency. The emission characteristics such as NOx, HC, CO and smoke of the various fuels were determined with the help of various equipment. The results show that rubber seed oil biodiesel and its blends have lower emission . With the better performance of the biodiesel and its blends on the engine, it is a good replacement to petroleum diesel.

Keywords: *Rubber seed oil, Biodiesel, Engine performance, Emission characteristics, Transesterification, Renewable energy.*

1.0 INTRODUCTION

The global environmental change and the issue for long term availability of traditional oil resources necessitate creating the substitute energy sources that give engine performance at par with the conventional fuel. Energy is an essential input for economic growth, social development, human welfare and improving the quality of life. Since their exploration, the fossil fuels continued as the major conventional energy source. With increasing trend of modernization and industrialization, the world energy demand is also growing at a faster rate (Nitin, 2012).

Interest in vegetable oils as alternative fuels for diesel engines, dates back to 1930s and

1940s. However, their use as viable substitutes for diesel fuel was not popular as it tends to clog fuel filters due to high viscosity. Heating and blending of vegetable oils with diesel was used to reduce the viscosity and improve volatility but this does not remove the polyunsaturated structure of the oils (Bora, 2009). Transesterification leads to the production of biodiesel, has been found to be an effective way of surmounting this problem. Despite this, the use of biodiesel has not yet become widespread, the main reason being the cheap and yet vast supply of petroleum based fuels. Biodiesel is an organic alternative fuel that can run in a compression ignition with little or no modification, as opposed to pure

oil that can require some modifications, to the vehicle. Many vehicle manufactures now cover a percentage of biodiesel usage in the warranty agreement of the vehicle. This means that a vehicle can use biodiesel without voiding the manufacturer's warranty. Biodiesel could also extend the life of your engine by 20L because it naturally lubricates the engine's moving parts cutting down on the friction created. Less friction also means less heat which in turn will reduce the frequency of heat related breakdowns (Pinnes 2007). Biodiesel is biodegradable meaning it will have no harmful effect on the environment in its liquid state. Biodiesel contains no harmful sulphur and is no toxic to humans or livestock. Sulphur emitted from engines burning petroleum based fuels forms sulphur dioxide which reacts with water to create sulphuric acids, in turn creating acid rain. Biodiesel contains no petroleum based product at all, it can however be blended with any amount of petroleum fuel to create a biodiesel blend.

Despite these advantages, there are still some problems associated with using biodiesel. Although engine manufactures may support biodiesel being used in their engines there are no long term field tests that prove that the use of biodiesel over the engines life may or may not increase the risk of premature wear to engine components. The long term effects of using biodiesel are not fully explored yet. Engine emissions are certified using either forecourt diesel or in some cases specially blended certification blend. By using biodiesel it may affect the engine NO_X emissions meaning the engine will fall outside of its certified specification (Pinner, 2007).

Compression ignition engines which run on diesel fuel are more widely used in transport on passengers and cargo, electric power generation, industry and agriculture compared to spark ignition engines. Hence, greater attention is being devoted to the use of biodiesel and its blends in these engines. Biodiesel and its blend with diesel have been employed as a fuel for a C.I engine without any modification in the existing system.This study presents the performance and emission characteristics of diesel engine using rubber seed oil biodiesel and its blends.

2.0 MATERIALS AND METHODS

The biodiesel was made from rubber seed oil by modifying a two-stage acid-base transesterification process. During the acid-catalysed stage, the amount of methanol used was 20% of the volume of oil plus 60% excess methanol. One litre of rubber seed oil and 40% of the required volume of methanol were measured and added to the heated rubber seed oil at 55^{0}C. The mixture was stirred gently for 5 minutes using a magnetic stirrer until it became milky and 1ml of 95% sulphuric acid was added to the mixture. Holding the temperature at 55^{0}C, the mixture was stirred gently for one (1) hour at 500 – 600rpm. The heat was removed and stirring continued for another hour after which the mixture was allowed to settle for two (2) hour. To the remaining 60% of the methanol 4.9g potassium hydroxide (KOH) was added to form potassium methoxide solution. 50% of this solution was added to the acid treated mixture and stirred gently for 5 minutes and allowed to settle to 6 – 12 hours after which the gylcerime was drained off. During the alkali-catalsed stage, the mixture was heated to 55^{0}C and the second half of the methoxide solution was slowly stirred in, mixing at the same speed for one (1) hour. On completion of the reaction, the product was poured into a separating funnel and allowed to settle for 18 – 24 hour. After

separation of the biodiesel and glycerol, the fatty acid methylester was washed with 2ml of 10% phosphoric acid added to warm distilled water and dried with anhydrous sodium sulphate. The biodiesel was self blended with the diesel fuel (Enweremadu, 2011). Diesel was used splash blended with the biodiesel in a conical flask with continuous stirring to ensure uniform mixing. The biodiesel was blended with the diesel fuel at a volume base of 5%, 10% and 20%. Blends were prepared at 25^0C at the ambient temperature of the blending location. The names of these blends were defined by the name of the biodiesel fuel followed by the volume fraction of the biodiesel in the blend.

Performance and emission test were carried out in single cylinder, four stroke TD-212-Small Engine Test set of TEcQuipment. The engine was directly coupled to an eddy current dynamometer which permitted engine monitoring. The engine and the dynamometer were interfaced to a control panel which was connected to a computer.

The fuel was supplied to the engine by an external tank. a glass burette attached parallel to the tank was sued for fuel flow measurement. The engine was ran at full load and the rated speed for all the test fuels. During the experiments, engine speed, engine torque, engine power and fuel consumption were measured and used to calculate the brake specific fuel consumption (BSFC), brake thermal efficiency (BTE), brake specific energy consumption (BSEC) and brake mean effective pressure (BMEP). Emission tests were carried out with Rosemount Analytical non-dispersive infrared gas analyzer (Model 880A) for CO, CO_2, and NO_X. Un-burnt hydrocarbons were measured with German-made flame ionization detector, Model VE7 while smoke was measured with Bosch type smoke meter (Model ETD02050). Oxides of nitrogen (NO_X), carbon monoxide (CO), un-burnt hydrocarbon (UHC) and smoke opacity were measured for exhaust emissions at full load and rated engine speed of 1700rpm. Tests were repeated three times
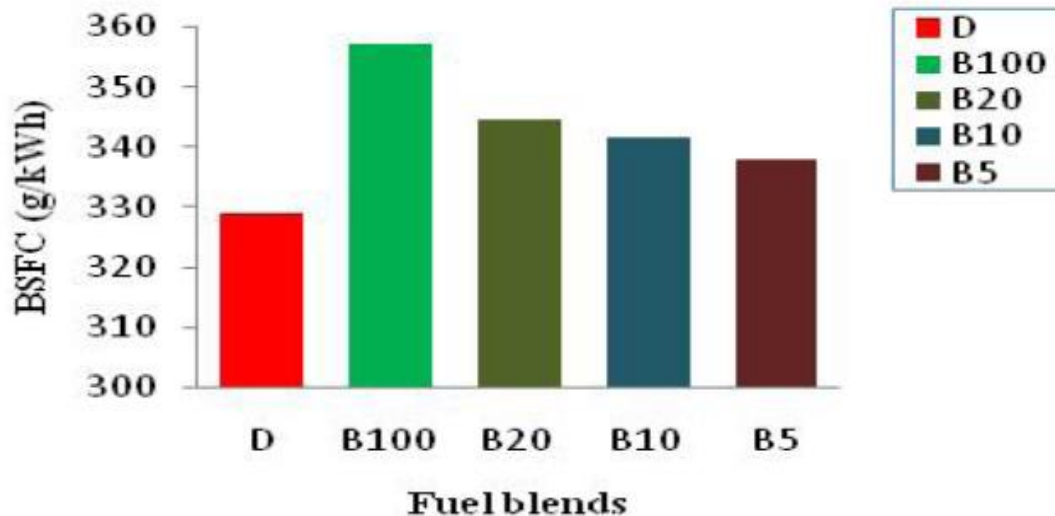

Figure 1: Comparison of BSFC for diesel and biodiesel diesel blends at full load

and the results of the three replications were averaged and reported.

3.0 RESULTS AND DISCUSSIONS

The results for engine performance and emission characteristic for petroleum diesel, rubber seed oil biodiesel and its blends as stated below

3.1 Engine Performance Parameters

Brake thermal efficiency (BTE) is the ratio between the power output and the energy introduced through fuel injection. Figure 2 shows that the brake thermal efficiency of rubber seed oil biodiesel and its blends with diesel fuel is lower compared with the diesel fuel. The brake thermal efficiency of blends

With increase in biodiesel content in the blends, the heating value of fuel decreases. Therefore, the brake specific fuel consumption of the fuel blends increase with biodiesel content. The brake specific fuel consumption of the biodiesel and its blends are higher compared to the petroleum diesel as show in Figure 1. This may be attributed to the lower viscosity, lower density and higher heating value of the petrol-diesel.

of the biodiesel lie between those of diesel and biodiesel. However, the decrease in brake thermal efficiency is not proportional to the increase in biodiesel content. The improved efficiency may be due to better lubricating properties of the blends as compared to the pure components.
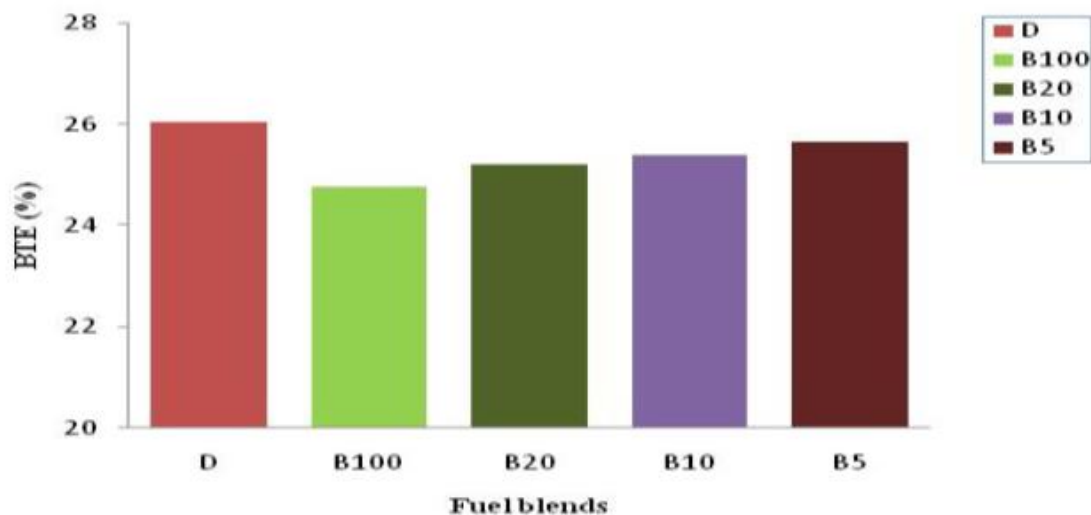

Figure 2: Comparison of BTE for diesel and biodiesel diesel blends at full load

3.2 Emission Characteristics

NO_X emissions increases in proportion to the biodiesel concentrations in the blend with pure biodiesel giving the maximum. Invariably all biodiesel have some levels of

oxygen bound to its chemical structure. Hence, oxygen concentration in biodiesel fuel might have caused the formation of NO_X. Being an oxygenated fuel, it also

supplies oxygen in addition to air inducted into the combustion chamber and this may aid the formation of NO_X. Another contributing factor maybe the possibility of higher combustion temperatures arising Increase in NO_X emissions from biodiesel fuels may also be due to advancing of injection timing brought about by more rapid transfer of pressure wave from fuel injection pump to fuel injector to open earlier. Faster pressure wave is as a result of higher bulb modulus of compressibility and The emission result show that the CO, smoke opacity and UHC decreases as the biodiesel content in the blends increase with B100 producing the best emission result.

from improved combustion as a larger part of the combustion of RSO biodiesel and its blends are completed before TDC due to lower ignition delay.

Consequently, a higher velocity of sound of biodiesel fuel relative to petrol-diesel. Advancing injection timing in a diesel engine advances phasing of combustion process leading to a longer period of time where temperatures are conductive for NO_X formation (Bora, 2009).

The CO, UHC and smoke opacity concentrations of all the biodiesel blending percentages were less than the petrol-diesel.
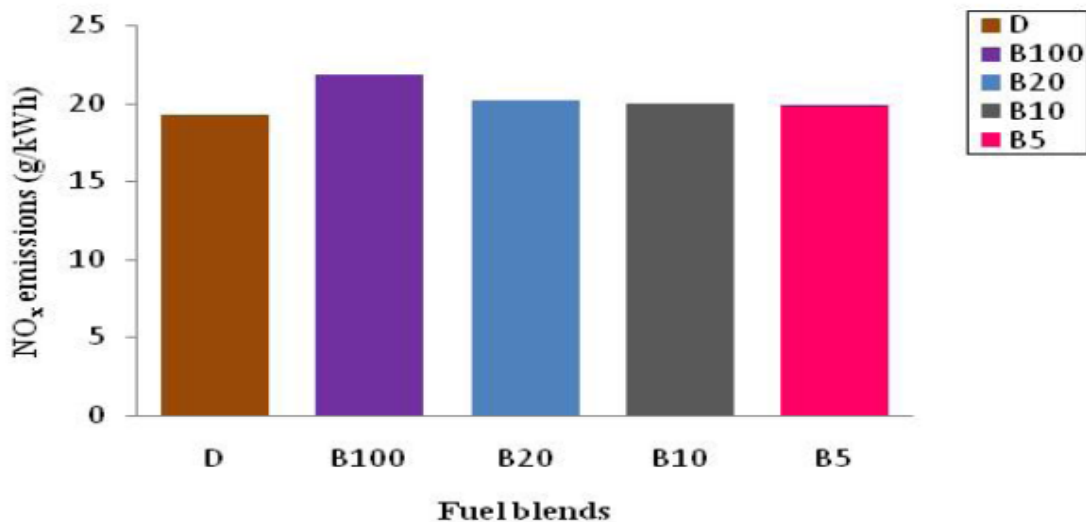
Figure 3: Comparison of NO_X emissions for diesel and biodiesel diesel blends at full load

The decrease in CO emissions from biodiesel and its blends may be due to the additional oxygen content in the fuel, which improves combustion in the cylinder. Biodiesel also has higher cetane number and it less compressible than diesel fuel. Increased cetane number of biodiesel fuel

lowers the probability of forming fuel-rich zone-and the advanced injection timing. All these result in shorter ignition delay, longer combustion and increase in complete combustion reaction regions. If a fuel is less compressible, the injection starts earlier and causes longer combustion duration.

Since biodiesel is an oxygenated fuel, it lead to a more compete and complete combustion resulting in decrease in UHC emissions. The higher cetane number of biodiesel fuel reduces delay period loading to lower UHC emissions. Therefore, the higher oxygen and the cetane number of biodiesel diesel fuel

blends tend to reduce UHC emissions when compared to petro-diesel fuel.

Since smoke is formed due to incomplete combustion, the oxygen content in B100 and its blends with diesel fuel may be more effective in enhancing better combustion, hence a decrease in smoke opacity compared to diesel fuel.
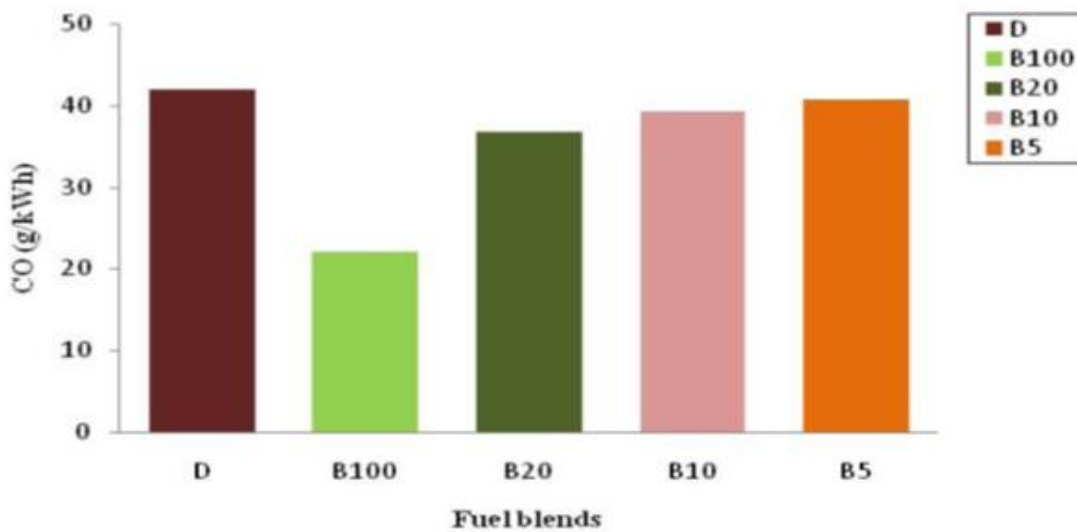
Figure 4: Comparison of CO emissions for diesel and biodiesel diesel blends at full load
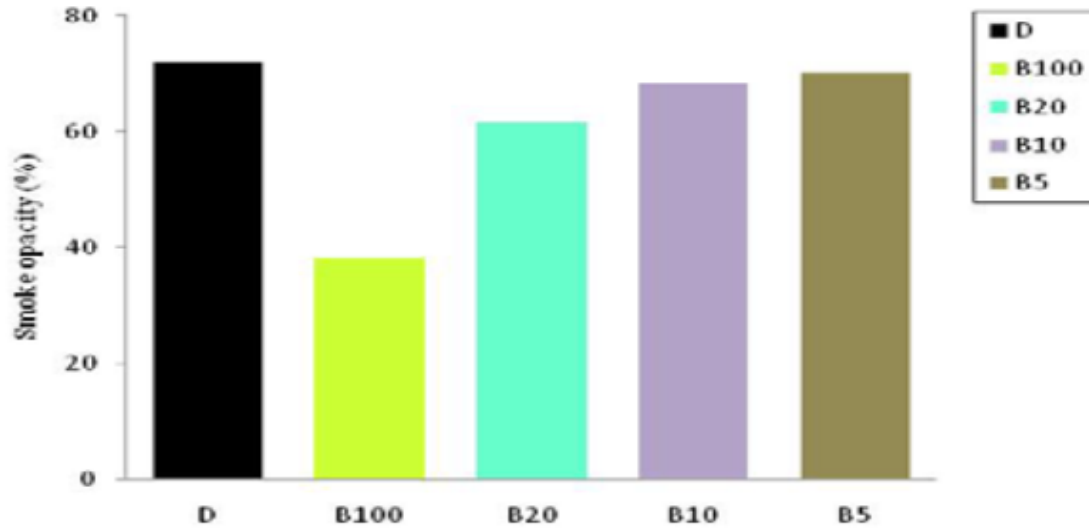
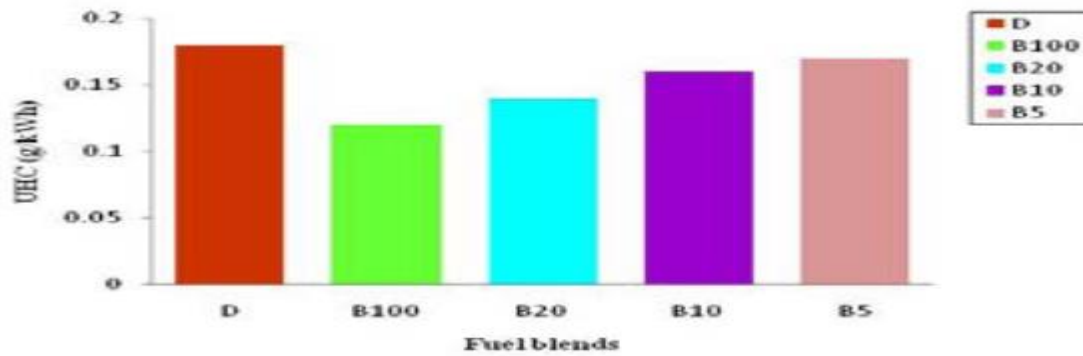**Figure 6: Comparison of smoke opacity for diesel and biodiesel-diesel blends at full load**

Figure 5: Comparison of UHC emissions for diesel and biodiesel diesel blends at full load

4.0 CONCLUSION

This study has demonstrated that methyl ester from rubber seed oil has a very strong potential for use as an alternative fuel in diesel engines. The performance of a TD-212 Small Engine Test Set when fuelled with the biodiesel and its blends with diesel fuel is very similar to that when fuelled with neat petro-diesel. These main conclusions from the work are as follows:

- The brake specific fuel consumption increased with increase in biodiesel in the fuel blends.
- The brake thermal efficiency of the engine fuel with pure rubber seed oil biodiesel and its blended fuel is lower compared to petrol-diesel.
- Smoke intensity, CO exhaust emissions, UHC decreased, whereas NO$_X$ emissions increased with increase in biodiesel content in the blends.
- The experimental results preliminary support the assertion that rubber seed oil biodiesel can be successfully used as a diesel fuel substitute in existing diesel engines without modifications but this requires long term and compressive tests.

REFERENCES

Bora, D. K. (2009): Performance of Single Cylinder Diesel Engine with Karabi Seed Biodiesel. Journal of Scientific and Industrial Research Vol. 68 pp 960-963.

Environmental Protection Agency (2002): Comprehensive Analysis of Biodiesel Impacts on Exhaust Emission. Draft technical Report EPA 420-p-02-001 (www.epa.gov/otaq/models/analysis/diodsl/p02001.pdf)

Handbook of Emission Reductions with Biodiesel (1999): (www.cytocultures.com/biodiesel%20Handbookhtml)

Hansen K. F. Jensan M. G (1997): Chemical and Biological Characteristics of Exhaust Emissions from a D. I. Diesel Engine Fuelled with rapeseed Methyl ester SAE Paper 1997, 971689.

Kac, A. (2001): The Foolproof way to make biodiesel.(http://journeytoforever.org/biodiesel_aleksnerhtml)

Lapuerta M. Amas O. and Fernardez R. (2008): Effects of Biodiesel Fuels on Diesel Engines Emissions. Progress in Energy and combustion Science. Vol. 34, pp 198 – 223.

Nitin S., Varma S. N. and Mukesh P. (2012): An Experimental Investigation of Performance and Exhaust emission of a diesel engine fuelled with Jetropha Biodiesel and its blends, Internal Journal of Energy and Environment. Vol. 3, pp 915 – 926.

Pinner, A. (2007): An Investigation into Biodiesel and its Potential role in the Replacement of Crude Oil, B.Eng Final Year Project, University of Hudders Field, pp 1-101.

Pinto A. C., Guarieiro L.L. N and others (2005): Biodiesel: An Overview Journal of Brazilian Chemical Society Vol. 16)16B), pp. 1313 – 1330.